Biomechanical investigations of sprint start technique and performance

Bezodis, Neil

Award date:
2009

Awarding institution:
University of Bath

BIOMECHANICAL INVESTIGATIONS OF SPRINT START TECHNIQUE AND PERFORMANCE

NEIL EDWARD BEZODIS

A thesis submitted for the degree of Doctor of Philosophy

University of Bath

School for Health

April 2009

Signature of author……..

N. E. Bezodis

ABSTRACT

Biomechanical investigations of sprint start technique and performance

N. E. Bezodis, University of Bath, 2009

The start is an important part of any athletics sprint event, and has thus been the focus of considerable biomechanical research. However, relatively little is known about how differences in technique beyond the 'set' position can influence the consequent performance levels. A series of empirical and theoretical investigations were therefore undertaken to advance the understanding in this area.

Initial investigations revealed the importance of appropriately quantifying performance. Horizontal external power production provided the most appropriate measure and was subsequently used to quantify the success associated with different aspects of technique. Block phase analyses of 13 trained and three international-level sprinters highlighted the importance of increasing hip extension and the rear leg push. It was revealed that over-extending the front ankle could impair performance due to an unfavourable increase in push duration. Empirical investigations of the first stance phase in international-level sprinters revealed the importance of configuration at touchdown - positioning the stance foot further behind the centre of mass and generating a large gravitational trunk-segment moment appeared beneficial for performance. Joint kinetics patterns were identified which assisted performance by augmenting horizontal centre of mass translation during stance.

To further investigate the first stance phase, a seven-segment angle-driven model was developed. Model evaluation revealed kinematic and kinetic outputs to match reality with a mean difference ranging from 5.2% to 11.1%. Individual-specific simulations identified alterations to stance leg angles at touchdown which influenced the centre of mass position and gravitational moment of the trunk, and consequently performance. Increases in the backwards velocity of the toe at touchdown and reductions in ankle dorsiflexion during early stance also improved performance by increasing the rate of horizontal force development. The combined empirical and theoretical understanding therefore highlighted several aspects of technique which could be altered in an attempt to improve sprint start performance.

PUBLICATIONS

Bezodis, N. E., Trewartha, G. and Salo, A. I. T. (2008). Understanding elite sprint start performance through an analysis of joint kinematics. In *Proceedings of XXVI International Symposium on Biomechanics in Sports* (edited by Y-H. Kwon, J. Shim, J. K. Shim and I-S. Shin) pp. 498-501. Seoul, Korea: Seoul National University Press.

Bezodis, N. E., Trewartha, G. and Salo, A. I. T. (2007). Choice of performance measure affects the evaluation of sprint start performance. *Journal of Sports Sciences*, **25**, *S72-S73*.

Conference presentations:

Bezodis, N. E., Trewartha, G. and Salo, A. I. T. (2008). Technique and performance during the elite sprint start. *24th Meeting of the BASES Biomechanics Interest Group*, Cardiff, UK.

Bezodis, N. E., Trewartha, G. and Salo, A. I. T. (2007). A comparison of initial step characteristics in elite sprinters. *23rd Meeting of the BASES Biomechanics Interest Group*, Liverpool, UK.

ACKNOWLEDGEMENTS

I would like to express my thanks to the following people, all of whom have contributed in some form towards the work presented in this thesis:

- Dr Aki Salo and Dr Grant Trewartha, who I have learnt so much from, and for their continued advice, support, opinion and hard work.

- Malcolm Arnold, Rob Ellchuk and their respective groups of sprinters for always being happy for me to turn up with my camera.

- The staff at the training facilities at the University of Bath and the University of Wales Institute, Cardiff for their assistance with data collection.

- James Corp and Harjinder Reehal for their technical assistance.

- All of the postgrads who I shared the last three and a half years with, especially Tom and Dom for always being willing for a coffee/9 holes.

- All my friends, including Cockers, Macca and the whole of 'sp1' for always providing a welcome distraction when I needed it most, and particularly to Big Luke and Nat for all the banter and fajitas.

- Mum and Dad for all of their support in its limitless forms. Thank you.

- Gwenie for helping to keep the last three and a half years so enjoyable, and for always putting a smile on my face.

TABLE OF CONTENTS

LIST OF FIGURES

Chapter 2

Chapter 3

Chapter 4

Chapter 5

Chapter 6

Chapter 7

Appendix C

Appendix D

Appendix F

LIST OF TABLES

Chapter 5

Chapter 6

Appendix B

NOMENCLATURE AND DEFINITIONS

Convention used to define the three principal axes throughout this thesis

x-axis	Medio-lateral horizontal axis
y-axis	Antero-posterior horizontal axis
z-axis	Vertical axis

Where appropriate, variables are referenced to one of these axes through a subscript character following the character representing that variable (e.g. v_y represents velocity (v) in the antero-posterior (y) direction).

Symbols used to represent variables in equations throughout the thesis

t	Time
d	Displacement
v	Velocity
a	Acceleration
F	Force
R	Reaction force
M	Moment
P	Power
E	Energy/Work
m	Mass
I	Moment of inertia
g	Acceleration due to gravity (9.81 $m \cdot s^{-2}$)
θ	Angular displacement
ω	Angular velocity
α	Angular acceleration
H	Angular momentum
O	Origin of the co-ordinate system
k	Stiffness co-efficient
b	Damping co-efficient
a_{z0}	Distance between the force platform surface and the *x*-*y* plane
ax	Force platform centre of pressure co-ordinate in the *x* direction
ay	Force platform centre of pressure co-ordinate in the *y* direction

py	Horizontal moment arm of proximal joint forces acting about a segmental centre of mass
pz	Vertical moment arm of proximal joint forces acting about a segmental centre of mass
dy	Horizontal moment arm of distal joint forces acting about a segmental centre of mass
dz	Vertical moment arm of distal joint forces acting about a segmental centre of mass
ε_j	A Fourier series applied to the angular acceleration time-history at joint *j*
j_n	Co-efficients for the n^{th} term (n = 1:5) of a Fourier series (where *n* = the frequency of the term in Hz) applied to the angular acceleration time-history at joint *j*

Convention used to define the power phases at each stance leg joint quantified in the inverse dynamics analysis

K_F^{1+}	First positive power phase ($^{1+}$) at the knee joint (K) during the swing ($_F$) phase. The same convention is used for the MTP (M), ankle (A), and hip (H) joints, the stance ($_S$) phase, and for the second positive ($^{2+}$) and any negative power phases ($^{1-}$, $^{2-}$).

Abbreviations used for terminology throughout the thesis

2D	Two-dimensional
C7	7^{th} cervical vertebra
CM	Centre of mass
EMG	Electromyography
HAT	Head-arms-trunk (i.e. a combined segment)
LDM	Laser distance measurement
LED	Light-emitting diode
MTP	Metatarsophalangeal
PB	Personal best

Symbols used to abbreviate statistical terminology throughout the thesis

df	Degrees of freedom
ρ	Spearman's rank order correlation co-efficient
p	Probability level
r	Pearson's product moment correlation co-efficient
s	Standard deviation
CV	Co-efficient of variation
ICC	Intraclass correlation co-efficient
RMS	Root mean square

Definitions of key terms used throughout the thesis

Technique	A specific movement strategy used to accomplish a particular task, including both kinematics (e.g. joint angles) and kinetics (e.g. resultant joint moments)
Performance	A measure of the success with which a particular task is accomplished
'Set' position	The position a sprinter adopts at the 'set' command, just prior to the start signal
Movement onset	The instant at which a sprinter moves in response to the start signal
Block exit	The instant at which a sprinter leaves the blocks (i.e. front foot contact is lost)
Block phase	The phase during which the sprinter is in contact with the blocks, commencing from the start signal
Push duration	The amount of time a sprinter spends pushing in the blocks (i.e. from movement onset to block exit)
Block velocity	The horizontal velocity of the whole body centre of mass at block exit
Block impulse	The product of the mean force produced and the push duration in the blocks - it determines block velocity (relative to mass)
Horizontal external power	The power contributing to translation of the centre of mass in a horizontal direction

Touchdown distance	The positioning of the touchdown foot relative to the CM at the onset of ground contact, with a positive value representative of the foot ahead of the CM
Foot touchdown velocity	The forward horizontal velocity of a specified point on the foot at the onset of stance, expressed relative to the ground
Empirical research	Systematic measurement of data through observation or experimentation
Descriptive research	The quantification of variables through direct measurement without intervention
Experimental research	The quantification of data associated with a direct intervention intended to manipulate technique
Theoretical research	Generation of hypothetical data through the replication of a system using a model-based representation
Internal validity	The degree to which an investigation measures what it purports to measure
External validity	The applicability of the results of an investigation to a 'real-world' setting
Simulation	A single iteration of a mathematical model
Step size	The time taken between successive samples during a simulation
Optimisation	A series of simulations used to search for a maximum/minimum, typically through the use of a specific algorithm
Matching optimisation	The process of attempting to match certain model outputs to known empirical values by systematically allowing specified model inputs to vary
Evaluation	The quantification of how well the model system represents reality (i.e. the closeness of model outputs to empirical data)

CHAPTER 1: INTRODUCTION

1.1. Research overview

Sprinting is a pure athletic endeavour, whereby the sole aim is to cover a specific short distance in the least possible time. Its appeal is therefore global - the 100 m at the 2008 Beijing Olympic Games was broadcast in over 200 countries worldwide, and 95 different nations were represented throughout the heats (IAAF, 2008). The 100 m world record holder is typically labelled 'the fastest man on Earth', and in Beijing, Usain Bolt re-affirmed this status by winning the 100 m in a world record time of 9.69 s.

A simple calculation reveals that Bolt achieved a velocity in excess of 10 metres per second when averaged across the entire race. However, as is the case with all of the athletics sprint events, the initial phase is covered at lower velocities due to the athlete starting from a stationary position. It has been demonstrated that striving to rapidly accelerate from stationary towards maximum velocity, thus reducing the amount of time spent running at sub-maximal velocities, is a favourable strategy for improved overall sprint performance (van Ingen Schenau *et al*., 1991, 1994; de Koning *et al*., 1992). The start is therefore a critically important part of a sprint, and any small improvement in sprint start performance could result in greater overall sprint performance. In sprinting, even seemingly small performance improvements can make a large, meaningful difference, as highlighted in the men's 100 m final at the 2004 Athens Olympic Games, where the fourth-placed finisher was only 0.04 s behind the gold-medallist.

Due to its clear importance in sprinting, the start has been the focus of considerable biomechanical research during the last 75 years. However, in the biomechanical literature the 'start' phase itself has not been clearly defined, and whilst some researchers have limited their analyses to the block phase, others have included one or more of the subsequent steps on the track. Whilst there exist several analyses of technique in the blocks (e.g. Atwater, 1982) and during the initial steps of a sprint (e.g. Jacobs and van Ingen Schenau, 1992), few studies have attempted to associate differences in technique with variations in levels of performance. Where studies have included both technique and performance related data (e.g. Mero *et al*., 1983;

Mendoza and Schöllhorn, 1993), the choice of measure with which to quantify performance has often appeared somewhat arbitrary, and has varied widely between studies. The two different performance measures used within the block phase study of Mendoza and Schöllhorn (1993) actually yielded conflicting assessments of the success of an experimental technique intervention. The use of different variables to measure performance may also explain why much of the early experimental sprint start research (e.g. Dickinson, 1934; Kistler, 1934; Henry, 1952) reached contrasting conclusions despite similar interventions, and there is thus a clear need for a common measure of performance to be adopted.

In addition to the conflicting performance measurement issues potentially limiting the current understanding of sprint start technique, there also exists a clear lack of kinematic data from beyond the 'set' position. Whilst many authors have documented 'set' position body configurations (e.g. Atwater, 1982; Mero, 1988), only linear kinematics of the centre of mass (CM) have typically been reported once the sprint has commenced. Although linear CM data provide important information, such data are largely indicative of performance and reveal little about the specific techniques used to achieve these translations. Furthermore, much of the previously presented technique data have been collected from sub-elite sprinters. A lack of information thus exists regarding the techniques used by sprinters capable of achieving international success. Whilst the collection of empirical data from high-level training sessions is possible with a suitably valid and unobtrusive methodological protocol, the experimental manipulation of technique is difficult due to the understandable opposition from international-level athletes and their coaches (Kearney, 1999). During recent years theoretical biomechanical methodology has been applied to several sporting activities to alleviate the need for direct measurement (e.g. Hiley and Yeadon, 2003a; King and Yeadon, 2004; Wilson *et al*., 2006). The use of a forward dynamics model in conjunction with a detailed empirical analysis therefore offers a useful approach through which the understanding of the sprint start in international-level sprinters can be advanced.

1.2. Statement of purpose

The aim of this thesis was to understand the aspects of sprint start technique that contribute to higher levels of performance.

1.3. Research questions

In order to provide a focus for the study and to help achieve the stated aim, a series of specific research questions were developed. A measure of performance was required in order to quantify the effects of differences in technique, and thus determine the most successful techniques. However, closer inspection of sprint start performance data previously presented by Mendoza and Schöllhorn (1993) revealed that the use of different performance measures (i.e. horizontal velocity at block exit or the time taken to reach 10 m) could potentially lead to contrasting conclusions. This fundamental issue has not been satisfactorily resolved, and it is not clear whether the use of different measures from a more specific phase (e.g. the block phase) could also lead to such conflicting results. Therefore, the first research question requiring investigation was:

i. **Does the choice of performance measure influence the identification of different levels of sprint start performance?**

If the choice of measure was found to influence the performance-based ranking of a group of sprinters, then the most objective measure must be determined prior to associating any aspects of technique with levels of performance. Furthermore, if externally-valid performance data are to be collected, consideration must be given to the fact that these data must be obtainable in a field-based environment, particularly if data are to be collected from international-level sprinters where the potential for control of the training schedule is limited (Kearney, 1999). An unobtrusive, yet valid, protocol must therefore be developed which can be used outside of the laboratory at training sessions. This thus led to the formation of the second research question:

ii. **What is the most appropriate measure of sprint start performance, and can it be accurately quantified in a field environment?**

Having identified a quantifiable and valid performance measure, different aspects of technique could therefore be confidently associated with the related levels of performance. In order to understand how the movement strategies adopted during the block phase and first post-block stance phase relate to higher levels of performance, a third research question was developed:

iii. Which kinematic technique variables are associated with higher levels of sprint start performance?

These kinematic aspects of technique would help to identify the movement patterns associated with the higher levels of sprint start performance, in particular those exhibited by international-level sprinters. However, whilst a kinematic analysis is a useful tool for identifying important movements, it yields limited understanding behind the causes of these movements. In order to determine these kinetic causes, inverse dynamics analyses are typically undertaken (Winter, 1990), and have been widely used in sprint research undertaken beyond the start phase (e.g. Mann, 1981; Johnson and Buckley, 2001). The use of a kinetic analysis in conjunction with a kinematic analysis would therefore provide information which would help to explain the kinematic aspects of technique, and thus the fourth research question posed:

iv. How are the more advantageous sprint start kinematics achieved, and why do they lead to improved performance?

In an attempt to further the understanding of a specific activity, biomechanists have increasingly developed computer-based forward dynamics models (e.g. Hiley and Yeadon, 2003a; King and Yeadon, 2004; Wilson *et al*., 2006). Such an approach allows the theoretical manipulation of variables, and can therefore be used to overcome the aforementioned limitations to applying direct experimental interventions with high-level athletes (Kearney, 1999). Forward dynamics modelling also negates some of the common limitations associated with empirical research involving human subjects, such as random variation, fatigue, and strength and co-ordination limits (Robertson *et al*., 2004). A theoretical research approach therefore offers great potential for advancing the understanding of sprint start technique and performance. However, in order to be able to apply a forward dynamics model

developed for such a purpose, its accuracy must be evaluated against empirical data. Consequently a fifth research question was developed:

v. **Can a realistic representation of sprint start technique and performance be achieved with a forward dynamics computer simulation model?**

Once sufficiently evaluated, a realistic simulation model could therefore be subsequently applied to make theoretical predictions about how specific technique changes could improve sprint start performance further. A sixth research question was thus developed, which could be addressed through the use of a fully evaluated forward dynamics model of a sprinter during the start:

vi. **Can selected hypothetical technique adjustments identify further performance improvements?**

These six research questions therefore provided a framework around which the thesis could progress. Specific biomechanical investigations designed to address these questions could thus be developed, allowing the aim of this thesis to be achieved.

1.4. Organisation of chapters

1.4.1. Chapter 2 - Review of literature

A review of the literature relevant to this thesis is provided in Chapter 2. This includes a discussion of research focussing on the sprint start, from both performance and technique perspectives. Literature concerned with methodological approaches and techniques used to conduct biomechanical investigations are also discussed. These include empirical data collection and reduction techniques - particularly concerning their appropriateness for application in the field with international-level sprinters, and theoretical simulation modelling methodology.

1.4.2. Chapter 3 - Developing an understanding of sprint start technique and performance

Three investigations designed to yield an increased understanding of fundamental sprint start technique and performance issues form the basis of Chapter 3. These include an investigation into the measurement of performance, an evaluation of the

accuracy with which performance data could be collected outside of a laboratory setting, and an initial group-based analysis intended to identify general aspects of technique which may be associated with higher levels of block phase performance. These studies also informed the empirical methodology adopted in subsequent chapters.

1.4.3. Chapter 4 - Lower limb angular kinematics during the block and first stance phases

This chapter includes a kinematic analysis of the techniques of three international sprinters. In addition to a block phase analysis, data from the first-post block stance phase were also collected in this investigation. The techniques were analysed on a single-subject basis alongside each sprinter's respective levels of performance in an attempt to identify kinematic aspects of sprint start technique associated with higher levels of performance.

1.4.4. Chapter 5 - Kinetic aspects of sprint start technique and their associations with kinematics and performance

Chapter 5 contains a kinematic and kinetic analysis of the techniques of three international sprinters during the first post-block stance phase. An inverse dynamics analysis was conducted to determine joint kinetics, and these kinetics are discussed in relation to the associated kinematics exhibited by each of the three sprinters, and their levels of performance.

1.4.5. Chapter 6 - Development and evaluation of a simulation model of a sprinter during the first post-block stance phase

This chapter provides a description of the development of a simulation model of a sprinter during the first post-block stance phase and an evaluation of its accuracy. The inputs required to characterise the model are detailed, including their origin and form, and the methods used to implement the model are explained. The model is objectively evaluated by comparing the model outputs to empirical data from the first post-block stance phase (collected in Chapter 5) and through a sensitivity analysis. The results of the evaluation are discussed, and the appropriateness of the model for application to investigate technique and performance during the first post-block stance phase is scrutinised.

1.4.6. Chapter 7 - Investigating the effects of technique adjustments on performance through simulation

A series of investigations are carried out using the forward dynamics model developed and evaluated in the previous chapter. The results of these investigations are used to enhance the understanding of how changes to sprint start technique could affect performance, furthering the understanding gained from the empirical research undertaken in Chapters 3-5.

1.4.7. Chapter 8 - Discussion

The major findings and insight gained from this research are discussed and summarised in Chapter 8. The research questions posed in Chapter 1 are addressed using the results obtained throughout each of the investigations undertaken in this thesis. The increased understanding of the sprint start that has been gained is presented. The appropriateness of the methodological approaches adopted is reviewed, and potential directions and applications for future research are proposed.

CHAPTER 2: REVIEW OF LITERATURE

2.1. Introduction

There has been considerable previous interest in the sprint start, which has provided knowledge surrounding many of its important aspects. This chapter will therefore aim to discuss and critique the relevant existing sprint start literature. However, the exact part of a sprint to which the "start" refers has rarely been identified. Studies which have explicitly stated an intention to investigate the sprint start have typically focussed on the block phase, although some have included analyses of one or several of the initial steps on the track. For the purposes of this current research, the block phase and each of the initial steps will be discussed as separate components of a sprint start. In addition to research focussing on the sprint start, this chapter will also discuss research relating to aspects of biomechanical methodology relevant to the investigations undertaken in this thesis.

2.2. Sprint Start Performance

2.2.1. The difficulty in quantifying sprint start performance

Success in any sprint event is evaluated based on the ability to cover a specific distance in the least possible time. However, when analysing only one particular part of a sprint, such as the very beginning, the exact definition of successful performance is less clear. For example, it is difficult to objectively determine whether reaching a specific distance (e.g. 5 m) earlier, or reaching this distance slightly later but with a greater instantaneous velocity, represents superior performance. This may partly explain why several different performance measures have been used in previous sprint start research. The use of different measures of performance is one potential reason why some experimental block phase studies have reported seemingly conflicting results, sometimes even within one study when two separate measures of performance have been employed (e.g. Henry, 1952; Mendoza and Schöllhorn, 1993).

Mendoza and Schöllhorn (1993) collected data from a group of seven sprinters with 100 m personal best (PB) times ranging from 10.4 to 10.8 s. Each sprinter performed a series of sprints from two different 'set' positions. In one condition the sprinters adopted their preferred position (pre-intervention), whilst in the other their position

was adjusted by the experimenter, with alterations made to the block spacing, front knee angle and proportion of body weight through the hands (post-intervention). The effects of these interventions upon performance were found to vary between subjects (Figure 2.1a), with three sprinters exhibiting an increase in block velocity (the horizontal velocity of the whole body CM at the instant of block exit) when using the post-intervention 'set' position (sprinters 2, 4 and 7), three showing a decrease (sprinters 3, 5 and 6) and one experiencing no change (sprinter 1). Whilst the logical conclusion would therefore have been that the interventions were beneficial for the starting performance of three sprinters, but detrimental for three others, further performance data suggested otherwise.

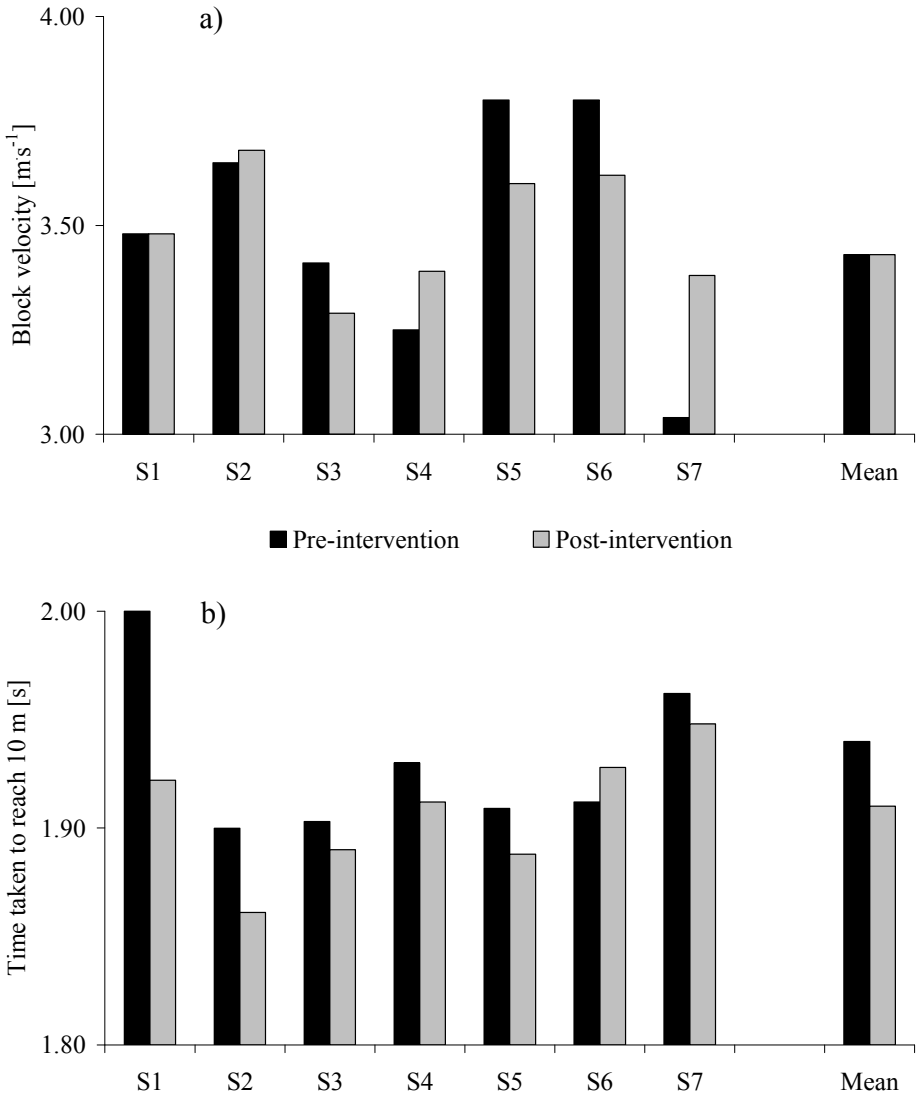

Figure 2.1. The effect of a specific block phase intervention upon a) block velocity and b) time taken to reach 10 m (from Mendoza and Schöllhorn, 1993).

The time it took each sprinter to reach the 10 m mark was also recorded by Mendoza and Schöllhorn (1993), and all but one of the sprinters (sprinter 6) reduced the time taken to reach 10 m from the post-intervention starting position (Figure 2.2b). These data thus conflicted with the block velocity data, suggesting that the determination of the effectiveness of an intervention, and quantification of performance during the start of a sprint, could depend largely upon the measure of performance adopted. Although it was not their aim, the data presented by Mendoza and Schöllhorn (1993) therefore highlighted a potentially far more important issue - the choice of variable used to quantify performance could possibly affect the conclusions reached in sprint start research. The discrepancies between the results obtained with these two variables identify limitations associated with the comparison of studies which have used widely different measures (e.g. one measured at block exit, and one at the 10 m mark) to assess sprint start performance.

A prime example of the effects of using different performance measures is apparent when comparing three of the early investigations into the effects of inter-block spacing upon sprint start performance (Dickinson, 1934; Kistler, 1934; Henry, 1952). Both Kistler (1934) and Henry (1952) determined that performance was improved with greater inter-block spacing, whereas Dickinson (1934) advocated the use of a more bunched start to improve performance. Although the methods and/or subjects may have had some effect on the results, a likely influence on the conclusions drawn was that Kistler (1934) and Henry (1952) reported performance based on impulse and block velocity, whereas Dickinson (1934) measured the time taken to reach 2.5 yards. Elongated starts have commonly been found to be associated with increased push durations (Harland and Steele, 1997), which may explain the larger block velocities observed by Kistler (1934) and Henry (1952). In contrast, the earlier block exits that typically occur when using bunched starts could have contributed to the shorter times elapsing to 2.5 yards observed by Dickinson (1934), in spite of potentially lower block velocities. Despite instigating relatively similar experimental interventions, Kistler (1934) and Henry (1952) thus reached opposing conclusions to those drawn by Dickinson (1934), possibly due to the choice of performance measure.

2.2.2. Variables used to measure performance in previous sprint start research

The variable most commonly used to measure sprint start performance has been block velocity (e.g. Henry, 1952; Gagnon, 1978; Vagenas and Hoshizaki, 1986; Mero, 1988; Mero and Komi, 1990; Guissard *et al*., 1992; Schot and Knutzen, 1992; Mendoza and Schöllhorn, 1993; Faverial *et al*., 2000; Parry *et al*., 2003; Mero *et al*., 2006). However, the use of block velocity as the sole measure of performance is potentially flawed. Velocity is directly determined by horizontal impulse production, and because impulse is equal to the product of force and time, an increased block velocity could therefore be due to either an increase in the net propulsive force generated, or to an increased push duration. Spending a longer time in the blocks conflicts with the 'least possible time' nature of a sprint (Mendoza and Schöllhorn, 1993), and therefore if an increased block velocity were associated solely with an increase in push duration, it would not be beneficial for overall sprint performance.

In an attempt to obtain a more complete understanding of performance, several studies have assessed performance using a discrete temporal measure in addition to block velocity. This has commonly been a measure of the time taken to reach a specific distance (e.g. Henry, 1952; Mero *et al*., 1983; Vagenas and Hoshizaki, 1986; Schot and Knutzen, 1992; Mendoza and Schöllhorn, 1993; Faverial *et al*., 2000; Parry *et al*., 2003; Mero *et al*., 2006), although great disparity has existed in the distances used, ranging from 2.5 to 50 yards. Other studies have adopted such measures of performance as velocity at a specific distance (e.g. Schot and Knutzen, 1992; Cousins and Dyson, 2004; Salo and Bezodis, 2004), or velocity at a distinct point such as first-step toe-off (e.g. Mero, 1988; Mero and Komi, 1990; Schot and Knutzen, 1992). Part of this discrepancy in the performance measures adopted could relate back to the fact that none of these studies have actually defined what they are referring to as the 'start' of a sprint, and thus quantifying the level of performance during a 'start' has been a somewhat arbitrary procedure. Whilst it has been suggested that the duration over which the 'start' has an influence on the entire sprint could range from one step to 50 yards (Schot and Knutzen, 1992), in the strictest terms it could be said to influence the entire race. It is therefore paramount that the variable chosen to measure performance provides an objective quantification of the performance of a sprinter during the specific phase of interest. For example, if analysing the block phase, an objective measure of performance between movement

onset and block exit is required, since a measure taken any further down the track will include the effects of subsequent steps and the techniques adopted beyond block exit.

The need to analyse additional information to block velocity or temporal measures when assessing sprint start performance was highlighted by van Coppenolle *et al*. (1989). The authors advocated the incorporation of both block time and block velocity into a single measure of block acceleration, as has been reported in several studies (e.g. Payne and Blader, 1971; Baumann, 1976; Gagnon, 1978; van Coppenolle *et al*., 1989; Guissard *et al*., 1992). Whilst Baumann (1976) reported the peak accelerations of the whole body CM during block phase, the use of this as a performance measure is limited since it typically occurs early in the block phase and is not representative of overall performance. Average block acceleration has been calculated by dividing the overall change in velocity during the block phase by the length of time over which this change has taken place (e.g. Payne and Blader, 1971; Baumann, 1976; Gagnon, 1978; van Coppenolle *et al*., 1989; Guissard *et al*., 1992). This is potentially a more useful measure of performance than block velocity due to the additional incorporation of time. Data from well-trained sprinters were presented by van Coppenolle *et al*. (1989) to show that whilst one athlete may exhibit a higher block velocity, another could have a higher acceleration due to a shorter push phase duration.

For the calculation of average block accelerations, van Coppenolle *et al*. (1989) advocated the removal of reaction time so that the time value used to calculate acceleration corresponded only to the time during which the sprinter was generating force against the blocks. Reaction times can vary greatly both between and within sprinters (Mero and Komi, 1990; Collet, 1999; Pain and Hibbs, 2007), and although the reaction to the gun is an important part of a sprint, it is independent from what actually happens once a sprinter has reacted (van Coppenolle *et al*., 1989). Whilst training to improve reaction times is no doubt important, particularly in the shorter sprint events, pre-movement time is an extraneous variable in situations where the aim is to understand technique and improve performance during the block phase and beyond.

Some researchers have taken the calculation of accelerations further and reported the power generated by a sprinter during the block phase (e.g. Cavagna *et al*., 1965; Mero *et al*., 1983; Mendoza and Schöllhorn, 1993). Cavagna *et al*. (1965) observed a peak power of 1500 W in a single sprinter (100 m PB = 10.3 s), Mero *et al*. (1983) reported a group mean power of 949 W (mean 100 m PB = 10.8 ± 0.3 s), whilst Mendoza and Schöllhorn (1993) found average block power in a group of sprinters to reach around 1500 W (100 m PBs ranging from 10.4 to 10.8 s). Despite relatively similar cohort ability levels, there were large differences in the mean power values reported by Mero *et al*. (1983) and Mendoza and Schöllhorn (1993), and the mean power value of Mendoza and Schöllhorn (1993) was similar to the peak power value reported by Cavagna *et al*. (1965). This suggests that different methods may have been employed in the calculation of power, which can be explained by the fact that power is a complex concept and several methods exist for the calculation of power during human movement (Winter, 1990). These differences primarily exist because different aspects of human power production are quantified with each method of measurement. It is therefore important to consider which aspect of power is fundamental when analysing performance during the start of a sprint.

Of these three studies which measured block power, Mero *et al*. (1983) did not state how block power was calculated, Cavagna *et al*. (1965) calculated it from low resolution film images, and Mendoza and Schöllhorn (1993) used a force platform. Unfortunately the manual synchronisation procedures used by Cavagna *et al*. (1965) (i.e. the camera operator gave a verbal start signal after initiating camera data collection) and their failure to report push durations limit the comparisons that can be drawn with these power data. Mendoza and Schöllhorn (1993) calculated mean block power from force platform data based on horizontal force and its time-integrals. It has already been established that the aim of a sprint is to translate the body over a specific horizontal distance in the shortest possible time. Therefore, the ability of a sprinter to produce power externally (i.e. against the track) is of interest. This power required to move the CM relative to the environment is termed external power (Cavagna *et al*., 1963; Winter, 1978; Stefani, 2006), and thus the external power calculated from horizontal forces, as measured in the blocks by Mendoza and Schöllhorn (1993) through a force platform, would potentially be of most interest as a measure of sprint performance. This is not the same as total power, since it ignores

the internal power associated with the relative motion of body segments (Winter, 1978), which are scarcely reflected in the motion of the CM during gait due to the reciprocal nature of limb movements. However, because reducing metabolic cost is not the main goal in sprinting (Caldwell and Forrester, 1992), neither the total power nor the efficiency of movement are considered to be of major importance when using power to quantify sprint performance.

2.2.3. Summary of sprint start performance measurement

A wide range of variables have previously been used in the quantification of sprint start performance. Whilst it appears that the use of markedly different performance measures (e.g. block velocity and time taken to reach 10 m) could influence the perceived performance success, it is not clear whether such a conflict exists when using less diverse variables such as those determined solely from the block phase (e.g. block velocity, average block acceleration, average block power). Furthermore, if the choice of performance measure does influence the identification of trials/sprinters associated with higher levels of performance, it is imperative that a single optimal performance measure is determined so that an objective quantification of performance can be achieved.

2.3. Sprint Start Technique

Sprint start technique has been the subject of a relatively large volume of research from a variety of different perspectives. Several studies have utilised a descriptive approach, documenting the techniques of both international and less-well-trained sprinters (e.g. Atwater, 1982; Mero *et al*., 1983). Other researchers have conducted experimental studies, administering specific interventions to technique and attempting to determine the subsequent effects upon performance (e.g. Henry, 1952; Schot and Knutzen, 1992). Both of the above modes of empirical research have been conducted over a variety of phases, ranging from solely the block phase up to and including several of the initial steps on the track.

2.3.1. The block phase of a sprint

Since starting blocks were introduced to the sprint events in 1928-29, there has been a large amount of sprint start research focussing on the block phase. Various kinematic, kinetic and muscle activity data have all been reported in an attempt to

describe the techniques used by sprinters covering a wide range of ability levels. Numerous experimental intervention studies have also been undertaken, the majority of which have adjusted the 'set' positioning of a sprinter through alterations to the set-up of the blocks in an attempt to improve performance.

Descriptive kinematic research

The majority of the kinematic block phase analyses document the joint angles adopted by sprinters when in the 'set' position (e.g. Borzov, 1978; Atwater, 1982; Mero *et al*., 1983; Mero, 1988; Mero and Komi, 1990; Čoh *et al*., 1998). These data have been collected from sprinters across a range of abilities, and have thus led to the identification of the positions exhibited by faster sprinters (Mero *et al*., 1983), as well as the proposition of optimum positioning (Borzov, 1978).

It was suggested by Borzov (1978) that leading sprinters tend to exhibit similar flexion angles in the lower limbs to each other, and thus use different block spacing (i.e. inter-block distance and distance between the front block and the start line) due to differing anthropometrics. Borzov (1978) quoted optimal average values as a front hip angle of 55°, a rear hip angle of 89°, the trunk orientated 14° below the horizontal, a front knee angle of 100°, and a rear knee angle of 129°, suggesting that when coaching beginners, these angles should be set and the blocks literally placed under the sprinter. However, Atwater (1982) collected data from a group of eight American national level sprinters and found trunk angles to range from 9° to 34° below the horizontal, and front knee angles to range between 79° and 112°. This implied that there was a large degree of variation present in 'set' position kinematics, even within a group of international sprinters. These suggestions have subsequently been reinforced by the relatively large standard deviations commonly observed when 'set' position kinematics have been reported from groups of sprinters (e.g. Mero *et al*., 1983; Mero, 1988; Mero and Komi, 1990; Čoh *et al*., 1998).

Mero *et al*. (1983) analysed the starts of 25 sprinters (100 m PBs ranged from 10.2 to 11.8 s), and retrospectively divided them into three sub-groups based on their CM velocity at the 2.5 m mark. The fastest group (n = 8) were found to adopt smaller angles at both hip joints in the 'set' position. Further tests revealed that these sprinters also had a greater percentage of fast twitch fibres (sampled from the vastus

lateralis), and typically scored more highly on standard strength and power tests such as the squat and counter-movement jumps. This led Mero *et al*. (1983) to suggest that the between-sprinter differences in 'set' position joint angles may be due to strength differences, with stronger sprinters able to adopt more acute joint angles and extend the joint over a greater range.

A large amount of kinematic sprint start data were collected from Slovenian national sprinters (males, n = 13, mean 100 m PB = 10.73 s; females, n = 11, mean 100 m PB = 11.97 s) by Čoh *et al*. (1998). Numerous correlation co-efficients between 'set' position kinematics and performance, quantified as the time taken to reach 5, 10, 20 and 30 m (as measured by photocells), were calculated. Results were somewhat inconclusive, with only a handful of moderately strong and statistically-significant relationships found. Whilst the results did suggest that an increased distance between the front block and the start line may be associated with a longer time taken to reach the majority of the measured distances, there were no strong correlations between any of the 'set' position joint angles and any of the performance measures. This again highlights that there is potentially no single optimal position to be adopted in the blocks, and that a large range of 'set' positions exist, independent of the levels of performance achieved.

A potentially more prudent use of the data available to Čoh *et al*. (1998) would have been to examine how these joint angles changed as the block phase progressed and large forces were generated. In a review of the biomechanics of the sprint start, Harland and Steele (1997) identified 17 research papers which reported data relating to block positioning and angular kinematics in the 'set' position. In contrast, only three papers were discussed which related to kinematic aspects of technique during the subsequent block phase. Two of these were qualitative coaching articles (Hoster and May, 1978; Korchemny, 1992), and one was an experimental investigation altering which leg was placed in the front block (Vagenas and Hoshizaki, 1986). To the author's knowledge, despite the existence of a large body of information regarding 'set' position joint kinematics and the linear kinematics of the CM during block exit, there still exist no studies which have quantitatively determined how the joint angles change during block exit. There is clearly a greater need for an analysis of technique during the block phase in addition to the abundance of data collected at

the very start of this phase. This would increase the understanding of how sprinters achieve the linear impulses and block velocities that are so readily reported.

Descriptive kinetic research

Kinetics are the underlying cause of any movement (Winter, 1990) and several studies have therefore included kinetic analyses in an attempt to further the understanding of the sprint start. One of the early kinetic studies was undertaken by Baumann (1976), who divided 30 male sprinters into three groups based on 100 m PB times (Group 1: n = 12, mean 100 m PB = 10.35 ± 0.12 s; Group 2: n = 8, mean 100 m PB = 11.11 ± 0.16 s; Group 3: n = 10, mean 100 m PB = 11.85 ± 0.24 s), and presented a detailed analysis of the recorded force time-histories. The fastest group generated greater total horizontal impulse during the push against the blocks (263 ± 22 Ns) than the other two groups (223 ± 20 Ns and 214 ± 20 Ns, respectively). As impulse production (relative to mass) determines the change in an object's velocity, and mean masses between groups were similar, the faster group of sprinters thus also achieved higher block velocities (3.6 $m \cdot s^{-1}$, compared to 3.1 $m \cdot s^{-1}$ and 2.9 $m \cdot s^{-1}$). The larger impulses of the fastest group were achieved despite spending the same mean amount of time pushing against the blocks as the intermediate group (369 ms), and less time than the slowest group (391 ms). The increased block velocities of the faster sprinters were therefore due to an increased average horizontal force production and not to an increase in the duration of the push against the blocks. Mero *et al*. (1983) also observed a faster group of sprinters to generate larger horizontal block impulses than their less-fast counterparts. Much like the results of Baumann (1976), there were no between-group differences in the duration of force production, thus differences were again due to the mean force generated. This led Mero *et al*. (1983) to suggest that the level of horizontal force produced is more important than the time taken to produce it. It therefore appears that the ability to generate a large amount of force, without spending overly long doing so, is an important aspect of the block phase.

Some studies have separated the forces generated into those applied against each of the separate blocks, using either two force platforms or strain gauges mounted in each foot plate of the blocks. In a group of seven male sprinters (100 m PB range from 10.8 to 11.2 s), Guissard and Duchateau (1990) found larger peak forces were

generated at the rear block. However, the rear leg only contributed 24% of the total impulse because the front leg was in contact with the blocks for over twice as long. This concurred with the data of Čoh *et al*. (2007), where the rear foot was found to contribute only 34% of the total impulse, and thus reinforced the previous suggestions of Payne and Blader (1971) that the front leg is a greater contributor to total impulse. The importance of the relative contribution of the two legs was highlighted by an experimental investigation in which the dynamic strength of each leg in 15 trained sprinters was assessed, before a series of sprint start trials were subsequently undertaken (Vagenas and Hoshizaki, 1986). It was found that when the stronger leg was placed in the front block, the group mean block velocity increased to 3.37 $m \cdot s^{-1}$ from a value of 3.12 $m \cdot s^{-1}$ when the weaker leg was in the front block ($p < 0.005$). Vagenas and Hoshizaki (1986) attributed these differences to the greater contribution from the front leg to total impulse production.

Although the front leg has a greater contribution to total impulse, it has been suggested that more skilled sprinters actually generate greater peak rear block forces, sometimes also applying less force on the front block than their less-skilled counterparts (van Coppenolle *et al*., 1989; Harland and Steele, 1997; Fortier *et al*., 2005). From two World Championships finalists, peak rear block forces of 1487 and 1333 N, and peak front block forces of 774 and 1062 N, contributing to total impulses of 301 and 308 Ns were recorded by van Coppenolle *et al*. (1989). These impulse values were associated with block exit velocities of 3.80 and 3.94 $m \cdot s^{-1}$, respectively. In contrast, these researchers also recorded data from a national level sprinter who exited the blocks with a velocity of 3.34 $m \cdot s^{-1}$. Whilst he was able to achieve a similar peak front block force (981 N) to the world class sprinters, his peak force against the rear block was considerably lower (442 N). This led van Coppenolle *et al*. (1989) to highlight the importance of force generation with the rear foot during the sprint start, although it must be considered that these kinetic differences may have been due to specific anthropometric or technique factors rather than ability level *per se*.

The conclusions of van Coppenolle *et al*. (1989) were reinforced by the results of Fortier *et al*. (2005), who compared a group of six trained sprinters (mean 100 m PB = 10.46 ± 0.11 s) with a group of six less well-trained sprinters (mean 100 m PB =

11.07 ± 0.30 s). Although the well-trained group were found to take slightly longer to reach peak rear block force generation (124 vs. 119 ms, $p < 0.05$) the mean peak forces were considerably greater than those generated by the less well trained group (1430 vs. 940 N, $p < 0.05$). The well-trained group also spent less *total* time pushing in the blocks (399 vs. 422 ms, $p < 0.05$). This led Fortier *et al*. (2005) to suggest an important role for rear leg block force generation, even if it led to a longer rear block contact, as it may not negatively affect total block time. These data must be treated with slight caution, as actual performance data (e.g. block velocity) were not reported, thus the results related to a division of groups based on past PB performances, rather than current levels of performance.

One further kinetic issue which has previously been highlighted is the angle of force application during block exit. Hafez *et al*. (1985) identified that although resultant velocity may be higher in one trial, the horizontal component of this velocity was sometimes less than in other analysed trials with lower resultant velocities. Furthermore, whilst horizontal block velocities were found to be greater in those sprinters with quicker PB times, these horizontal block velocities did not appear to be related to the total resultant block force. This supported previous suggestions (Payne and Blader, 1971; Baumann, 1976) that a good start is characterised by the generation of high horizontal impulses, rather than simply high impulses. This aspect of technique has been associated with the angle between the horizontal and a line joining the CM to the front toe at block exit, which has been found to range between 32° and 42° in well-trained sprinters (Mero *et al*., 1983; Mero, 1988). It has been suggested that provided this angle does not negatively affect the subsequent steps, it should be as low as possible at block exit in order to facilitate horizontal impulse generation (Payne and Blader, 1971).

Descriptive muscle activity research

Several studies have utilised electromyography (EMG) to record muscle activity during the sprint start. The gluteus maximus of the rear leg has been observed to be the first muscle active during the block phase (Mero and Komi, 1990; Čoh *et al*., 2007). Whilst Guissard and Duchateau (1990) observed the biceps femoris to be first muscle recruited in both legs, they did not collect data from the gluteus maximus. Rear leg biceps femoris activation was found to be followed shortly after by

quadriceps (rectus femoris, vastus lateralis and vastus medialis) and then calf muscle (soleus and gastrocnemius) activation (Guissard and Duchateau, 1990; Figure 2.2). The rear leg quadriceps have been found to be typically only active during the early part of the rear block push phase, deactivating prior to the rear foot leaving the block to keep this foot clear of the track during the subsequent rear leg swing phase (Guissard and Duchateau, 1990; Čoh *et al*., 2007). During the remainder of rear block contact, only the biceps femoris and calf muscles were found to remain active (Guissard and Duchateau, 1990).

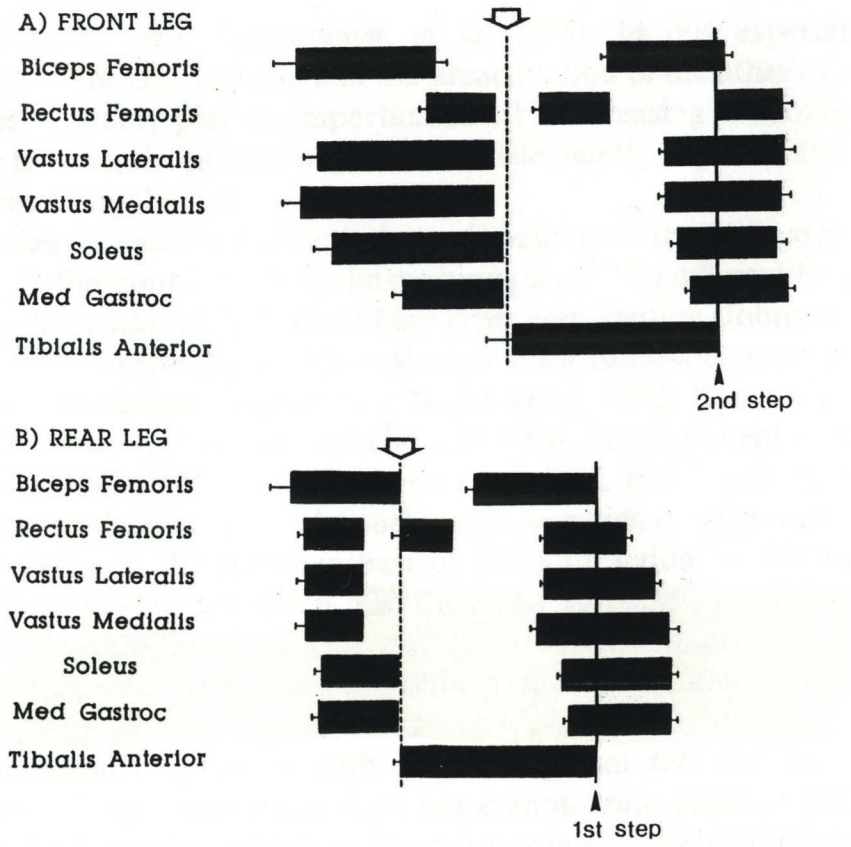

Figure 2.2. Durations of electromyographical activity for selected front (A) and rear (B) leg muscles during the block phase and first two steps of seven trained sprinters (mean ± *s*; from Guissard and Duchateau, 1990). For each leg, the arrows indicate the instant at which the foot left the block, with the second vertical line indicating the subsequent ground contact with that leg.

In the front leg, the vastii muscles have been typically found to be active throughout virtually the entire push phase in the blocks, activating soon after the initial gluteus maximus and biceps femoris activation, and remaining active almost until the instant

of block exit (Guissard and Duchateau, 1990 - Figure 2.2; Čoh *et al*., 2007). In contrast to the vastii muscles of the quadriceps, the rectus femoris muscle only became active during the late part of the block phase (Guissard and Duchateau, 1990), potentially due to its biarticular nature being a limiter of early hip extension. The front leg soleus has been observed to activate considerably earlier than the gastrocnemius muscle (Guissard and Duchateau, 1990), which was suggested to be due to knee flexion in the 'set' position. This would have shortened the biarticular gastrocnemius, whereas the uniarticular soleus muscle remained in a prestretched position (Guissard and Duchateau, 1990). In both legs, dorsiflexion was observed at the ankle during the early part of the push phase, and thus any activity in the calf muscles was initially eccentric in nature (Mero and Komi, 1990).

Experimental alterations to block spacing

Much of the early sprint start research focused on the effects of altering the positioning of the blocks in an attempt to experimentally manipulate 'set' position kinematics. It is widely accepted that increasing the distance between the two blocks induces an increase in total block force and in push duration, and thus greater total block impulses and hence block velocities (Dickinson, 1934; Kistler, 1934; Henry, 1952; Schot and Knutzen, 1992). Whilst the front foot forces have been found to be independent of interblock spacing (Kistler, 1934), more elongated starts led to greater forces being exerted by the rear foot. However, whether these increases actually represent an improvement in performance is less clear. As stated previously, the choice of performance measure with which to assess the effects of such an intervention can influence its perceived success. The apparent contradiction between the results of Kistler (1934), Dickinson (1934) and Henry (1952) has been attributed to a relative time loss incurred when generating a forceful push against the blocks (Stock, 1962). This had led to the widespread acceptance that an intermediate inter-block spacing provides the best platform for block phase performance, allowing sprinters to generate relatively large forces without spending detrimental amounts of time doing so (Sigerseth and Grinaker, 1962; Stock, 1962; Hoster and May, 1978; Harland and Steele, 1997).

It was originally suggested that positioning the CM as close to the start line as possible was important in sprinting as it moved the sprinter closer to the finish line

and thus reduced the total distance to be covered during a race (Dickinson, 1934). This was not only achieved by reducing the inter-block distance, but also by reducing the distance between the front block and the start line. When adjusting this distance, Menely and Rosemier (1968) found a small but non-statistically-significant decrease in the time taken to reach 10 yards as the distance between the front block and the start line was reduced. Reis and Fazenda (2004) measured the distance between the front block and the start line as chosen by 15 male sprinters (of unstated ability level). The authors found a moderately strong, significant relationship between this distance and the time taken to reach 20 m and 60 m, suggesting that those sprinters who reached these distances earlier adopted a front foot position closer to the start line. However, the causality of this cannot be determined, and it may relate back to the suggestions of Mero *et al*. (1983) regarding 'set' position kinematics, with the faster sprinters able to adopt such positions in the blocks due to their greater strength. The highly variable block settings used by eight international-level sprinters (interblock spacing ranged from 0.15 m to 0.38 m, and distance between front block and the start line ranged from 0.32 m to 0.58 m; Atwater, 1982) support the notion that there appears to be no single optimum block positioning suitable for all.

Another aspect of block positioning that has been experimentally altered is the medio-lateral inter-block spacing (Parry *et al*., 2003). The lateral distance between the toes was adjusted between 0.24 and 0.52 m, and 22 university-level sprinters completed a series of sprints to 30 m. Split times at each 5 m were measured by photocells. It was found that a wider foot placement led to advantages in terms of the time taken to reach 5 and 10 m, although by 15 m these differences were negated, and even appeared to reverse at 20 m. These inconclusive results suggest that the medio-lateral placement of the feet has little effect on performance, in terms of the time taken to reach specific distances. The random error typically associated with the use of photocells (Yeadon *et al*., 1999) may also have affected the small differences observed between conditions, and influenced the apparently contradictory results at different 5 m intervals. There has been little further research in this area, potentially because the medio-lateral foot spacing in sprint races is relatively fixed due to the design of the starting blocks.

Experimental alterations to block obliquity

One further feature of the block settings which can be manipulated by the sprinter is the angle of the block faces. Several authors have therefore conducted studies where these block obliquities have been experimentally altered, and the consequent effects on performance determined (e.g. Guissard *et al*., 1992; Cousins and Dyson, 2004; Mero *et al*., 2006). Guissard *et al*. (1992) found that as front block obliquity decreased from 70° to 30° (relative to the track), mean block velocity increased from 2.37 $m \cdot s^{-1}$ to 2.94 $m \cdot s^{-1}$ without affecting the total duration of the push phase (these low block velocities were likely due to the relatively low ability level of the 17 sprinters studied - 100 m PBs ranged from 10.4 to 11.9 s). The authors suggested that this was due to an increase in the initial length of the calf muscles, and a reduction in the coupling time between the initial stretch and subsequent shortening of these muscles.

Cousins and Dyson (2004) altered the obliquities of both blocks independently, and recorded the forces produced against each block by five sprinters of unstated ability level. It was found that the greatest horizontal forces were achieved using the smallest angles at each block (30° on the front block, 50° on the rear), although it was not stated whether there was any effect on push duration. Mero *et al*. (2006) also altered the angle of both block faces (either both at 40° or both at 65°), and calculated joint kinetics and muscle-tendon lengths throughout the block phase. The results again revealed that smaller block angles induced greater block velocities. Mero *et al*. (2006) determined that these increased block velocities were largely due to elongated initial muscle-tendon lengths of the gastrocnemius and soleus, which contributed to greater peak ankle moments and powers and thus higher block velocities, confirming the previous theories of Guissard *et al*. (1992).

2.3.2. The initial steps of a sprint

As highlighted in section 2.2, the choice of either block velocity or the time taken to reach 10 m as a performance measure can affect the conclusions reached in sprint start research (Mendoza and Schöllhorn, 1993). This implies that alterations can be made by a sprinter during the early steps of a sprint in order to decrease the time taken to cover a specific distance despite a lower block velocity. The initial post-block steps during a sprint start thus possess the potential to have a considerable

effect upon performance. Sprinters continue to rapidly accelerate after leaving the blocks as they strive to achieve their maximum velocity. This acceleration is an important part of a sprint, because if a sprinter is able to reach their maximum velocity earlier, the time spent running at submaximal velocities will be reduced, thus reducing the time taken to cover a specific sprint distance (van Ingen Schenau *et al*., 1991). Although the analysis has not been as thorough as that focusing on the block phase, numerous biomechanical investigations have been undertaken regarding the technique of sprinters during the initial steps after block exit.

Descriptive kinematic research

Descriptive kinematic variables from the initial steps of eight international standard sprinters have previously been documented (Atwater, 1982; Table 2.1). Mean values for the first flight time (0.049 s), contact time (0.193 s) and step length (1.02 m) have also been reported by Mero (1988) for a group of trained sprinters (mean 100 m PB = 10.79 ± 0.21 s), with the contact time and step length in particularly close agreement with those observed by Atwater (1982). Salo *et al*. (2005) reported respective contact times of 0.200, 0.173, 0.159 and 0.135 s for the first four steps of a sprinter (100 m PB = 10.80 s), and durations of 0.045, 0.058, and 0.074 s for the second, third and fourth flight phases, respectively. Both the flight times and contact times are similar to those presented by Atwater (1982), showing a consistent trend for stance duration to decrease and flight duration to increase (after the initial post block-exit flight phase) as a sprint progresses from the blocks. The trends for increasing step length and flight time, and decreasing contact time, have been shown to continue for at least the first ten steps of a sprint (Čoh and Tomažin, 2006).

Table 2.1. Selected mean kinematic descriptors of the initial four steps of a maximal sprint in a group (n = 8) of American national level sprinters (from Atwater, 1982).

	Flight 1*	Flight 2	Flight 3	Flight 4
Flight Time [s]	0.063	0.043	0.060	0.069
Step Length [m]	1.00	1.11	1.31	1.46
	Stance 1	Stance 2	Stance 3	Stance 4
Contact Time [s]	0.196	0.179	0.164	0.152

* Flight 1 = from front block clearance to first contact on track.

Touchdown distance (the positioning of the touchdown foot relative to the CM at the onset of ground contact, with a positive value representative of the CM posterior to the foot) has also been documented during the first three steps after block clearance (Mero *et al*., 1983). It was found that the CM moved progressively backwards relative to the point of ground contact as the sprint progressed. After being 0.13 m ahead of the point of stance foot contact at first touchdown, the CM was 0.04 m ahead by second touchdown and was 0.05 m behind the point of ground contact by the instant of third touchdown (Mero *et al*., 1983). The CM has been found to remain behind the stance foot at touchdown during all subsequent ground contacts in a sprint (Mann *et al*., 1984; Hunter *et al*., 2005), with touchdown distances of up to 0.40 m reported at the 50 m mark (Alexander, 1989). It has been shown that touchdown distance is related to the braking impulse magnitude observed during the early part of stance in the acceleration phase (Hunter *et al*., 2005).

In a detailed analysis of the second post-block stance phase, Jacobs and van Ingen Schenau (1992) extended the understanding of CM positioning relative to the stance foot. The authors determined that sprinters adopt a strategy whereby the CM is first rotated about the stance foot, before an extension of the stance leg joints occurred which increased the distance between the CM and the foot. This was attributed to the maximisation of horizontal motion, since during the early part of the stance phase an extension of the stance leg would only serve to translate the CM vertically. Therefore, the CM first appeared to be rotated in front of the stance foot so that the subsequent extension would have a grater influence upon horizontal motion. However, the techniques behind this overall rotation and extension of the CM about the foot were not described by Jacobs and van Ingen Schenau (1992). The contributions of each of the stance leg joints and segments used to achieve this favourable increase in horizontal motion therefore remained unclear.

Descriptive kinetic research

Stance phases during any form of gait are commonly divided into braking and propulsive phases based upon the orientation of the antero-posterior force vector, with a period of both braking (negative) and propulsive (positive) impulse contributing to the net propulsive impulse. The initial ground contacts of a sprint are no different (e.g. Mero *et al*., 1983; Mero, 1988; Salo *et al*., 2005). Mero (1988)

observed the braking phase to last for 12.9% of total stance duration during the first post-block step. Although Salo *et al*. (2005) found the absolute duration of the braking phase not to differ by more than 2 ms during each of the first four post-block contacts (12 - 14 ms), the braking phase duration was found to increase when expressed as a percentage of total stance duration over these first four steps (from 6.3 to 9.9%), due to the gradual decrease in total stance time. It is likely that this percentage continues to increase until maximum velocity is reached, where the braking phase has been reported to endure for 44% of stance (Mero and Komi, 1986). The mean peak braking force magnitude was also found to increase over the first four steps (215, 348, 421 and 672 N, respectively) by Salo *et al*. (2005). Because absolute braking phase duration did not change, the magnitude of the braking impulse thus also increased. These increased braking impulses, due to a concurrent increase in braking force magnitude, contributed to a decrease in the net propulsive impulse over each of the first four steps (Salo *et al*., 2005).

Net propulsive impulse determines the change in velocity during stance, and the large values generated during the initial steps of a maximal sprint rapidly accelerate the sprinter from their block velocity towards their maximum attainable velocity. Net propulsive impulse values between 87 and 91 Ns have been reported during the first stance phase of a sprint (Mero, 1988; Salo *et al*., 2005), with magnitudes of 63, 61 and 54 Ns found to be present during each of the subsequent three stance phases, respectively (Salo *et al*., 2005). Net horizontal impulses (and consequently acceleration) are thus greatest during the first step on the track, and decrease as a sprint progresses. Values of 20 Ns have been reported at 14 m (Johnson and Buckley, 2001), 18 Ns at 16 m (Hunter *et al*., 2005), and 0 Ns by 40 m (Mero and Komi, 1994), the latter indicating that there is no net change in velocity during contact.

When studying a group of 25 sprinters, Mero *et al*. (1983) observed that those who took longer to reach a distance of 2.5 m exhibited a greater relative loss in velocity during early stance than their faster counterparts in both the first (11.3% vs. 3.5%) and second (8.8% vs. 3.7%) post-block ground contacts. The fact that the faster sprinters exhibited less deceleration is indicative of a decreased braking impulse during the first two post-block contacts, and it thus appears that minimising braking impulse may reduce the time taken to reach 2.5 m – an apparent improvement in

performance. If a smaller braking impulse can be achieved without affecting a decrease in the subsequent propulsive impulse, then net propulsive impulse and thus the change in forward horizontal velocity will also increase. In order to achieve a reduction in braking impulse magnitude, a sprinter must either decrease the magnitude of the braking force, or the duration of the application of this braking force.

The magnitude of a braking force has been suggested by Mann and Sprague (1980, 1983) and Putnam and Kozey (1989) to be a function of both touchdown distance and foot touchdown velocity (the antero-posterior horizontal velocity of the foot at the onset of stance, relative to the ground). Braking forces have been found to exist from the first post-block stance onwards (Mero *et al*., 1983; Mero, 1988; Salo *et al*., 2005) despite the CM being positioned anterior to the point of ground contact (Mero *et al*., 1983), suggesting that a positive touchdown distance (i.e. CM posterior to the stance foot) is not the sole cause of a braking force. When analysing the second stance phase of seven well trained sprinters (mean 100 m PB = 10.6 ± 0.2 s), Jacobs and van Ingen Schenau (1992) observed a marked contraction of the gluteus maximus and hamstrings muscles just prior to ground contact, which caused a reduction in foot touchdown velocity. In accordance with previous suggestions of Putnam and Kozey (1989), Jacobs and van Ingen Schenau (1992) proposed that this action was utilised to assist a decrease in the magnitude of the braking force, although due to the descriptive nature of the study this could not be confirmed. Whilst no studies currently exist which associate changes to braking force magnitude with concurrent changes in kinematic parameters during the initial steps of a sprint, the kinematics during trials with either high or low braking forces (relative to the mean value recorded in the study) have been analysed later in the acceleration phase at the 16 m mark (Hunter *et al*., 2005). The trials with lower braking forces during early stance were found to be associated with a decreased foot touchdown velocity ($p < 0.001$), supporting the theories of Putnam and Kozey (1989) and Jacobs and van Ingen Schenau (1992).

In addition to a reduction in foot touchdown velocity, Hunter *et al*. (2005) also found that the trials with lower braking forces were associated with a smaller touchdown distance (i.e. CM less far behind stance foot, $p < 0.01$). It was proposed that a

decrease in foot touchdown velocity partly reduced the braking force. Whilst Hunter *et al*. (2005) attributed the reduction in touchdown distance to being a required response for the maintenance of balance, it may actually be a consequence of the lower foot touchdown velocity reducing the distance that the foot is placed in front of the CM at touchdown. A reduction in touchdown distance may, however, also have a more direct influence on the impulse characteristics during stance. The magnitude of the previously described rotations required to position the CM suitably far ahead of the stance foot (Jacobs and van Ingen Schenau, 1992) would therefore not be as great in order for extension to have a beneficial effect. The application of the results of Hunter *et al*. (2005) to the current area of research must be considered with caution, however, as not only were data collected at the 16 m mark rather than during the initial few post-block steps, the cohort studied were not actually sprinters – they participated in sports involving sprint running. It must also be acknowledged that the components of a ground reaction force vector are part of one single entity, and are not separate measures, thus, a decrease in braking impulse could also affect the vertical impulse (Hunter *et al*., 2005).

Despite the existence of several studies containing kinematic and external kinetic data during the initial steps of a sprint, few have combined these in order to compute joint kinetics. Ito *et al*. (1992) collected joint power data from the first 19 steps of a sprint from force and video data by moving the start line relative to the force platform over a series of trials, and reported general trends in the results in abstract form. The authors found that during the first half of each swing phase, the hip flexors typically generated positive power, whilst the knee extensors exhibited negative power, and the magnitudes of both increased from steps one to five, before reaching a plateau. During the first half of the stance phase, the hip extensors were observed to produce and maintain a high level of positive power, whilst the ankle and knee extensors exhibited progressively greater negative power from steps one to thirteen. During the latter half of the contact phase, the ankle plantarflexors were found to produce a high level of positive power.

In a previously discussed study (Jacobs and van Ingen Schenau, 1992), the authors also analysed mean joint kinetics during the second stance phase after block exit in seven well-trained male sprinters. During a stance phase with a mean duration of

175 ms, the resultant hip joint moment was extensor dominant until the last 55 ms, when it became flexor dominant. Due to the continual extension of the hip throughout stance, the hip joint power followed a similar pattern to the moment time-history. The resultant knee joint moment was briefly flexor dominant at touchdown, before becoming and remaining extensor dominant throughout the remainder of stance, reaching a mean peak value of 140 Nm, 88 ms prior to toe-off. The resultant ankle joint moment was plantarflexor throughout stance, reaching a mean peak value of 245 Nm, 78 ms before the end of the stance phase. Due to the initial period of dorsiflexion during the first 60 ms of stance, the ankle initially acted as an energy absorber (negative power), before generating large amounts of positive power (mean peak = 2192 W) during the latter part of stance, although the total work performed at each joint during stance was not reported. Jacobs and van Ingen Schenau (1992) attributed the temporal sequencing of the peak powers from hip to knee to ankle to a proximal-to-distal power transfer, which had previously been suggested to be achieved via the actions of the biarticular biceps femoris and gastrocnemius muscles (Grégoire *et al.,* 1984). The results presented by Jacobs and van Ingen Schenau (1992) provided some welcome initial insight into how sprinter's techniques were achieved. However, the inclusion of a full kinematic analysis and external forces alongside an analysis of the internal joint kinetics would allow the effects of these internal and external forces upon the individual joint and segment rotations to be determined, thus potentially extending the understanding of how techniques are achieved during the initial steps of a sprint.

Descriptive muscle activity research

After each leg had exited its block, Guissard and Duchateau (1990) observed the rectus femoris and tibialis anterior muscles to be activated during the respective early swing phase (Figure 2.2), in order to assist flexion at the hip and ankle joints. By mid-swing, rectus femoris activity had ceased (Guissard and Duchateau, 1990), and was replaced by biceps femoris activity, which has been attributed to an attempt to reduce foot touchdown velocity (Jacobs and van Ingen Schenau, 1992). This action has also been shown to be assisted by activation of the gluteus maximus muscles in studies where it has been included in the analysis (e.g. Mero and Komi, 1990; Jacobs and van Ingen Schenau, 1992; Čoh *et al*., 2007). Just prior to ground contact,

Guissard and Duchateau (1990) identified activation of several extensor muscles, namely soleus, gastrocnemius, rectus femoris and the vastii group.

At touchdown in the first stance phase, biceps femoris and tibialis anterior activity were found to cease, whilst the extensor muscles all remained highly active (Guissard and Duchateau, 1990; Figure 2.2). A similar trend was observed during the second stance phase in the contralateral leg (Guissard and Duchateau, 1990; Jacobs and van Ingen Schenau, 1992). During this second stance phase, the mean muscle activity time-histories presented by Jacobs and van Ingen Schenau (1992) showed a consistent level of activation in the gluteus maximus throughout stance, whereas semitendinosus activity decreased markedly around mid-stance. At around the same time, activity levels of the quadriceps and plantarflexor muscles increased rapidly, reaching peak levels just before, or at, toe-off. This muscle activity pattern was consistent with the previously discussed proximal-to-distal joint kinetics pattern found to exist during the second stance phase of a sprint (Jacobs and van Ingen Schenau, 1992), highlighting a specific strategy used in an attempt to accelerate during the early part of a sprint.

2.3.3. Summary of sprint start technique research

There exists a large volume of knowledge regarding the sprint start. However, there are still numerous important aspects of sprint start technique which remain under-investigated and lacking in research. Very little is known about the kinematic changes which occur during the block and first stance phases, with the current understanding of angular kinematic aspects of technique limited to the ‘set’ position. Whilst the linear kinematic and kinetic aspects of technique are well described, it is not well understood how the individual joints and segments contribute to these. The combination of a detailed kinematic analysis with a full internal joint kinetics analysis would assist the understanding of how these kinetics influence the kinematics. The association between these angular data and the horizontal motion of a sprinter could also then be identified, furthering the understanding of both how and why specific aspects of technique could influence performance.

2.4. Biomechanical modelling and potential applications to the sprint start

Theoretical models are often developed in biomechanical research to further the current level of understanding in situations where the collection of large volumes of data is difficult, or where intervention is either not possible or could negatively affect the desired outcome. Theoretical models of sprinting have been previously developed (e.g. Borzov, 1978; Mann, 1985), involving the proposition of an 'ideal' technique, based on a coalition of descriptive kinematic results. Mann (1985) presented values representative of 'poor', 'average' and 'good' technique for parameters such as joint and linear kinematics at touchdown, step length and frequency, and horizontal velocity. These were based on data collected from international-level American sprinters during competition, and were intended to provide a framework model of high-level performers. Whilst analysing and documenting the kinetic and kinematic aspects of the techniques adopted by international sprinters, and the consequent creation of a statistical-based model can yield useful data to which less-well-trained sprinters and their coaches can refer and train towards, alternative modes of modelling potentially offer further benefits.

Theoretical simulation models can be developed in addition to empirical data collection and analysis in order to achieve greater understanding of a biomechanical system (Yeadon and Challis, 1994). Such an approach is based around the formulation of a mathematical model, representative of a specific system of interest, in an attempt to make predictions about the behaviour of this system. These forward dynamics models permit numerous alterations to be made, which is often not possible with empirical research involving human subjects. A forward dynamics modelling approach negates problems associated with the 'law of the single variable' - individual aspects of technique can be manipulated without any subsequent effects on other aspects as would commonly occur in experimental settings. Computer-based simulation models also alleviate other potentially confounding effects associated with human research such as random variation, the effects of fatigue, limits to strength and coordination, and the requirement for treatment within an ethical manner (Robertson *et al*., 2004). Additionally, a forward dynamics modelling approach used in high-level sport can overcome the fact that athletes are seldom willing for any experimental manipulation of their training routine to take place (Kearney, 1999), particularly during the competitive season when their performance

is ideally at its highest level. Such models have therefore been previously used in dynamic sporting applications. However, aside from some initial work regarding the development of a theoretical model of a sprinter during the block phase, which was recently presented in abstract form (Jessop and Pain, 2007), forward dynamics simulation modelling has not been widely used to study sprint biomechanics.

2.4.1. Modelling human movement

Forward dynamics simulation models are typically mathematical formulations of Newtonian systems (Yeadon and Challis, 1994). During activities such as sprinting, the human body can therefore be considered as a mechanical system comprising a series of connected rigid masses with fixed inertial properties. The mechanical properties of a human have been represented by such a linked segment system in numerous biomechanical studies (e.g. Hatze, 1981a; Bobbert *et al*., 1987; Alexander, 1990; Liu and Nigg, 2000), with adjacent segments connected at frictionless joints where the exertion of equal and opposite reaction forces is assumed. Linked segment models of the entire human body have varied greatly in their complexity, with previous examples ranging from as few as two (Alexander, 1990) to 17 segments (Hatze, 1981a) and beyond. The required complexity of a model is often dependent upon the research question of interest. Whilst simple representations can neglect important aspects of the human body, they have been useful in obtaining fundamental understanding of movements, such as in jumping (Alexander, 1990). In contrast, more complex representations require numerous input parameters in order to function correctly and can therefore over-complicate the situation.

An important aspect of any human body model is its interaction with the surrounding environment. In sprinting, the contact between the foot and the ground must be modelled appropriately, with realistic representations of the ground reaction forces achieved. Some simple models of ground contact during gait have directly connected the distal end of the leg with the ground (e.g. Alexander, 1990), ignoring the foot segment altogether. Others have included a foot segment, but limited its motion by attaching it to the ground (e.g. Onyshko and Winter, 1980; Chou *et al*., 1995). However, these approaches do not reflect the realistic situation, where the body is not anchored to the ground during stance, and surface compliance is present.

The foot-ground interface has been modelled with a viscoelastic representation in up to three dimensions using spring-damper systems (e.g. Gilchrist and Winter, 1996; Marhefka and Orin, 1996, 1999; Bruneau and Ouezdou, 1999; King and Yeadon, 2002, 2004; Gittoes, 2004; Wilson *et al*., 2006). Whilst Coulomb friction models (Badoux, 1964) have previously been adopted when modelling the antero-posterior ground reaction forces (e.g. Gerritsen *et al*., 1995; Gilchrist and Winter, 1997; Wojtyra, 2003), their use renders the simulation of ground contact unnecessarily complex, as friction can be incorporated into the horizontal spring-damper systems. One problem with the commonly used viscoelastic representations of ground contact is that the forces are discontinuous upon impact, as they are immediately affected by the initial velocity in the spring due to the damping term (Marhefka and Orin, 1996). In reality, contact forces should start from zero and increase over time. Marhefka and Orin (1996) therefore proposed the use of a ground contact model in which damping is dependent on the change in spring length. The damping thus increases as the spring compresses, mimicking reality where an increased area of the sprinter's spiked shoe and the track would come into contact. Subject-specific stiffness and damping co-efficients for use with non-linear ground contact models have been previously determined using matching optimisations (matching simulated data with known empirically-recorded data, e.g. Gittoes, 2004; Wilson *et al*., 2006; Yeadon *et al*., 2006), and these ground contact models have been successfully incorporated into dynamic human motion simulations.

2.4.2. Dynamic packages for multi-body model formation

As human body models become more sophisticated, the task of developing the equations that describe their motion increases in complexity – a total of 2,300 hours were reportedly required in the development of Hatze's (1981a) 17 segment model of long jumping. Because human body models are mathematical formulations of Newtonian systems, software packages exist which assist with the development of the equations of motion for a system which has been explicitly defined by the user. One such programme is AUTOLEV, which uses Kane's method for formulating the equations of motion (Kane *et al*., 1983), and can generate computer source code in FORTRAN, C or Matlab™ formats, allowing subsequent manipulation of the code by the user. AUTOLEV has previously been used to successfully create complex computer simulation models of sporting movements (e.g. Brewin *et al*., 2000; King

and Yeadon, 2002, 2004; Yeadon and King, 2002; Yeadon and Brewin, 2003). Other software packages exist for specific modelling purposes, such as facilitating the relatively convenient development of muscle-based models (e.g. SIMM). One recently developed software package is Simulink®, within which SimMechanics® can be used to create a model as a series of bodies connected by joints using a block-based system. The properties of all blocks within the system can be specified, and the associated equations of motion can therefore be determined from this user-defined block structure and its properties. Simulink® and SimMechanics® have been increasingly used to develop computer based models of biological systems in recent years (e.g. Jessop and Pain, 2007; Son *et al*., 2008).

The models developed within these software packages provide the framework of a human body representation. However, in order to simulate the motion of a human, they require activation. The choice of input data to drive a forward dynamics model is somewhat dependent on the construction of the model, in particular which elements are represented in its structure, and also on the purpose of the model. Human body models have previously been driven by either muscle activity, net torques acting about the joints, or angular accelerations of the joints themselves.

2.4.3. Muscle-driven models

Muscle-driven models are relatively complex in nature, consisting of representations of individual muscles (e.g. Thelen *et al*., 2003). The more detailed muscle-driven models use the muscle model of Hill (1938), and thus contain contractile and elastic elements (e.g. Zajac *et al*., 1984; Pandy *et al*., 1990; van Soest *et al*., 1993; Seyfarth *et al*., 2000). This approach can therefore incorporate the bi-articular nature of muscles, and allow the establishment of a causal relationship between muscle activation profiles and the calculated movement pattern (Jonkers *et al*., 2002). However, due to the complexity of muscle-driven models, it is difficult to obtain the required muscle-specific parameters. Therefore few muscle-driven models have been evaluated by comparing simulated with actual recorded performances, and output data have typically only been compared with group ensemble data (e.g. Pandy *et al*., 1990; van Soest *et al*., 1993)

2.4.4. Torque-driven models

A slightly more simplistic representation of the effect of muscular contractions is to include torque generators at each joint, such as in the models developed by Riley and Kerrigan (1998), King and Yeadon (2002, 2004) and Yeadon *et al*. (2006). These generators represent the net torque acting about a joint due to all biological structures crossing that particular joint. Torque generators typically vary between zero and maximum activation, and are used to open and close the joints. Values relating to initial activation, onset time and ramp time commonly act as inputs for torque generators, as used by King and Yeadon (2002). These simulations allow the torque about a single joint to be quantified directly, although they cannot completely represent the action of biarticular muscles. The torque parameters can be estimated from empirical data collected using an isokinetic dynamometer, with individual joint torques measured over a range of angular displacements and velocities, as demonstrated by King and Yeadon (2002) and Yeadon *et al*. (2006). Surface plots can be fitted to these empirical data in order to create the inputs necessary for a torque-driven model. The activation profiles and peak magnitudes of these joint torques can then be varied in an attempt to determine the effect upon performance (e.g. Riley and Kerrigan, 1998; King and Yeadon, 2004). However, there are limitations associated with the use of isokinetic testing to obtain joint torque data, due to the common requirement for the torque-angular velocity relationship and the angle range of isovelocity torque data to be extended. A further potential limitation to the success of a torque-driven model is the fact that the simulation control schemes are often somewhat basic, typically using a 'bang-bang' control theory with a single 'on-off' repetition during the entire movement. Whilst the inclusion of additional 'on-off' repetitions may improve the model, they can cause a large increase in the number of input parameters, such as in the model developed by Roos (2007).

2.4.5. Angle-driven models

In contrast to a torque-driven modelling approach, the technique used in a movement can be recreated by driving the joint angular acceleration profiles within a forward dynamics model, and simulating the resulting motion of the whole body (e.g. van Gheluwe, 1981; Brewin *et al*., 2000; Yeadon and Hiley, 2000; Yeadon and Brewin, 2003; Hiley and Yeadon, 2003a, 2003b, 2007; Gittoes, 2004; Wilson *et al*., 2006;

Yeadon *et al*., 2006). This allows the technique used by the human model-representation to be directly manipulated, a useful approach when attempting to determine how alterations to technique affect the performance outcome. A major advantage associated with the use of angle-driven models is that the output can be directly evaluated against kinematic data from actual performances (e.g. van Gheluwe, 1981; Brewin *et al*., 2000; Yeadon and Hiley, 2000; Wilson *et al*., 2006), with a satisfactory evaluation giving confidence in the theoretical data generated. However, care must be taken to ensure that the alterations to joint torques associated with changes in the angular acceleration time-histories do not lie beyond the physiological limits for specific joint angles or angular velocities.

2.4.6. Model evaluation

The applicability of model results to an applied human setting is dependent upon the structure of the model, and in particular how accurately it represents reality. Model output data must therefore be evaluated against directly comparable empirical data in order to increase confidence in the output (Yeadon and Challis, 1994). Without any evaluation, the model results and associated conclusions could have minimal relevance to the intended system of interest (Yeadon and King, 2002).

The extent of the evaluation of human body models in previous literature has varied widely, from no evaluation at all, through to the detailed comparisons with a range of empirical data, such as those undertaken by Cole *et al*. (1996), Yeadon and King (2002) and King *et al*. (2006). Model evaluations have commonly involved the development of an objective cost function. This function typically comprises the difference between specific model outputs and the associated data from empirical analyses. When evaluating their torque-driven model of jumping for height, King *et al*. (2006) included such variables as joint angles and trunk orientation, linear and angular momenta at take-off, and the overall root mean square (RMS) difference between actual and simulated ground reaction forces. It is important that the evaluation undertaken, and the cost function developed, is appropriate for the intended purpose of the model (Yeadon and King, 2002). Whilst a comparison of simulated and actual kinetic variables may be important for an injury investigation, the accuracy of simulated kinematic variables is of greater importance when attempting to gain further insight into technique. The variables used when evaluating

a model against criterion data must therefore be considered based on the specific aims of the model itself.

2.4.7. Model application

Although few authors have utilised forward dynamics models when conducting sprint-based research, the potential for their application clearly exists. If a suitably accurate model representation of a sprinter can be developed and evaluated, it can be used to modify aspects of sprint technique that have previously been difficult to investigate, and subsequently simulate the effects on performance. In accordance with the aforementioned 'law of the single variable', it is possible to systematically alter individual input parameters and determine the resulting effects on performance. Numerous output data from the model can also be viewed in an attempt to obtain further understanding regarding why the observed changes in performance were achieved. There also exists the possibility to search for specific optimal outputs, by performing numerous iterations with varying input conditions. The specific inputs (variables relating to technique, strength, or timing, depending on the type of model employed) which led to this optimal performance can then be identified, as performed by King and Yeadon (2004) and Hiley and Yeadon (2007) in analyses of tumbling and asymmetric bar gymnastics, respectively.

2.4.8. Summary of modelling approaches to biomechanical investigations

Theoretical computer simulation models provide a useful addition to empirical research. They allow results to be generated which may otherwise be unobtainable in a comparable timescale, if at all. In order to ensure the validity of these modelled data, the output data from a forward dynamics model must be evaluated against comparable criterion data. After such an evaluation, confidence can be placed in the results generated using the theoretical model. The model can therefore be used to investigate specific biomechanical research questions, for example those concerned with identifying the techniques associated with higher levels of performance.

2.5. Data collection and processing in sprint biomechanics investigations

It is important that any data collected in a biomechanical investigation are accurate, and that they are useful and relevant for addressing the specific research questions. When attempting to collect data during high-level sport, the biomechanist often

possesses less control over the environment due to restrictions to access and protocol. The appropriateness of the study design and apparatus used to collect these data must therefore be considered, both in terms of their external and internal validity. Once collected, raw data in biomechanical research studies are seldom instantly useful. In order to yield meaningful, accurate data which can be used for descriptive purposes or in a theoretical model, these data must be processed. Aspects of raw data processing which are particularly important for dynamic human movements such as sprinting include the appropriate smoothing of noise and the application of inertia data.

2.5.1. Validity

The validity associated with the collection of data relates to whether the test or apparatus measures what it purports to measure (Thomas and Nelson, 1999). This firstly comprises the external validity of the data collection environment itself - whether the results can be confidently extrapolated to an applied sprint setting. Secondly, the internal validity of the measurement is important - whether the results are sufficiently accurate, and there is no major measurement error or bias.

External validity

One limitation of empirical research previously highlighted was that athletes, particularly full-time professionals, are often unwilling to change their training schedule for the sake of research (Kearney, 1999). Therefore if data from high-ability sprinters are required in order to address a specific research question, the external validity of such data is a critical issue. If it is not possible to collect data from a competition setting, due to such issues as access and interference restrictions, then training sessions during the competitive season offer a viable alternative. However, in order to maintain the external validity of the data collected at these sessions, there should be minimal intrusion from the researcher.

Internal validity

When striving to maintain external validity by collecting data during competition or high-performance training sessions, the internal validity of a research study can often be negatively affected (Atkinson and Nevill, 2001). It is therefore vital that any experimental set-up is performed with sufficient precision to minimise the level of

measurement error inherent to the collected data. However, even with such precautions, measurement error can seldom be entirely alleviated. It is important to assess the magnitude of these measurement errors by determining the concurrent validity associated with the set-up (Hopkins, 2000).

Concurrent validity relates to the agreement between a measured value and its true criterion (Thomas and Nelson, 1999) and has often been assessed using statistics such as paired t-tests or correlation co-efficients. A paired t-test approach is limited for this purpose because it simply compares the mean values of the two methods. Whilst the mean values can be equal, the random error between measurements can be large, leading to a decreased likelihood of detecting significant error (Atkinson and Nevill, 1998; Altman and Bland, 1983). Correlation co-efficients provide a measure of the linear association between measurements obtained from the two methods. Whilst it is desirable that the correlation between two methods is high (i.e. values increase and decrease together), this is only relative, as it provides a measure of association rather than agreement (Altman and Bland, 1983). Correlation co-efficients can therefore not determine any systematic bias, and their magnitude is also affected by the heterogeneity of the sample. If the inter-trial variation is high compared to the level of measurement error, the correlation co-efficient will be high, whereas if the inter-trial variation is low, then the co-efficient will be lower (Altman and Bland, 1983).

The limits of agreement approach (Altman and Bland, 1983; Bland and Altman, 1999) for assessing concurrent validity is insensitive to sample heterogeneity, and can be used to separate systematic bias from random error. It also provides a practically meaningful way of assessing the accuracy of measurement through the determination of limits between which true values can be expected to lie 95% of the time (Atkinson and Nevill, 1997). The difference scores between new and criterion measures for each data sample (i.e. new value minus true value) can be plotted against the mean value of the new and criterion measures (Altman and Bland, 1983; Bland and Altman, 1995; 1999). This provides a means through which the systematic and random errors can be viewed with greater ease than in a simple scatter-plot of one method against the other (Altman and Bland, 1983; Atkinson *et al*., 2005), whilst plotting the difference scores against either the new or criterion score would identify

a relationship between difference and magnitude when in reality one does not exist (Bland and Altman, 1995) . Bland-Altman plots can be used to ascertain the presence of heteroscedasticity by assessing the errors relative to the magnitude of the measured value, and if present this can be accounted for by log transformation and calculation of ratio, rather than absolute, limits of agreement (Bland and Altman, 1986). The actual limits of agreement are calculated from the standard deviation of all the difference scores between the new and criterion values (Bland and Altman, 1986). For normally-distributed difference score data, which is common due to any inter-subject or inter-trial clustering being removed when assessing difference scores as estimates of measurement error, one standard deviation equates to 68% limits of agreement. In order to obtain 95% limits of agreement, these are typically multiplied by 1.96 (Bland and Altman, 1986), or by the appropriate cumulative probability and degrees of freedom (*df*) from the *t*-distribution if the sample size is not sufficiently large (i.e. $n < 120$; Thomas and Nelson, 1999; Hopkins, 2000).

2.5.2. Apparatus used to measure sprint start performance

There are numerous pieces of apparatus available for collecting the data necessary to analyse sprint start performance. Whilst some offer potentially higher levels of accuracy, their use can be limited by the environment in which they must operate. Therefore in order to obtain accurate sprint start data during high level performances, without altering the typical training or competition environment, the choice of appropriate apparatus is an important issue.

Force transducers

Force platforms are regularly used during human movement analyses due to the relative ease of their implementation, and their high resolution and accuracy. Division of the force data by subject mass yields acceleration data, with velocity and position data obtained through integration of this acceleration time-history (Davies and Rennie, 1968). External power can also be calculated as the product of force and velocity (e.g. Davies and Rennie, 1968; Willems *et al*., 1995). Since Payne *et al*. (1968) investigated the use of a force platform for studying the sprint start, several researchers have used force platforms to determine impulse (e.g. Baumann, 1976; Mero, 1988; Čoh *et al*., 2007), block velocity (e.g. Baumann, 1976; Mero, 1988; Mero *et al*., 2006; Čoh *et al*., 2007), block acceleration (e.g. Baumann, 1976;

Guissard *et al*., 1992) and block power (e.g. Mendoza and Schöllhorn, 1993). However, as force platforms are typically no longer than 0.90 m, it is unlikely that forces through both the hands and the feet can be recorded on one platform, and ignoring the hands will potentially yield slightly false estimates of total force and the associated variables. As sprinters also seldom train on force-instrumented running tracks, some researchers have used force transducers implanted in the starting blocks themselves (e.g. van Coppenolle *et al*, 1989; Guissard and Duchateau, 1990; Lemaire and Robertson, 1990; Fortier *et al*., 2005), although due to calibration and orientation issues, these have not been widely used.

Video analysis

Automatic video analysis systems offer a relatively time-efficient means with which to collect displacement data. However, current requirements for marker attachment to the sprinter could affect technique and performance, and combined with the fact that sprint training often takes place in an outdoor setting, they cannot be used unobtrusively to collect externally valid high-performance data. Manual video analyses provide a useful alternative which require no intrusion on the researcher's part, yet offer the opportunity for data to be collected in an externally valid situation. Despite being more time-consuming due to the requirement for operator-led digitising, manual video analyses are a commonly adopted approach for obtaining biomechanical data during the sprint start. Displacement data are recovered, and velocities can be determined through differentiation (Winter, 1990), with block velocities typically estimated by extracting the value at the instant of block exit (e.g. Mero and Komi, 1990; Schot and Knutzen, 1992; Čoh and Tomažin, 2006).

The determination of acceleration, forces and external power from video analyses is a process typically associated with considerable error due to noise in the original displacement data being amplified as higher derivatives are calculated (Winter, 1990). Rigorous set-up and methodology can assist the reduction of the magnitude of the noise, particularly in displacement and velocity time-histories. However, the acceleration, force and external power time-histories may potentially still contain relatively high levels of noise. If force transducer apparatus are unavailable and these acceleration or kinetic data are required, even as mean values, the manual video

analysis methods used to collect and calculate them must therefore be assessed to ensure that they exhibit an acceptable level of internal validity.

Laser distance measurement

In order to obtain data from distances beyond the block phase, several force platforms or video cameras would be required, or the camera field of view must be widened. Whilst the former are incredibly cost and time-intensive, the latter could lead to an unacceptable resolution of the target image, leading to inaccurate motion analysis results. The collection of displacement data beyond the block phase would allow the assessment of any additional measures of performance required at distances further down the track. Velocities at specific distances or points in the step cycle could be calculated, as could times elapsing to specific distances. These data have occasionally been obtained through the use of a laser distance measurement (LDM) device, which records the displacement of a target object (e.g. a sprinter) relative to the reference system at specified small divisions in time (e.g. Chelly and Denis, 2001; Arsac and Locatelli, 2002; di Prampero *et al*., 2005; Morin *et al*., 2006).

The accuracy of LDM-obtained velocity data has only previously been evaluated through a comparison with split times over 3-10 m ranges using either photocells (Chelly and Denis, 2001; di Prampero *et al*., 2005; Morin *et al*., 2006) or video cameras (Arsac and Locatelli, 2002; Harrison *et al*., 2005) and has not included a comparison at the start of a sprint. Photocells are not suitable for a sufficiently accurate comparison over such short distances, due to the errors in velocity estimates associated with such factors as the beams being broken by different parts of the body (Yeadon *et al*., 1999). Harrison *et al*. (2005) carried out a comparison of LDM device and video methods, concluding that these two methods provided similar average velocities over 3 m sections. However, this conclusion was limited by the fact that the authors compared LDM device data with hip marker motion, rather than the motion of the whole body CM. The displacement data obtained with an LDM device relate to the motion of a point on the surface of a subject (typically in the lumbar region) which is tracked by the operator. Data from the LDM device may therefore closely mimic the motion of hip markers, although they may not necessarily be representative of the path of the CM, which is a product of the motion of all segments. It is therefore important to determine whether the displacement data

obtained through an LDM device are comparable to CM displacement, because as highlighted in section 2.2, it is the ability to horizontally translate the CM which dictates performance in sprinting.

2.5.3. Single-subject analyses

Sprint start studies (section 2.3) have typically adopted a group-based study design, and either analysed the mean data from all subjects (e.g. Mero, 1988; Jacobs and van Ingen Schenau, 1992), or the mean data from sub-groups based on their PB times (e.g. Baumann, 1976; Mero *et al*., 1983). Such group-based analyses can be useful for identifying general trends associated with a specific activity of interest, such as identifying aspects of techniques associated with sprinters capable of achieving higher levels of performance (e.g. Baumann, 1976; Mero *et al*., 1983; Fortier *et al*., 2005). However, group-based analyses can sometimes cause different strategies or techniques to be overlooked, by simply focussing on mean data from the entire cohort.

Closer inspection of the data presented by Mendoza and Schöllhorn (1993) revealed not only performance quantification issues (as discussed in section 2.2), but a further methodological issue related to group-based analyses of the sprint start. If the block velocity data collected by Mendoza and Schöllhorn (1993; Figure 2.1a) were considered solely for the entire group, as indicated by the columns on the far right hand side, it would be concluded that the intervention had no effect upon block velocity, as the average values of block velocity between the pre- and post-intervention conditions across the whole group were identical. However, viewing the data at an individual subject level indicates that the pre-intervention condition was superior for three of the sprinters and that the post-intervention condition was superior for three others, with one sprinter showing no change in block velocity between conditions. Therefore only one of the seven subjects (i.e. sprinter 1) actually followed the mean trend from all of the subjects. This reinforces previous comments suggesting that that displacement, velocity and acceleration time-histories from the start of a sprint are highly individual (Payne and Blader, 1971; Baumann, 1976; Bhowmick and Bhattacharyya, 1988) and should be analysed as such.

Previously advocated ideas relating to the analysis of results on an individual level in biomechanical investigations (e.g. Dufek *et al*., 1995; Bates, 1996; Dixon and Kerwin, 2002) therefore appear to be particularly applicable to sprint start research. Human movement analyses often present results as the average value obtained by a group of subjects, in an attempt to generalise this to a wider population without regard to the performance of any single individual (Stergiou and Scott, 2005). Standard deviations are commonly also presented to show the variation within the group, but this inter-subject variability is representative of variations between individuals performing the same task. Therefore, although it is typically treated as error and is accommodated by increasing the number of subjects or trials, inter-subject variability can often reflect the adoption of different individual strategies to accomplish one common task (Bates *et al*., 2004). This form of variability violates the homogeneity of variance assumption, compromising data validity and it thus should not be analysed on a whole-group basis (Bates *et al*., 2004). Few studies have analysed the sprint start using a multiple single-subject design, and the remaining majority may thus have masked individual differences in technique or strategy by averaging them all into a mean whole group value. Whilst group-based analyses can provide a useful starting point for the analysis of the technique of sprinters during the start, it is important to consider that each individual may adopt a different technique. There may therefore not be a single optimum technique that is applicable to all sprinters, and the data should thus be analysed on an appropriate level.

2.5.4. Data smoothing

The raw displacement data collected during manual video analyses are a combination of both the desired signal of interest and undesired random noise, due largely to operator error in landmark location when digitising (Wood, 1982). Noise is typically of lower amplitude than human movement displacement time-histories, and is often more apparent at higher frequencies due to the low frequencies commonly associated with human movement (Figure 2.3). Whilst displacement data are paramount for accurate analyses of motion during the sprint start, their first and second derivatives are also required for the calculation of variables such as resultant joint moments and powers. As mentioned previously, noise is amplified when derivates are calculated (Winter, 1990), and thus even minimal noise in the displacement data can have a marked effect upon the velocity and acceleration time-histories. Owing to the

typically non-deterministic, low amplitude, high frequency nature of noise, it can be treated to varying extents. Numerous smoothing routines exist which attempt to reduce the noise in a signal whilst leaving the true signal of interest unaffected.

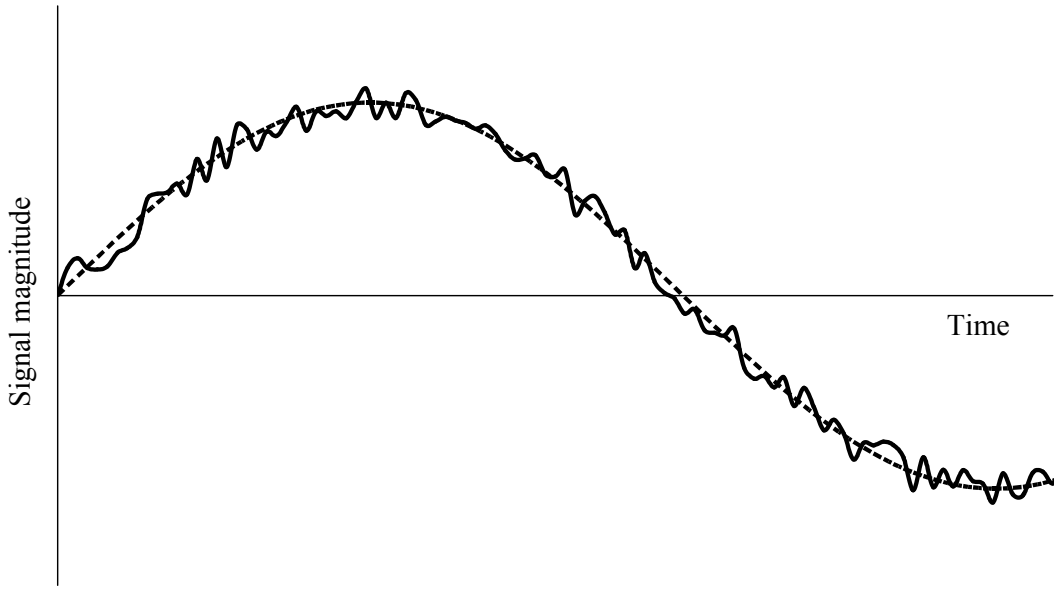

Figure 2.3. A typical example of a recorded signal containing noise (solid line) and the true signal of interest (dotted line).

Polynomial functions

Polynomial approximations can be fitted to displacement data and numerically differentiated in order to obtain the higher derivatives (Zernicke *et al*., 1976). Such representations are effective for relatively simple analyses such as CM motion during flight (McLaughlin *et al*., 1977), although they can over-smooth displacement data in more complex situations (Pezzack *et al*., 1977). Depending on the order of the polynomial fitted, these techniques typically produce smoother functions, at the expense of local detail (Burkholder and Lieber, 1996). Whilst this may be detrimental for analyses during impacts such as a single ground contact phase in a sprint, it has potential applications when local detail is not required, such as for an overall representation of motion during an entire sprint, or phase of a sprint.

Spline functions

Splines are a series of polynomials joined together at knots, and have been found to exhibit greater smoothing accuracy compared to both simple and stepwise

polynomial smoothing techniques (Burkholder and Lieber, 1996). The Generalised Cross-Validated Spline (Woltring, 1985) can be used to automatically determine the tightness of a fit in each region of the data, whereas other splines, such as the quintic spline of Wood and Jennings (1979) permit the operator to define the level of smoothing. Using digitised displacement data of a falling golf ball, Vaughan (1982) found a quintic spline to provide the best estimate of acceleration, whilst the Butterworth digital filter and cubic splines experienced problems at the data end-points. However, the acceleration of a falling golf ball is constant due to the effects of gravity, and these results may not be applicable for sprinting where segmental angular accelerations and linear joint centre accelerations vary throughout, and the choice of smoothing factor could largely influence the results (Soudan and Dierckx, 1979).

Fourier analyses

Fourier techniques represent a signal as a series of weighted sine and cosine terms. They can be used to transform data into the frequency domain, with harmonics above a specific frequency removed prior to an inverse transformation back to the time domain. The determined Fourier co-efficients can also be used to directly compute velocity and acceleration (Hatze, 1981b; Cappozzo and Gazzani, 1983). Fourier analyses ideally require data to be periodic in nature (Wood, 1982), and thus the non-periodic trends associated with displacement data in sprinting, particularly at the start, may limit the application of Fourier analyses for smoothing raw sprint data.

Digital filtering

Low-pass digital filters can be used to remove high-frequency noise through the attenuation of all data above a specified cut-off frequency (Winter, 1990). A low-pass Butterworth digital filter has been shown to accurately estimate acceleration from noisy video-based displacement data when compared to criterion acceleration data using a mechanically-driven segment designed to mimic human motion (Pezzack *et al*., 1977). Data are often passed bi-directionally through these filters in order to sharpen the cut-off and alleviate any phase-lag (Winter, 1990). One important issue when using a digital filter is the selection of a cut-off frequency that results in optimal removal of noise whilst leaving the majority of the true signal unaffected. Whilst a simple visual inspection of the curves is subjective and unlikely

to be repeatable with significant accuracy, several objective and repeatable methods for determining an appropriate cut-off frequency exist. These include the use of regression equations (Yu *et al*., 1999), procedures based on the assumption of noise being white in nature (Challis, 1999), or a residual analysis of the difference between filtered and unfiltered signals over a wide range of cut-off frequencies (Winter, 1990). The frequency content of noise within displacement time-histories has also been shown to differ in each of the principal directions (Giakas and Baltzopoulos, 1997a) and between anatomical sites (Angeloni *et al*., 1994; Giakas and Baltzopoulos, 1997b), and thus separate cut-off frequencies are typically required for each individual landmark in each direction.

Whilst polynomial, spline and Fourier functions can be numerically differentiated in order to obtain the first and second derivatives, digital filtering processes cannot differentiate data (Wood, 1982). This has previously been overcome by the application of finite difference equations, such as the second central difference method (Miller and Nelson, 1973). A further consideration when using filters is the potential to introduce end-point error due to the recursive nature of a filter (Vaughan, 1982). This can be alleviated by collecting additional data outside of the period of interest. Whilst for the sprint start this would not require alterations to the field of view to the rear of the blocks, it would require a lengthening of the field of view to cover an area further down the track. This would result in a smaller target image and hence decreased accuracy when digitising. This can be combated by padding the data at the end, using linear extrapolation or reflection procedures rather than simple duplication of the end-point (Smith, 1989; Vint and Hinrichs, 1996). Where real kinematic data are available either side of the phase of interest, such as prior to movement in the block phase, it has been proposed that the number of additional frames of data required need not exceed ten (Smith, 1989). However, if real data are not available, and extrapolation or reflection procedures are used, it has been suggested that the data should be padded with twenty additional points (Smith, 1989).

If joint kinetics are required to address a specific research question, inverse dynamics analyses are typically undertaken, and have been widely used for such purposes in previous sprinting investigations (e.g. Mann and Sprague, 1980; Mann, 1981; Jacobs

and van Ingen Schenau, 1992; Johnson and Buckley, 2001; Hunter *et al*., 2004; Bezodis *et al*., 2008). Inverse dynamics analyses require both kinematic and kinetic data as inputs, which typically originate from two separate systems (e.g. video camera and force platform). The kinematic data will therefore require smoothing in order to reduce noise and yield acceptable acceleration data for use in the inverse dynamics calculations. However, it has been suggested that the kinetic data should also be smoothed to the same extent, for example using the same cut-off frequency (van den Bogert and de Koning, 1996; Bisseling and Hof, 2006). Failure to do so could create artificial impact peaks in the computed internal joint forces and resultant joint moments. These would potentially occur because higher frequency components of the kinetic data would not be negated by the true high frequency accelerations in the kinematic data which were removed by smoothing, although further research is warranted in this area.

2.5.5. Human body inertia modelling

The collection of joint centre displacement time-histories during the sprint start, and subsequent smoothing procedures to reduce the effects of noise, enables the calculation of several kinematic variables, such as joint angular displacements and their derivatives. However, in order to obtain kinetic results or data relating to CM motion, further processing is necessary. The properties of each segment to be included in the human body model are required. Individual segmental CM locations, masses and moments of inertia enable the calculation of whole body CM displacement and kinetic variables such as resultant joint moments and powers. There are numerous methods which can be employed for the calculation of these individual segmental properties, each of which possess inherent advantages and disadvantages for modelling the body of a sprinter.

Cadaver-based methods

Cadaver-based methods provide segmental inertia properties in ratio form, determined from the dissection of human cadavers (e.g. Dempster, 1955; Clauser *et al*., 1969; Chandler *et al*., 1975). This enables the calculation of individual segmental masses and CM locations for any subject based on a simple knowledge of whole body mass and individual segment lengths. They thus allow the calculation of segmental inertia data in a short space of time, with minimal anthropometric

measurements required. However, a major limitation associated with the use of cadaver-based methods is the age and former health status of the cadaver samples. The cadaver specimens have typically come from elderly males, often smaller in size than the average white male (Dempster, 1955), and it is unlikely that the mass distribution of a trained sprinter would be similar to that of the population sampled in these cadaver-based studies.

Medical imaging methods

Segmental inertia properties have been estimated based on the tissue distribution measured using imaging techniques such as gamma-mass scanning (e.g. Zatsiorsky and Seluyanov, 1983), computerised tomography (Ackland *et al*., 1988), magnetic resonance imagery (Mungiole and Martin, 1990) and dual energy X-ray absorptiometry (Durkin *et al*., 2002). Using images obtained at regular intervals along the body, the tissue dimensions and properties can be used to compute the required segmental masses, moments of inertia and CM locations. However, not only has the potentially harmful radioactive nature of the gamma-mass and computerised tomography scanning techniques restricted their use, the limited availability and high cost further inhibit the use of such methods, particularly with a large group of subjects.

Medical imaging methods have also been used to obtain data from groups of subjects and present it in ratio form (Zatsiorsky and Seluyanov, 1983). Whilst this could again potentially be limited by the characteristics of the studied population, Zatsiorsky and Seluyanov (1983) recruited one hundred young male physical education students (mean age = 23.8 ± 6.2 years), thus providing segmental inertia data that are more appropriate when studying athletic populations. One limitation of the data presented by Zatsiorsky and Seluyanov (1983) is that the ratios relate to segments with somewhat unconventional endpoints, rather than the often used, and more easily identifiable, joint centres. Subsequent adjustments by de Leva (1996) have allowed the application of these data with standard joint centre time-histories. These data would thus be particularly useful when studying a large group of subjects from an athletic background, as the only measurement required is total body mass, and the mean ratio data can be retrospectively applied.

Mathematical methods

Mathematical models involve the representation of the human body as a series of geometric solids (e.g. Whitsett, 1963; Hanavan, 1964; Jensen, 1978; Hatze, 1980; Yeadon, 1990). Subject-specific anthropometric measurements enable the dimensions of each solid to be determined, which can be combined with density data obtained from cadaver-based studies in order to compute the required inertia properties of each segment. The initial use of a single solid to represent each segment by Whitsett (1963) and Hanavan (1964) did not account for the irregular shape of many segments, and the subsequent models of Jensen (1978), Hatze (1980) and Yeadon (1990) therefore divided segments into a combination of several smaller solids. These models thus require a large number of anthropometric measurements to be taken from the subject. The model of Hatze (1980) required 242 anthropometric measurements, and thus the collection and analysis of data are time consuming processes. The model of Yeadon (1990) requires a more practical 95 measurements, which are used to calculate the properties of 40 solids. These solids can subsequently be grouped in order to obtain human body models comprising various numbers of segments depending on the required level of precision. Yeadon (1990) stated that his model requires approximately 30 minutes of the subject's time and can predict body mass to within 3%. When subject-specific inertia properties are required, mathematical models therefore offer a viable alternative. They are useful for obtaining more detailed human body models or in situations where kinetic variables are determined from highly-trained populations whose anthropometrics are likely to be considerably different from more generic athletic populations.

2.5.6. Summary of data collection and processing issues

There are clearly numerous issues which must be addressed when collecting and processing biomechanical data in order to obtain accurate and reliable data which are suitable for addressing the posed research questions. When researching high-level sport, it is important that data are collected during appropriate performances, and the associated threats to the accuracy of such data must be considered, reduced and quantified. Numerous options exist for reducing the noise levels in the collected data, and for the creation of an appropriate representation of the inertia characteristics of a sprinter. The choice of a suitable method for each of these processes must be based

on the research question and variables of interest, as there exists no single method that is universally superior to all others.

2.6. Chapter Summary

This chapter has reviewed relevant literature in order to determine the current state of the body of knowledge surrounding sprint start technique and performance, and to discuss key findings from previous research. Areas requiring further research were identified, including the necessity to identify the most appropriate measure of sprint start performance prior to associating changes in technique with differences in levels of performance. Methods and equipment for obtaining accurate performance data were discussed, and the difficulties associated with obtaining internally valid data in more externally valid field-based settings were identified. When considering aspects of sprint start technique which required further insight, there appeared to be a lack of knowledge relating to kinematic changes which occur during the block phase and first post-block stance phase. Additionally, despite the widespread collection of external kinetic data, few researchers have combined this with concurrently collected kinematic data in order to calculate the internal joint kinetics and understand the causes behind the observed techniques. Virtually all of the previous sprinting literature discussed in this chapter (sections 2.2 and 2.3) employed empirical research designs by measuring and reporting technique-related variables, sometimes after experimental interventions which were designed to directly manipulate technique. However, the review of theoretical biomechanical methodology (section 2.4) revealed forward dynamics modelling to be a potential mode of research which could be applied to sprinting in order to further develop informed theories which would otherwise not be possible with empirical research alone.

The review of literature informed the overall aim of this thesis, which was to understand the aspects of sprint start technique and performance that contribute to higher levels of performance. The research questions, as previously stated in Chapter 1, were developed in order to achieve this aim, and a series of investigations were undertaken to address these research questions. Empirical analyses of kinematic and kinetic data were employed alongside a theoretical analysis using a forward dynamics model. Each of the investigations are described and discussed in the subsequent chapters of this thesis.

CHAPTER 3: DEVELOPING AN UNDERSTANDING OF SPRINT START TECHNIQUE AND PERFORMANCE

3.1. Introduction

Biomechanists and coaches often endeavour to determine certain aspects of sporting techniques which appear to result in high levels of performance, and as highlighted in the previous chapter, the sprint start is no exception. However, because the measurement of sprint start performance is not currently an entirely clear concept, a range of measures have previously been used to quantify sprint start performance. The use of relatively diverse performance measures, such as block velocity and the time taken to reach 10 m, could provide conflicting assessments of performance success (Mendoza and Schöllhorn, 1993). However, it is not known whether the choice of performance measure during a more specific phase could also influence the outcome of a study. For example, could a series of block phase performances be ranked in conflicting orders using different variables obtained solely at block exit?

In Chapter 1, research question i posed *does the choice of performance measure influence the identification of different levels of sprint start performance?* If the use of different performance measures affects the ranking of a series of trials, the conclusions reached will thus be dependent on the choice of measure. The first aim of this chapter was therefore to determine whether the choice of performance measure influences the performance-based ranking of a series of sprint starts within a group of trained sprinters. If the identification of the highest performing sprinter is influenced by the choice of performance measure, then research question ii must be addressed - *what is the most appropriate measure of sprint start performance, and can it be accurately quantified in a field environment?* By considering the aims of a sprint and what constitutes a successful sprint start, an appropriate performance measure will be identified. However, as highlighted in the previous chapter, externally valid sprint data must typically be collected outside of a laboratory setting where no direct intervention from the biomechanist is possible. As this could potentially limit the internal validity of the collected data, a separate investigation evaluating the accuracy of the data collection and processing methods will be undertaken to determine whether the chosen performance measure can be accurately quantified in a field environment. The second aim of this chapter was therefore to

evaluate the accuracy with which the selected performance measure could be obtained at a coach's planned session with no intrusion.

Having evaluated the validity with which the chosen performance measure can be obtained in the field, the techniques of sprinters can confidently be compared to their associated levels of performance. Returning to the data collected in the field from the group of trained sprinters, certain kinematic aspects of technique could therefore be identified in an attempt to address research question iii - *which kinematic technique variables are associated with higher levels of sprint start performance?* Additionally, instead of just focussing on technique in the 'set' position, as has often been undertaken in the past, an analysis including data from the whole block phase will be included. The final aim of this chapter was therefore to begin to identify some of the key aspects of technique associated with higher levels of performance.

3.2. Methods

3.2.1. Participants

Thirteen male sprinters, ranging in ability level from university club level to World junior 100 m champion, provided written consent for data to be collected at their indoor sprint start training sessions. The Local Research Ethics Committee approved biomechanical investigations which did not involve any invasive procedures to be undertaken during training sessions, as was the case for all studies presented throughout this thesis. In order to remain unobtrusive, and to avoid any errors associated with skin movement artefact or out of plane rotations, no markers were attached to the sprinters in this study or throughout this thesis. For this study, data were collected at the University of Bath indoor track just prior to the competition phase of the indoor season. Basic anthropometric characteristics were obtained from the sprinters prior to the training session, and are presented in Table 3.1 alongside their 100 m PB times.

Table 3.1. Descriptive characteristics for the 13 sprinters.

Sprinter ID	Height [m]	Mass [kg]	Age [years]	100 m PB [s]
A	1.77	85.2	18	10.35
B	1.70	78.3	21	10.53
C	1.85	84.2	20	10.70
D	1.81	76.5	21	10.90
E	1.74	71.9	22	11.10
F	1.79	74.3	21	11.19
G	1.73	61.6	17	11.2
H	1.69	69.5	31	11.2
I	1.80	60.3	16	11.3
J	1.80	58.4	16	11.3
K	1.81	73.1	21	11.55
L	1.78	78.6	28	11.6
M	1.84	82.0	19	11.6

100 m personal best (PB) times reported to the nearest 0.1 s are hand timed.

3.2.2. Data collection

A high-speed digital video camera (Motion Pro®, HS-1, Redlake, USA) was mounted on a tripod, 8.00 m away from the centre of the running lane, with the lens centre 1.00 m above the ground, directly in line with the start line. An area of 2.00 m horizontally by 1.60 m vertically was calibrated, using four corner points of a rectangular calibration frame. The calibration frame was located centrally inside a field of view 2.50 m wide, with its mid-point at the start line. Images were collected at a resolution of 1280 × 1024 pixels using a shutter speed of 1/1000 s, an open iris, and a sampling frequency of 200 Hz. Due to the indoor conditions, an additional 4000 W of lighting was used to provide a sufficiently bright image. An LDM device (LDM-300C, Jenoptik, Germany) operating at 100 Hz was positioned approximately 20 m behind the start line in the centre of the lane to obtain data relating to the displacement of the lumbar region of the sprinter (as described in section 2.5.2). The exact distance between the LDM device and the start line was determined during a static trial prior to data collection so that all LDM device distances could subsequently be expressed relative to the start line (0.00 m).

Following coach directed warm-ups, all 13 sprinters completed a series of three maximal effort sprints to 30 m commencing from starting blocks. Each sprinter adjusted the blocks according to their personal preference, and all wore their own spiked shoes. Tight fitting clothing was worn by all sprinters, which assisted the subsequent video analysis. Each sprint was initiated by the experimenter, who provided standard '*on your marks*' and '*set*' commands. The experimenter then gave the start signal by pressing a custom designed trigger button. This sent signals to the camera, the LDM device, and a sounder device. The sounder acted as an auditory stimulus mimicking the starting signal present in competition. After each sprint, sprinters were allowed their normal recovery (approximately 8-10 minutes) in order to facilitate subsequent performance without the effects of fatigue.

3.2.3. Data processing

The raw video files were viewed to determine the occurrence of specific events, each of which was defined as follows:

- Movement onset: the first video frame in which movement was visible (which always occurred at the head).
- Rear foot off: the first frame in which the rear foot lost contact with the rear block.
- Block exit: the first frame in which the front foot lost contact with the front block.
- First stance touchdown: the first frame in which the rear block foot made contact with the track.

From these event timings, phase durations were calculated as follows:

- Rear foot push duration: movement onset to rear foot off.
- Total push phase duration: movement onset to block exit.
- First flight duration: block exit to first stance touchdown.

The video files were subsequently imported into digitising software (Peak Motus®, v. 8.5, Peak Performance, USA). All digitising was performed at full resolution, and with a zoom factor of 2.0, allowing points to be digitised at every half-pixel. The resolution of measurement was therefore 0.00098 m. Eighteen specific anatomical points (vertex, seventh cervical vertebra (C7), shoulder, elbow, wrist, third

metacarpal, hip, knee, ankle and second metatarsophalangeal (MTP) joint centres) were manually digitised from the frame prior to movement onset through to ten frames after touchdown. The horizontal and vertical scale factors calculated from the calibration frame were applied in order to align scale the raw digitised co-ordinates and thus obtain absolute displacement data. The raw displacement time-histories from each trial were then exported from the digitising software, and all subsequent analysis took place using custom routines developed in Matlab™ (v. 7.4.0, The MathWorks™, USA).

In order to alleviate any potential effects of end-point error when smoothing the data, the first frame was backwards-replicated ten times, and ten frames of data were included post-touchdown (Smith, 1989). It was decided to replicate the frame prior to movement onset since it was assumed that the sprinter was stationary during this time. Residual analyses (Winter, 1990) were performed individually for each of the 36 time-histories (i.e. a horizontal and a vertical component for all of the 18 anatomical points), due to the likelihood of differing noise content at each anatomical site and in each of the principal directions (Angeloni *et al*., 1994; Giakas and Baltzopoulos, 1997a, 1997b). The determined optimal cut-off frequencies were used to obtain filtered displacement time-histories by passing the raw displacement data bi-directionally through a fourth-order Butterworth digital filter. Cut-off frequencies ranged from 16 to 28 Hz. All filtered displacement data were combined with segmental inertia data (de Leva, 1996) in order to create a 14-segment model (head, trunk, upper arms, forearms, hands, thighs, shanks, feet). Inertia data for the feet were taken from Winter (1990), as they corresponded to more easily identifiable endpoints, and allowed for a linked segment model to be created. The mass of each sprinter's spiked shoes were measured prior to data collection, and the appropriate mass was added to both feet. The mass ratios of all segments were adjusted accordingly to ensure that their sum remained equal to one after the inclusion of this additional mass. The whole-body CM displacement time-history was calculated from the segmental data using the summation of segmental moments approach. Joint angles were calculated (Figure 3.1), and all linear and angular displacement time-histories were subjected to second central difference calculations (Miller and Nelson, 1973) in order to derive their corresponding velocities.

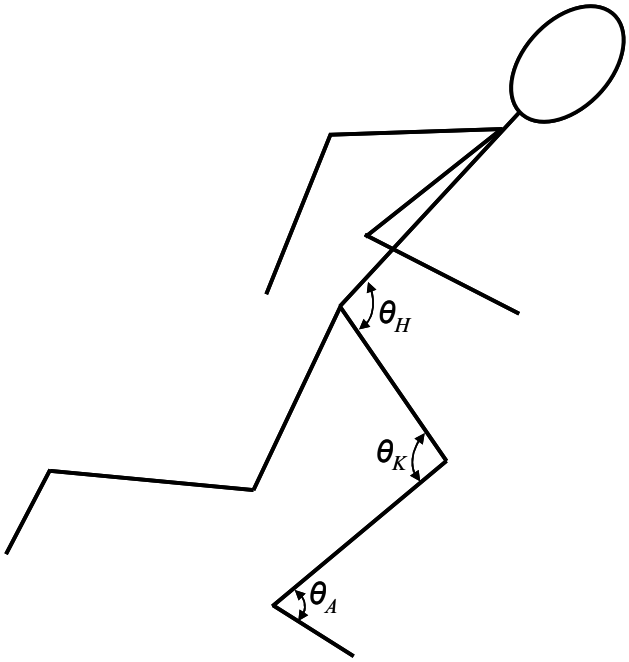

Figure 3.1. Convention used to describe positive (extension/plantarflexion) changes in joint angles at the hip (θ_H), knee (θ_K) and ankle (θ_A).

Joint angles at specific events ('set' position, rear foot off, block exit and touchdown) and peak angular velocities during the block phase were identified. All angular data were reported in degrees to conform to the majority of previous sprinting research (e.g. Atwater, 1982; Mero *et al*., 1983; Mann *et al*., 1984; Mann and Herman, 1985; Mero and Komi, 1990). The time at which these peak values occurred were expressed as a percentage of the duration of the push phase. Step length was calculated as the difference between the horizontal position of the front block MTP joint one frame prior to block exit, and the horizontal position of the contralateral MTP joint at first stance touchdown. Touchdown distance was calculated as the difference between this MTP co-ordinate at touchdown, and the horizontal position of the CM in the same frame, with a positive value representing the stance foot MTP ahead of the CM. The instantaneous horizontal velocity of the MTP at touchdown (relative to the track) was also identified.

Calculation of performance measures

Block velocities have previously been estimated from manual video analyses by extracting the first derivative of a smoothed displacement time-history at the instant of block exit (e.g. Mero and Komi, 1990; Schot and Knutzen, 1992; Čoh and Tomažin, 2006). However, alternative manual video analysis methods for the

estimation of take-off velocity have previously been applied to track and field events such as the triple jump (Yu and Hay, 1996) and hurdles (Salo and Scarborough, 2006). After any take-off, be it before a hurdle, from the long jump runway, or out of the blocks, the motion of a body's CM is determined by the laws of projectile motion. Ignoring air resistance, horizontal velocity is constant during the subsequent flight phase, and block velocity can thus be calculated using displacement data from this flight phase. For the current study, block velocity was calculated using the raw CM displacement data from each frame of the first flight phase, using the procedures outlined by Salo and Scarborough (2006). Assuming constant horizontal velocity during flight, the first derivative of a linear polynomial fitted through these data can therefore be used as a measure of block velocity (Figure 3.2). The validity of this method, and of other available methods for the calculation of block velocity from kinematic data, was also evaluated against criterion kinetic data (see section 3.2.5).

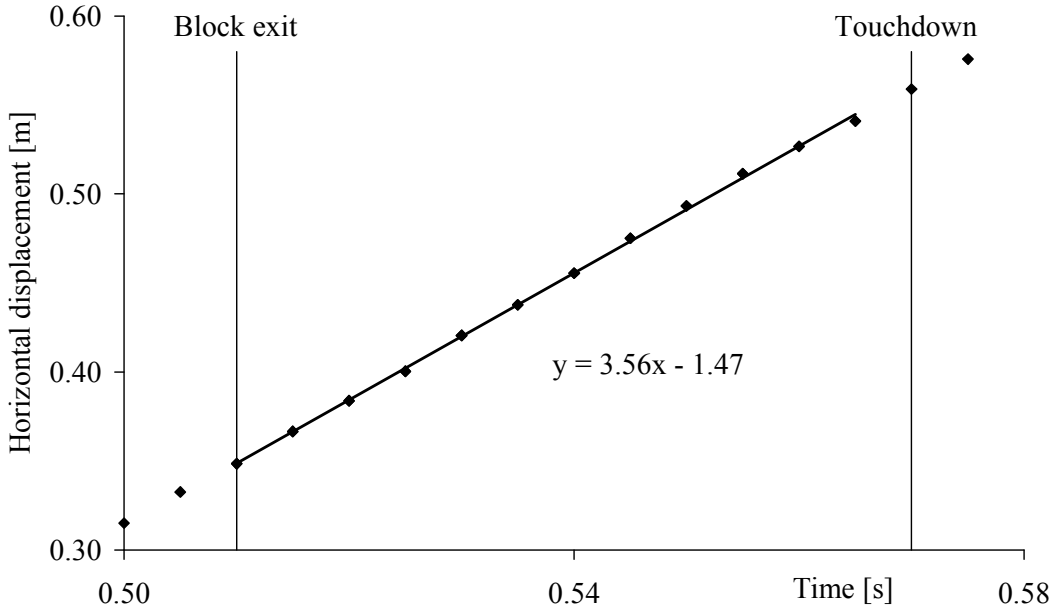

Figure 3.2. Method used to determine block velocity. Raw horizontal CM displacement data (♦) were extracted during flight (i.e. from block exit to one frame prior to touchdown), and fitted with a linear function. The first derivative of this function represented the horizontal CM velocity (3.56 $m \cdot s^{-1}$) throughout the first flight after block exit (ignoring air resistance).

Average horizontal block acceleration ($\bar{a}_Y$) was calculated based on the change in horizontal velocity during a specific phase (Δv_Y) divided by the associated duration of that phase (Δt):

$$\bar{a}_Y = \frac{\Delta v_Y}{\Delta t} \qquad [3.1]$$

As a sprinter commences the block phase with zero velocity, their Δv_Y during the block phase is equal to their velocity at block exit (i.e. block velocity). Whilst Δt could be obtained from the overall change in time from the sounder activating to block exit, the first part of this relates to the reaction time prior to the sprinter moving. As highlighted in the previous chapter, reaction times can vary greatly both within and between sprinters (van Coppenolle *et al*., 1989; Collet, 1999; Pain and Hibbs, 2007). Therefore, although reaction time is an important part of sprinting, it is independent from the actual block phase performance. Removal of pre-movement time from the Δt value gives the duration of the active pushing phase in the blocks, and thus yields a more accurate indication of start performance for the current purposes. Total push phase duration was thus used for Δt rather than total block time.

The power which contributed to the net change in horizontal CM motion (hereafter termed average horizontal external power) during the push phase in the blocks was calculated based on mechanical principles. As sprint performance is related to the ability to translate the CM in a horizontal direction, the change in energy in the antero-posterior (y-axis) direction (E_Y) is of primary interest. This energy is therefore equal to a sprinter's kinetic energy, and was thus calculated based on knowledge of their mass (m) and horizontal velocity (v_Y):

$$E_Y = \frac{m \cdot v_Y^{\,2}}{2} \qquad [3.2]$$

The average horizontal external power ($\overline{P}_Y$) generated during a specific phase (e.g. the push phase in the blocks) is equal to the change in energy between the start and end of that phase, divided by the associated time duration:

$$\overline{P}_Y = \frac{\Delta E_Y}{\Delta t} \qquad [3.3]$$

Combining equations 3.2 and 3.3 therefore yields an equation from which average horizontal external power can be calculated, based on knowledge of horizontal velocity at the start (v_{Y_i}) and end (v_{Y_f}) of the phase of interest, the duration of this phase, and the mass of the sprinter:

$$\overline{P}_Y = \frac{m(v_{Y_f}{}^2 - v_{Y_i}{}^2)}{2 \cdot \Delta t} \qquad [3.4]$$

The LDM device was used to obtain displacement and velocity-based measures of performance from beyond the block phase, for inclusion in the comparison of performance measures. It was important to obtain LDM device velocity time-histories that were relatively smooth functions, independent of any within-step fluctuations, as these could influence instantaneous velocity values taken from a specific point on the curve due to the changes in velocity which occur within a step cycle. The overall motion of a sprinter's CM during the acceleration phase, excluding these fluctuations during each individual stance phase, is one of increasing velocity with decreasing acceleration. A polynomial function can be fitted to the raw LDM device data to remove both the random noise and the genuine within-step velocity fluctuations that could affect the results. It was decided to fit the polynomial to the displacement data, as these were the raw data recorded by the LDM device, and to subsequently derive the associated velocities.

The raw displacement data obtained with the LDM device were fitted with a fifth-order polynomial function using the 'polyfit' and 'polyval' functions in Matlab™. The polynomial order was determined by the author based on RMS differences between the polynomial and raw data. A residual analysis was undertaken to identify a polynomial order which provided a close match to the known underlying trends of the displacement and velocity profiles, without starting to incorporate any within-step velocity fluctuations. The polynomial start point was identified from where the

raw displacement values increased and remained greater than 2 standard deviations above the mean noisy pre-start signal level (informed from pilot comparisons between LDM device and high-speed video movement onsets). As the training sessions consisted of maximal effort sprints to 30 m, the raw LDM device data were truncated 50 data points after displacement exceeded 30 m, so that polynomial endpoint error would not affect the values recorded at 30 m (Wood, 1982). The displacement polynomial was numerically differentiated with respect to time in order to yield a fourth-order representation of the velocity profile. The time at which displacement equalled 10, 20 and 30 m was identified, as were the corresponding velocity values at these points.

From the high-speed camera and LDM device, nine measures of performance were thus obtained, all of which had been used in previous sprint start research. These were:

- Block velocity (from high-speed video data)
- Average horizontal block acceleration (from high-speed video data)
- Average horizontal external block power (from high-speed video data)
- Time to 10 m (from LDM device data)
- Time to 20 m (from LDM device data)
- Time to 30 m (from LDM device data)
- Velocity at 10 m (from LDM device data)
- Velocity at 20 m (from LDM device data)
- Velocity at 30 m (from LDM device data)

Because smaller sprinters require less power to translate their CM to the same extent as a larger sprinter, average horizontal external block power values were also normalised using leg length and mass data, based on the functions presented by Hof (1996; Appendix A). This yielded a tenth performance measure. It was not necessary to normalise the velocity or acceleration data, as neither of these variables are biased by the mass of a sprinter.

3.2.4. Statistical analysis

Due to equipment problems, no LDM device data were available for sprinter A. For each of the variables used to quantify performance, the mean performances of the

remaining 12 sprinters were therefore ranked from 1 (best) to 12 (worst). Spearman's rank order correlation co-efficients (ρ) were then calculated from these ordinal data to determine whether different performance measures ranked the mean performances of the 12 sprinters in the same order, or whether the choice of performance measured affected the ranking of the sprinters. Once the chosen performance measure had been identified, Pearson's product moment correlations (r) were calculated between selected technique variables and this measure of performance. As LDM device data were not required for this, the individual means obtained from all 13 sprinters were included. These correlations allowed the identification of aspects of technique that were associated with higher levels of performance. Statistical significance was accepted below a probability (p) level of 0.05.

3.2.5. Method accuracy evaluation - high-speed video

The previously described high-speed video set-up (section 3.2.2) was replicated in a laboratory with identical field of view, calibration and camera settings to those used at the track. The starting blocks were firmly spiked into a 1 cm thick rubber mat which was strongly bonded to a sheet of thin steel, which in turn was securely bolted to a 0.900 x 0.600 m force platform (Kistler, 9287BA, Kistler Instruments Ltd., Switzerland) operating at 1000 Hz. The force platform data were used to obtain criterion measures of block velocity against which the video data were compared. White tape of width 0.05 m was used to create a representation of the start line directly in front of the force platform, so that the hands were placed on the front edge of the platform. The starting blocks were again adjusted to the preference of the sprinter, with the constraint that the blocks must remain on the force platform in order to ensure that all points of ground contact were on the platform. This constraint meant that a slightly bunched start was enforced, which may have marginally reduced the block velocity of the subject (Henry, 1952). However, this reduction was common to both the criterion and video measures of block velocity, and would thus have no detrimental effect on the primary aim of this part of the study, which was to evaluate the accuracy of the video method. In contrast, allowing a freely chosen starting position with the hands placed in front of the force platform would yield an incorrect velocity value from the force data due to not all of the ground reaction forces generated throughout the block phase being recorded (i.e. those through the hands during the early part would be ignored).

One trained male sprinter (age = 23 years, mass = 62.3 kg, height = 1.71 m, 100 m PB = 11.20 s) provided consent and completed a series of 20 sprint start trials from the blocks mounted on the force platform. Multiple trials from a single subject provided data to address the second part of research question ii - *what is the most appropriate measure of sprint start performance, and can it be accurately quantified in a field environment?* - as the measurement errors being investigated (i.e. due to equipment set-up, data processing and data reduction) were operator- and system-dependent, and not due to subject-dependent biological variation. It would therefore be feasible to extrapolate the magnitude of the observed measurement error to situations using an identical video data collection protocol (i.e. same field of view, camera settings, calibration and data processing), such as that carried out at the track with the group of 13 trained sprinters in this chapter.

In each trial of this method accuracy evaluation, the sprinter raised in to the 'set' position upon standard starting commands from the investigator. The investigator subsequently pressed a trigger button, again sending a signal to the sounder device and high-speed video camera, and additionally to the computer collecting the force platform data. The trigger signal was also transmitted to a series of 20 light-emitting diodes (LEDs; Wee Beastie Ltd, UK) placed in the camera view, one of which illuminated every 1 ms. This allowed synchronisation of the force and video data to the nearest millisecond based on the number of LEDs illuminated in the first frame of video data.

The raw horizontal force data were extracted and integrated in order to obtain the associated velocity data (Davies and Rennie, 1968). It was decided not to smooth these data, as any noise present in the raw signal would decrease in magnitude during the integration procedures (Willems *et al*., 1995). Pilot tests confirmed this, as it was found that digital filtering (with a cut-off frequency determined from residual analysis) altered these force-derived block velocity values by less than 0.005 $m \cdot s^{-1}$. Movement onset time was defined as the frame in which the horizontal force first increased, and then subsequently remained, two standard deviations above the mean horizontal force recorded during the first 50 ms. Block exit time was determined as the frame in which horizontal force first dropped below a threshold of 10 N (this was

different to the threshold used to identify movement onset due to the vibrations of the blocks on the force platform rendering the previously used threshold inaccurate). The corresponding velocity at the instant of block exit was thus identified and recorded as the criterion measure of block velocity. Force platform power values were calculated from the product of the force and velocity time-histories (e.g. Davies and Rennie, 1968; Willems *et al*., 1995), and were averaged across the push phase to yield a criterion measure of average horizontal external power. Average horizontal external power was also calculated using discrete force platform block velocity (v_{Y_f}) and push phase duration (Δt) values in equation 3.4 (v_{Y_i} = zero in the blocks), to directly verify the formulation of the external power equation previously derived for use with the high-speed video data.

The video data were reduced and processed exactly as outlined in section 3.2.3, in order to directly replicate the protocol used in the field. In addition to the previously described calculation of block velocity (Salo and Scarborough, 2006; Figure 3.2; hereafter termed the '*flight polynomial*' method), block velocity was also calculated using two alternative methods, and the accuracy of all three was determined in an attempt to identify the most valid method. The '*flight displacement*' method (Yu and Hay, 1996) yielded a block velocity value through extraction of the horizontal CM displacement co-ordinates during the first and last frames of flight, and division of the difference between them by the associated change in time. A '*digital filtering*' method was also used, in which the filtered horizontal CM velocity at the instant of block exit was calculated. In order to obtain this value, raw horizontal CM displacement time-histories from movement onset to first touchdown underwent a residual analysis to determine optimal cut-off frequencies (Winter, 1990). The raw displacement data were then passed bi-directionally through a fourth-order Butterworth digital filter, before velocities were calculated using second central difference equations (Miller and Nelson, 1973). Block acceleration and average horizontal external block power were also calculated (equations 3.1 and 3.4) using the block velocity estimates from each of these three video methods alongside push durations identified visually from the video data. These video-based power values were then compared to criterion power data calculated from force platform-derived block velocity and push duration data.

Difference scores were calculated between each video method estimate of block velocity and each force platform criterion measure for all 20 trials (i.e. video method minus criterion score). These difference scores were then separately plotted for each video method against the mean value of that video method and the criterion measure of block velocity to check for heteroscedasticity (Altman and Bland, 1983; Bland and Altman, 1995, 1999). The 95% limits of agreement were calculated from the standard deviation (*s*) of all the difference scores between the new and criterion values (Bland and Altman, 1986). As the sample size was 20 in this part of the current study, the appropriate critical *t*-value at the two-tailed 95% confidence level was 2.093 (Thomas and Nelson, 1999; Hopkins, 2000). Therefore, 95% limits of agreement presented in the Bland-Altman plots were equal to the standard deviation of the difference scores multiplied by 2.093. Previous force transducer-based measures of block velocity (Table 3.2) were identified from sprinters covering a range of ability levels similar to the 13 studied in the field in the current chapter (see Table 3.1 for PBs of current group). These values provided a range of block velocities that could be expected in a cohort of this ability level, thus providing data against which the limits of agreement associated with the current video-based methodology could subsequently be contextualised.

Table 3.2. Force transducer-based estimates of block velocity for male sprinters of a similar ability range to the 13 sprinters in the current study (mean ± *s*).

Study	n	PB [s] (range if reported)	Block velocity [$m \cdot s^{-1}$]
Baumann (1976)	12	10.35 ± 0.12 (10.20 – 10.60)	3.60 ± 0.20
Baumann (1976)	8	11.11 ± 0.16 (10.90 – 11.40)	3.10 ± 0.15
Baumann (1976)	10	11.85 ± 0.24 (11.60 – 12.40)	2.90 ± 0.20
Mero (1988)	8	10.79 ± 0.21 (10.45 – 11.07)	3.46 ± 0.32
Mero and Komi (1990)	4	10.76 ± 0.19	3.42 ± 0.38
Mero and Komi (1990)	4	10.82 ± 0.23	3.50 ± 0.22
Čoh *et al*. (1998)	13	10.73 ± 0.20	3.20 ± 0.19

The video sequences from each trial were digitised a second time, on a separate occasion, and repeatability co-efficients (Bland and Altman, 1986) were calculated for each block velocity calculation method. These were equal to the product of the

appropriate *t*-value (2.093) and the standard deviation of the differences between paired retest measurements. They were thus directly comparable to the 95% limits of agreement and could be used alongside them to additionally compare the repeatability agreement within each new method itself (Bland and Altman, 2003). Intraclass correlation co-efficients (ICC) were also calculated between the initial block velocity data for the 20 trials and the 20 redigitised values, giving further indication of the retest reliability of the video-based methods.

3.2.6. Method accuracy evaluation - laser distance measurement device

One further evaluation was undertaken in order to quantify the accuracy associated with the performance data obtained with the LDM device. Ten trained sprinters (males: n = 7, age = 23.9 ± 5.4 years, 100 m PB = 10.76 ± 0.64 s ranging from 9.98 to 11.55 s; females: n = 3, age = 20.7 ± 1.2 years, 100 m PB = 12.48 ± 0.35 s ranging from 12.11 to 12.80 s) ranging in ability from university to international level participated in this part of the study. Whilst the ability level of each sprinter would affect the observed velocity magnitudes at different distances, it was deemed that this would not influence the study outcome in which the aim was to compare measures of velocity between two separate instruments. Unlike the use of correlation co-efficients for assessing concurrent validity, the limits of agreement approach adopted in the current study would not be affected by the wide-ranging ability levels of this heterogeneous group (Altman and Bland, 1983).

Data were collected at four separate track-based training sessions at the University of Bath during the outdoor season. The LDM device was set-up as described previously in section 3.2.2. Additionally, the high-speed video camera (200 Hz) was located perpendicular to the direction of the running lane, approximately 35 m from the centre of the lane. At each session, the camera was placed perpendicular to a different distance from the start line, so that video data were collected at distances of 1, 5, 10 and 30 m. Due to the triggering options available in the camera set-up, and the length of time a sprinter typically takes to reach 30 m, it was not possible to synchronise the camera and the LDM device. However, this was not considered to be problematic, since both the camera and LDM device yielded data relating to the instant at which a sprinter reached a specific distance. The velocity of a sprinter at this distance could thus be derived separately for each device. The camera field of

view was approximately 5.00 m wide, with an area of 4.50 × 1.60 m (2.25 m either side of the distance of interest) calibrated in order to obtain scaled displacement data. A shutter speed of 1/1000 s was used with an open iris, and images were captured at a resolution of 1280 × 1024 pixels. LDM device data collection was initiated manually at the 'set' command, whilst video data collection was initiated manually just prior to the sprinter entering the field of view (except for the 1 m comparison where it was automatically triggered with the start signal).

The LDM device data were processed using the polynomial functions described in section 3.2.3 in order to obtain velocity data at the target distance. Whole-body CM displacements were required from the video data for use as the criterion against which to compare the LDM device data. Raw whole-body CM displacements were obtained from video data using the same inertia modelling procedures as described in section 3.2.3, with velocities calculated using second central difference equations (Miller and Nelson, 1973). Using these video data, the first frame in which the raw CM displacement equalled or exceeded the specific target distance was noted. At this point in time, the phase of the step cycle (i.e. stance or flight) that the sprinter was in was identified from the video clip, and the closest adjacent contrasting phase (i.e. flight or stance) was also identified. The combined duration of these stance and flight phases yielded the duration of the step cycle occurring at the target distance (Figure 3.3). For the comparison at the 1 m mark, the sprinters were typically in mid-stance. As the two adjacent flight times were different in length, the mean duration of the two flight phases was utilised in order to obtain total step duration. In order to determine velocity at the target distance without any influence of the phase of the step cycle, this step duration was applied so that it was evenly spaced either side of the frame in which the target distance was reached (e.g. if the step duration was 41 frames and the target distance was passed in frame number 67, the *target distance step cycle* was deemed to commence at frame 47 and terminate at frame 87; Figure 3.3). This enabled analysis of a complete step starting from an arbitrary point in the step cycle, but in which the sprinter passed the specific target distance at mid-step. The mean value of all raw CM velocities during this *step at the target distance* thus provided a value representing the velocity of the sprinter at the target distance, independent of the effects of the phase of the step cycle the sprinter was in as they reached this distance.

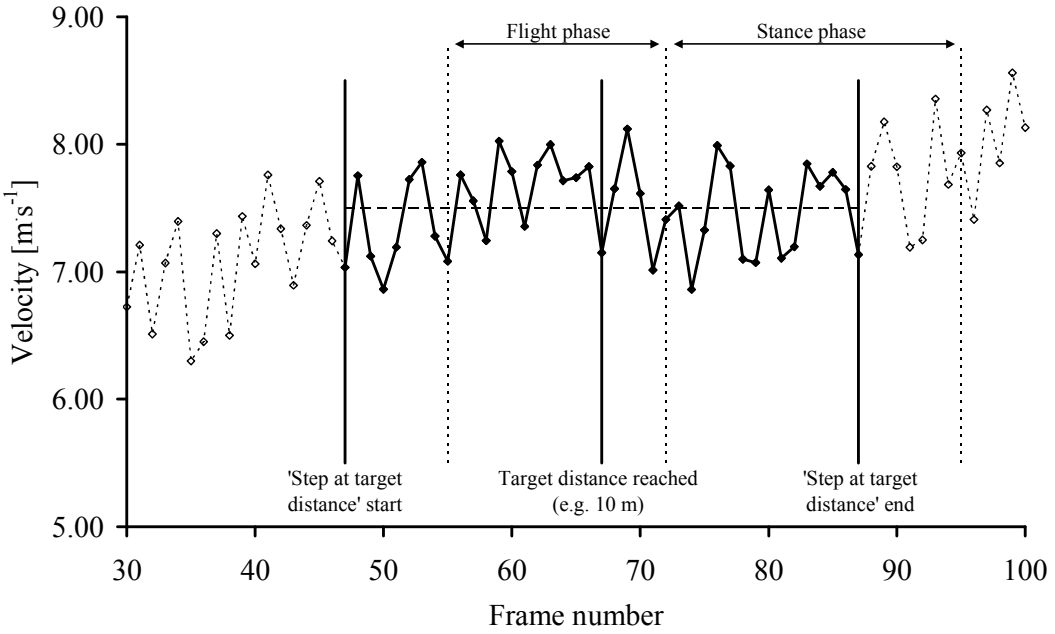

Figure 3.3. Calculation of velocity at the target distance from raw high-speed video data. The frame in which the target distance was first reached was identified (# 67). The closest touchdown or take-off was identified (#72) and the duration of the step cycle either side of this event was determined (#55 - #95). This duration (i.e. 41 frames) was then applied evenly either side of the frame in which the target distance was reached in order to obtain a *step at the target distance*. The mean value of all the raw velocities during this step thus yielded an estimate for velocity at the target distance independent of any step cycle fluctuations (dashed horizontal line).

Although the raw video data contained noise, this would likely have had minimal effect on the determined velocities over a complete step cycle due to its presumed random nature. The high-speed video velocity values would therefore be comparable to those obtained with the LDM device. To confirm this, one trial (at the 10 m mark) was redigitised on ten separate occasions to quantify any effects of noise in the high-speed video data on the determined velocity value. The reliability of the high-speed video velocity values were subsequently determined by calculating a co-efficient of variation (CV) from the ten redigitisations. As with the high-speed video analysis, a limits of agreement approach was used to determine the level of agreement between the LDM device data and the criterion data. Pilot data collected with the LDM device

were used to identify the range of velocities that could be expected at each of the 1, 5, 10 and 30 m marks (Table 3.3). These provided data against which the quantified limits of agreement could subsequently be contextualised in order to determine their appropriateness for the desired purpose.

Table 3.3. Pilot data used to assist the evaluation of the limits of agreement for the LDM device.

Sprinter	100 m PB [s]	Number of trials	1 m velocity [m·s^{-1}]	5 m velocity [m·s^{-1}]	10 m velocity [m·s^{-1}]	30 m velocity [m·s^{-1}]
1	9.98	2	4.59 ± 0.02	7.03 ± 0.05	8.42 ± 0.08	9.86 ± 0.10
2	10.22	10	4.29 ± 0.05	6.86 ± 0.05	8.26 ± 0.09	9.91 ± 0.34
3	10.51	4	4.43 ± 0.05	7.07 ± 0.07	8.45 ± 0.05	9.96 ± 0.20
4	10.90	4	4.05 ± 0.06	6.33 ± 0.06	7.63 ± 0.09	9.21 ± 0.12
5	11.20	8	3.99 ± 0.19	6.42 ± 0.14	7.79 ± 0.05	9.14 ± 0.01
6	11.55	8	4.00 ± 0.14	6.36 ± 0.06	7.70 ± 0.10	9.17 ± 0.10

3.3. Results and discussion

This section will be split into five separate parts, the first reporting whether the choice of performance measure influenced the performance-based ranking of the main group of sprinters. Following this, a discussion proposing the best measure of performance will be undertaken, drawing on theory, previous research and the current results. The evaluation of the high-speed video and LDM device protocols will form the next two sections, to show that this chosen performance measure can be accurately obtained in track-based situations. Finally, the data from the main group of 13 sprinters will be revisited, with certain aspects of technique analysed to establish associations with levels of performance as quantified by the chosen measure.

3.3.1. The effect of choice of measure on performance-based ranking

The rank orders of the 12 sprinters (i.e. excluding sprinter A) when using each different performance measure are presented in Table 3.4. No two measures ranked the performances of all sprinters in the same order, and thus no two measures were perfectly correlated. Whilst the ‘time to’ and ‘velocity at’ measures obtained beyond the block phase with the LDM device were closely matched to each other (i.e.

correlation co-efficients from 0.91 to 0.99, all $p < 0.01$), correlations between these and the block phase measures were weaker (ranging from 0.66 to 0.85, all $p < 0.05$). Confirming the proposal identified from the results of Mendoza and Schöllhorn (1993), this highlighted that contrasting conclusions could be reached when assessing block performance based on measures obtained either at block exit, or measures obtained further down the track.

Table 3.4. Rank order of 12 sprinters for each of the 10 measures of performance.

	B	C	D	E	F	G	H	I	J	K	L	M
Block velocity [$m \cdot s^{-1}$]	2	1	11	6	5	4	8	7	3	10	12	9
Average block acceleration [$m \cdot s^{-2}$]	3	2	12	5	1	4	7	6	11	9	10	8
Average horizontal external power [W]	2	1	10	4	3	6	8	11	12	7	9	5
Normalised block power	1	2	12	5	3	4	6	7	8	9	11	10
Time to 10 m [s]	2	3	10	5	1	4	11	8	9	7	12	6
Time to 20 m [s]	2	3	10	4	1	5	12	8	9	7	11	6
Time to 30 m [s]	2	3	10	4	1	5	12	8	9	7	11	6
Velocity at 10 m [$m \cdot s^{-1}$]	1	2	10	4	3	5	11	9	8	7	12	6
Velocity at 20 m [$m \cdot s^{-1}$]	1	3	10	4	2	5	12	9	7	8	11	6
Velocity at 30 m [$m \cdot s^{-1}$]	1	3	10	4	2	6	12	5	9	7	11	8

Sprinter A was excluded due to no LDM device data. Sprinters were ranked from 1 (best) to 12 (worst). A ranking of one was given for the highest velocity, the highest acceleration, the highest average horizontal external power, and the lowest time. If all measures ranked the sprinters in the same order, it would be expected that the same number would appear down each individual column (i.e. each sprinter would be ranked in the same position when using any performance measure).

Spearman's rank order correlations between each of the video-based measures quantifying performance at block exit were typically moderate to strong. The correlation co-efficient between block velocity and average block acceleration was 0.68 ($p < 0.05$), between block velocity and average horizontal external block power was 0.50 ($p = 0.10$), and between average block acceleration and average horizontal external block power was 0.80 ($p < 0.01$). However, no two of these measures ranked all 12 sprinters in the same order, since none were correlated with a perfect co-efficient of 1.00. Despite some significantly strong correlations, any rank order correlation co-efficient lower than 1.00 indicates inconsistency in the performance-based ranking of these 12 sprinters. This could thus lead to contrasting conclusions if different measures of performance, even those obtained solely from the block phase, were used to assess the relative success of a particular aspect of technique.

The Spearman's rank order correlation co-efficient between average horizontal external block power and its normalised values was 0.66 ($p < 0.05$), which reinforced the influence of different subject morphologies upon the absolute magnitudes of power generated, and thus the need to normalise power data to account for this. However, when average horizontal external block power data were normalised, they still ranked the trials in a conflicting order from both block velocity and block acceleration ($\rho = 0.88$ and 0.92, respectively; both $p < 0.01$). Therefore, even when body size was accounted for in these power data, a perfect match between measures was not observed. The contrast in the ranking of Sprinter J with each of the different block phase performance measures illustrates well how the choice of performance measure could influence the perceived ability of one single sprinter within a group of sprinters (3rd highest block velocity, 11th highest acceleration, 12th highest average horizontal external power, and 8th highest normalised power; Table 3.4).

3.3.2. The identification of an objective measure of sprint start performance

The results presented in Table 3.4 confirmed that the choice of performance measure affects the ranking of sprinters based on their levels of performance, as no two of the ten measures were perfectly correlated. Therefore, if attempting to associate technique variables with improvements in performance, the choice of performance measure could affect the conclusions reached. It is thus important to determine which measure yields the most objective representation of sprint start performance. Also, because researchers often focus on different parts of the sprint start and acceleration phase, the ideal measure of performance should be sufficiently flexible so that the results and conclusions from studies investigating different phases (such as one or more of the post-block steps rather than the block phase) can be readily compared. As the results presented in Table 3.4 relate to the block phase, block phase performance is primarily considered for the purpose of this section. At the end of the following discussion it will be shown that the chosen performance measure is an appropriate measure for any part of the sprint start.

Many of the authors who have studied block phase technique have utilised performance measures from specific distances or events further along the track, such as those measured with the LDM device in the current study. These measures have included the times taken to reach certain distances (from 2.5 yards to 50 m) from the

start line (e.g. Henry, 1952; Stock, 1962; Menely and Rosemier, 1968; Payne and Blader, 1971; Baumann, 1976; Gagnon, 1978; Vagenas and Hoshizaki, 1986; Mendoza and Schöllhorn, 1993; Čoh *et al*., 1998; Parry *et al*., 2003; Mero *et al*., 2006), the instantaneous velocity at a specific distance (e.g. Stock, 1962; Mero *et al*., 1983; Cousins and Dyson, 2004; Salo and Bezodis, 2004), or the velocity at the end of a specific step cycle (e.g. Mero, 1988; Schot and Knutzen, 1992; Rodano *et al*., 1994; Čoh *et al*., 1998).

Whilst measuring performance at a distance further down the track does provide meaningful sprint performance data, its direct relevance to technique and performance during just the block phase is questionable. It must be acknowledged that as the distance at which performance is measured moves further from the start line, the value obtained will move continually closer to the key performance indicator in sprinting (i.e. the time taken to reach the finishing distance). However, the time taken to reach these distances, and thus the performance levels measured at them, is a function of the techniques used in every step prior to that distance, and not just technique during the block phase. This was reinforced by the current results, whereby correlation co-efficients calculated between all measures of performance beyond block exit and those obtained from the block phase did not exceed 0.85. This indicates inconsistency between the performance-based ranking of sprinters at block exit, and their ranking at 10, 20 or 30 m. Performance should therefore ideally be quantified during just the phase over which technique is analysed, allowing the observed performance levels to be directly attributed to the observed techniques.

Several authors who have analysed block phase technique have also reported performance based on measures obtained at block exit. The most common of these has previously been block velocity (e.g. Dickinson, 1934; Henry, 1952; Baumann, 1976; Gagnon, 1978; Vagenas and Hoshizaki, 1986; Mero, 1988; van Coppenolle *et al*., 1989; Mero and Komi, 1990; Guissard *et al*., 1992; Schot and Knutzen, 1992; Mendoza and Schöllhorn, 1993; Čoh *et al*., 1998; Čoh and Tomažin, 2006; Gutiérrez-Dávila *et al*., 2006; Mero *et al*., 2006). However, the use of block velocity as an objective measure of block performance possesses inherent limitations. The instantaneous horizontal velocity of a sprinter at block exit is directly determined by the amount of horizontal impulse that they can generate during the push in the blocks

– greater impulse generation leads to a higher block velocity. Because this impulse magnitude is the product of the mean horizontal force generated and the time duration over which it was generated, a greater block velocity could, however, simply be the result of spending longer in contact with the blocks rather than increasing the average force produced. Whilst sprinters should clearly strive to produce large horizontal velocities at block exit, these should not be primarily achieved through an increase in the duration of the push phase in the blocks, as this conflicts with the 'least possible time' nature of overall sprint performance (Mendoza and Schöllhorn, 1993). The limitations associated with the use of block velocity can be illustrated by considering two sprinters who leave the blocks with identical velocities. If performance was assessed based on block velocity, they would be deemed to be of equal ability. However, if one of these sprinters had spent less time in the blocks generating this increase in velocity, this would clearly be representative of superior performance, but this would be overlooked by using block velocity to quantify performance.

Whilst the reporting of separate velocity and temporal variables could be used to assess performance, the relative importance of each would be open to interpretation. It would therefore potentially be difficult to determine whether a sprinter with a low velocity achieved in a short time duration, or a sprinter with a higher velocity achieved in a longer space of time exhibited the highest levels of performance. A single variable that incorporates both the change in velocity of a sprinter and the associated time duration over which this velocity increase was achieved would thus appear to provide a more meaningful, objective measure of performance. By definition, acceleration quantifies the rate of change in velocity, and thus appears to be a suitable variable. Average block accelerations have been reported by several authors (e.g. Payne and Blader, 1971; Baumann, 1976; Gagnon, 1978; van Coppenolle *et al*., 1989; Guissard *et a*l., 1992), and have been calculated most commonly by dividing the overall change in velocity by the associated push duration against the blocks. This therefore provides a measure of performance which incorporates the changes in both velocity and time into one single variable.

Another variable that also quantifies both the changes in velocity and time is power. The results in section 3.3.1 showed that average horizontal external block power and

acceleration did not rank the performance of all sprinters in the same order (Spearman's rank order correlation co-efficient = 0.92 when using normalised block power). As sprinting is generally considered to be a power based event, and power production (a kinetic variable) ultimately determines the acceleration (a kinematic variable) of a sprinter, the quantification of performance based on power potentially provides the most appropriate value. Depending on their body mass, all sprinters must perform a specific amount of external work in order to translate their body horizontally towards the finish line. However, it is the rate at which they are able to perform this work that determines their performance level, and this is quantified by a sprinter's horizontal external power production against the track/blocks. Therefore, whilst the time taken to reach the finish is the key performance indicator in sprinting, it is power production which determines this, and is thus of critical importance.

Theoretical studies have suggested that the most preferable strategy in short sprints is one in which maximal power is produced from the very start (van Ingen Schenau *et al*., 1991, 1994; de Koning *et al*., 1992). Based on these models, less time would be taken to reach the finish line due primarily to a reduction in the time taken to reach maximum velocity, despite more energy being theoretically lost to air resistance and thus velocity being reduced at the end of the race (van Ingen Schenau *et al*., 1994). A large power production from the very start of a race is therefore important because it reduces the time spent running at submaximal velocities (de Koning *et al*., 1992; van Ingen Schenau *et al*., 1994). The generation of power during the block phase and initial post-block steps is thus a vitally important contributor to overall sprint performance.

Horizontal external power production determines the horizontal motion of a sprinter's CM, and is typically calculated from force platform recordings (e.g. Davies and Rennie, 1968; Mendoza and Schöllhorn, 1993). However, the average horizontal external power production during a specific phase of interest can also therefore be retrospectively calculated based on the resulting motion of the CM. It was shown earlier in this chapter that this can achieved based on knowledge of the initial and final velocities and the change in time associated with a specific phase of interest (equation 3.4). Using average horizontal external power as a measure of performance therefore incorporates the important aspects of both velocity and time. The

appropriateness of average horizontal external power for the measurement of sprint start performance can be determined by defining exactly what it quantifies.

Horizontal external power can only be produced during stance because during flight the sole force acting on the sprinter is weight (ignoring drag due to air resistance). Average power relates to the sum of any negative and positive power phases, where power is positive when the CM undergoes acceleration and negative when the CM decelerates. Not all horizontal external power production in sprinting is positive, as there are typically negative periods present in the block phase and in every subsequent ground contact. The first horizontal CM movement in the blocks is usually backwards due to ankle dorsiflexion (Mero *et al*., 2006), and the CM has been found to decelerate due to the presence of braking forces during the early part of stance, from the first post-block ground contact onwards (Mero *et al*., 1983). The net horizontal external power generated during each analysed period (e.g. block phase or individual stance) is thus of importance, because this incorporates both the positive and negative contributions to the change in motion of a sprinter. Equation 3.4 therefore yields a net value encompassing power associated with both increases and decreases in velocity during a specific phase. Horizontal external power relates to the rate of work performed against a specific object in order to translate the whole body CM in a horizontal direction. This therefore quantifies the power generated against the blocks/track, and does not include any internal power associated with individual segmental movements relative to the CM. Average horizontal external power, as quantified by equation 3.4, therefore provides a comprehensive, objective measure of performance during the sprint start. It can be defined as quantifying the overall net amount of power generated by a sprinter against the track/blocks in an attempt to translate the CM in a horizontal direction (in the least possible time).

Average horizontal external power can also be used to assess any specific part of the sprint start since in the block phase or any of the subsequent post-block stance phases maximum power generation is the aim (i.e. performing work to increase velocity to as high a level as possible in the least possible time). Because power is a kinetic variable whose magnitude is affected by the size and mass of a sprinter, absolute power data will likely yield different results to normalised power data. This was demonstrated by the moderate relationship ($\rho = 0.66$) between these two variables

presented in section 3.3.1. Since larger sprinters require greater magnitudes of power in order to reach the finish line, the use of absolute power as a measure of performance will favour these larger sprinters. Normalised power values should therefore be used to obtain objective performance measures for inter-subject comparisons.

3.3.3. Video methods accuracy validation

The comparison of three different methods of data processing (*digital filtering*, *flight displacement* and *flight polynomial*) enabled the identification of the most valid method for determining block velocity from the high-speed video data. Bland-Altman plots illustrating the systematic bias and 95% limits of agreement between each of the three high-speed video processing methods and the criterion force platform data are presented in figures 3.4a-c.

The *digital filtering* method showed the weakest agreement with the criterion data (Figure 3.4a), exhibiting 95% limits of agreement of ± 0.190 $m \cdot s^{-1}$. Both the *flight displacement* (Figure 3.4b) and *flight polynomial* (Figure 3.4c) methods showed stronger agreement, (± 0.056 and ± 0.048 $m \cdot s^{-1}$, respectively). Systematic bias was also greatest in the *digital filtering* method (0.084 $m \cdot s^{-1}$) compared to values of 0.018 $m \cdot s^{-1}$ and 0.005 $m \cdot s^{-1}$ for the *flight displacement* and the *flight polynomial* methods, respectively. Due to the markedly lower level of accuracy clearly associated with the *digital filtering* method, all further calculations were only performed for the two more accurate methods. The ICC values for the *flight displacement* method and the *flight polynomial* method were 0.84 and 0.90, respectively, both indicative of high levels of retest reliability. Repeatability co-efficients (Bland and Altman, 1986) for the *flight displacement* method and the *flight polynomial* method were ± 0.063 and ± 0.053 $m \cdot s^{-1}$, respectively.

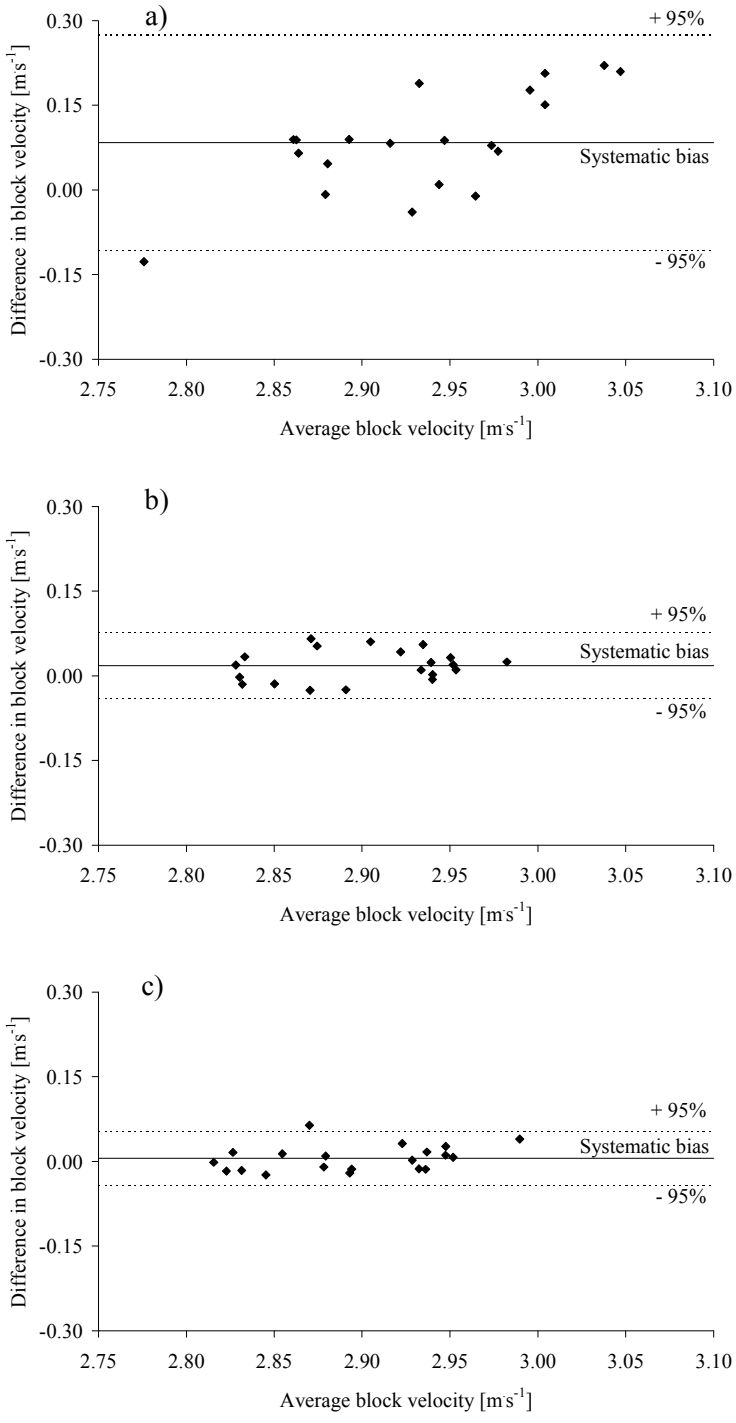

Figures 3.4a-c. Bland-Altman plots illustrating systematic bias and 95% limits of agreement between the criterion measure and a) the *digital filtering* method, b) the *flight displacement* method, and c) the *flight polynomial* method. For each of the 20 trials, the difference between the criterion and the selected video estimate of block velocity is plotted on the y-axis (video minus criterion) against the average of the video and criterion estimates on the x-axis.

The data presented in Figure 3.4a indicated that proportional systematic and random error existed between the *digital filtering* method and the force platform criterion data. The systematic error appeared to increase at higher block velocities, as indicated by the trend for values to increase from the bottom left to the top right of Figure 3.4a. The random error appeared to increase at lower block velocities, as indicated by the greater spread of values towards the left hand side of Figure 3.4a. It has been suggested that such biased data require log transformation if they are to be put to further use (Atkinson *et al*., 2005). However, as the *digital filtering* method (Figure 3.4a) was clearly less valid than the other two methods (Figures 3.4b and 3.4c) and would thus not be the chosen method for the calculation of block velocity, it was decided not to calculate the log-transformed ratio limits of agreement to account for this heteroscedasticity.

Although the filter used for the *digital filtering* method was recursive in nature, and incorporated data points either side of the frame of interest, the noise levels in each of these points likely differed. This method was not able to account for individual fluctuations in noise magnitude between points, and the exact smoothed value at block exit was therefore typically less accurate (Figure 3.4a) than those values obtained with the other two methods (Figures 3.4b-c). The *flight displacement* and *flight polynomial* methods both use data points across a wider time interval, which appears to reduce the random effects of noise in the raw data upon the determined block velocity value.

Neither the *flight displacement* method nor the *flight polynomial* method exhibited any proportional systematic or random error when compared with the criterion force platform data, and both data sets were homoscedastic in nature (Figures 3.4b and 3.4c). The *flight polynomial* method exhibited less systematic bias (0.005 $m \cdot s^{-1}$) than the *flight displacement* method (0.018 $m \cdot s^{-1}$). The positive values for systematic bias associated with both methods imply that these absolute video estimates of block velocity were marginally higher than the force platform criterion values. The systematic error associated with these two methods was small, with the bias of the *flight polynomial* method representing less than 0.2% of the mean criterion block velocity value (2.89 $m \cdot s^{-1}$).

The random element of measurement error was quantified by the 95% limits of agreement, and would likely have been introduced by factors such as operator error during digitising. The slightly smaller limits of agreement associated with the *flight polynomial* method (± 0.048 $m \cdot s^{-1}$) indicate that less random error was present than when using the *flight displacement* method (± 0.056 $m \cdot s^{-1}$). As both methods were calculated from exactly the same digitisation of one trial, this shows that the *flight polynomial* method is a more accurate method with which to determine block velocity. It appears that any digitising error in the two video frames used for the *flight displacement* method had a larger effect on the estimate of block velocity than with the *flight polynomial* method. Whilst the random error due to digitising is typically white in nature, using just the two endpoint frames (as in the *flight displacement* method) could lead to a less accurate velocity estimate because the noise may not be evenly distributed over both frames. In contrast, by fitting a linear polynomial through all the flight data (as in the *flight polynomial* method), the average of several values (typically around 15-20) were used to estimate velocity, which potentially further reduced the effects of the random noise introduced by operator error. When compared to the range of block velocities presented in Table 3.2, the magnitude of the 95% limits of agreement associated with the *flight polynomial* method (± 0.048 $m \cdot s^{-1}$) is clearly small. This method therefore provides a sufficiently high level of precision which would allow the confident distinction between different levels of performance.

The stronger retest ICC co-efficient associated with the *flight polynomial* method (0.90) indicated that the block velocity values were also more repeatable and reliable than those obtained using the *flight displacement* method (0.84). This may again be due to the fact that any error (or difference in the case of a retest analysis) in the two endpoint co-ordinates would have a larger effect on block velocity calculated using the *flight displacement* method than using the *flight polynomial* method. The repeatability co-efficient for the *flight polynomial* method (± 0.053 $m \cdot s^{-1}$) was very similar in magnitude to the 95% limits of agreement, confirming that this method was the most appropriate of the three video-based methods for determining accurate block velocity data.

In order to assess the accuracy with which the determined performance measure (i.e. average horizontal external power) could be quantified with the full video analysis protocol, the block velocity values obtained using the *flight polynomial* method were used with the video-based estimates of push phase duration to calculate average horizontal external block power using equation 3.4. Prior to this, the force platform values of v_{Y_f} and Δt (v_{Y_i} = zero in the blocks) were input into equation 3.4 to verify the correct formulation of this equation for the calculation of power. Identical magnitudes of power to those obtained from the mean value of the product of force and velocity time-histories from the force platform were obtained, indicating that equation 3.4 can confidently be used to calculate average horizontal external power from accurate v_{Y_f}, v_{Y_i} and Δt values. Using the high-speed video values of v_{Y_f} and Δt from all 20 trials, a systematic bias of 5 W was identified in the calculation of average horizontal external power, with 95% limits of agreement of $\pm$ 24 W compared to the criterion power values calculated solely from force platform data. The only previously presented block power data using a force platform showed magnitudes in excess of 1500 W in a group of sprinters (with 100 m PBs ranging from 10.4 to 10.8 s; Mendoza and Schöllhorn, 1993). The error associated with the measurement of power from a high-speed video protocol (i.e. 95% limits of agreement ± 24 W) was therefore less than 1.6% of the magnitudes of power which could be expected from a group of well-trained sprinters, indicating a high and appropriate level of validity associated with this high-speed video analysis protocol.

Section conclusion

Both the *flight displacement* and *flight polynomial* methods provided a high level of validity for calculating block velocity from high-speed video data. However, the *flight polynomial* method showed a slightly higher level of accuracy, with lower systematic bias and less random error. A high level of validity was also observed in average horizontal external power values obtained from these video data. This confirmed that an unobtrusive video data collection and processing protocol can be used to obtain average horizontal external power data - the selected objective measure of performance - in an externally valid setting without compromising the internal validity of these data. Data collected using this protocol, such as the descriptive block phase data obtained from 13 sprinters in a field-based setting (i.e. at

an indoor track) in this chapter, can therefore be analysed and discussed (section 3.3.5) with full confidence in their validity.

3.3.4. Laser distance measurement device method accuracy validation

The first part of this validation incorporated a verification of the method used to obtain a criterion velocity value against which to compare the LDM device estimates. The mean velocity value from the 10 redigitisations of one high-speed video trial at 10 m was 7.66 ± 0.01 $m \cdot s^{-1}$ (CV = 0.15%). It is likely that the nature of the method used, in which values were averaged over approximately 40 frames, and the typically white nature of noise due to operator error, negated any influence of random error upon these velocity values. The low CV value indicated that this method provided a repeatable measure of average step velocity at a specific distance from video data.

Systematic bias and 95% limits of agreement were calculated between the LDM device estimates and the high-speed video measures of velocity at specific distances (Table 3.5). There was a general overall trend for the magnitude of the systematic bias to decrease as the measurement distance (relative to the start line) increased. The large systematic bias observed at the early parts of a sprint (particularly at 1 m) were not wholly due to measurement artefact, as indicated by a retrospective analysis of the relative horizontal distance between the lumbar point (at which the LDM device was aimed) and the CM of a sprinter during the first second of a sprint (Figure 3.5). The lumbar point was approximately 0.40 m behind the CM in the 'set' position, but after movement onset as the sprinter rose from the blocks and began to accelerate, his posture became more upright, and thus the relative horizontal distance between the lumbar point and CM decreased (Figure 3.5). At any specific time after block exit, the lumbar point had therefore covered a greater distance than the CM, and must have thus also travelled at a higher mean velocity than the CM. As the LDM device is one-dimensional in nature, and can only measure the horizontal displacement between the device and the lumbar point at which it is aimed, velocity values higher than the actual CM velocity would be obtained during the early part of a sprint, particularly at 1 m (as indicated by the large positive systematic bias in Table 3.5). By one second, at which point the sprinter had typically covered just over 2 m, the relative distance between the lumbar point and the CM had fallen to approximately 0.10 m (Figure 3.5).

Table 3.5. Systematic bias and 95% limits of agreement between the laser distance measurement device and criterion video data at 1, 5, 10 and 30 m during a sprint.

Distance [m]	Number of trials	Systematic bias [m·s^{-1}]	95% limits of agreement [m·s^{-1}]
1	22	0.407	± 0.182
5	14	0.133	± 0.207
10	30	0.161	± 0.112
30	10	0.057	± 0.130

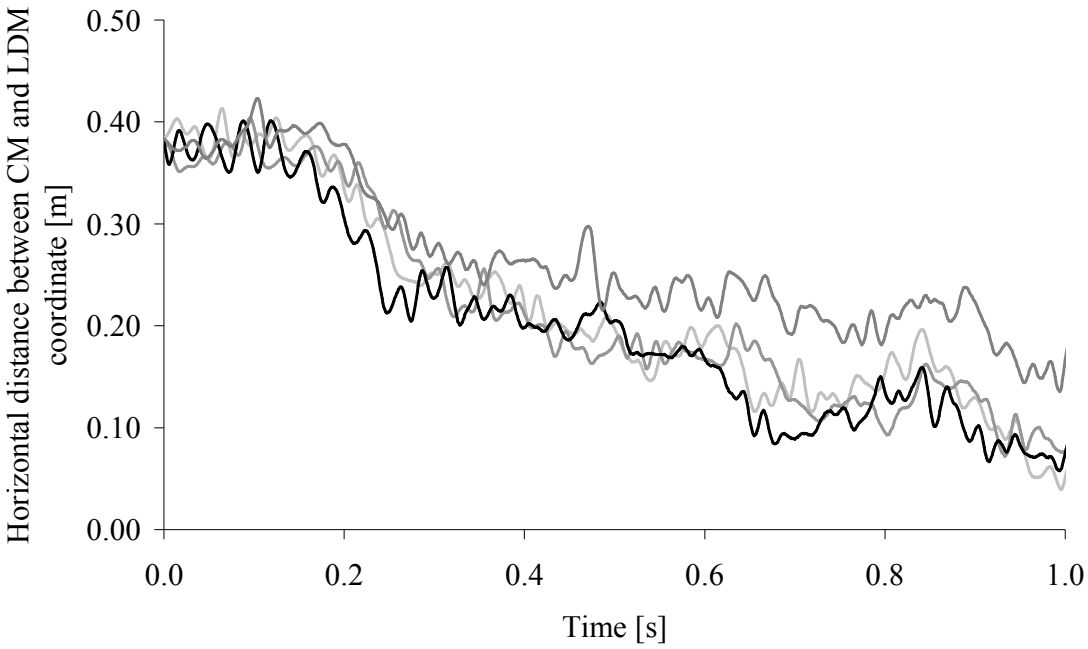

Figure 3.5. Raw horizontal difference in displacement between the centre of mass (from high-speed video) and the lumbar point (from LDM device) during the first second of a sprint for four trials of a sprinter.

The horizontal distance between the CM and the lumbar point will never be likely to reach a value of 0.00 m, because the CM will typically remain in front of the lumbar point throughout the duration of a sprint. However, a levelling-off of the gradient in Figure 3.5 would mean that velocity data (i.e. the first derivative) obtained with the two devices would match more closely, and this was confirmed in the current study by the considerably lower systematic biases observed at distances beyond 1 m (Table 3.5). This also concurred with video data previously collected by Slawinski *et al*. (2004), who found that although there is a phase shift in the individual within-step

fluctuations in horizontal velocity between the CM and the lumbar point during constant velocity running, overall changes in displacement and velocity across one step were similar. Therefore, by smoothing out the within-step fluctuations in the raw LDM device data, a non-biased representation of the motion of a sprinter can be achieved from a LDM device beyond the early parts of a sprint commencing from blocks, once a sprinter has adopted a more upright stance.

In terms of the random error associated with LDM device measurement, the 95% limits of agreement were highest during the first 5 m of the sprint. The values of 0.182 and 0.207 $m \cdot s^{-1}$ obtained at 1 and 5 m, respectively, combined with the high systematic bias (particularly at the 1 m mark) suggested that the error associated with LDM device estimates of velocity during the early part of a sprint was somewhat high, particularly when compared with the range of values presented in Table 3.3. By the 10 m mark, more accurate measures of velocity (95% limits of agreement = 0.112 $m \cdot s^{-1}$) were obtained with the LDM device. This level of random error then increased slightly at the 30 m mark (0.130 $m \cdot s^{-1}$), possibly due to the divergence of the laser beam as the sprinter moved further from the start line. Movement of any segments near to the lumbar point, any clothing movement, or even a large leg retraction and thus high foot displacement behind the sprinter could all have affected the velocity estimate here, because a greater area of the target object was measured by the wider laser beam at these distances. However, the errors associated with LDM device estimates of velocity at 10 and 30 m can be considered acceptable within the context of the range of velocities (> 0.80 $m \cdot s^{-1}$) previously observed at these distances (Table 3.3).

Section conclusion

The high systematic bias and random error associated with LDM device velocity data during the first 5 m of a sprint potentially limits its use during these early distances. However, the lower limits of agreement at 10 m and beyond indicate that the LDM device can be used to obtain estimates of velocity from these parts of a sprint with acceptably low levels of random error. The LDM device data which were obtained and included in the comparison of performance measures earlier in this chapter (i.e. velocity at 10, 20 and 30 m used in section 3.3.1) thus possessed an acceptable

degree of validity for the desired purpose. It is recommended, however, that the current LDM device protocol should not be used to obtain velocity data from distances of less than 10 m in a sprint. Such data will not be representative of CM motion due to the errors associated with the gradually changing posture as a sprinter rises out of the blocks during this early part of a sprint.

3.3.5. Aspects of sprint start technique associated with higher levels of performance

It was previously determined that average horizontal external block power provides an objective measure of performance, and when normalised it can be used for inter-subject comparisons. It was also proven that these power data can be accurately obtained from high-speed video footage alone. Therefore, the techniques used by the 13 sprinters studied in this chapter can be analysed in an attempt to identify any aspects of technique that appear to be associated with higher levels of performance. A Pearson product moment correlational analysis approach was taken, whereby technique-related variables were correlated with normalised average horizontal external block power. A mean value was calculated from all three trials for each sprinter, and these 13 values for each variable were used in the correlation calculations. The selection of technique variables which were considered to be potentially important to performance was initially based on the literature reviewed in Chapter 2.

Prior to analysing the technique variables, a Pearson's product moment correlation was calculated between normalised average horizontal external block power and the individual sprinters' 100 m PB times. A statistically significant moderate to strong negative correlation ($r = -0.73$, $p < 0.01$) existed, which revealed a general trend for those sprinters who were able to achieve a powerful block phase to also maintain a higher level of overall average power production throughout the remainder of a sprint, and thus reach the finish line earlier. Whilst normalised average horizontal external block power and 100 m PB have not previously been correlated, the correlation co-efficient between block velocity and 100 m PB from the current data ($r = -0.70$, $p < 0.01$) coincided exactly with the value reported by Mero (1988) from a group of eight sprinters (with 100 m PB times ranging from 10.45 to 11.07 s).

The Spearman's rank order correlations between block phase performance and performance at 10, 20 and 30 m discussed in section 3.3.1 were all below 0.85, which suggested that they may be potentially problematic if used solely as performance measures due to ranking sprinters in contrasting orders. However, the fact that these relationships between block performance and performance up to 30 m were all moderately strong and positive (all $\rho > 0.66$, all $p < 0.05$) suggests that a successful start is typically associated with higher levels of performance later on. These findings suggest that similar demands are present during the block phase and subsequent phases, and that training to improve block technique and performance should not hinder performance during subsequent phases of a sprint.

The Pearson's product moment correlations between peak block phase joint extension angular velocity magnitudes (hip, knee and ankle of both legs) and normalised average horizontal external block power were generally low, with only two correlation co-efficients exceeding ± 0.35. These were both associated with the hip joints – the rear hip with a correlation co-efficient of 0.37 ($p = 0.22$) and the front hip of 0.56 ($p < 0.05$). Although these results cannot be compared with previously published data since angular kinematics during block exit have not been reported, they suggest the existence of a trend for performance levels to increase as sprinters extend their hips with a greater velocity, particularly the front hip. It was also observed that those sprinters who extended their rear hip over a greater range during the rear block phase ($r = 0.41$, $p = 0.17$), or exhibited a greater rear hip angle at rear block exit ($r = 0.51$, $p = 0.08$), tended to exhibit greater normalised average horizontal external block power, although these findings were not statistically significant. In addition to this apparent trend for greater rear hip extension and velocity to facilitate performance, a greater push duration with the rear leg, expressed as a percentage of the entire block phase, was also associated with higher normalised average horizontal external block power ($r = 0.50$, $p = 0.09$). Although forces were not measured, and thus impulses could not be calculated, these kinematic data suggested an importance associated with the rear leg push against the blocks, particularly with the rear hip. This concurred with previous data presented by Lemaire and Robertson (1990) who, similar to Payne and Blader (1971), highlighted the potential for increased rear leg action in the blocks to facilitate performance.

When the temporal pattern of peak leg joint angular velocities was considered, it was found that all 13 sprinters showed a rear leg sequencing of knee then hip, followed by ankle (Figure 3.6a). In contrast, with the front leg, all sprinters aside from sprinter A showed a proximal to distal sequencing from the hip to the knee and then the ankle (Figure 3.6b). Proximal to distal joint extension strategies are commonly associated with power producing tasks (Grégoire *et al*., 1984; van Ingen Schenau *et al*., 1987), and the occurrence of such a pattern in the front leg during block exit could thus be expected. The early peak knee joint angular velocity in the rear leg could be due to it starting from a more extended angle in the 'set' position (subject means ranged from 95 to 122°) than the front leg (78 to 95°). The rear knee therefore could not extend for too long as its extension range was small due to its starting position, thus limiting its contribution to force production. The knee therefore reached peak extension angular velocity prior to the hip, which may have also been due to the musculature surrounding the hip working to extend the trunk against gravity.

Several kinematic variables beyond block exit were also determined, although neither first flight duration, nor first step length were even moderately related to normalised average horizontal external block power ($r = 0.10$, $p = 0.75$; $r = 0.20$, $p = 0.52$, respectively). This suggests that a greater block phase performance does not appear to affect the flight time or step length of the next phase. This is important since it suggests that striving to increase block power and thus performance is a beneficial strategy and does not appear to negatively affect the subsequent motion of the sprinter. When considering the kinematics at the end of this first flight phase, a large range of mean values existed across the stance leg joint angles, touchdown distance and foot touchdown velocity of the 13 sprinters (Table 3.6). Not only does this show considerable inter-subject variation, the large standard deviations associated with some variables also revealed that intra-subject variation existed between the three trials for some sprinters.

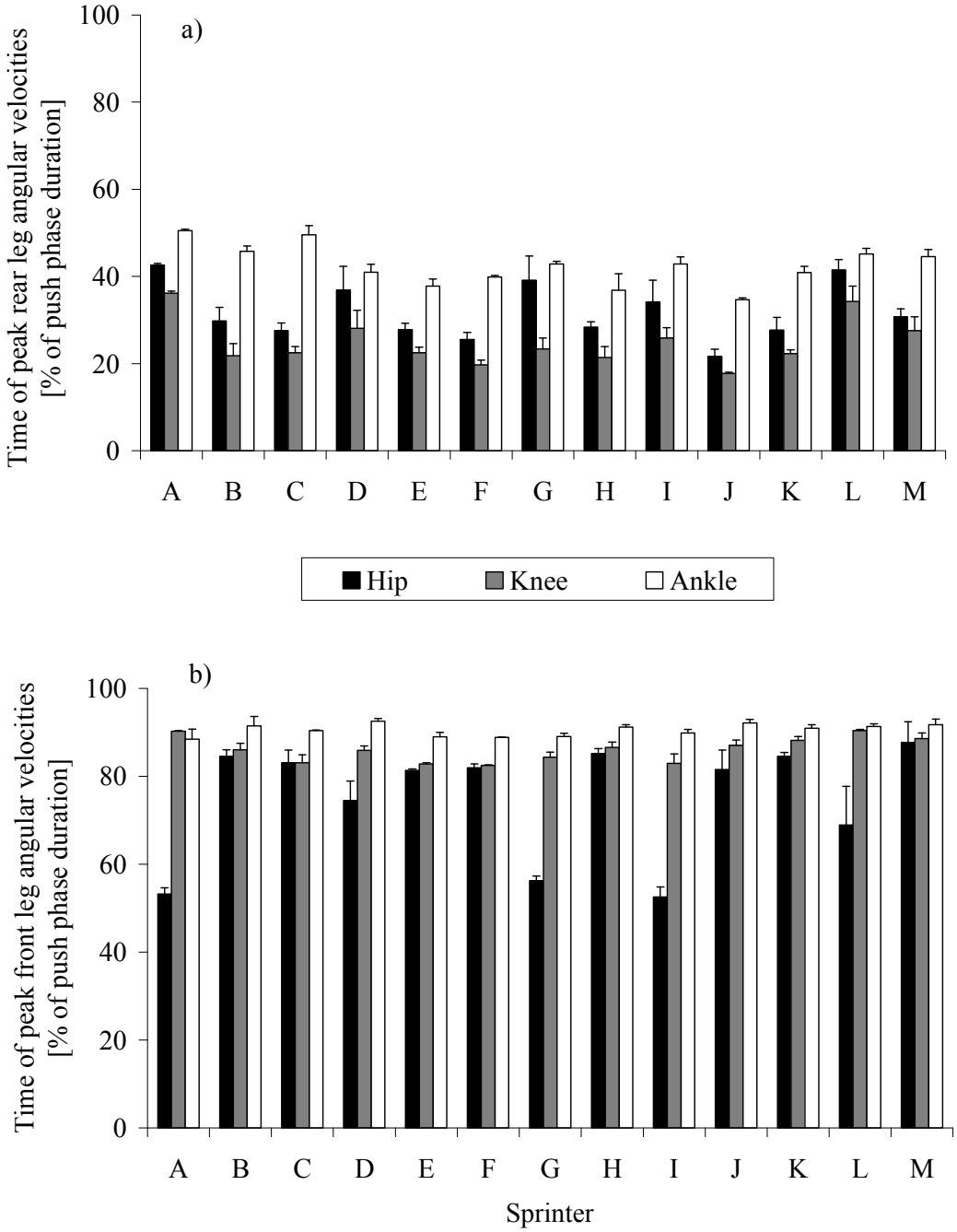

Figure 3.6. Timing of peak joint extension angular velocities at a) the rear leg and b) the front leg expressed as a percentage of total push phase duration.

Table 3.6. Kinematic variables at touchdown for each of the 13 sprinters (mean ± *s*).

	Angle [°]				Touchdown	Touchdown
Sprinter	Trunk	Stance hip	Stance knee	Stance ankle	distance [m]	velocity [m·s^{-1}]
A	42 ± 1	98 ± 2	94 ± 1	91 ± 3	-0.151 ± 0.025	0.98 ± 0.27
B	36 ± 1	103 ± 1	99 ± 1	98 ± 2	-0.268 ± 0.004	0.83 ± 0.62
C	32 ± 1	99 ± 6	102 ± 6	102 ± 3	-0.285 ± 0.064	0.99 ± 0.94
D	45 ± 1	111 ± 6	94 ± 5	100 ± 6	-0.215 ± 0.030	1.03 ± 0.98
E	16 ± 2	73 ± 2	93 ± 1	83 ± 1	-0.165 ± 0.011	1.27 ± 0.11
F	28 ± 5	91 ± 6	100 ± 2	95 ± 3	-0.220 ± 0.013	1.44 ± 0.26
G	41 ± 3	103 ± 5	99 ± 3	94 ± 4	-0.186 ± 0.047	0.83 ± 0.22
H	34 ± 3	91 ± 6	101 ± 4	95 ± 0	-0.104 ± 0.030	0.90 ± 0.42
I	31 ± 1	96 ± 5	106 ± 9	96 ± 2	-0.172 ± 0.026	0.58 ± 0.37
J	29 ± 2	79 ± 5	89 ± 5	83 ± 3	-0.029 ± 0.071	0.68 ± 1.00
K	29 ± 1	97 ± 3	115 ± 2	100 ±1	-0.225 ± 0.024	0.61 ± 0.43
L	30 ± 3	98 ± 5	110 ± 3	96 ± 1	-0.219 ± 0.003	0.29 ± 0.34
M	25 ± 2	86 ± 7	103 ± 5	93 ± 2	-0.167 ± 0.040	1.14 ± 0.57
Min	16	73	89	83	-0.285	0.29
Max	45	111	115	102	-0.029	1.44

All joint angles are the relative angles between two segments, whereas trunk angle is expressed relative to the horizontal. Touchdown distance defines the horizontal distance between the stance foot MTP and the CM, and touchdown velocity relates to the horizontal velocity of the MTP. Min and max values indicate the minimum and maximum mean values, respectively.

Despite the large range in values for these touchdown kinematics, they were, however, not strongly associated with the block phase performance of the sprinters. Correlations between normalised average horizontal external block power and trunk, hip, knee and ankle angles at touchdown were 0.12, 0.09, -0.27 and 0.05, respectively. A slightly stronger trend between touchdown distance and normalised block power (r = -0.35, p = 0.25) may suggest that despite the largely inconsistent effects on individual configuration at the stance leg joints and the trunk, there was a tendency for a more powerful block phase to assist the whole body CM being further in front of the stance foot at touchdown, although this was not statistically significant.

Section conclusion

The fact that all of the technique variables from the block phase correlated with normalised average horizontal external block power at a strength of 0.60 or below, and that only one (front hip peak extension angular velocity) was significantly

correlated, is a meaningful finding in itself. It suggests that, in a relatively heterogeneous group of sprinters, there are no single aspects of technique that lead directly to higher levels of block performance, and that the techniques of sprinters during the block phase were somewhat individual. It would therefore be preferable to analyse block phase technique on a multiple single-subject level, as advocated for biomechanical analyses by Bates (1996). However, findings related to improving high-level performance would therefore be more insightful if sprinters towards international ability-level were analysed. Furthermore, the low correlation co-efficients between normalised average horizontal external block power and the analysed kinematics at first stance touchdown also suggested that these variables were not largely affected by block phase performance. However, because considerable variation existed between the positions exhibited at the onset of stance across the group, determining whether these different kinematics at touchdown could affect the subsequent levels of performance attained during the first stance phase of a sprint presents an interesting area for further investigation.

3.4. Chapter summary

This chapter aimed to address some of the methodological issues associated with the measurement of sprint start performance, and to identify certain aspects of technique which were associated with higher levels of performance amongst a group of 13 trained sprinters. The calculation of ten different performance measures revealed that no two measures ranked all sprinters in the same order of performance, even if using different measures obtained solely from the block phase. This clearly answered research question i - *does the choice of performance measure influence the identification of different levels of sprint start performance?* - yes, it does. Contrasting conclusions previously reached in sprint start research could therefore be partly due to the use of different performance measures.

In order to answer the first part of research question ii - *what is the most appropriate measure of sprint start performance, and can it be accurately quantified in a field environment?* - several performance measures were considered. It was suggested that velocity based measures of performance are limited due to their lack of inclusion of the time taken to achieve this change in velocity. Average horizontal external power was proposed as the most appropriate, objective measure, as it determines the overall

performance level of a sprinter, and would ideally be high from the very start of a sprint. Using normalised average horizontal external power values was also shown to allow accurate inter-subject comparisons.

In order to address the second part of research question ii, the accuracy of a specific high-speed video protocol which could be used for unobtrusive field-based data collection was evaluated. It was shown that block velocity and average horizontal external block power data could be obtained through manual video analysis (digitising) without any intrusion from the biomechanist, and most importantly without any major decrement to internal validity. The technique data from the group of 13 trained sprinters were therefore analysed in an attempt to begin to address research question iii - *which kinematic technique variables are associated with higher levels of sprint start performance?* The role of hip extension, particularly with the rear leg, was one aspect of technique that appeared to be potentially important in the achievement of high block phase performance. It was also identified that striving to improve block phase performance did not appear to detrimentally affect performance during the remainder of a sprint, and is thus a useful aspect to focus on in training. However, considerable variation existed in the techniques used by this heterogeneous group, and it was proposed that techniques should subsequently be considered on an individual-specific basis, ideally focussing on highly-trained sprinters in order to understand how the highest levels of performance are achieved.

CHAPTER 4: LOWER LIMB ANGULAR KINEMATICS DURING THE BLOCK AND FIRST STANCE PHASES

4.1. Introduction

The investigations in Chapter 3 identified aspects of technique necessitating greater attention, and methodological considerations requiring inclusion in subsequent analyses. The range of techniques used by the studied group of trained sprinters highlighted the existence of considerable inter-subject variation during the block phase. However, because only weak correlations between specific kinematic technique variables and performance (quantified by normalised average horizontal external power production) were observed, it was proposed that greater insight would be gained if sprinters were studied on a single-subject basis. Furthermore, when using these subject-specific data to address research question iii - *which kinematic technique variables are associated with higher levels of sprint start performance?* - such data would provide more meaningful answers if collected from well-trained sprinters capable of achieving high levels of performance.

In addition to the range in kinematic variables exhibited during the block phase by the sprinters studied in Chapter 3, data from the end of the first flight phase also revealed that a wide range of body configurations were adopted at first stance touchdown. Therefore, as well as extending the analysis to international-level sprinters, further insight could also be obtained by including the first post-block stance phase in the current analysis. The aim of this chapter was therefore to identify key angular kinematic aspects of the block phase and first stance techniques of three international-level sprinters. Any inter-subject differences in technique could then be associated with the individual sprinters' performance levels in an attempt to understand how higher levels of performance are attained.

4.2. Methods

4.2.1. Participants

Three international-level male sprinters (subject information is presented in Table 4.1) provided consent for a training session to be videotaped for analysis at the University of Bath outdoor track during the early part of the outdoor competition season. Data collection sessions were designed to coincide exactly with each

sprinter's training schedule, and thus took place on days in which start and acceleration phase training occurred. There was therefore no intrusion or change to the coach's planned programme, and external validity was thus maintained.

Table 4.1. Descriptive characteristics for the three sprinters.

	N	P	Q
Age [years]	19	30	19
Mass [kg]	80.4	74.9	81.4
Height [m]	1.81	1.76	1.78
100 m PB [s]	10.22	9.98	10.51
No. of runs	4	4	3

4.2.2. Equipment set-up

An unobtrusive manual video analysis approach (as described and validated in Chapter 3) was used, so that high-performance data could be collected from the international sprinters' training sessions with no interference from the experimenter. Each trial commenced from a start line marked perpendicularly across a lane of the 100 m straight on an outdoor synthetic track. A high-speed video camera (Motion Pro®, HS-1, Redlake, USA) operating at 200 Hz was located on the infield. The camera was positioned perpendicular to the running lane, 40.00 m from the lane centre (mid-zoom range) and 0.75 m in front of the start line. A shutter speed of 1/1000 s was used, alongside an open iris, and images were collected at a resolution of 1280 × 1024 pixels. Prior to the training session, a two-dimensional (2D) area of 3.50 m horizontally × 1.60 m vertically was calibrated using a four-point rectangular calibration frame positioned centrally inside a 4.00 m wide field of view. This enabled the collection of full body kinematic data from movement onset through to the end of the second flight phase.

4.2.3. Data collection

Following a coach-directed warm-up, each sprinter completed three (sprinter Q) or four (sprinters N and P) maximum effort sprints to 30 m, commencing from starting blocks. The blocks were adjusted to the preference of each sprinter, who wore their own spiked shoes. An experienced starter initiated each trial with verbal '*on your*

marks' and '*set*' commands. The starter then gave the start signal by pressing a custom designed trigger button, which sent signals to initiate camera data collection, and to activate a sounder device. The sounder acted as an auditory stimulus mimicking the starting signal present in competition. After each trial, sprinters were allowed their normal recovery (about 8-10 minutes) in order to facilitate performance without the effects of fatigue.

4.2.4. Data processing

The raw video clips were viewed to determine the instants of movement onset, block exit, first stance touchdown, first stance toe-off and second stance touchdown. These conformed with the definitions used in Chapter 3, where movement onset was defined as the first visible head movement, whilst block exit/toe-off were identified as the first frame in which the foot had clearly lost contact with the block/track, and touchdowns were identified as the first frame in which the foot clearly regained contact with the track. Block, flight and stance phase durations were determined from these event timings. As not all of the sprinters started with the same leg in the rear block, the legs were referred to as front and rear block leg for the block phase, with the rear block leg subsequently being referred to as the stance leg, and the front block leg as the swing leg, during the first post-block stance phase.

The raw video files were imported into digitising software (Peak Motus®, v. 8.5, Peak Performance, USA). All digitising was performed at full resolution, and with a zoom factor of 2.0, allowing points to be digitised at every half-pixel. The resolution of measurement was therefore 0.00156 m. Eighteen specific anatomical points (vertex, C7, shoulder, elbow, wrist, third metacarpal, hip, knee, ankle and second MTP joint centres) were manually digitised from one frame prior to movement onset until touchdown of the second stance phase. This enabled velocity at the end of the first stance phase, in addition to at block exit, to be calculated using the *flight polynomial* method (as outlined in section 3.2.3). The horizontal and vertical scale factors calculated from the calibration frame were applied to align scale the raw digitised co-ordinates and obtain absolute displacement time-histories. These were subsequently expressed relative to the start line at ground level as the origin of the global co-ordinate system. The raw displacement time-histories were then exported

from Peak Motus®, and all subsequent data analysis took place using custom routines developed in Matlab™ (v. 7.4.0, The MathWorks™, USA).

As in the previous chapter (section 3.2.3), the first data point for each time-history (i.e. that from the stationary 'set' position) was replicated ten times prior to filtering in order to alleviate any potential endpoint error (Smith, 1989). No padding was required at the latter end of the data set, since data from the second flight phase were sufficient to alleviate error in the filtered data obtained from the first stance phase (i.e. there were at least ten true data points beyond the phase of interest; Smith, 1989), and only raw displacement data from the second flight phase were required for the velocity calculations using the *flight polynomial* method. The padded displacement time-histories were digitally filtered by passing the raw data bi-directionally through a fourth-order Butterworth digital filter (Winter, 1990). Cut-off frequencies were determined using a residual analysis approach in order to obtain the most appropriate degree of minimal signal distortion and maximum noise removal (Winter, 1990). Residual analyses were performed individually for each of the 36 time-histories (i.e. a horizontal and a vertical component for all of the 18 anatomical points) for reasons described previously in section 3.2.3. The cut-off frequencies used ranged from 15 to 28 Hz.

All filtered displacement data were combined with segmental inertia data (de Leva, 1996) in order to create a 14-segment model (head, trunk, upper arms, forearms, hands, thighs, shanks, feet). To account for the mass of the spiked shoes 0.20 kg was added to the mass of each foot, consistent with previous sprinting research (e.g. Hunter *et al*., 2004; Bezodis *et al*., 2008), and the mass ratios of all segments were adjusted accordingly to ensure that their sum remained equal to one after the inclusion of this additional mass. The whole-body CM displacement time-histories were consequently calculated from the segmental data using the summation of segmental moments approach. Ankle, knee and hip angles were calculated, conforming to the same convention used in Chapter 3 (Figure 3.1). All linear and angular displacement time-histories were subjected to second central difference calculations (Miller and Nelson, 1973) in order to derive their corresponding velocity time-histories. Block velocity and first stance take-off velocity were calculated using the *flight polynomial* method. Average horizontal external powers during the push

against the blocks and the first stance phase were calculated from these velocity values and the associated phase durations, using equation 3.4 as outlined in Chapter 3 (page 60). These were again normalised (Hof, 1996; Appendix A) to account for body size, and thus facilitate inter-subject comparison.

Joint angles at specific events (e.g. block exit, first stance toe-off) and the changes in each joint angle during the block and first stance phases were calculated. The peak extension angular velocities were identified for each of the legs during their respective block contacts, and for the stance leg during the first stance phase. Touchdown distance was calculated by calculating the difference between the horizontal co-ordinates of the stance foot MTP and the whole body CM at first stance touchdown, with a positive value representing the stance foot MTP ahead of the CM.

4.3. Results

4.3.1. The block phase

The greatest average horizontal external block power was achieved by sprinter N (1406 ± 38 W; Table 4.2), who also exhibited the highest mean block velocity (3.48 ± 0.06 $m \cdot s^{-1}$). However, when power data were normalised to account for differences in body stature, sprinter P exhibited a greater mean power (6.33 ± 0.27), and thus in accordance with the argument developed in Chapter 3, a higher level of performance. Despite spending the longest mean time generating force in the blocks (0.360 ± 0.005 s), sprinter Q achieved the lowest mean block velocity (3.32 ± 0.08 $m \cdot s^{-1}$).

Table 4.2. Performance descriptors during the block phase (mean ± *s*).

	N	P	Q
Push duration [s]	0.346 ± 0.005	0.330 ± 0.004	0.360 ± 0.005
Block velocity [$m \cdot s^{-1}$]	3.48 ± 0.06	3.43 ± 0.06	3.32 ± 0.08
Average horizontal external power [W]	1406 ± 38	1337 ± 47	1245 ± 57
Normalised power	5.94 ± 0.16	6.33 ± 0.27	5.29 ± 0.20

Sprinter P extended his rear hip over the greatest mean range during rear block contact, with ranges of 10° and 15° greater than those of sprinters N and Q, respectively (Table 4.3). Sprinter P also exhibited the greatest mean peak hip angular velocity, which occurred later in the phase than the peak angular velocities of sprinters N and Q (by 5 and 8%, respectively). Sprinter Q exhibited less rear knee extension (8 ± 0°) and a lower mean peak rear knee angular velocity (116 ± 18°·s^{-1}) than sprinters N (22 ± 5° and 268 ± 59°·s^{-1}) and P (19 ± 1° and 216 ± 19°·s^{-1}). At rear block exit, sprinter Q was more flexed at all three of the rear leg joints than sprinters N and P (Table 4.3). Due to a problem with the camera set-up, no rear ankle data were available for sprinter P in the 'set' position. Sprinters N and Q exhibited similar mean amounts of rear ankle dorsiflexion during the early block phase (-6 ± 2 and -5 ± 1°, respectively). However, sprinter N subsequently plantarflexed his rear ankle over a mean range of 5° more than sprinter Q, and achieved a mean peak rear ankle angular velocity 51°·s^{-1} higher than sprinter Q.

Table 4.3. Rear leg joint kinematics during the rear block contact phase (mean ± *s*).

		N	P	Q
Hip	Peak ω [°·s^{-1}]	317 ± 27	329 ± 76	252 ± 29
	Time of peak ω [%]	31 ± 2	36 ± 2	28 ± 2
	Δ angle during phase [°]	31 ± 2	41 ± 8	26 ± 3
	Angle at end of phase [°]	124 ± 2	128 ± 4	105 ± 2
Knee	Peak ω [°·s^{-1}]	268 ± 59	216 ± 19	116 ±18
	Time of peak ω [%]	28 ± 1	19 ± 1	23 ± 2
	Δ angle during phase [°]	22 ± 5	19 ± 1	8 ± 0
	Angle at end of phase [°]	146 ± 6	137 ± 4	128 ± 4
Ankle	Peak ω [°·s^{-1}]	347 ± 47	n/a	296 ± 45
	Time of peak ω [%]	41 ± 2	n/a	37 ± 2
	- Δ angle during phase [°]	-6 ± 2	n/a	-5 ± 1
	+ Δ angle during phase [°]	+24 ± 4	n/a	+19 ± 2
	Angle at end of phase [°]	143 ± 3	139 ± 4	134 ± 4

The Δ joint angle data represent the overall range of extension. For the ankle joint, data are split into initial dorsiflexion (-) and subsequent plantarflexion (+) magnitudes.

At the front leg during the block phase, sprinter N extended his hip over a smaller mean range (109 ± 4°; Table 4.4) than sprinters P and Q, but extended his knee (78 ± 2°) and plantarflexed his ankle (55 ± 4°; Figure 4.1) over a greater mean range. Sprinter N also exhibited the greatest mean front knee (169 ± 1°) and ankle (162 ± 2°) joint angles at block exit, whereas sprinter P exhibited the greatest mean front hip angle at block exit (166 ± 2°). Whilst mean peak hip and knee extension angular velocities were similar between all three sprinters (30 and 33°·s^{-1} difference between highest and lowest mean value for hip and knee, respectively), sprinter N exhibited a peak mean front ankle plantarflexion velocity (597°·s^{-1}) that was 135°·s^{-1} and 133°·s^{-1} higher than sprinters P and Q, respectively. This peak angular velocity occurred at around 90% of the total block phase durations, and is also illustrated by the gradients of the ankle joint angle displacement time-histories during this late part of the block phase (Figure 4.1).

Table 4.4. Front leg joint kinematics during the block phase (mean ± *s*).

		N	P	Q
Hip	Peak ω [°·s^{-1}]	507 ± 23	537 ± 2	520 ± 12
	Time of peak ω [%]	83 ± 3	52 ± 5	71 ± 19
	Δ angle during phase [°]	109 ± 4	116 ± 4	118 ± 2
	Angle at end of phase [°]	163 ± 3	166 ± 2	158 ± 3
Knee	Peak ω [°·s^{-1}]	582 ± 11	560 ± 8	549 ± 19
	Time of peak ω [%]	85 ± 2	85 ± 1	82 ± 1
	Δ angle during phase [°]	78 ± 2	75 ± 3	66 ± 1
	Angle at end of phase [°]	169 ± 1	166 ± 3	158 ± 3
Ankle	Peak ω [°·s^{-1}]	597 ± 34	462 ± 38	464 ± 12
	Time of peak ω [%]	90 ± 1	89 ± 1	89 ± 1
	- Δ angle during phase [°]	-21 ± +7	-9 ± 3	-19 ± 2
	+ Δ angle during phase [°]	+55 ± 4	+41 ± 3	+41 ± 2
	Angle at end of phase [°]	162 ± 2	155 ± 2	145 ± 1

The Δ joint angle data represent the overall range of extension. For the ankle joint, data are split into initial dorsiflexion (-) and subsequent plantarflexion (+) magnitudes.

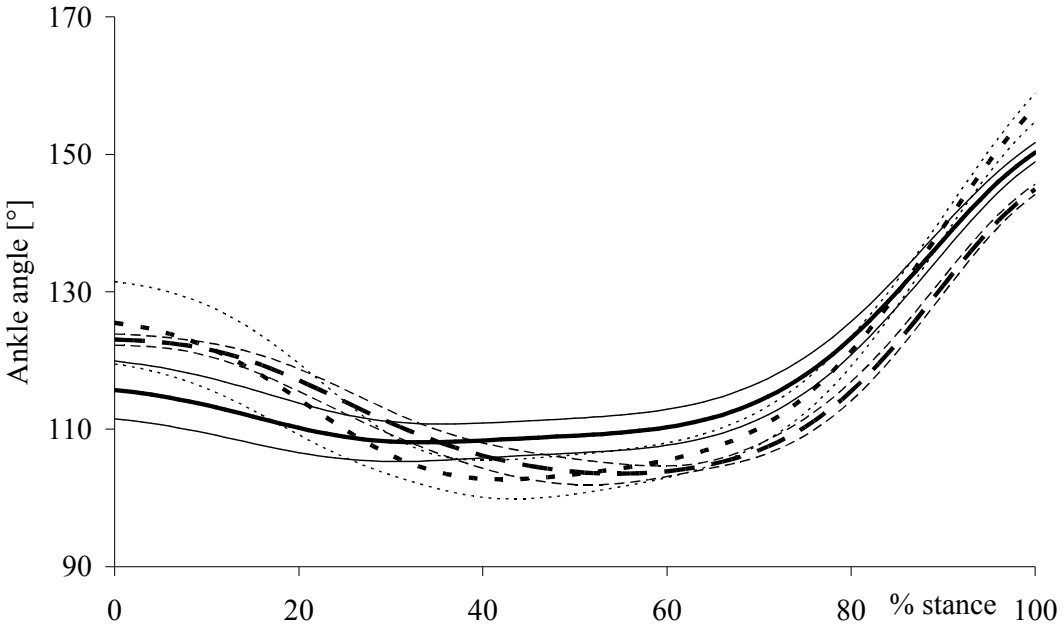

Figure 4.1. Front ankle angle time-histories during the block phase for each sprinter (mean ± *s*; sprinter N = dotted line; sprinter P = solid line; sprinter Q = dashed line).

4.3.2. The first stance phase

At first touchdown, all three sprinters landed with a negative touchdown distance, indicating that their CM was in front of their stance foot MTP at the onset of stance. The mean touchdown distance of sprinter N (-0.265 ± 0.011 m) was greater in magnitude than that of sprinters P (-0.220 ± 0.014 m) and Q (-0.195 ± 0.019 m). Whilst sprinters P and Q exhibited similar mean first stance phase durations (0.190 ± 0.008 s and 0.187 ± 0.003 s respectively; Table 4.5), sprinter N spent less time in stance (0.170 ± 0.004 s). Sprinter N exhibited a slightly higher mean average horizontal external power than sprinter P (by 19 W). However, sprinter P achieved a higher level of first stance phase performance, because when normalised to account for differences in body size, the power production of sprinter P (9.97 ± 0.44) was greater than sprinters N (8.99 ± 2.34) and Q (6.24 ± 1.29). Sprinter P also increased his horizontal velocity to the greatest mean extent (1.30 ± 0.17 $m \cdot s^{-1}$), 0.13 $m \cdot s^{-1}$ greater than the change in velocity achieved by sprinter N and 0.36 $m \cdot s^{-1}$ greater than that of sprinter Q. Sprinter P achieved the greatest mean range of extension at the hip (70 ± 6°) and knee (53 ± 7°) joints during stance, and was more extended at all three stance leg joints by toe-off than sprinters N and Q (Table 4.6).

Table 4.5. Performance descriptors during the first post-block stance phase (mean ± *s*).

	N	P	Q
First stance duration [s]	0.170 ± 0.004	0.190 ± 0.008	0.187 ± 0.003
Horizontal velocity increase [m·s^{-1}]	1.17 ± 0.18	1.30 ± 0.17	0.94 ± 0.10
Average horizontal external power [W]	2126 ± 553	2107 ± 367	1457 ± 300
Normalised power	8.99 ± 2.34	9.97 ± 1.74	6.24 ± 1.29

Table 4.6. Stance leg joint kinematics during the first stance phase (mean ± *s*).

		N	P	Q
Hip	Peak ω [°·s^{-1}]	474 ± 42	516 ± 28	525 ± 19
	Time of peak ω [%]	61 ± 4	59 ± 0	34 ± 28
	Δ angle during phase [°]	66 ± 2	70 ± 6	61 ± 5
	Angle at end of phase [°]	161 ± 2	165 ± 3	160 ± 2
Knee	Peak ω [°·s^{-1}]	526 ± 63	456 ± 40	489 ± 41
	Time of peak ω [%]	0 ± 0	13 ± 27	51 ± 1
	Δ angle during phase [°]	35 ± 4	53 ± 7	42 ± 1
	Angle at end of phase [°]	148 ± 3	152 ± 1	142 ± 3
Ankle	Peak ω [°·s^{-1}]	664 ± 28	583 ± 74	725 ± 40
	Time of peak ω [%]	76 ± 2	78 ± 3	81 ± 1
	- Δ angle during phase [°]	-11 ± 1	-8 ± 1	-11 ± 2
	+ Δ angle during phase [°]	+47 ± 2	+45 ± 5	+52 ± 3
	Angle at end of phase [°]	140 ± 3	148 ± 6	139 ± 1

The Δ joint angle data represent the overall range of extension. For the ankle joint, data are split into initial dorsiflexion (-) and subsequent plantarflexion (+) magnitudes.

Whilst all of the performance outcome data were related to horizontal CM motion, vertical CM motion during the first stance phase was also considered. Sprinter Q exhibited a greater increase in vertical CM position during the first stance phase compared to sprinters N and P, particularly during the latter part of stance (Figure 4.2). By the end of stance, the CM of sprinter Q was on average 0.037 ± 0.005 m higher than its vertical position at touchdown, compared to values of 0.008 ± 0.009 and 0.011 ± 0.007 m for sprinters N and P, respectively.

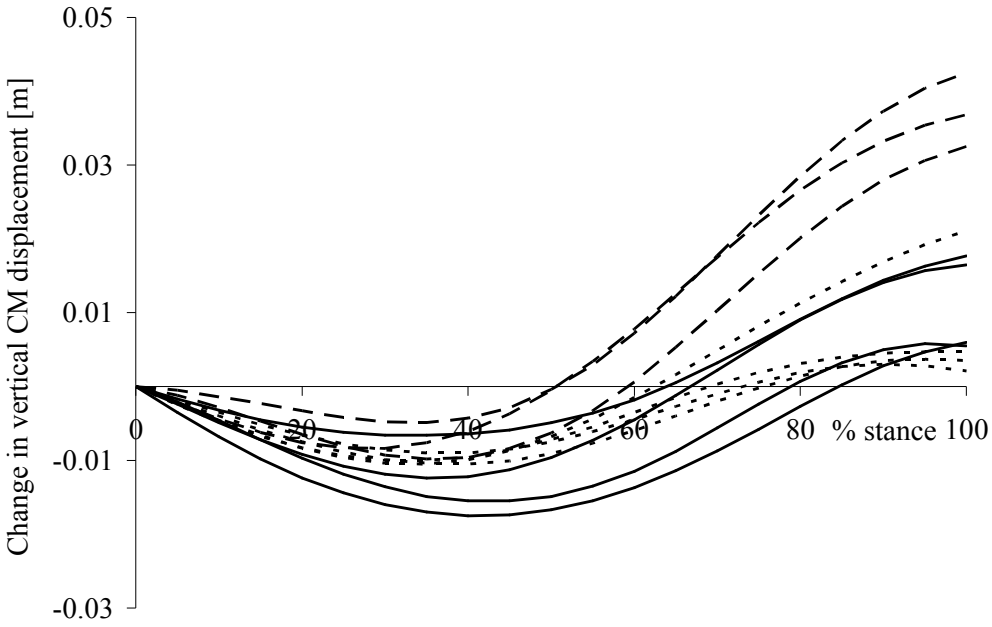

Figure 4.2. Changes in vertical centre of mass displacement (relative to the position at touchdown) during the first stance phase for all trials of each sprinter (sprinter N = dotted line; sprinter P = solid line; sprinter Q = dashed line).

4.4. Discussion

The higher performance levels of sprinter P in both the blocks and the first stance phase (as indicated by his greater normalised power production; Tables 4.2 and 4.5) were consistent with his ability level (i.e. 100 m PB of 9.98 s; 0.24 s and 0.53 s superior to the PBs of sprinters N and Q, respectively). The analysed lower leg angular kinematics provided some insight towards understanding how these greater levels of performance were achieved, and will be discussed separately for each phase, starting with the block phase.

4.4.1. The block phase

Although sprinter P only exhibited slightly higher mean peak angular velocities at both hip joints during the block phase than sprinters N and Q (Tables 4.3 and 4.4), he exhibited a greater mean range of extension at the rear hip (41 ± 8°) compared to sprinters N (31 ± 2°) and Q (26 ± 3°), and at the front hip (116 ± 4°) compared to sprinter N (109 ± 4°). Combined with a shorter mean push phase duration (0.330 ± 0.004 s), sprinter P therefore produced higher average hip extension velocities across the push phase, particularly at the rear hip. It is possible that this increased rear hip

action exhibited by sprinter P may have helped him to achieve the highest levels of performance (Table 4.2) by increasing velocity to a greater extent during the early part of the block phase through the generation of large forces against the rear block. The rear hip extensor muscles (gluteus maximus and biceps femoris) have previously been shown to be the first leg muscles activated during the block phase (Mero and Komi, 1990), and to remain active throughout the duration of rear block contact (Guissard and Duchateau, 1990; see Figure 2.2). The other major muscles in the rear leg activate later and do not contract for as long as the hip extensors (Guissard and Duchateau, 1990; Mero and Komi, 1990). It is therefore highly likely that recruitment of the large musculature surrounding the hip joint plays a key role in the generation of forces against the rear block. As peak horizontal forces in excess of 1500 N have previously been recorded against the rear block (van Coppenolle *et al*., 1989), the contribution of these forces to performance is clear. This may therefore also partly explain the observed tendency for an increased rear hip action (increased range of motion, greater angle at block exit, larger peak angular velocity) to be associated with increased performance amongst the group of trained sprinters in the previous chapter (section 3.3.5).

The importance of rear leg action during the block phase has also been previously suggested by Fortier *et al*. (2005), who recorded greater rear peak horizontal force magnitudes and impulses in a group of sub-10.70 s sprinters compared to their counterparts with 100 m PBs between 10.70 and 11.40 s. In addition to observing greater rear peak horizontal forces in the better group of sprinters, Fortier *et al*. (2005) also observed these sprinters to exhibit a decreased *total* block time. This suggests that increased force generation with the rear leg does not induce a potentially unfavourable increase in total push phase duration. A greater contribution from the rear leg could therefore be one aspect of technique that would assist the generation of large horizontal forces in the least possible time - a requirement for successful block performance advocated by Baumann (1976) and Mero *et al*. (1983), and discussed in Chapter 2. Increased rear leg involvement during the block phase thus appears to be synonymous with a powerful start (i.e. greater velocity achieved in less time) and consequently with higher performance levels. However, whilst the current data add further weight to the previous suggestions that better starters typically exhibit a stronger rear leg action (Payne and Blader, 1971; van Coppenolle

et al., 1989; Lemaire and Robertson, 1990; Fortier *et al*., 2005), it must be remembered that the front leg is the greater contributor to total impulse due largely to its greater contact time and thus its importance cannot be discounted.

In contrast to the more pronounced hip action of sprinter P, sprinter N exhibited a larger and faster extension of the more distal knee and ankle joints during the block phase (Tables 4.3 and 4.4, Figure 4.1). This was particularly true at the front ankle where sprinter N's mean range of plantarflexion (55 ± 4°; Table 4.3 and Figure 4.1) was considerably greater than that of sprinters P and Q (41 ± 3 and 41 ± 2°, respectively), and mean peak angular velocity (597 ± 34°·s^{-1}; Table 4.3) also exceeded that of sprinters P (462 ± 38°·s^{-1}) and Q (464 ± 12°·s^{-1}). The muscles which work to plantarflex the front ankle joint (i.e. gastrocnemius and soleus) have previously been found to be active during the latter part of the block phase (Guissard and Duchateau, 1990; Figure 2.2). The increased plantarflexion of the front leg ankle joint could therefore be associated with the extra 0.016 s on average that sprinter N spent pushing in the blocks compared to sprinter P (Table 4.2), particularly because this plantarflexion occurred at a greater rate towards the end of the block phase (Figure 4.1).

The greater mean amount of time that sprinter N spent in the blocks (0.346 ± 0.005 s) compared to sprinter P (0.330 ± 0.004 s) could partly explain his higher mean block velocity (3.48 ± 0.06 m·s^{-1} vs. 3.43 ± 0.06 m·s^{-1}), as he spent longer generating force against the blocks, thus achieving a larger total horizontal impulse. However, this did not appear to augment overall block performance, as sprinter N generated less normalised average horizontal external block power (5.94 ± 0.16) than sprinter P (6.33 ± 0.27). These data suggest that the higher block velocity achieved by sprinter N was predominantly due to a longer push phase duration, rather than any concurrent increase in average force production. This provides further justification for the use of power rather than velocity as a measure of performance, by providing kinematic evidence from international-level sprinters to reinforce the argument developed in Chapter 3. These data suggested that an increased contribution from the front ankle joint could potentially augment block velocity, but that this occurred at the expense of time spent in the blocks, rather than being a strategy to produce more power. Due to front ankle plantarflexion occurring largely during the late block phase, increasing

this ankle movement will only slightly increase total force generation, since the forces generated during this time are low (Mero *et al*., 1983; Mero and Komi, 1990). Whilst this will increase total horizontal impulse and thus block velocity, the extra time spent generating these low forces does not appear to be beneficial for block phase performance. It must be considered, however, that too little plantarflexion may also not benefit performance. At the front ankle during the block phase, sprinter Q exhibited similar amounts of dorsiflexion to sprinter N, and similar amounts of plantarflexion to sprinter P (Table 4.4) and thus a much smaller overall increase in ankle angle. Sprinter Q may therefore have only obtained a minimal contribution from the front ankle towards block performance, and whilst sprinter N potentially used the front ankle for too great a contribution, an intermediate degree of overall plantarflexion, as exhibited by sprinter P may be optimum for assisting performance.

4.4.2 The first stance phase

During the first stance phase, the leg joints of all three sprinters extended continuously, aside from some initial dorsiflexion at the ankle joint (Table 4.6). This differs from mid-acceleration phase (16 m mark) where some sprinters were observed by Hunter *et al*. (2005) to exhibit knee flexion during early stance, whilst during the maximum velocity phase, an initial period of knee flexion was observed in all four of the well-trained sprinters studied by Bezodis *et al*. (2008). Sprinter P exhibited the greatest mean range of extension at both the hip (70 ± 6°) and knee (53 ± 7°) joints, with sprinter Q showing less hip extension (61 ± 5°) and sprinter N considerably less knee extension (35 ± 4°). Sprinter P was also able to limit the amount of dorsiflexion during early stance (8 ± 1°) compared to sprinters N and Q (11 ± 1° and 11 ± 2°, respectively). It is possible that this may have provided a more stable base against which the aforementioned larger hip and knee extension of sprinter P were augmented.

When the total net extension at all three leg joints were summed (i.e. hip extension + knee extension – ankle dorsiflexion + ankle plantarflexion), sprinter P achieved a mean total extension of 160 ± 13°, greater than that of sprinters N (137 ± 7°) and Q (144 ± 3°). The higher total range of extension at the leg joints of sprinter P likely contributed to his greater performance (normalised average horizontal external power = 9.97 ± 1.74; Table 4.5) by translating his CM over a greater distance and at a

greater rate during stance. However, this concept can be better understood by comparing the techniques and performances of sprinters N and Q who both achieved similar mean amounts of total net leg joint extension.

Despite actually exhibiting a slightly lower total range of net leg joint extension ($137 \pm 7°$ vs. $144 \pm 3°$), sprinter N generated greater mean normalised average horizontal external power (8.99 ± 2.34) than sprinter Q (6.24 ± 1.29) during the first stance phase, which is indicative of higher levels of performance. Also, although sprinter N spent less time in stance (0.170 ± 0.004 s) than sprinter Q (0.187 ± 0.003 s), the greater power production of sprinter N still induced a greater increase in horizontal velocity (1.17 ± 0.18 m·s^{-1} vs. 0.94 ± 0.10 m·s^{-1}). It therefore appeared that the leg extension of sprinter N occurred in such a fashion that it had a more beneficial effect upon performance. The CM displacement data presented in Figure 4.2 revealed that sprinter Q increased the vertical CM position to a greater extent during stance than sprinter N in all trials, including the one trial where sprinter N exhibited an atypically large increase in vertical CM motion during the second half of stance. This suggests that the leg extension of sprinter Q propelled the CM in a more vertical direction, whereas sprinter N was able to limit the increase in vertical CM position and achieve greater horizontal motion, as indicated by the performance data presented in Table 4.5.

Jacobs and van Ingen Schenau (1992) analysed the second stance phase of a sprint, and suggested that during this early part of a sprint, sprinters adopted a specific strategy to augment horizontal motion and prevent unwanted additional increases in vertical motion. It was proposed that an initial rotation of the CM about the stance foot was required, to position the CM further in front of this foot. This was followed by an overall extension of the stance leg, increasing the distance between the stance foot and the CM. These two actions thus directed the body in a more favourable horizontal direction. It would therefore appear that positioning the foot further behind the CM at the onset of stance reduced the requirement for rotation, allowing the hip and knee extension which occurred from touchdown for all sprinters in the current study to be directed more favourably.

Although Jacobs and van Ingen Schenau (1992) did not present any touchdown distances, Mero *et al*. (1983) previously found the point of contact on the foot to be 0.04 m behind the CM at the onset of the second stance phase in a group of trained sprinters. In the same study, Mero *et al*. (1983) reported a mean touchdown distance of -0.13 m from the first stance phase, indicating that the CM was further ahead of the stance foot at the onset of the first stance phase compared to the second. The slightly lower negative magnitudes compared to the mean values presented in the current study can be explained by the fact that Mero *et al*. (1983) measured touchdown distances from the point of foot contact (i.e. the toe). The initial rotation of the CM about the stance foot prior to leg extension may therefore be less important for performance during the first stance phase (than during the second and all of the remaining steps) if a large negative touchdown distance (stance foot further behind the CM at touchdown) can be achieved. The mean difference in touchdown distance between sprinters N and Q (0.070 m) may therefore partly explain their contrasting performance success. As the CM of sprinter N was further in front of the stance foot MTP at touchdown than that of sprinter Q, the subsequent leg extension of sprinter Q would have caused a greater (and earlier) increase in the vertical component of CM motion (Figure 4.2). In contrast, sprinter N was in a more favourable position at touchdown, and despite a shorter stance phase duration and less total leg extension than sprinter Q, this extension was directed in a more advantageous horizontal direction and was thus more beneficial for performance.

Although the CM motion is determined due to the laws of projectile motion once a sprinter leaves the blocks, the individual segments can still be repositioned around the CM during the subsequent flight phase. The differences in touchdown distance, and subsequent differences in performance, between sprinters N and Q during the first stance phase suggest that it may be beneficial to attempt to 'pull' the foot back relative to the CM during flight in order for leg extension during the subsequent stance phase to propel the sprinter in a more favourable, horizontal direction.

4.4.3. Conclusion

The results presented in this chapter revealed some interesting angular kinematic aspects of technique which appeared to influence performance. During the block phase, increased extension at the hip joints, particularly in the rear leg, appeared

favourable for improved performance, whereas an increased front ankle motion appeared less beneficial. The performance data also reinforced the ideas developed in Chapter 3 regarding the limitations associated with velocity as a performance measure. An analysis of the joint angular kinematics during the first post-block stance phase revealed differences in technique between international-level sprinters which could potentially affect performance. It appeared that landing with the stance foot further behind the CM was beneficial for performance, since it allowed the subsequent leg extension to occur in a more favourable horizontal direction.

4.5. Chapter summary

This chapter investigated the techniques used by international-level sprinters during both the block phase and the first post-block stance phase, attempting to associate aspects of their techniques with their individual performance levels. Data were collected at coach-led training sessions in an attempt to obtain high-performance data which could be used to address research question iii - *which kinematic technique variables are associated with higher levels of sprint start performance?* An increased push with the rear leg in the blocks, particularly from the hip, was suggested to assist the generation of average horizontal external power during the block phase. Whilst greater motion at the more distal joints (particularly the front leg ankle joint) appeared to potentially assist an increase in block velocity, such a strategy was identified as being detrimental for overall performance (i.e. average horizontal external power production). These data illustrated an aspect of technique which would be identified as being beneficial for performance based on block velocity, yet detrimental when based on average horizontal external block power. This was due to the reliance upon the low forces generated during the late part of the block phase as the ankle plantarflexed. These specific kinematics which were associated with an unfavourable increase in block velocity in international-level sprinters therefore further addressed research question ii - *what is the most appropriate measure of sprint start performance, and can it be accurately quantified in a field environment?* These empirical data thus reinforced the theoretical justification presented in Chapter 3 for the use of average horizontal external power as a measure of performance.

The kinematic data collected from the first post-block stance phase were also used to address research question iii. These data revealed that a larger extension of each of

the leg joints during stance potentially appeared to benefit performance. However, it was suggested that the direction of leg extension was also important for performance, since the primary aim in sprinting is to enhance horizontal translation. Landing with the stance foot further behind the whole body CM at touchdown may therefore have improved performance by initiating stance from a position which facilitated the influence of leg extension upon horizontal, rather than vertical, motion. It could not be determined, however, whether positioning the foot further back relative to the CM may eventually inhibit performance beyond a limit. This would therefore be an interesting area worthy of further investigation.

The data presented in this chapter provided an interesting insight into the differences in the kinematic aspects of technique within a group of three international-level sprinters during the first stance phase. However, whilst the analysis increased the understanding of technique during this important part of a sprint, it remained unclear how these techniques (and ultimately the levels of performance) were achieved. An analysis of the individual joint kinetics alongside kinematics from the first stance phase would therefore assist the understanding of the causes of these techniques, furthering the current body of knowledge by addressing research question iv - *how are the more advantageous sprint start kinematics achieved, and why do they lead to improved performance?*

CHAPTER 5: KINETIC ASPECTS OF SPRINT START TECHNIQUE AND THEIR ASSOCIATIONS WITH KINEMATICS AND PERFORMANCE

5.1. Introduction

The kinematic analysis presented in Chapter 4 advanced the current understanding of the techniques used by international-level sprinters during the first stance phase and how individual differences could influence performance. However, since observed kinematics are the result of a complex series of muscular contractions, the causes of these techniques should be investigated. A kinetic analysis is therefore required to determine the underlying causes of motion (Winter, 1990). By concurrently collecting video and force platform data, an inverse dynamics approach can be utilised in order to calculate the individual joint kinetics: resultant joint moments, joint power and joint work. The observed kinematics and resulting performance can then be attributed to work being performed by the muscle groups crossing specific joints during certain parts of the stance phase.

Joint kinetics have previously been documented in sprint research, although the majority of studies have been undertaken during the maximum velocity phase (e.g. Mann and Sprague, 1980; Mann, 1981; Bezodis *et al*., 2008) or the mid-acceleration phase (e.g. Johnson and Buckley, 2001; Hunter *et al*., 2004). To the author's knowledge, only one study (Jacobs and van Ingen Schenau, 1992) has provided detailed joint kinetics during early acceleration, from the second stance phase. Also, joint work has only previously been reported at maximum velocity (Bezodis *et al*., 2008), and the results presented in Chapter 4 revealed that the joint movement patterns are distinctly different during the first stance phase when a sprinter is attempting to rapidly accelerate. Although the aforementioned studies have reported resultant joint moments and powers, few have attempted to associate them with performance. Joint kinetics are directly representative of the rotational motion caused at joints, whereas performance in sprinting is essentially a horizontal concept - who can cover a specific horizontal distance in the least possible time? Therefore, it is important to understand how the observed rotational joint actions contribute to translation, particularly of the whole body CM.

In order to address research question iv - *how are the more advantageous sprint start kinematics achieved, and why do they lead to improved performance?* - the aim of this study was to analyse the joint moments, powers and work produced by international-level sprinters during the first step of a sprint. This kinetic analysis can be used to address research question iv by answering several specific questions, namely: What are the net joint moments and powers acting at the stance leg joints during the stance phase and preceding swing phase? Which joints generate energy to accelerate the body? How do these joint kinetics contribute to performance? This therefore allows the previously identified kinematic aspects of technique to be explained in greater detail, and the kinetic aspects of technique which contribute to the observed motion, and ultimately to performance, to be identified.

5.2. Methods

5.2.1. Participants

Three sprinters, all of whom had reached the final of European or World Indoor Championships within the last two years, provided consent to participate in this study. Relevant characteristics for the sprinters are presented in Table 5.1. Data were collected at the National Indoor Athletics Centre, Cardiff in the pre-competition phase of the indoor season. The data collection session was designed to coincide exactly with the sprinters' training schedule, so that external validity was maintained. This data collection took place approximately 18 months after the data collection in Chapter 4, by which time the 100m PBs of sprinters N and Q had improved by 0.08 s and 0.23 s, respectively.

Table 5.1. Descriptive characteristics for the three sprinters.

	N	Q	R
Age [years]	21	20	26
Gender	M	M	F
Mass [kg]	82.6	86.9	60.5
Height [m]	1.81	1.78	1.76
60 m PB [s]	6.55	6.63	7.84*
100 m PB [s]	10.14	10.28	12.72*

* Indicates PB for hurdles at the same distance.

5.2.2. Equipment set-up

A start line of 0.05 m thickness was affixed across one lane of an indoor running track so that the sprinters would land with their first ground contact on a 0.900 × 0.600 m force platform (Kistler, 9287BA, Kistler Instruments Ltd., Switzerland), sampling at 1000 Hz. The platform was covered with a fitted piece of the synthetic track surface, which was 11 mm thick and was firmly affixed with double-sided adhesive tape. From pilot testing with the three sprinters, it was determined that the start line should be placed 0.06 m from the nearest edge of the force platform so that contact would occur near the centre of the platform. Three high-speed digital video cameras (Motion Pro®, HS-1, Redlake, USA) were located at specific positions in order to obtain the relevant video footage for analysis (Figure 5.1).

One camera (camera 1) was positioned to capture full body kinematics during the block and first flight phases, whilst another (camera 2) was positioned to capture full body kinematics during the first stance phase and start of the second flight phase. These two cameras operated at 200 Hz and were positioned 25.00 m away from the centre of the running lane (mid-zoom range), perpendicular to the direction of the sprint, and with the lens centre 1.00 m above the ground. Camera 1 was located 0.25 m in front of the start line, whilst camera 2 was located 0.95 m in front of the start line. An area of 2.00 m horizontally × 1.60 m vertically was calibrated for each of these two cameras, using a rectangular calibration frame positioned inside a field of view 2.50 m wide, as detailed in Chapter 3. Both cameras collected images at a resolution of 1280 × 1024 pixels with a 1/1000 s shutter speed and an open iris. A third camera (camera 3), operating at 1000 Hz, was positioned to capture detailed lower leg video footage during the first stance phase. This camera was located 9.00 m away from the centre of the running lane, perpendicular to the direction of the sprint, 0.20 m above the ground. The camera was positioned 0.51 m in front of the start line so as to be directly in line with the centre of the force platform, and operated with a 1/1000 s shutter speed and an open iris. An area of 0.720 m horizontally × 0.490 m vertically was calibrated inside a field of view encompassing the entire width of the force platform (i.e. 0.900 m), and images were collected at a resolution of 800 × 600 pixels. The data from camera 3 were used to obtain high-speed, high-resolution images of ground contact, which were subsequently utilised in the development and evaluation of a simulation model in Chapter 6. An additional

8400 W of lighting was positioned around the capture area in order to increase the brightness of the collected images.

The three digital video cameras were synchronised to one another, and to the force platform, by a custom designed trigger system. Data collection was initiated by the pressing of a trigger button which sent a signal to each of the cameras and to the force platform. All devices initiated data capture upon the next epoch after receiving this trigger signal. Camera 3 (1000 Hz) and the force platform (1000 Hz) therefore began collecting data within 0.001 s of the trigger signal, whilst cameras 1 and 2 (200 Hz) began collecting data within 0.005 s. In order to synchronise all devices to within 0.001 s, a series of 20 LEDs (Wee Beastie Ltd, UK) were placed in the view of both of the 200 Hz cameras. At each 0.001 s interval after the trigger signal, one LED was illuminated until all were activated 0.020 s after the trigger signal. The data collected with cameras 2 and 3 could thus be synchronised based on the number of LEDs illuminated in the first frame of the collected video files. The trigger signal was sent to a sounder device which acted as an auditory start signal to which the sprinters responded, representative of that occurring in competitive situations.

5.2.3. Data collection

Following a coach-directed warm-up, each sprinter completed a series of four (sprinter R) or five (sprinters N and Q) maximum effort sprints to 30 m, commencing from starting blocks. The blocks were adjusted to the preference of each sprinter, who wore their own spiked shoes. Each trial was initiated by an experienced starter, who followed standard '*on your marks*' and '*set*' commands by pressing the custom trigger button to simultaneously initiate data collection and activate the sounder. After each trial, sprinters were allowed their normal recovery (about 8-10 minutes) in order to facilitate performance without the effects of fatigue.

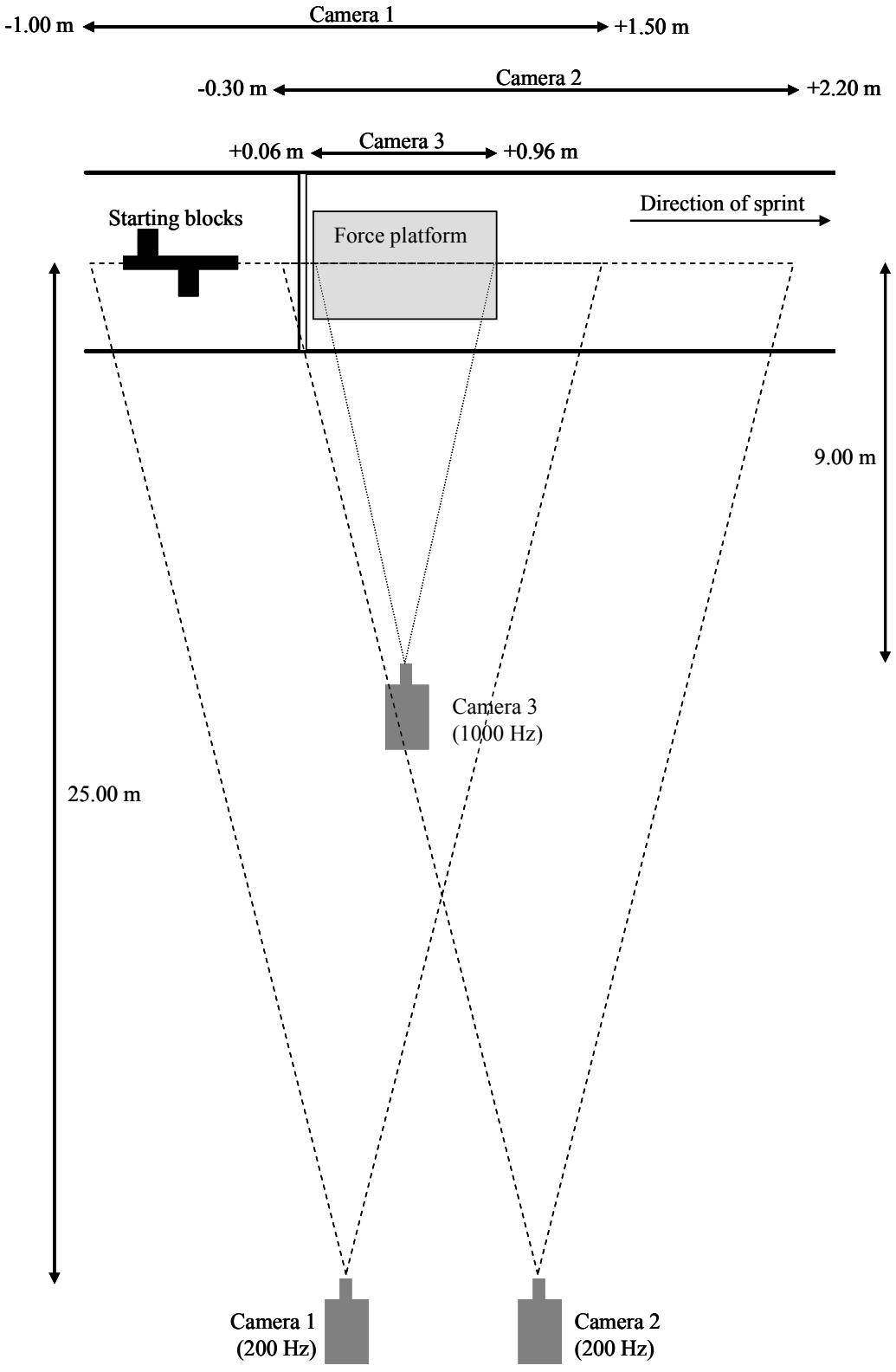

Figure 5.1. Plan view of the data collection set-up, including field of view limits (relative to the start line) for each of the three cameras (not to scale).

5.2.4. Data processing

The raw video clips from camera 1 were viewed to determine the instants of movement onset, rear foot off and block exit, as defined in Chapter 3 (movement onset was first visible head movement, rear foot off and block exit were the first frame in which the foot had clearly lost contact with the block). Other events and phases were defined as follows:

- First stance touchdown: identified to the nearest ms from the force platform data as the first frame in which the raw vertical force data exceeded, and remained above, 2 SD of the mean value during the zero load period.
- Toe-off: identified as the next frame in which the raw vertical force data fell back below this 2 SD threshold.
- Rear leg push duration: the time from movement onset to rear foot off.
- Block phase duration: the time from movement onset to block exit.
- First flight duration: the time from block exit to first stance touchdown.
- First stance duration: the time from first stance touchdown to first stance toe-off.

As not all of the sprinters started with the same leg in the rear block, the legs were referred to as front and rear block leg for the block and first flight phases, and then subsequently as stance and swing leg for the first stance phase (therefore the rear block leg became the stance leg and the front block leg became the swing leg).

The raw video files were imported into digitising software (Peak Motus®, v. 8.5, Peak Performance, USA). All digitising was performed at full resolution, and with a zoom factor of 2.0, allowing points to be digitised at every half-pixel. The resolution of measurement was therefore 0.00098 m for cameras 1 and 2, and 0.00056 m for camera 3. Using the data from cameras 1 and 2, 20 specific anatomical points and joint centres were digitised (vertex, C7, shoulder, elbow, wrist, hip, knee, ankle and MTP joint centres, fingertips and halluces). For camera 1, digitising commenced one frame prior to movement onset, and continued until 10 frames after first touchdown. For camera 2, digitising commenced 10 frames prior to touchdown and continued until 10 frames after toe-off. From camera 3, the MTP joint centre and hallux of the touchdown foot were digitised from 10 frames prior to touchdown until 10 frames after toe-off. The horizontal and vertical scale factors calculated from each camera's

calibration frame were applied to align scale the raw digitised co-ordinates. All raw displacement time-histories were expressed relative to the start line at ground level as the origin of the global co-ordinate system. These raw displacement data were then exported from Peak Motus®, and all of the subsequent data analysis took place using custom routines developed in Matlab™ (v. 7.4.0, The MathWorks™, USA).

For reasons described subsequently in the inverse dynamics section of these methods (pages 123-130), a single cut-off frequency was required for the filtering of all kinematic data. It was decided that this should be based on minimising the signal to noise ratio in the stance leg. Therefore, for all trials the raw horizontal and vertical displacement time-histories from the stance leg (toe, MTP, ankle, knee, hip) separately underwent residual analyses in order to determine the cut-off frequency which provided the most appropriate degree of minimal signal distortion and maximum noise removal (Winter, 1990). The mean value from all of these trials determined optimal cut-off frequencies (24 Hz) was therefore applied to all 40 kinematic time-histories bi-directionally through a fourth-order Butterworth digital filter (Winter, 1990). Any co-ordinate time-histories which did not contain 10 additional frames of data due to a particular landmark not being in the field of view for a full 10 frames either side of contact were padded via reflection prior to filtering in order to reduce the effects of any endpoint error (Smith, 1989). Potential endpoint error in the camera 1 data prior to movement onset was alleviated by padding the digitised data using 10 replications of the last 'set' position frame prior to movement onset, for reasons explained in Chapter 3.

The filtered displacement data were combined with individual specific segmental inertia data (Yeadon, 1990; see Appendix B for individual values). These were calculated from 95 anthropometric measurements taken on each sprinter by an experienced experimenter. To account for the mass of the spiked shoes 0.20 kg was added to the mass of each foot (e.g. Hunter *et al*., 2004; Bezodis *et al*., 2008). The division of spike mass between the two foot segments was determined directly from the ratio of forefoot:rearfoot length, assuming an equal division of mass across the length of the spike (e.g. if forefoot length was 0.08 m and rearfoot length was 0.16 m, 0.067 kg was added to the forefoot and 0.133 kg to the rearfoot). The whole body CM displacement time-histories were consequently calculated from the

segmental data using a summation of segmental moments approach, and joint angles were determined. Absolute segment angles were also determined, with an angle of 0° representing horizontal orientation, and positive increases in segment angle relating to an anti-clockwise rotation of the proximal endpoint about the distal endpoint (when viewed from the right hand side with the sprinter running from left to right).

Extension at the hip and knee joints, and plantarflexion at the ankle and MTP joints, were defined as positive (Figure 5.2). A plantarflexion/dorsiflexion definition (e.g. Stefanyshyn and Nigg, 1997) was used at the MTP joint rather than the sometimes used flexion/extension definition in order to coincide with ankle motion (i.e. plantarflexion at both the ankle and the MTP joint related to a downwards rotation of the distal endpoint). All linear and angular displacement time-histories were subjected to second central difference calculations (Miller and Nelson, 1973) in order to derive their corresponding velocity time-histories. Block exit velocity was calculated using the *flight polynomial* method, as described previously in section 3.2.3. Average horizontal external block power was calculated from this velocity value and the duration of the push phase against the blocks, using equation 3.4 (page 60).

Joint angles and angular velocities at specific events (set position, block exit, touchdown and toe-off) were identified. As touchdown and toe-off were defined at 1000 Hz from the force platform data, the time-histories of the kinematic variables reported at these events were resampled at 1000 Hz using an interpolating cubic spline. This provided a more appropriate representation of the exact value at touchdown/toe-off, as the first 200 Hz video frame could occur up to 4 ms after touchdown/toe-off. Pilot work revealed that this was necessary, because in trials where this 4 ms difference did exist at touchdown, variables such as horizontal toe velocity and knee angular velocity were different between the more accurate interpolated value and the slightly delayed 200 Hz value by as much as 0.76 $m \cdot s^{-1}$ and 91° $\cdot s^{-1}$, respectively.

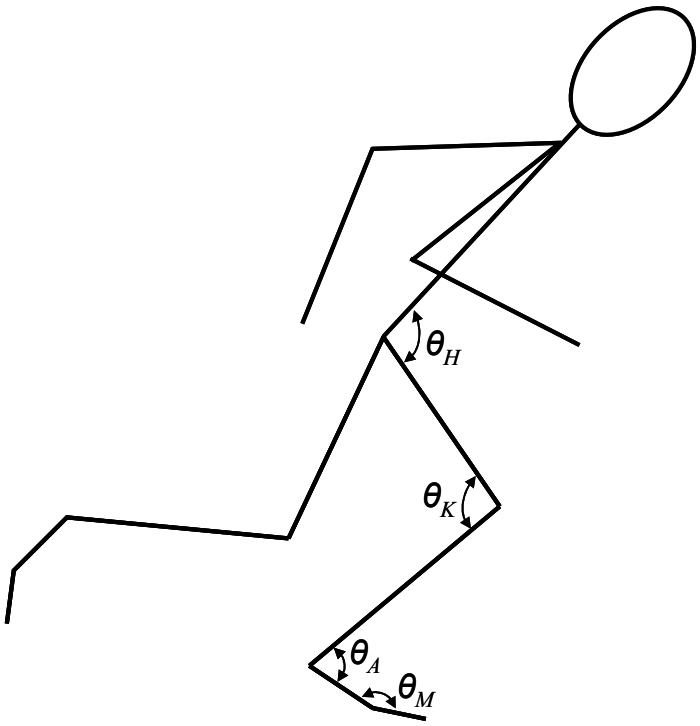

Figure 5.2. Convention used to describe positive (extension/plantarflexion) changes in leg joint kinematics and kinetics.

Peak joint angular velocities during the block, flight and stance phases were identified, as were the times at which these peak values occurred. These times were expressed as percentages of the total phase duration to facilitate inter-trial and inter-individual comparison. Step length was calculated as the difference between the horizontal displacement of the front block hallux one frame prior to block exit, and the horizontal displacement of the rear block hallux at first stance touchdown (from camera 1 data resampled at 1000 Hz). The difference between this latter co-ordinate and the horizontal co-ordinate of the CM during the same touchdown frame was taken as a measure of touchdown distance, with a positive value representing the stance foot hallux ahead of the CM at touchdown. The instantaneous velocity of the stance foot hallux at touchdown was also identified from the camera 1 data resampled at 1000 Hz, and provided a measure of foot touchdown velocity. Hallux data were used as opposed to the MTP (as used in chapters 3 and 4) since the hallux was identified as the landmark closest to the point which made contact with the track. To aid readability, absolute values of all variables were presented. For certain inter-subject comparisons, selected normalised variables were also presented to account for the effects of body stature on their magnitude (Hof, 1996; Appendix A).

For all variables to be reported solely from the force data, the raw horizontal and vertical force data were passed bi-directionally through a fourth-order Butterworth digital filter (Winter, 1990) with a cut-off frequency of 150 Hz (the mean value from residual analyses of all trials). This removed the majority of the high frequency noise without markedly affecting the magnitude of the impact peaks which occurred shortly after touchdown. Peak forces during the braking and propulsive phases were identified from the filtered horizontal and vertical force data. The horizontal braking, propulsive and net propulsive impulses were calculated through numerical integration (Trapezium Rule) of the horizontal force data, and the net vertical impulse was calculated through integration of the vertical force data after the removal of body weight (determined from a static trial). Using the horizontal impulse data, the changes in horizontal velocity across each frame were calculated, and combined with the initial velocity previously calculated from camera 1 in order to obtain absolute instantaneous horizontal velocity values throughout stance. The product of the absolute horizontal velocity and the horizontal force time-histories yielded the horizontal external power time-history, from which the mean value was calculated and normalised (Hof, 1996; Appendix A).

The centre of pressure data were calculated from the separate channels of data recorded through the force platform. This allowed adjustment of the a_{z0} value (the distance between the force platform surface and the *x*-*y* plane) to account for the thickness of the track surface affixed to the force platform, and was performed using the following equations:

$$M_x = s_x \cdot (F_{z1} + F_{z2} - F_{z3} - F_{z4}) \qquad [5.1]$$

$$M_y = s_y \cdot (-F_{z1} + F_{z2} + F_{z3} - F_{z4}) \qquad [5.2]$$

$$ax = (F_x \cdot a_{z0} - M_y) / F_z \qquad [5.3]$$

$$ay = (F_y \cdot a_{z0} + M_x) / F_z \qquad [5.4]$$

The variables F_{z1} to F_{z4} represented the four vertical force data channels, s_x and s_y were the distances between the sensors and the *x*- and *y*-axes, M_x was the platform moment about the *x*-axis, M_y was the platform moment about the *y*-axis, and *ax* and *ay* were the centre of pressure co-ordinates in the *x* and *y* direction, respectively. For the force platform used in this study (Kistler, 9287BA, Kistler Instruments Ltd., Switzerland), s_x and s_y were fixed values of 210 and 350 mm, respectively. Without any additional material on the force platform surface, a_{z0} was -52 mm. Thus with the additional piece of track surface, which was 11 mm thick, a_{z0} was adjusted to -63 mm.

Inverse dynamic analysis of joint kinetics

A 2D inverse dynamics analysis was undertaken to determine the resultant joint moments acting about the four joints of the stance leg during the first stance phase. Although the MTP joint was included in one of the earliest investigations of joint kinetics (Elftman, 1940), it has not been widely used in subsequent joint kinetics analyses. Since Elftman (1940) proposed that the muscles about the MTP joint exert moments large enough to warrant separate consideration, to the author's knowledge the only study to have included an MTP joint when calculating joint kinetics during sprint running was that conducted by Stefanyshyn and Nigg (1997), who identified a mean peak plantarflexor moment of 112 Nm. This suggests that the MTP joint could play an important role in sprinting, a notion that was recently reinforced by Krell and Stefanyshyn (2006), and is thus an essential joint to include in kinetic analyses of the lower leg in sprinting. Ignoring this joint will therefore likely create an artificially high ankle joint moment due to the omission of a plantarflexor moment at the distal end of the rearfoot segment. This will also have consequent effects on the calculated knee and hip joint moments, and the MTP joint was therefore incorporated into the current analysis.

Joint kinetics were calculated starting from the external ground reaction forces measured between the foot and the ground, and continuing up the limb to calculate the forces acting at the MTP, ankle, knee and hip joints. The raw horizontal and vertical force data were downsampled to 200 Hz by identifying the frames which corresponded temporally to a frame of video data, and removing the four redundant force data frames between each of these points across the entire length of the force

data. These downsampled force data could then be combined with the filtered joint centre displacement time-histories obtained from camera 2, and the appropriate individual specific segmental inertia data (Yeadon, 1990; Appendix B) to calculate the resultant joint moments. Resultant joint moments were also calculated for the same leg from the instant it left the rear block until the instant of touchdown (i.e. the rear leg swing phase) using the joint centre displacement time-histories obtained from Camera 1. Forces at the toe were thus known (i.e. zero) during this phase, allowing inverse dynamics calculations to be carried out.

The first part of the analysis involved the calculation of the internal joint forces acting at each of the four leg joints, based upon Newton's Second Law of Motion:

$$\sum F = m \cdot a \qquad [5.5]$$

A free body diagram (Figure 5.3) was used to summarise all forces acting on the n^{th} segment. With known segmental accelerations, the unknown joint reaction forces at the proximal end of the segment could thus be calculated.

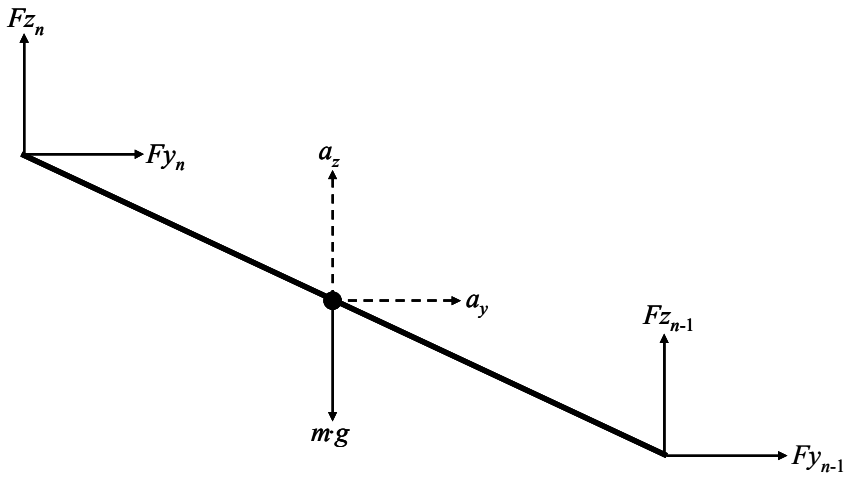

Figure 5.3. Free body diagram of the n^{th} segment of the leg, including all forces acting on the segment, and the resulting accelerations.

The horizontal and vertical internal joint forces were then calculated in a distal to proximal direction. This therefore commenced at the known ground reaction forces acting at the centre of pressure during stance, and at the toe during flight where the external forces acting were zero. Segmental CM accelerations were calculated

through double differentiation of the respective displacement time-histories, using second central difference equations (Miller and Nelson, 1973). The internal joint forces were thus calculated using the following equations:

$$Fy_n = m \cdot a_y - Fy_{n-1} \qquad [5.6]$$

$$Fz_n = m \cdot a_z - Fz_{n-1} + m \cdot g \qquad (g = 9.81 \text{ m·s}^{-2}) \qquad [5.7]$$

For the calculation of resultant joint moments at each end of the n^{th} segment, Newton's Second Angular Analogue was used (equation 5.8). This states that the sum of all moments (M) acting about a segment is equal to the product of its moment of inertia (I) and its angular acceleration (α):

$$\sum M = I \cdot \alpha \qquad [5.8]$$

A further free body diagram (Figure 5.4) was used to summarise all of the moments acting on the n^{th} segment.

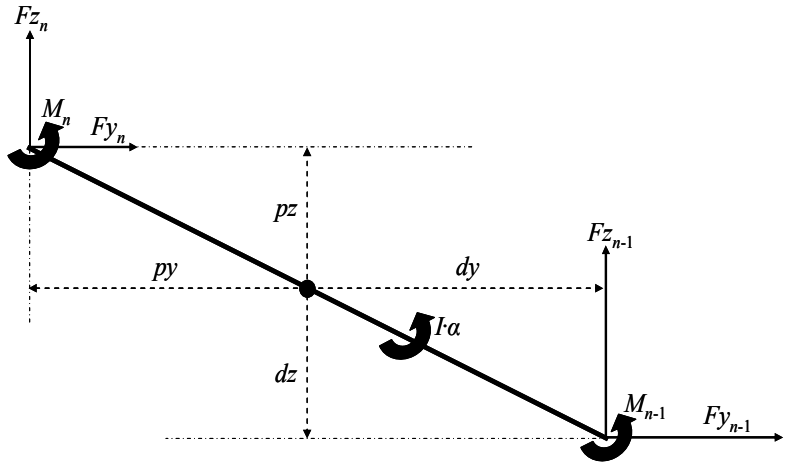

Figure 5.4. Free body diagram of the n^{th} segment of the leg, including all moments acting on the segment, and the resulting angular acceleration.

Again starting at the distal end of the system, where the moment is known, resultant joint moments were calculated at each of the leg joints, using the following equation [5.9] based on the sum of all moments acting about the segment CM:

$$M_{n-1} + M_n + (Fz_{n-1} \cdot dy) + (Fy_{n-1} \cdot dz) - (Fz_n \cdot py) - (Fy_n \cdot pz) = I \cdot \alpha$$

where *dy*, *dz*, *py* and *pz* represent the proximal (*p*) and distal (*d*) moment arms in the horizontal (*y*) and vertical (*z*) directions. The resultant joint moments were reported using the same convention as that used for the angular kinematics (Figure 5.2), with extension/plantarflexion defined as positive. The power at each joint (*P*) was then calculated as the product of the resultant moment (*M*) and the angular velocity (ω):

$$P = M \cdot \omega \qquad [5.10]$$

The power time-histories for the rear leg swing phase and the first stance phase were divided into periods of continuous positive or negative power. Based on the convention used by Winter (1983), these power phases were primarily defined by the joint at which they occurred (M = MTP joint, A = ankle joint, K = knee joint, H = hip joint). Subscript terms were used to define whether the phases related to swing/flight ($_F$) or stance ($_S$). Superscript terms were used to specify whether these were phases of power generation (e.g. $^{1+}$, $^{2+}$) or power absorption (e.g. $^{1-}$, $^{2-}$), with the numbers relating to the order of the phases. For example, K_F^{2+} relates to the second power generation phase at the knee joint during the swing phase. Ignoring any minor fluctuations, four major phases were defined at the knee during the swing phase (i.e. from rear foot off until touchdown). These were phases of positive (K_F^{1+}), negative (K_F^{1-}), positive (K_F^{2+}) and finally negative (K_F^{2-}) power (Figure 5.5a). At the hip joint, three phases were defined: an initial positive power phase (H_F^{1+}), a brief negative power phase (H_F^{-}), and a further positive power phase (H_F^{2+}; Figure 5.5b). Power production during the swing phase at the ankle and MTP joints was negligible and thus power phases at these joints were not defined in the current analysis.

The major power phases were also identified at each joint during stance. Ignoring minor initial fluctuations at the MTP joint, phases of negative (M_s^-; A_s^-; K_s^-) followed by positive power (M_s^+; A_s^+; K_s^+) were defined at the MTP, ankle and knee joints, respectively (Figures 5.6a-c). The hip joint power time-history was divided into an initial phase of positive power (H_s^+) followed by a phase of negative power (H_s^-;

Figure 5.6d). The amount of work done at each joint during each power phase was calculated as the time-integral (Trapezium Rule) of the joint power time-history during the appropriate time period. This yielded the total amount of energy absorbed (during negative power phases) and generated (during positive power phases) at each of the joints. Similar to the kinematic data, several kinetic variables were normalised to facilitate inter-subject comparison where appropriate (Hof, 1996; Appendix A)

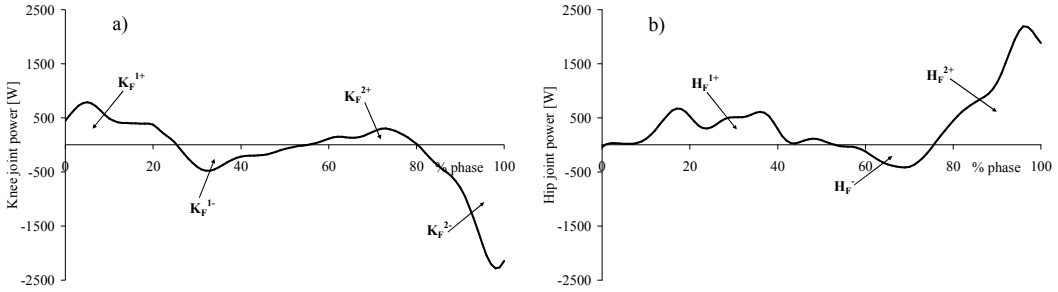

Figure 5.5a-b. Definition of power phases at the knee and hip joints during the rear leg swing phase. This phase was abbreviated by a subscript F (for flight), as S was used for stance. Figures are taken from one individual trial, but are representative of the typical power phases for all 3 sprinters.

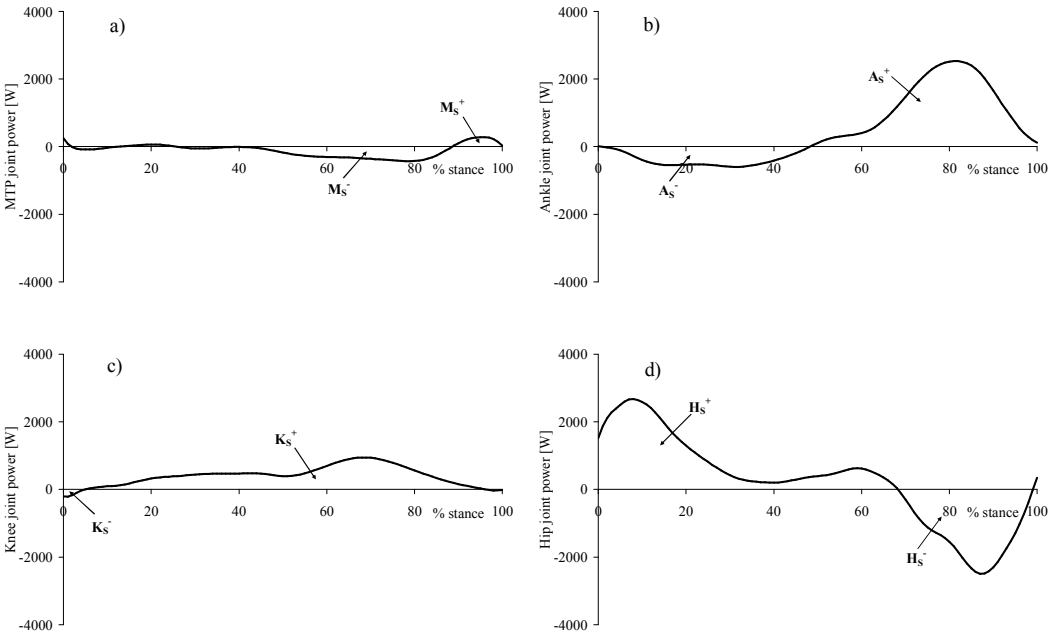

Figure 5.6a-d. Definition of power phases at each of the leg joints during the stance phase. Figures are taken from one individual trial, but are representative of the typical power phases for all 3 sprinters.

Processing of raw input data for inverse dynamics analyses

Inverse dynamic analyses require kinematic, kinetic and segmental inertia data, and thus the accuracy of these data is paramount for appropriate joint kinetic data to be obtained. Inertia data, and in particular kinematic data, have been shown to have the largest influence on joint kinetic outputs (Challis and Kerwin, 1996; Riemer *et al*., 2008). This informed the decision to use individual specific inertia data, and two high-resolution video cameras, each with a relatively small field of view. However, despite this approach, the raw kinematic data obtained from any manual video analysis will unavoidably contain some level of noise, due largely to random operator error when identifying anatomical landmarks (Wood, 1982). As higher derivatives are calculated, the noise is amplified and can thus have an increasingly detrimental effect on velocity and acceleration time-histories. Both linear (equations 5.6 and 5.7) and angular (equation 5.9) segmental accelerations are required for inverse dynamic analyses, and thus any noise in these time-histories will largely affect the determined joint kinetics.

The smoothing of kinematic input data is thus of critical importance, with low-pass digital filters commonly used to reduce this noise which typically dominates the higher end of the frequency spectrum, in contrast to the lower-frequency true signal of interest (Winter, 1990). Noise and true signal do not, however, occur at separate, distinct frequencies; instead some overlap exists. It must therefore be considered that low-pass filtering in an attempt to reduce the effects of noise could have one of two detrimental effects on the filtered signal. The use of too high a cut-off frequency will not remove sufficient noise, and the acceleration time-histories and calculated joint kinetics will be overly noisy and difficult to accurately interpret. Too low a cut-off frequency will result in much smoother acceleration time-histories, but at the expense of the higher frequency content of the true acceleration signal being omitted. In previous sprinting joint kinetics research, reported cut-off frequencies for kinematic data have ranged from 8 Hz (Hunter *et al*., 2004) to 20 Hz (Jacobs and van Ingen Schenau, 1992; Belli *et al*., 2002). The kinetic data, which are typically obtained through a force platform, will also contain some degree of noise. The previous sprinting joint kinetics studies which have reported the filtering methods applied to kinetic data have all used cut-off frequencies of 75 Hz (Jacobs and van

Ingen Schenau, 1992; Johnson and Buckley, 2001; Hunter *et al*., 2004), considerably higher than the cut-off frequencies applied to the kinematic data.

Bisseling and Hof (2006) suggested that applying different cut-off frequencies to the raw force and kinematic data used in an inverse dynamics analysis can create artefacts in the resulting joint kinetic data. When investigating the knee joint moment during a landing impact phase, they proposed that in reality the contribution of the ground reaction force was neutralised by the moments generated by high segmental accelerations. When they filtered both the kinematic and force data at 100 Hz they observed a gradual, but slightly noisy, rise in the resultant knee joint extensor moment towards a peak value (~300 Nm) approximately 80 ms after landing. Secondly, when the same kinematic data were filtered at a lower cut-off frequency (20 Hz) than the force data (100 Hz), a large extensor peak (~150 Nm) occurred approximately 20 ms after landing. This was followed by a brief period of flexor dominance 10 ms later, before the main extensor peak was reached around 80 ms after landing. However, when the force and video cut-off frequencies were again matched, this time at 20 Hz, the resultant knee joint moment was very similar in overall shape and magnitude to that observed when filtering both force and video at 100 Hz. The only slight difference was that it was smoother, most likely due to a lower level of noise in the kinematic acceleration data due to the lower cut-off frequency. Bisseling and Hof (2006) suggested that the real segmental accelerations contained frequencies considerably greater than 20 Hz, and that by low-pass filtering the kinematic data at 20 Hz, they had removed some of the true acceleration data. This therefore led to problems when the concurrently collected force data were filtered at 100 Hz, as the higher frequency kinematic data were removed, despite these being produced as a result of the high frequency kinetic data, which were maintained.

Filtering the video data at a lower cut-off frequency than the force data thus creates inconsistencies in the frequency content of the two data sets (van den Bogert and de Koning, 1996; Bisseling and Hof, 2006; van den Bogert and Su, 2008). This can lead to false impact joint moments due to the removal of the high frequency segmental accelerations which corresponded to the high frequency impact ground reaction forces (Bisseling and Hof, 2006). It has therefore been proposed that both the video

and force data used in an inverse dynamics analysis should be filtered using the same cut-off frequency (van den Bogert and de Koning, 1996; Bisseling and Hof, 2006; van den Bogert and Su, 2008). This maintains only data of corresponding frequency content, and thus no mismatch is created by removing the high frequency acceleration data associated with the high frequency forces at impact. Ideally, the cut-off frequency would be as high as possible in order to maintain as much of the true force and acceleration signals as possible. However, in reality, as more high frequency content of the kinematic data is included, the amount of noise included markedly increases. The selected cut-off frequency should therefore be as high as possible, without being so high that the acceleration time-history remains largely affected by noise, and the joint kinetics become uninterpretable.

Based on the results presented by Bisseling and Hof (2006), the rapid periods of change between flexor and extensor dominance at the knee and hip joints previously reported during the initial part of sprinting stance (e.g. Mann and Sprague, 1980; Mann, 1981; Johnson and Buckley, 2001; Bezodis *et al*., 2008) could potentially be artefact introduced by applying a lower cut-off frequency to the video data than the force data. Whilst this rapid change from extensor to flexor to extensor dominance after touchdown, sometimes within 30 ms, has been reported by the above authors, none have offered a physiological explanation of how or why such an action would occur. It is possible that these periods of rapid change were due to the internal joint forces - calculated by equating the sum of all forces acting on a segment with the product of the segment's mass and its acceleration (i.e. equations 5.6 and 5.7, page 120). For example, at the ankle joint an artificially high internal joint force would be required to counter the large impact ground reaction force and match the acceleration data from the foot segment which were of lower frequency due to the higher degree of filtering. This erroneous internal joint force would then be used in the equation (i.e. equation 5.9, page 121) for calculating the resultant joint moment acting about the knee, creating a spurious extension peak.

It was therefore decided to undertake a pilot analysis to determine the effects of different force and video filter cut-off frequencies, using a systematic approach in an attempt to determine whether impact peaks in the resultant joint moments could be false transients introduced by inappropriate methodology. The raw force and joint

centre displacement time-histories (both at 200 Hz after the force data were downsampled to match the corresponding video frames) from one trial were filtered at several different cut-off frequencies, and the resulting knee joint moments were calculated in a four segment leg model (forefoot, rearfoot, shank and thigh), using the standard inverse dynamics approach as outlined previously. These knee joint moments were calculated with various force and video cut-off frequencies, and are presented in Figures 5.7a to 5.7g. The horizontal internal joint forces at the knee, which partly affected the calculation of these knee joint moments, were also extracted from the analysis and are presented in Figures 5.8a to 5.8g.

From the data with least filtering, where both the force and video were filtered at 75 Hz (V75F75; Figure 5.7g), it is apparent that although the knee joint moment was relatively noisy, most likely due to a high noise content in the kinematic data, there was no clear impact peak. However when the video cut-off frequency was reduced to 40 Hz (V40F75; Figure 5.7f) and then 20 Hz (V20F75; Figure 5.7d), an impact peak appeared in the knee joint. This was associated with an increased internal joint force peak just after impact (Figures 5.8f and 5.8d). Whilst frequency components up to 75 Hz remained in the ground reaction force data soon after impact with these two methods, the higher frequency components of the acceleration data calculated from the video were removed (above 20 Hz in V20F75 and above 40 Hz in V40F75). Thus when determining the internal joint forces, the term related to the product of the segment's mass and acceleration (in equations 5.6 and 5.7, page 120) lacked some of the high frequency data which was included in the external ground reaction force term. Whilst the ground reaction force exhibited a large impact peak, the segmental acceleration data were missing this peak due to the use of a lower cut-off frequency. Therefore, much like the data reported by Bisseling and Hof (2006), a spurious high frequency component was required in the internal joint force in order to satisfy Newton's Second Law and ensure that the sum of all forces were equal to the product of the segment's mass and acceleration. This peak in the internal joint force was subsequently included when equating the sum of all moments acting about the segment to the product of that segment's moment of inertia and angular acceleration (i.e. equation 5.9, page 121), thus creating a similarly spurious extension peak in the calculated resultant joint moment.

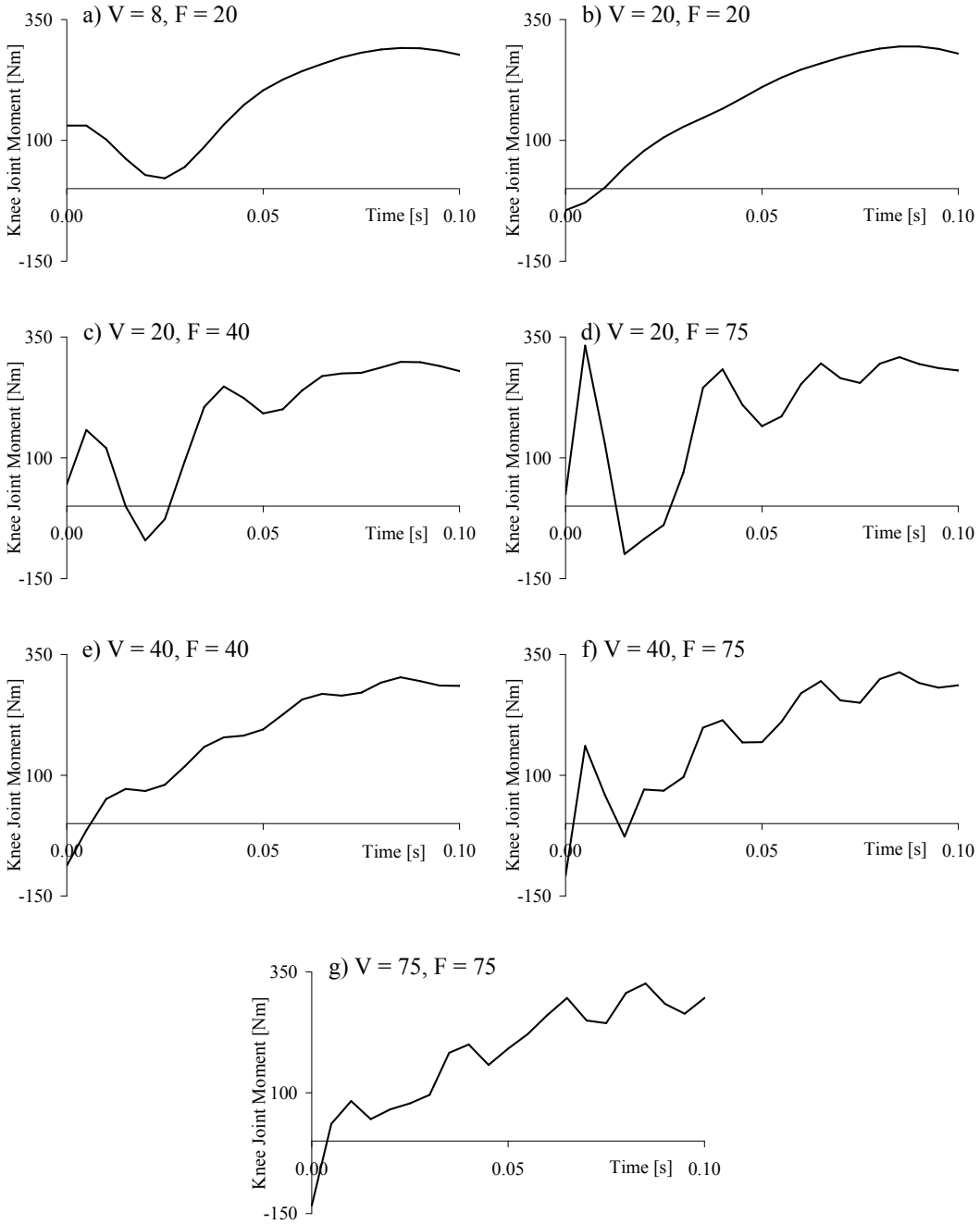

Figure 5.7. Knee joint moment calculated using video (V) and force (F) data filtered at different cut-off frequencies (in Hz).

In contrast, when the video and force cut-off frequencies were again matched, for example both at 40 Hz (V40F40; Figure 5.7e) or 20 Hz (V20F20; Figure 5.7b), there was no sign of an impact peak in the knee joint moment time-history, much like when using the V75F75 method (Figure 5.7g). The only differences between these two data sets and the V75F75 data set appeared to be in the overall noise content of the knee joint moment. As the cut-off frequency decreased, the amount of noise in

the knee joint moment time-history also decreased. This was logical, and was due to the decreased magnitude of noise in the kinematic data, again confirming the findings of Bisseling and Hof (2006).

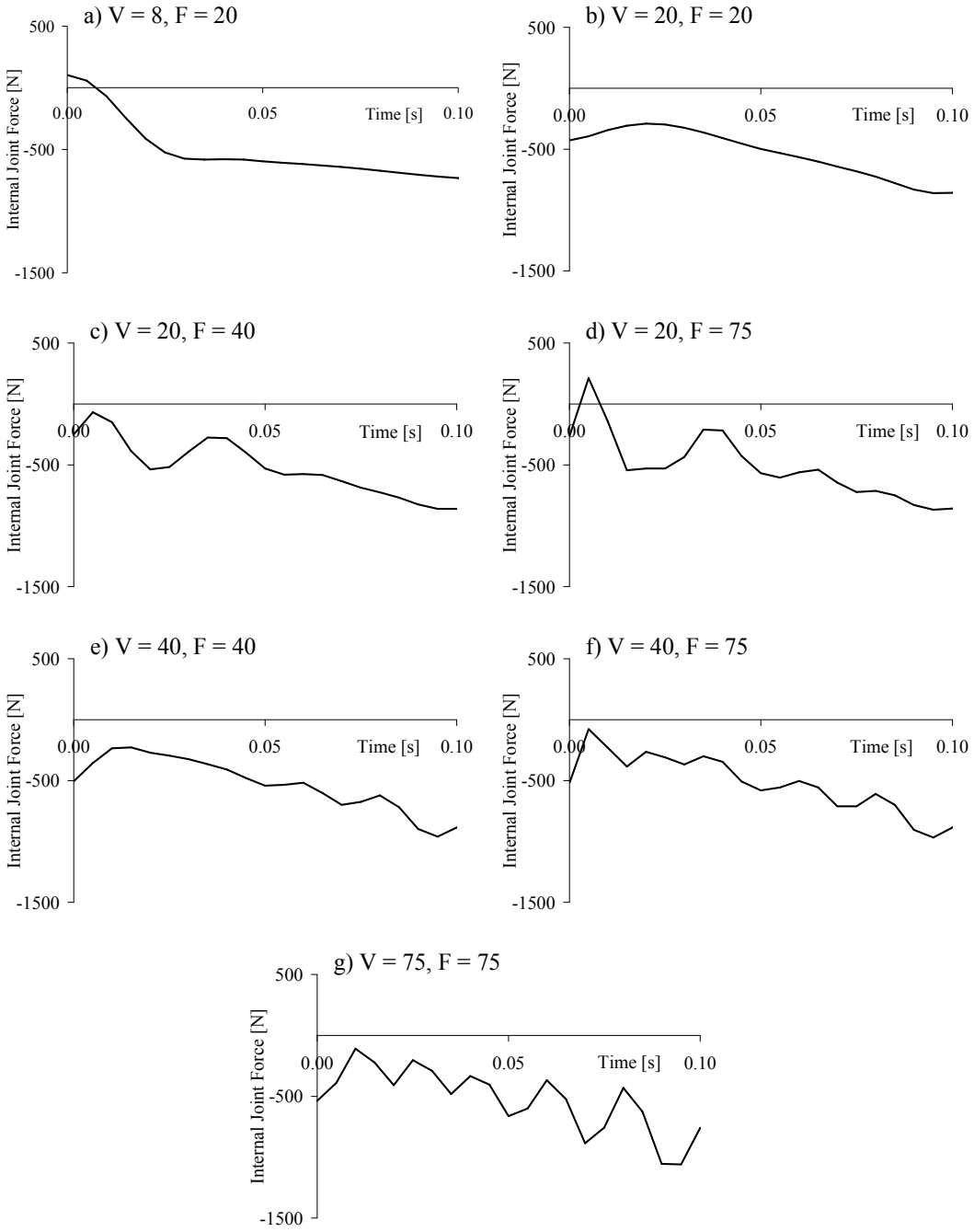

Figure 5.8. Horizontal internal knee joint force calculated using video (V) and force (F) data filtered at different cut-off frequencies (in Hz).

Further evidence to reinforce the theory of filtering force and video data at the same cut-off frequencies when processing inverse dynamics data became apparent when

the video data were filtered at 8 Hz, and the force data at 20 Hz (V8F20; Figure 5.7a). These force data were thus exactly the same as those used in the V20F20 calculations, containing considerable attenuation of the ground reaction force impact peaks. Whilst the V20F20 produced relatively smooth joint moment time-histories with no impact peaks, reducing the video cut-off frequency to 8 Hz (V8F20) reintroduced an early extension moment to the knee joint moment time-history (Figure 5.7a). It therefore appeared that by removing further acceleration data of a frequency content between 8 and 20 Hz, the force and video data again became mismatched. This implies that if the video cut-off frequency was lower than the force cut-off frequency, irrespective of the absolute cut-off frequency values used, a spurious internal joint force peak, and thus an artefact in the resultant joint moment, was generated soon after impact. As both the difference between the respective cut-off frequencies, and the absolute value of the cut-off frequencies decreased (e.g. from V25F75 to V40F75 to V8F20), the frequency and magnitude of these extension moment peaks was also reduced. However, any difference between the force and video cut-off frequencies meant that there were no segmental acceleration data at frequencies corresponding to the higher end of the ground reaction force data frequency spectrum, and thus false impact peaks could have been produced.

It is acknowledged that force data filtered at a low cut-off frequency are no longer fully representative of the true force data, as the impact peaks are markedly attenuated. However, the same holds true for the kinematic data. Whilst the signals are smoother when they are filtered at a low cut-off frequency, and much of the noise is removed, they too are not fully representative of the true signal, as they also lack any high frequency components. Ideally, the data would not require filtering at all, and the truest representation of the joint kinetics could be obtained. However, this is seldom the case, and whilst even filtering at a very high frequency would mean that little or no true signal are removed, the typical levels of noise in kinematic data limits this approach. A considerable degree of low-pass filtering must therefore be performed in order to obtain acceleration time-histories that are not overly affected by noise. The magnitude of the filtering required to achieve this will depend on such factors as the system and set-up used to collect the kinematic data, the movement being analysed and the operator experience (Wood, 1982). However, both the currently presented data and previous research suggest that the force data should be

filtered at the same cut-off frequency. This will yield the most realistic representation of the true joint kinetic data, with minimal effects of noise from the kinematic data, and more importantly no artificial impact peaks generated by un-matched higher frequency force data. Consequently, a two-way approach was adopted for filtering the force data. For the inverse dynamics analysis in the current study, the force data were filtered at a cut-off frequency of 24 Hz, matching that applied to the kinematic data. Alternatively, variables calculated solely from the ground reaction forces were obtained from data filtered at a higher frequency of 150 Hz to preserve the impact peaks.

5.3. Results

5.3.1. The block phase

During the push against the blocks, sprinter Q generated the greatest mean average horizontal external power (1482 ± 109 W; Table 5.2). Whilst sprinter N generated greater absolute mean power than sprinter R, their mean power production was similar when normalised to account for body stature (4.84 and 4.66, respectively). The average horizontal external power production of sprinter Q contributed to a mean increase in horizontal velocity (3.55 $m \cdot s^{-1}$) that was 0.36 $m \cdot s^{-1}$ and 0.45 $m \cdot s^{-1}$ greater than that of sprinters N and R, respectively. Sprinter N spent the least mean time pushing in the blocks (0.357 s), 0.014 s and 0.029 s less than the push phase durations of sprinters Q and R, respectively.

Table 5.2. Performance descriptors during the block phase (mean ± *s*).

	N	Q	R
Push phase duration [s]	0.357 ± 0.009	0.371 ± 0.009	0.386 ± 0.008
Rear foot push duration [s]	0.194 ± 0.018	0.191 ± 0.009	0.198 ± 0.013
Block velocity [$m \cdot s^{-1}$]	3.19 ± 0.09	3.55 ± 0.14	3.10 ± 0.05
Average horizontal external power [W]	1182 ± 96	1482 ± 109	760 ± 36
Normalised power	4.84 ± 0.39	5.87 ± 0.43	4.66 ± 0.22

During the push phase in the blocks, all sprinters showed a sequencing of peak rear leg angular velocities in the order of knee, hip, ankle, MTP (Table 5.3). At the front leg, the hip reached peak extension velocity first, followed by the knee and ankle

almost synchronously, and slightly later the MTP joint (Table 5.4). Sprinter Q exhibited the greatest mean peak front hip ($715 \pm 98°\cdot s^{-1}$) and knee ($968 \pm 120°\cdot s^{-1}$) angular velocities. Sprinter R exhibited the largest mean peak front ankle plantarflexion velocities ($1079 \pm 33°\cdot s^{-1}$), whilst sprinter N exhibited lower mean peak front MTP plantarflexion velocities ($611 \pm 215°\cdot s^{-1}$) than the other two sprinters.

Table 5.3. Rear leg joint kinematics during the rear block contact phase (mean ± *s*).

		N	Q	R
Hip	Peak ω [°·s^{-1}]	308 ± 90	313 ± 58	254 ± 38
	Time of peak ω [%]	31 ± 8	40 ± 2	31 ± 5
	Δ angle during phase [°]	27 ± 5	29 ± 5	23 ± 2
	Angle at end of phase [°]	107 ± 3	95 ± 4	106 ± 5
Knee	Peak ω [°·s^{-1}]	310 ± 34	215 ± 43	199 ± 25
	Time of peak ω [%]	26 ± 2	24 ± 5	23 ± 3
	Δ angle during phase [°]	22 ± 4	11 ± 4	-3 ± 1
	Angle at end of phase [°]	114 ± 3	125 ± 2	136 ± 3
Ankle	Peak ω [°·s^{-1}]	354 ± 50	590 ± 73	551 ± 77
	Time of peak ω [%]	39 ± 3	42 ± 2	48 ± 3
	- Δ angle during phase [°]	-5 ± 2	-6 ± 1	-2 ± 2
	+ Δ angle during phase [°]	+17 ± 3	+32 ± 4	+43 ± 4
	Angle at end of phase [°]	134 ± 4	145 ± 6	150 ± 2
MTP	Peak ω [°·s^{-1}]	513 ± 131	456 ± 125	582 ± 117
	Time of peak ω [%]	46 ± 3	49 ± 2	52 ± 1
	Δ angle during phase [°]	17 ± 2	-6 ± 8	-9 ± 3
	Angle at end of phase [°]	140 ± 4	146 ± 4	155 ± 4

The Δ joint angle data represent the overall range of extension. For the ankle joint, data are split into initial dorsiflexion (-) and subsequent plantarflexion (+) magnitudes.

Table 5.4. Front leg joint kinematics during the block phase (mean ± *s*).

		N	Q	R
Hip	Peak ω [°·s^{-1}]	588 ± 35	715 ± 98	591 ± 41
	Time of peak ω [%]	65 ± 20	70 ± 25	67 ± 18
	Δ angle during phase [°]	112 ± 3	123 ± 6	118 ± 2
	Angle at end of phase [°]	162 ± 3	175 ± 3	162 ± 1
Knee	Peak ω [°·s^{-1}]	799 ± 54	968 ± 120	762 ± 37
	Time of peak ω [%]	91 ± 2	92 ± 1	93 ± 1
	Δ angle during phase [°]	91 ± 2	88 ± 5	65 ± 2
	Angle at end of phase [°]	176 ± 2	175 ± 1	171 ± 1
Ankle	Peak ω [°·s^{-1}]	783 ± 68	911 ± 96	1079 ± 33
	Time of peak ω [%]	90 ± 1	92 ± 1	94 ± 1
	- Δ angle during phase [°]	-14 ± 1	-14 ± 3	-7 ± 2
	+ Δ angle during phase [°]	+57 ± 4	+43 ± 2	+53 ± 3
	Angle at end of phase [°]	154 ± 2	149 ± 3	156 ± 2
MTP	Peak ω [°·s^{-1}]	611 ± 215	783 ± 171	800 ± 107
	Time of peak ω [%]	96 ± 1	97 ± 1	97 ± 0
	Δ angle during phase [°]	-5 ± 5	0 ± 5	-9 ± 6
	Angle at end of phase [°]	147 ± 5	148 ± 5	151 ± 6

The Δ joint angle data represent the overall range of extension. For the ankle joint, data are split into initial dorsiflexion (-) and subsequent plantarflexion (+) magnitudes.

5.3.2. The rear leg swing phase

During the rear leg swing phase, the angle at the rear leg MTP joint remained relatively constant (Figure 5.9a). An MTP dorsiflexion angular velocity was generated during the late part of the phase (Figure 5.9b) which served to decrease the MTP angle slightly before touchdown. From a somewhat plantarflexed position at rear foot block exit (Figure 5.9e), the ankle joint exhibited a dorsiflexion angular velocity throughout the majority of the swing phase (Figure 5.9f), decreasing the ankle angle further (Figure 5.9e), although all sprinters exhibited slight plantarflexion prior to touchdown in some trials. The resultant joint moments generated about the MTP and ankle joints during the rear leg flight phase were negligible (Figures 5.9c and 5.9g), and thus power production was also minimal (Figures 5.9d and 5.9h).

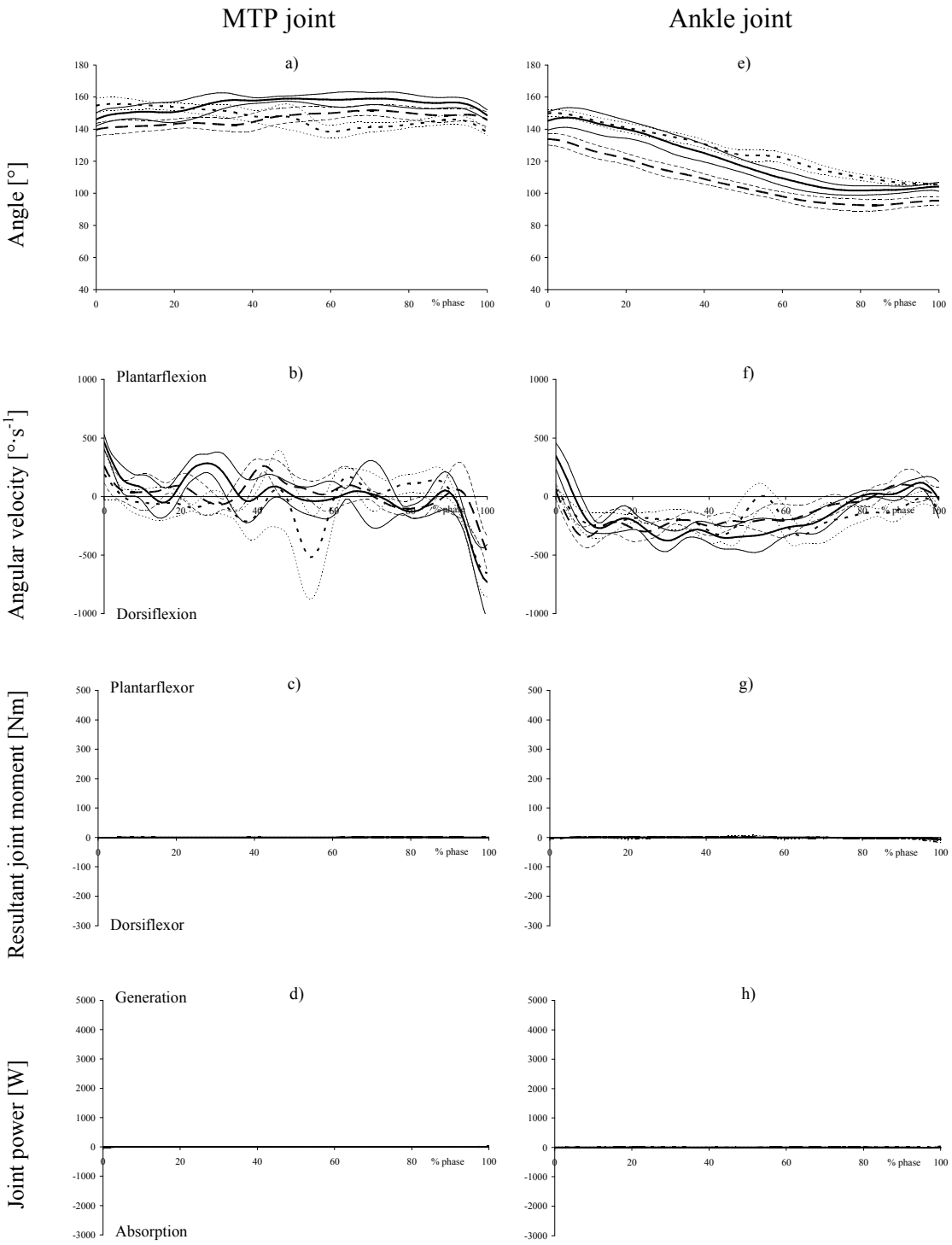

Figures 5.9a-h. MTP and ankle angular kinematic and kinetic time-histories during the rear leg swing phase (i.e. from rear foot off the block until first stance touchdown) expressed relative to phase duration (mean ± *s*; sprinter N = dotted line; sprinter Q = dashed line; sprinter R = solid line). Figures c, d, g and h are provided in Appendix C on a larger scale.

At rear block exit, there was a relatively large flexion angular velocity at the knee joint (Figure 5.10b), combined with a knee flexor moment (Figure 5.10c), which decreased the knee angle during the first half of the rear leg flight phase (Figure 5.10a). A reduction in the flexor moment and a subsequent knee extensor moment reduced the flexion angular velocity so that by mid-phase, the knee began to extend. The peak in this mean extensor moment was greater for sprinter N (68 ± 29 Nm) than sprinters Q (20 ± 8 Nm) or R (13 ± 4 Nm). Soon after mid-phase, sprinters Q and R generated knee flexor moments, which started to attenuate its extension angular velocity. On average, sprinter N did not exhibit this flexor moment until 79 ± 2 % of the phase. However, sprinter N generated greater mean peak knee flexor moments during the late swing phase (182 ± 31 Nm) than sprinters Q (80 ± 6 Nm) and R (79 ± 16 Nm). The knee flexor moment caused an absorption of energy during the late part of the phase (K_F^{2-}; Figures 5.10d and 5.11), particularly in sprinter N due to his larger extension velocity than sprinters Q and R (Figure 5.10b).

For all three sprinters, hip joint angular velocity was minimal at rear block exit (Figure 5.10f), as a hip flexor moment was active (Figure 5.10g) to halt the extension which had previously occurred during rear block contact, and to commence a period of hip flexion (Figure 5.10e). At around mid-phase, the resultant joint moment about the hip joint became extensor, reducing the flexion velocity, and causing hip extension by around 75% of the phase. A considerable amount of energy was generated at the hip joint during the remainder of the phase (H_F^{2+}; Figure 5.11), as the extensor moment remained high. Sprinter N exhibited a large mean peak hip moment (363 ± 52 Nm) during the late swing phase and a much higher mean peak hip power (3959 ± 1444 W) than sprinters Q (2067 ± 181) and R (1742 ± 366 W).

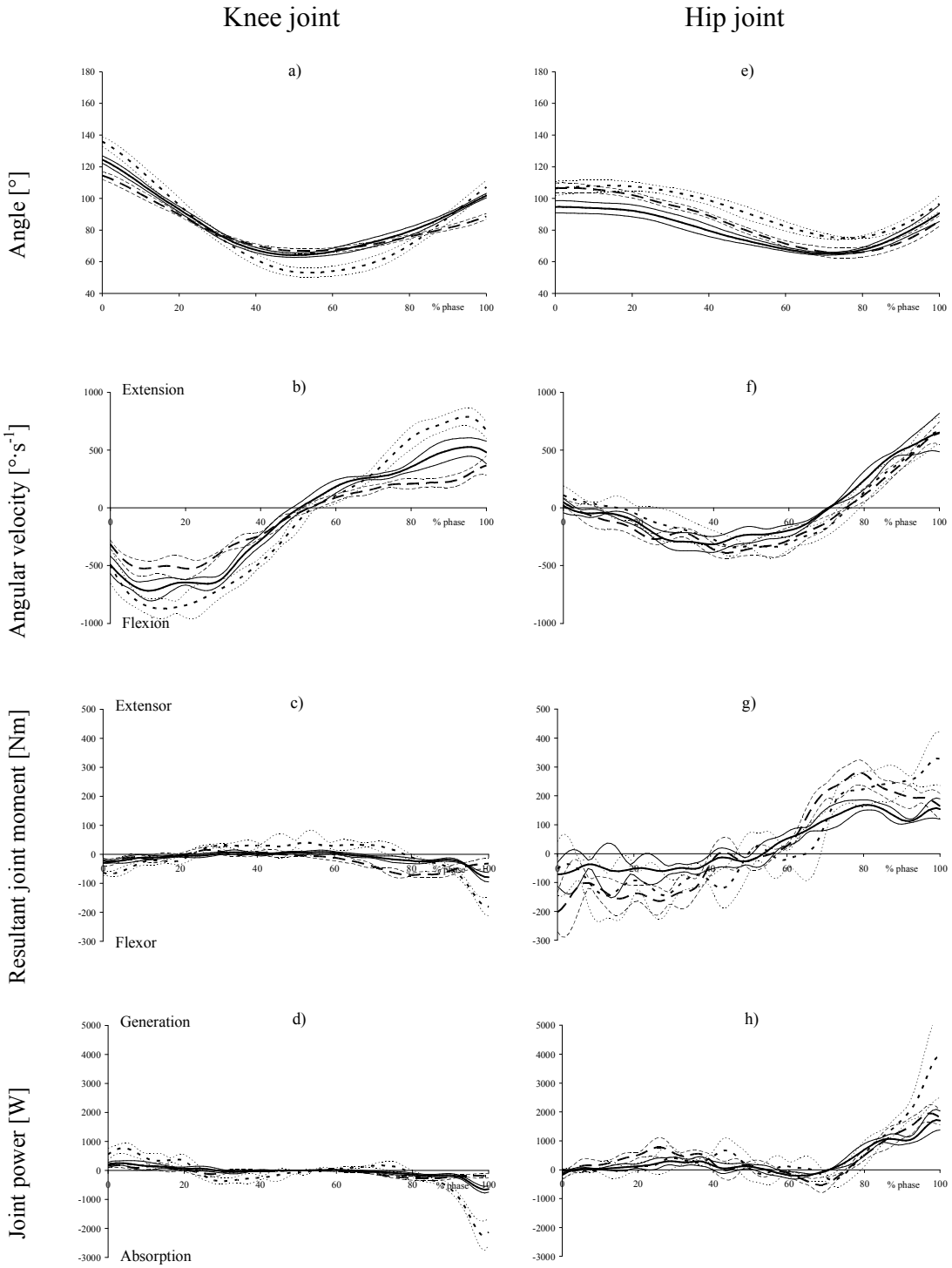

Figures 5.10a-h. Knee and hip angular kinematic and kinetic time-histories during the rear leg swing phase (i.e. from rear foot off the block until first stance touchdown) expressed relative to phase duration (mean ± *s*; sprinter N = dotted line; sprinter Q = dashed line; sprinter R = solid line.

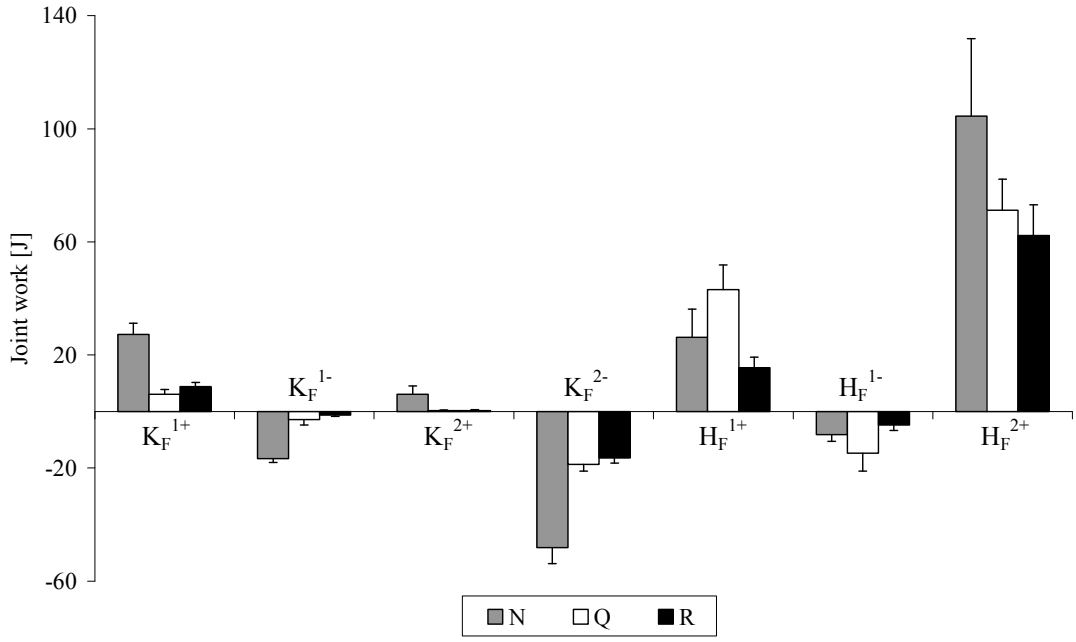

Figure 5.11. Energy generation and absorption at the knee and hip joints during each of the power phases of the rear leg swing phase (mean ± *s*). Variables beginning with K refer to the knee joint, and those beginning with H refer to the hip joint. A '+' sign indicates power generation, whereas a '-' sign indicates power absorption. See section 5.2.4 (page 121) for a complete explanation of the symbols.

The mean duration of the flight phase (front foot block exit to touchdown) of sprinter R (0.056 ± 0.009 s) was less than that of sprinters N and Q (0.073 ± 0.012 and 0.072 ± 0.008 s, respectively). Sprinter R also exhibited a shorter mean first step length (0.95 ± 0.01 m) than sprinter N (1.09 ± 0.03 m), who in turn had a shorter step length than sprinter Q (1.13 ± 0.02 m). The same trend remained when step lengths were normalised to leg length, with values of 1.06 ± 0.02, 1.14 ± 0.03 and 1.19 ± 0.04 for sprinters R, N and Q, respectively.

5.3.3. The stance phase

In terms of power production, sprinter Q generated a greater mean average horizontal external power (2671 ± 80 W) during the first stance phase than sprinters N (2071 ± 139 W) and R (1419 ± 40 W). When normalised to account for differences in body stature, the mean power production of sprinter Q remained the largest (10.57 ± 0.32). However, sprinter R generated slightly more relative power (8.70 ± 0.24) than sprinter N (8.48 ± 0.57). Sprinter R exhibited the shortest mean

stance duration (0.177 ± 0.007 s) and a slightly lower mean increase in velocity (1.13 ± 0.03 $m \cdot s^{-1}$) than sprinters N and Q. The mean stance durations of sprinters N (0.193 ± 0.008 s) and Q (0.191 ± 0.003 s) were similar, and thus due to a greater mean horizontal external power production, sprinter Q achieved a greater increase in horizontal velocity (1.39 ± 0.02 $m \cdot s^{-1}$) than sprinter N (1.26 ± 0.02 $m \cdot s^{-1}$).

External kinetics

Sprinter N generated a greater mean peak horizontal braking force (-731 ± 181 N) than sprinters Q (-147 ± 79 N) and R (-312 ± 67 N; Figure 5.12a). This remained the case when values were normalised (sprinter N = -0.90 ± 0.22; sprinter Q = -0.17 ± 0.09; sprinter R = -0.52 ± 0.11). Sprinter N also showed a larger mean peak vertical force during braking (1211 ± 90 N) than sprinters Q (605 ± 76 N) and R (891 ± 37 N; Figure 5.12b), although when normalised to account for body stature, the mean peak vertical impact forces of sprinters N and R were identical (1.49 ± 0.11 and 1.49 ± 0.06, respectively; sprinter Q = 0.71 ± 0.09). Sprinter Q generated greater mean propulsive peaks in both the horizontal (1094 ± 16 N) and vertical (1857 ± 17 N) directions than sprinter N (938 ± 52 N and 1697 ± 102 N), who in turn generated greater peaks than sprinter R (631 ± 11 N and 1200 ± 39 N). The same trend was also apparent when these respective horizontal and vertical peak values were normalised (sprinter Q = 1.28 ± 0.02 and 2.17 ± 0.02; sprinter N = 1.15 ± 0.06 and 2.09 ± 0.13; sprinter R = 1.06 ± 0.02 and 2.01 ± 0.07).

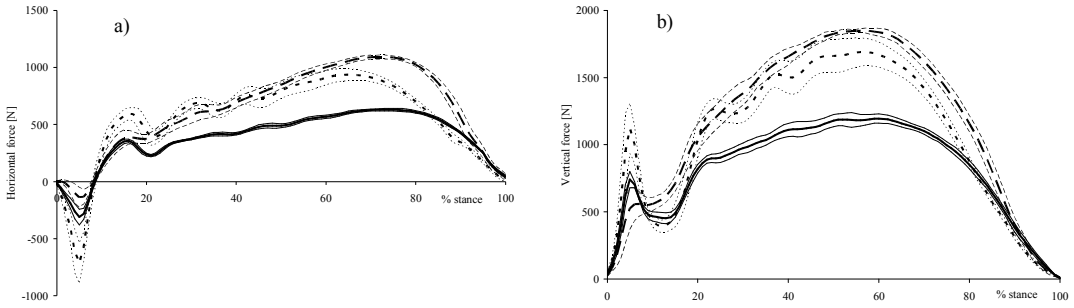

Figures 5.12a-b. Time-histories of absolute horizontal and vertical force production during stance expressed relative to the duration of the phase (mean ± *s*; sprinter N = dotted line; sprinter Q = dashed line; sprinter R = solid line).

Kinematics and joint kinetics at touchdown

At touchdown, all three sprinters exhibited a negative touchdown distance (Table 5.5). Sprinter N positioned his foot the furthers behind his CM, both in absolute

(-0.086 ± 0.028 m) and normalised (-0.089 ± 0.031) terms. Sprinter N also touched down with a somewhat high mean horizontal toe velocity of 2.29 ± 0.63 $m \cdot s^{-1}$, whereas the mean toe velocity of sprinter Q at touchdown was zero (Table 5.5).

Table 5.5. Linear kinematics at touchdown (mean ± *s*).

	N	Q	R
Horizontal toe velocity [$m \cdot s^{-1}$]	2.29 ± 0.63	0.00 ± 0.15	0.78 ± 0.41
Touchdown distance [m]	-0.086 ± 0.028	-0.045 ± 0.022	-0.052 ± 0.014
Normalised touchdown distance	-0.089 ± 0.031	-0.048 ± 0.023	-0.057 ± 0.016

For all sprinters, there was a trend for horizontal toe velocity at touchdown to increase linearly with peak braking force magnitude across all individual trials, and this appeared to be fairly strong for sprinters N and R (Figure 5.13a). The trends between touchdown distance and peak braking force magnitude (Figure 5.13b) were more variable. Sprinter R exhibited a relatively strong positive trend, whereas sprinters N and Q exhibited weaker positive and negative trends, respectively.

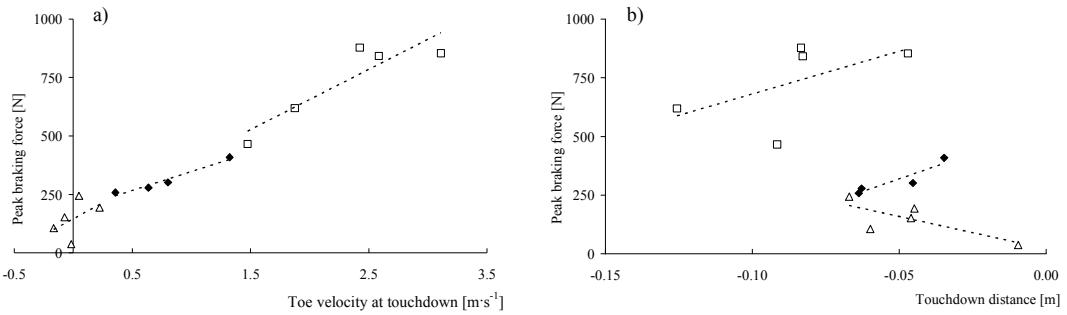

Figures 5.13a-b. Scatter-plots and individual trend lines for a) toe touchdown velocity and b) touchdown distance against peak braking force magnitude (sprinter N = squares; sprinter Q = triangles; sprinter R = diamonds).

In terms of joint angular kinematics at touchdown, sprinter R exhibited a greater mean MTP angle (148.1 ± 3.3°) than sprinters N and Q (Figure 5.14a), whilst sprinter N exhibited the greatest mean ankle angle (107.2 ± 2.5°; Figure 5.14e). All three sprinters exhibited rapid MTP dorsiflexion at touchdown (Figure 5.14b), whilst ankle joint angular velocities were relatively small (Figure 5.14f). At the knee and hip joints (Figure 5.15), sprinter Q touched-down with a less extended stance knee

joint (90.1 ± 1.3°) than sprinters N (102.1 ± 4.1°) and R (99.3 ± 1.7°; Figure 5.15a). Sprinter Q also exhibited a lower mean knee extension angular velocity at touchdown (297 ± 82°·s^{-1}) than sprinter R (459 ± 88°·s^{-1}), whilst that of sprinter N was higher still (747 ± 71°·s^{-1}; Figure 5.15b). For all three sprinters, the stance hip was in a relatively flexed position at touchdown (92.6 ± 3.7, 87.6 ± 2.5 and 89.0 ± 4.1° for N, Q and R, respectively; Figure 5.15e), and hip extension angular velocity was high (752 ± 72, 610 ± 76 and 609 ± 124°·s^{-1} for N, Q and R, respectively; Figure 5.15f). Ankle (Figure 5.14g) and MTP (Figure 5.14c) joint moments were negligible at touchdown for all sprinters, and whilst sprinters Q and R also exhibited negligible knee joint moments (Figure 5.15c), the flexor moment which had appeared during the latter part of the flight phase remained present at the knee joint of sprinter N at touchdown. At the hip joint (Figure 5.15g), all three sprinters exhibited an extensor moment at touchdown.

Kinematics and joint kinetics during the stance phase

At both the MTP and ankle joint, all three sprinters exhibited similar angular kinematic patterns (Figure 5.14). The MTP angle initially decreased from the onset of stance, and continued to do so for the majority of the stance phase, aside from a brief period of plantarflexion for sprinters Q and R between about 15 and 35% of stance. Towards the end of the stance phase (at around 70%) there was a further increase in the MTP dorsiflexion angular velocity, which was followed by a rapid increase in plantarflexion velocity, with peak values occurring at 98-99% of stance. The ankle angular kinematics showed two clear phases, an initial dorsiflexion for approximately the first half of stance, and a subsequent plantarflexion during the second half, with mean peak plantarflexion angular velocities occurring between 89% (sprinter N) and 92% (sprinter R) of stance (i.e. sprinter Q reached peak plantarflexion velocity between these two percentage times).

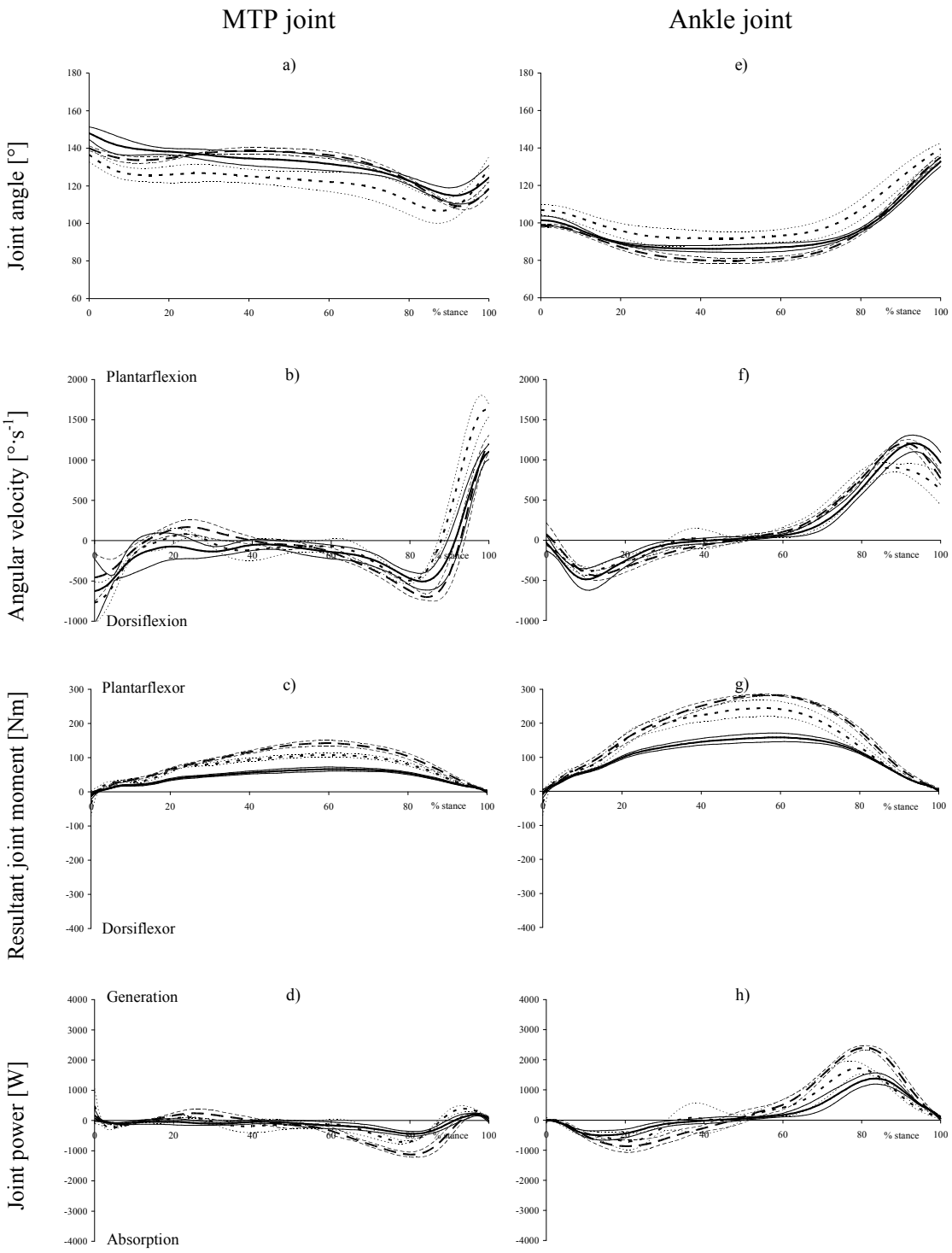

Figures 5.14a-h. MTP and ankle angular kinematic and kinetic time-histories during stance expressed relative to stance duration (mean ± *s*; sprinter N = dotted line; sprinter Q = dashed line; sprinter R = solid line).

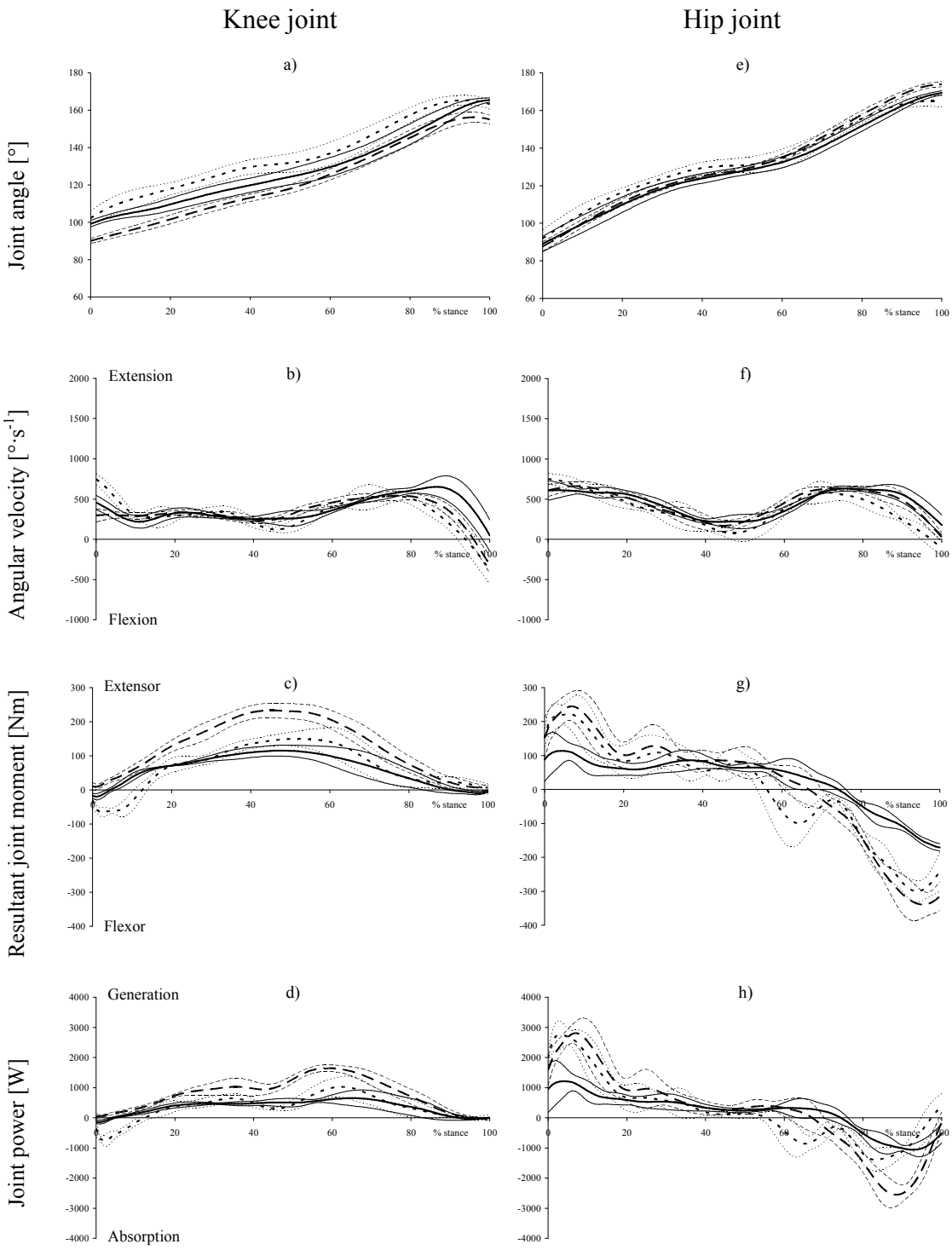

Figures 5.15a-h. Knee and hip angular kinematic and kinetic time-histories during stance expressed relative to stance duration (mean ± *s*; sprinter N = dotted line; sprinter Q = dashed line; sprinter R = solid line).

In terms of the joint kinetics, aside from small dorsiflexor moments at touchdown, both the MTP and ankle joints experienced plantarflexor moments throughout stance (Figures 5.14c and 5.14g). The mean peak ankle joint moments (246 ± 24, 284 ± 2 and 169 ± 13 Nm for sprinters N, Q, and R, respectively) were around twice as large as the mean peak MTP moments for all three sprinters (108 ± 5, 143 ± 8 and 67 ± 6 Nm for sprinters N, Q, and R, respectively). There was a period of negative power at the MTP joint (M_S^-) soon after mid-stance (Figure 5.14d), which was followed by a small positive power phase (M_S^+) with mean values peaking between 94% (sprinter N) and 97% (sprinters Q and R) of stance. At the ankle joint, a phase of negative power (A_S^-) existed for the first half of stance, which was followed by a period of positive power (A_S^+) peaking at between 78% (sprinter N) and 83% (sprinter R) of stance, and yielding 2.5 - 3.0 times more energy than was previously absorbed (Figures 5.14h and 5.16).

The knee and hip joints extended throughout the entire stance phase, aside from a slight knee flexion occurring just prior to toe-off (Figures 5.15a and 5.15e). Sprinter N was typically more extended at the stance knee and hip joints at touchdown than sprinters Q and R. Sprinter N also typically maintained a more extended knee joint throughout stance, but the hip was only more extended than sprinters Q and R for around the first half of stance. For all sprinters, the mean angular velocity profiles at the hip and knee both showed a double peak, the first occurring at or soon after touchdown. The knee angular velocity then decreased to a minimum extension velocity around mid-stance, before increasing again to a mean peak angular velocity between 75% (sprinter N) and 87% (sprinter R) of stance. Having peaked soon after touchdown, the hip extension angular velocity then decreased to a minimum value near mid-stance before increasing to a mean peak extension velocity between 71% (sprinter N) and 76% (sprinter R) of stance. Over the duration of the stance phase, sprinter Q exhibited the greatest range of extension at the stance hip (86.4 ± 3.1°) and ankle joints (36.5 ± 1.1°), with sprinter R exhibiting the greatest range at the knee joint (66.1 ± 1.3°). Sprinter N exhibited the largest mean peak extension angular velocity at the stance hip (797 ± 50°·s^{-1}) and knee (728 ± 25°·s^{-1}), whilst sprinter Q exhibited the lowest mean peak knee angular velocity (562 ± 57°·s^{-1}).

The knee joint moment was extensor throughout the whole stance phase, aside from sprinters N and R generating a brief flexor moment at touchdown, and some small flexor moments just prior to toe-off (Figure 5.15c). The mean peak knee moments occurred between 46% (sprinter Q) and 53% (sprinter N) of stance, and sprinter Q generated considerably greater peak knee moment magnitudes, both in absolute (234 ± 21 Nm) and normalised (0.29 ± 0.03) terms than sprinters N (157 ± 27 Nm; 0.20 ± 0.04) and R (116 ± 16 Nm; 0.22 ± 0.03). Sprinter N absorbed a considerable amount of energy at the knee joint during early stance (-10.3 ± 1.59 J; phase K_S^-) whilst sprinter R absorbed only a negligible amount (-0.75 ± 0.41 J) and sprinter Q merely -0.01 ± 0.02 J (Figure 5.16). A large positive power phase (K_S^+) subsequently occurred at the knee joint, with mean peak magnitudes occurring at between 59% (sprinter Q) and 65% (sprinter R) of stance. A considerable amount of energy was therefore generated at the knee, with sprinter Q producing over twice as much (154.1 ± 17.3 J) as sprinters N (76.8 ± 21.8 J) and R (64.6 ± 13.4 J).

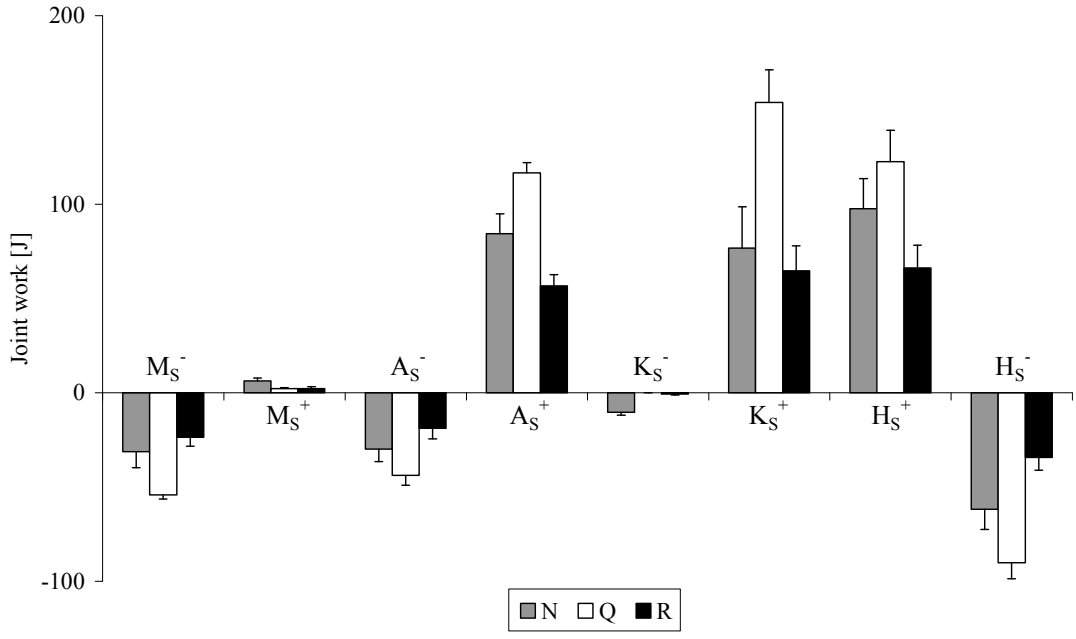

Figure 5.16. Energy generation and absorption at the leg joints during each of the power phases during stance (mean ± *s*). Variables beginning with M refer to the MTP joint, A refers to the ankle joint, K to the knee joint, and H to the hip joint. A '+' sign indicates power generation, whereas a '-' sign indicates power absorption. See section 5.2.4 (page 121) for a complete explanation of the symbols.

The mean hip moment (Figure 5.15g) remained extensor for the first half of stance, before becoming flexor dominant between 57% (sprinter N) and 75% of stance (sprinter R). The flexor moment then typically increased in magnitude, reaching mean peak values between 95% of stance (sprinter N) and toe-off (sprinter R). As the hip was extending throughout stance, there was a phase of large positive power generation (H_S^+), which peaked between 4% (sprinters N and R) and 7% (sprinter Q) of stance. During this H_S^+ phase, considerable energy was generated at the hip joint by all three sprinters (97.6 ± 16.0, 122.6 ± 16.6 and 66.2 ± 12.1 J for sprinters N, Q, and R, respectively; Figure 5.16). This was followed by a negative power phase (H_S^-) once the moment became flexor dominant, with mean peak magnitudes occurring between 81% (sprinter N) and 93% (sprinter R) of stance (Figure 5.15h). The gravitational moment of the trunk segment about this hip joint during stance was also calculated, which would tend to cause flexion at the hip due to the relatively large mass of the trunk, and its orientation. Gravitational moments were fairly consistent throughout stance for each sprinter, with mean peak values of 140 ± 4, 134 ± 3 and 97 ± 1 Nm exhibited by sprinters N, Q and R, respectively (Figures 5.17a to 5.17c).

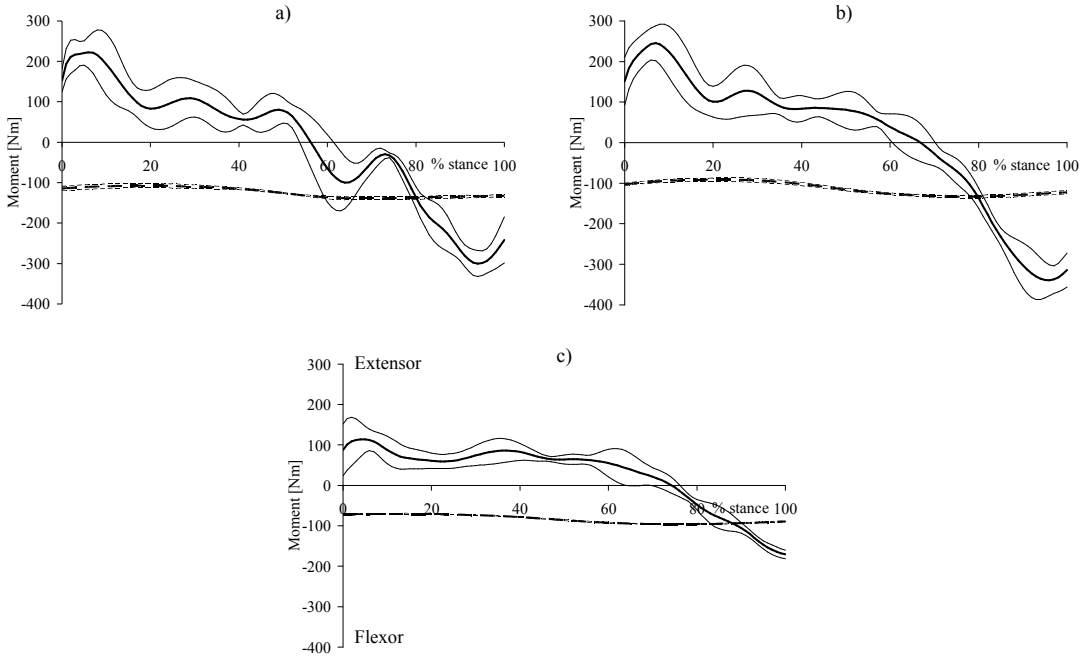

Figure 5.17a-c. Resultant hip joint moment (solid line) and trunk segment gravitational moment (dashed line) throughout the stance phase for sprinters N (a), Q (b) and R (c), respectively (mean ± *s*).

The angular orientations of the stance leg and trunk segments throughout the duration of the stance phase were also determined (Figures 5.18 - 5.20). These indicated that the thigh rotated in a clockwise direction throughout stance (when viewed from the right hand side with the sprinter running from left to right), with the rotational velocity decreasing only towards the end of stance. Shortly before the rotation of the thigh segment began to slow, the rearfoot segment began to rotate in a clockwise direction, closely followed by the forefoot segment. In contrast, the shank and trunk segments remained in a relatively fixed position throughout the entire stance phase. Sprinter Q exhibited the greatest thigh angle at touchdown (i.e. the greatest anticlockwise rotation from a vertical orientation) and proceeded to subsequently rotate the thigh segment over the greatest distance during stance (Figure 5.19a). Sprinter Q also typically rotated the rearfoot segment over a greater range than the other two sprinters, with a more rapid rotation during the latter part of stance (Figure 5.19b).

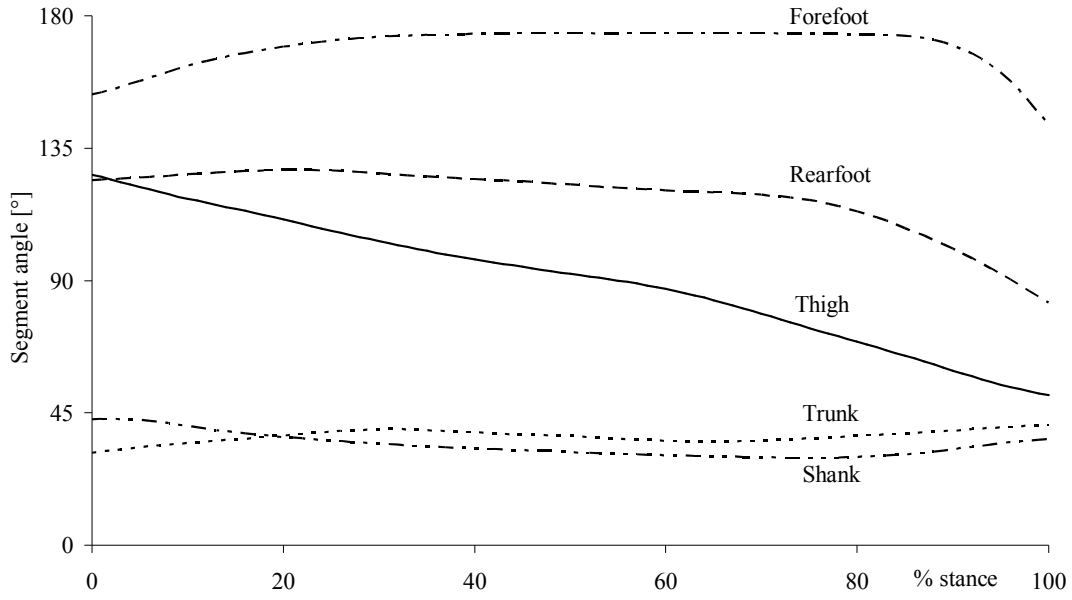

Figure 5.18. Typical example of segmental angular displacements during stance (from one trial of sprinter R). An angle of 0° represents a horizontal orientation, with a positive angle representing an anti-clockwise rotation of the proximal endpoint about the distal endpoint (when viewed from the right hand side with the sprinter running from left to right).

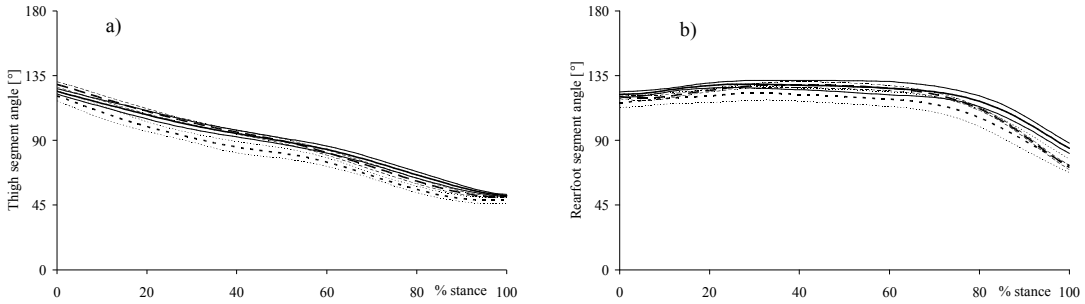

Figures 5.19a-b. Thigh (a) and rearfoot (b) segment rotations for each of the three sprinters during stance (mean ± *s*; sprinter N = dotted line; sprinter Q = dashed line; sprinter R = solid line).

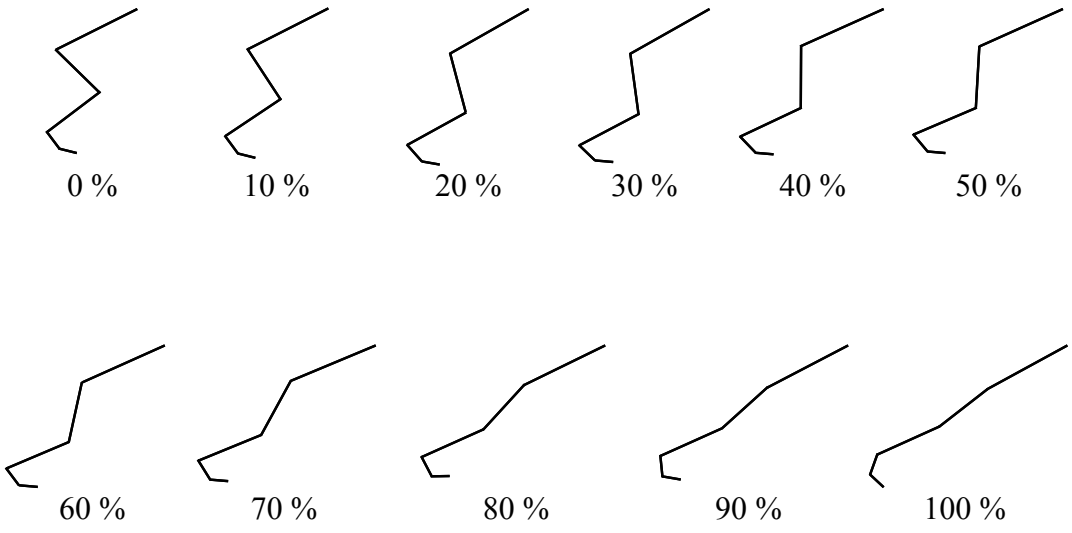

Figure 5.20. Representative stick figure diagram (forefoot, rearfoot, shank, thigh, and trunk segments) of a sprinter (N) during the first stance phase (at every 10% of stance).

Kinematics and joint kinetics at toe-off

By toe-off, the hip joints of the sprinters were nearing full extension (164.8 ± 3.1, 174.0 ± 1.4 and 169.4 ± 1.1° for sprinters N, Q, and R, respectively; Figure 5.15e). This represented mean increases in hip angle during stance of 72.2 ± 4.3, 86.4 ± 3.1 and 80.4 ± 3.7° for sprinters N, Q, and R, respectively. Compared to the hip, the knee joint was typically less close to full extension (162.7 ± 2.6, 155.1 ± 2.4 and 165.4 ± 1.1° for sprinters N, Q, and R, respectively; Figure 5.15a), and had covered a smaller

range of motion during stance (60.6 ± 5.2, 65.0 ± 2.1 and 66.1 ± 1.3° for sprinters N, Q, and R, respectively). The mean ankle joint angles at toe-off were 139.2 ± 3.4, 134.9 ± 1.7 and 132.6 ± 2.4° for sprinters N, Q, and R, respectively (Figure 5.14e), representing respective mean increases in angle of 32.0 ± 2.6, 36.5 ± 1.3 and 31.1 ± 2.3° from touchdown.

5.4. Discussion

5.4.1. The block phase

The primary reason for the camera focussing on the block and flight phases (i.e. camera 1) was to determine an accurate block exit (and thus first touchdown) velocity, and to obtain rear leg joint kinetics during the swing phase. However, this camera also provided accurate kinematic data from the block phase. Although it was not the main aim of this chapter, the current data can thus be briefly compared to the data presented in Chapter 4 in order to either reinforce the techniques and findings previously identified, or identify other aspects of the techniques utilised by international-level sprinters during the block phase. These block phase data can also be used to compare within-subject between the data presented in this and the previous chapter. This could offer some interesting insight regarding the techniques and performances of sprinters N and Q as their current levels of performance had changed from those achieved 18 months previously.

In the current chapter, sprinters N and Q both extended their rear knee during rear block contact (mean total range of extension = 21.6 ± 3.6 and 10.7 ± 4.2°, respectively), whereas sprinter R actually exhibited a net flexion (-2.8 ± 0.7°). At the rear hip joint, the overall mean increase in joint angle during the rear block push was 27.1 ± 4.5, 28.9 ± 5.0 and 23.1 ± 2.2° for sprinters N, Q, and R, respectively. Sprinter R may therefore not have used the rear leg push to full advantage, which may have inhibited her generation of block velocity (Table 5.2). Sprinter Q, who generated the greatest average horizontal external power in the blocks, exhibited the highest front hip and knee angular velocities (Table 5.4) and extended his front hip over a greater range (122.9 ± 6.2°) than sprinters N and R (112.2 ± 3.4 and 118.1 ± 1.9°, respectively; Table 5.4). Sprinter Q also only extended his front ankle by 29.6 ± 3.5°, compared to the mean increases of 42.9 ± 3.0 and 45.9 ± 2.4° exhibited by sprinters N and R, respectively. Therefore, although he spent slightly longer in the blocks than

sprinter N, sprinter Q spent this time more favourably by extending the powerful proximal leg joints.

When compared to the data presented in Chapter 4 (Tables 4.3, 4.4 and 4.5), sprinters N and Q both spent an additional 0.011 s pushing in the blocks in the current investigation. Sprinter Q was able to increase average horizontal external power production by 237 W compared to the investigation presented in Chapter 4, which resulted in a 0.23 $m \cdot s^{-1}$ increase in block velocity. This was associated with an increased contribution from the front leg, where mean peak angular velocities in the hip, knee and ankle joints had increased by 195, 419 and 447º$\cdot s^{-1}$, respectively. The total range of motion at the hip and knee joints therefore increased by 17 and 22º respectively, and both of these joints were 17º more extended at block exit than in the previous investigation (indicating that the initial 'set' positioning of sprinter Q had hardly changed). At the ankle joint, the plantarflexion range of motion was only 2º greater, suggesting that sprinter Q had avoided potentially detrimental large increases in front ankle range of motion despite the larger angular velocities achieved at this joint. In the rear leg, sprinter Q increased his peak ankle angular velocity by 294º$\cdot s^{-1}$ and increased its plantarflexion range of motion by 13º. Angular velocities in the hip and knee had also increased by 61 and 99º$\cdot s^{-1}$, respectively. Both of these joints extended by an additional 3º throughout the rear block contact phase, thus also suggesting an increased contribution from all of the rear leg joints towards the higher performance levels of sprinter Q observed in the current chapter.

Although sprinter N also spent an additional 0.011 s pushing in the blocks in the current investigation, his block velocity decreased by 0.29 $m \cdot s^{-1}$, and thus his performance clearly suffered (average horizontal external power production was 224 W lower). It became clear that Sprinter N had markedly changed his 'set' positioning, since although a similar amount of extension was achieved in the rear hip and knee joints between investigations (4º and 0º mean difference, respectively), sprinter N was considerably less extended at both of these joints by rear block exit in the current chapter (17 and 32º less at the hip and knee, respectively). As peak rear leg angular velocities had not changed by more than 42º$\cdot s^{-1}$ (in either direction), these data suggested that sprinter N may therefore have used the rear leg joints over a less favourable range of motion in the current investigation. In the front leg, sprinter N

exhibited higher mean peak angular velocities at the hip, knee and ankle in the current investigation (by 81, 217 and 186º·s^{-1}, respectively). However, although knee range of motion increased by 13º, front hip range of motion actually decreased slightly. Accompanied with a slightly larger increase in the plantarflexion range of motion at the ankle joint in the current investigation, the over-reliance on extension at the less proximal front leg joints may again, as suggested in Chapter 4, have negatively affected the performance of sprinter N.

Whilst there are clearly individual differences in block phase technique between international-level sprinters, the findings from this chapter, both independently and when compared against data from Chapter 4, reinforced some of the important aspects of block phase technique highlighted in Chapter 4. These included the importance of the push against the rear block, and a greater extension of the more proximal rather than distal front leg joints when attempting to enhance performance. Intra-subject comparisons across relatively large time-scales offer an interesting area of future work which would clearly assist the development of training strategies. With consistent inertia models and additional measurement of dynamic strength and power (e.g. using isokinetic dynamometer testing and vertical and countermovement jumps), it could be possible to further understand the effects of intra-subject changes in ability upon technique and ultimately performance between seasons.

5.4.2. The rear leg swing phase

From the moment that the rear foot left the blocks until it touched down on the track to commence the first stance phase, there were negligible resultant joint moments generated about the MTP (less than 1 Nm; Figure 5.9c and Appendix C). At the ankle joint, sprinters Q and R exhibited resultant joint moments of less than 3 Nm and sprinter N less than 10 Nm until just before touchdown where a slight dorsiflexor moment was generated (up to 20 Nm for sprinter N, and 10 Nm for sprinters Q and R; Figure 5.9g and Appendix C). These small ankle joint moments were consistent with previous joint kinetics analyses during the swing phase (e.g. Mann and Sprague, 1980; Mann, 1981; Johnson and Buckley, 2001). The knee flexor moment present during the late swing phase was consistent with previous observations at the 16 m mark (Johnson and Buckley, 2001) and at maximum velocity (Mann and Sprague, 1980; Mann, 1981). This existed to absorb energy during late swing (phase $K_S{}^{2-}$;

Figure 5.11) and thus decelerate the rotation of the shank. Sprinter N generated the greatest knee extensor moment during mid-swing (Figure 5.10c), which contributed to a greater extension velocity of the knee at touchdown than sprinters Q and R (Figure 5.10b). Sprinter N thus required the largest knee flexor moment just prior to and at touchdown in an attempt to reduce this extension velocity. The consequences of this will be addressed subsequently during the discussion of the stance phase (section 5.4.3).

The rear hip flexion after rear block exit (Figure 5.10e) occurred due to a considerable flexor moment (Figure 5.10g) as energy was generated by the hip flexor muscles (phase H_F^{1+}; Figure 5.11). This flexion velocity was subsequently decelerated by eccentric hip extensor activity (phase H_F^-). The continued extensor moment then acted to extend the hip once flexion velocity had been reduced to zero, consistent with previous observations at the 16 m mark (Johnson and Buckley, 2001). There was thus a large hip extensor moment and extension angular velocity at the end of the swing phase, associated with a phase of considerable energy generation at the hip (phase H_F^{2+}). Sprinter N exhibited the greatest hip extensor moment during the late part of the swing phase, which contributed to a larger hip power production (Figure 5.10h) and thus greater energy generation (Figure 5.11) than the other two sprinters. This large hip moment may also have partly contributed to the high knee extension velocity of sprinter N. A hip extensor moment in a swinging leg would tend to rotate the shank in an anti-clockwise direction, which would typically increase the potentially detrimental forward horizontal velocity of the foot at touchdown. Therefore, some of the previously described high knee flexor moment of sprinter N during late swing may have been required not only in response to the knee extensor moment observed during mid-swing, but also to this hip extensor moment.

The overall resultant joint moment patterns during the rear leg swing phase were generally consistent with previous data from the latter phases of a sprint. Negligible ankle and MTP moments, combined with a hip moment changing from flexor to extensor dominance during mid swing and a knee extensor moment during mid swing which became flexor dominant during late swing, appeared to be the strategy used in preparation for the first stance phase. Large hip, and to some extent knee,

extensor moments (as generated by sprinter N) may have increased the requirement for a knee flexor moment during late swing in order to decelerate the swinging shank. Failure to arrest this knee flexor moment by the end of the flight phase would potentially be detrimental to the subsequent weight acceptance and extension required during stance.

5.4.3. The stance phase

The results from each of the separate joints will firstly be discussed, commencing with the MTP joint which has previously been largely ignored in sprint research. The overall kinetics patterns from all four stance leg joints will then be discussed with a view to how they were used to achieve the observed levels of performance. This will consider how the rotational joint actions helped to augment the horizontal motion of the sprinters.

Kinematics and kinetics at each joint

The plantarflexor resultant joint moment at the MTP throughout stance (Figure 5.14c) was in agreement with the only known previous MTP joint moments in sprinting, recorded from club-level sprinters wearing training shoes (Stefanyshyn and Nigg, 1997). Consistent with the observed angular velocity profile (Figure 5.14b), there was a noticeable phase of energy absorption (M_S^-) at the MTP during late stance, which for sprinters Q and R exceeded the energy absorbed at the ankle joint during phase A_S^- (Figure 5.16). The energy absorbed at the MTP joint during the M_S^- phase exceeded that generated during the subsequent phase (M_S^+) of MTP plantarflexion by a factor of 5.0, 24.3 and 11.4 for sprinters N, Q and R, respectively (Figure 5.16). Whilst these differences may have been due to individual differences in the active and passive biological structures surrounding the MTP joint, this cannot be determined from the current analysis. The stiffness of the spiked shoes, of which each sprinter wore their own individual pair, would also have affected the MTP joint moment, and thus influenced the joint kinetics. However, the MTP joint kinematics and kinetics presented in Figure 5.14 revealed that considerable movement occurred at the MTP joint during the first stance phase of a sprint and that mean peak plantarflexor moments in excess of 100 Nm were generated. All of the above reinforce the need for inclusion of the MTP joint in future analyses of the lower leg

during the start of a sprint, providing sufficiently accurate foot kinematic data can be obtained.

Much like at the MTP joint, the resultant ankle joint moment was also predominantly plantarflexor throughout stance (Figure 5.14g). This pattern was consistent with previous sprinting research, ranging from the second stance phase (Jacobs and van Ingen Schenau, 1992) to the 16 m mark (Johnson and Buckley, 2001) and the maximum velocity phase (e.g. Mann and Sprague, 1980; Mann, 1981; Bezodis *et al*., 2008). The mean peak plantarflexion moment magnitudes for the male sprinters (264 ± 24 Nm for sprinter N and 284 ± 2 Nm for sprinter Q) were close to the corresponding mean value (approximately 245 Nm) observed during the second stance phase by Jacobs and van Ingen Schenau (1992). Although the occurrence of a phase of energy absorption (A_S^-) followed by a phase of energy generation (A_S^+) at the ankle joint was also consistent with previous sprinting literature (e.g. Mann and Sprague, 1980; Mann, 1981; Jacobs and van Ingen Schenau, 1992; Johnson and Buckley, 2001; Bezodis *et al*., 2008), the magnitudes of the energy changes in each of these two power phases were considerably different from those observed previously at maximum velocity (Bezodis *et al*., 2008).

In the current study, sprinters N, Q and R generated more energy at the ankle than they absorbed by a factor of 2.8, 2.7 and 3.0, respectively (Figure 5.16). During the maximum velocity phase in well-trained and international sprinters, this ratio was found to be less than 0.6 (whole group mean), and thus the amount of energy absorbed exceeded the subsequent energy generated (Bezodis *et al*., 2008). Although Jacobs and van Ingen Schenau (1992) did not compute joint work in their analysis of the second stance phase, their ankle joint power time-histories were similar in shape and magnitude to those in the current study, with energy generation clearly much greater than absorption. At the 16 m mark, Johnson and Buckley (2001) presented ankle joint power time-histories which showed negative power phases of similar magnitude to the subsequent positive power phases (i.e. a factor of around 1.0). These current and previously published data therefore suggest that the net energy generated at the ankle joint gradually decreases from a large positive value to a negative value as a sprint progresses towards maximum velocity. However, this could be partly dependent on ability level or the absolute velocity attained by the

sprinters. Belli *et al*. (2002) found that nine trained middle-distance runners running at their maximum velocity (8.86 ± 0.56 m·s^{-1}), generated greater energy with the ankle joint musculature than was absorbed. It is therefore possible that at lower maximum velocities, net energy absorption may not be required at the ankle. However, at the high maximum velocities exhibited by well-trained sprinters, high vertical impact forces must be absorbed and it is possible that the ankle joint thus has to absorb more energy than it can generate (i.e. net energy absorption during stance).

The positive knee joint angular velocity from touchdown to toe-off (Figure 5.15b) was consistent with previous data from the second stance phase (Jacobs and van Ingen Schenau, 1992). However, the current data contrasted with those previously collected at 16 m mark, where some, but not all, sprinters flexed the knee during the early part of stance (Johnson and Buckley, 2001), and at the maximum velocity phase, where knee flexion was evident during early stance for all sprinters (Bezodis *et al*., 2008). This suggests that as a sprint progresses, increased flexion occurs at the knee joint during early stance, whilst during the initial steps, sprinters are able to extend their knee joints throughout stance and generate positive power. It is possible that due to the increased vertical forces experienced during the latter phases of a sprint (Bezodis *et al*., 2008), knee flexion is inevitable unless the musculature surrounding the knee possesses the strength to maintain knee joint configuration. The initial knee flexor moment at touchdown exhibited by Sprinter R, and in particular sprinter N (Figure 5.15c) may have been related to their greater braking and impact forces (Figures 5.12a and 5.12b) compared to sprinter Q. Although these peak impact forces (~2 BW) were still considerably lower than those observed at maximum velocity (>4 BW; Bezodis *et al*., 2008) and thus knee flexion did not occur, the knee joint was still required to absorb some of the energy associated with this impact (10.1 J during phase K_S^- for sprinter N; Figure 5.16).

As sprinter Q exhibited only minimal braking and impact forces, and thus did not require a knee flexor moment to counter these forces, he could begin to generate a more favourable knee extensor moment from the onset of stance. This may have allowed him to subsequently produce much greater peak knee extensor moments than sprinters N and R, which occurred earlier in stance (Figure 5.15c). As the knee joint extended throughout the majority of stance (Figure 5.15a), the power generated at the

joint was predominately positive. Sprinter Q was thus able to obtain an increased contribution from the knee joint, generating considerably greater energy (154.1 ± 17.3 J) than sprinters N (76.7 ± 21.8 J) and R (64.6 ± 13.4 J; Figure 5.16), and this remained true when these energy data were normalised using the convention of Hof (1996; Q = 0.19, N = 0.10, R = 0.12). It has previously been suggested that positive knee extensor power is initially used to terminate the negative vertical velocity present at touchdown in the maximum velocity phase, before playing a role in generating positive vertical and horizontal velocity for the remainder of stance (Mann, 1981). The initial negative vertical velocity would be greater during the maximum velocity phase where flight durations are longer (i.e. a greater time over which gravity can accelerate the CM) than at the start of a sprint. As there is a lower initial negative vertical velocity to be reversed during the start of a sprint, the knee may therefore have an increased role in the generation of positive power, and thus acceleration of the sprinter. The increased knee extensor joint moment and joint power of sprinter Q may therefore have helped him to achieve higher levels of performance, by contributing to his overall horizontal external power production during the first stance phase. Further kinetic analyses of other international-level sprinters may strengthen the identification of this aspect of technique as an important implication for coaching and training.

One further reason why sprinter N may have exhibited a knee flexor moment during the initial part of stance could be due to the aforementioned large knee flexor moment during the late swing phase not being terminated prior to touchdown. The knee flexor moment of sprinter N during the late flight phase (Figure 5.10c) was generated in an attempt to reduce the large knee extension angular velocity (Figure 5.10b) caused previously by the hip and knee extensor moments. However, this appeared unsuccessful because at touchdown, the knee extension angular velocity of sprinter N remained much higher than sprinters Q and R (Figure 5.15b), and thus the horizontal toe velocity of sprinter N was also high (2.29 ± 0.63 m·s^{-1}). It has previously been suggested that this horizontal foot velocity at touchdown is related to an increase in braking forces (Putnam and Kozey, 1989; Jacobs and van Ingen Schenau, 1992). The much larger mean peak braking force of sprinter N (-731 ± 181 N), in comparison to that of sprinter Q (-147 ± 79N) who was able to reduce his mean horizontal toe velocity to zero (0.00 ± 0.15 m·s^{-1}) at touchdown,

reinforced this. This theory was also supported by the trends for peak braking force magnitude to increase concurrently with toe touchdown velocity for all sprinters (Figure 5.13a). These braking forces occurred despite all sprinters exhibiting a negative touchdown distance (i.e. the CM ahead of the stance toe at touchdown; Table 5.5). These results suggested that during the first stance phase of a sprint, the magnitude of the braking force was increased by a greater horizontal velocity of the toe at touchdown. Therefore, if the toe was moving faster relative to the ground at touchdown, braking impulse was greater and thus the reduction in horizontal CM velocity during early stance was also greater. The less clear trends between touchdown distance and peak braking force magnitude between each of the three sprinters (Figure 5.13b) suggested that touchdown distance may not have as direct an effect on braking force magnitude, and that this relationship may be more individual specific.

The resultant knee joint moment time-histories contrasted in shape with many of those previously presented in sprint analyses (e.g. Mann and Sprague, 1980; Mann, 1981; Johnson and Buckley, 2001; Hunter *et al*., 2004; Bezodis *et al*., 2008), which contained high frequency flexor and extensor peaks soon after touchdown. There is reason to believe that these previously observed peaks may likely be artefacts that can be largely attributed to the use of different cut-off frequencies between processing the force and video data (Bisseling and Hof, 2006). Based on the previously outlined argument in section 5.2.4, is it proposed that the knee joint moments presented in Figure 5.15c represent a truer picture of the real knee joint moment. However, further investigation is warranted and these methods should also be applied to the maximum velocity phase where much of the previous research which has observed these impact peaks has been focused.

Whilst the resultant moments at the three distal joints became increasingly extensor during the first half of stance, the hip extensor moment peaked soon after touchdown (Figure 5.15g), as the hip generated a large amount of energy during the early part of stance (Figure 5.15.h and 5.16). This large hip extension moment was a continuation of the moment which was active during the latter part of the rear leg swing phase (Figure 5.10g). As previously mentioned, this was likely an attempt to decrease the forward momentum of the whole swing leg prior to touchdown, thus reducing the

velocity difference between the foot and the ground, assisting a reduction of the braking force magnitude (Putnam and Kozey, 1989; Jacobs and van Ingen Schenau, 1992).

The hip extension angular velocity peak soon after touchdown (Figure 5.15f) reflected the fact that after the hip had been able to extend rapidly during the non-weight bearing swing phase (Figure 5.10f), the hip joint had to subsequently act to support the weight of the upper body, and thus its capacity for extension was reduced. This resulted in a decrease in extension velocity around mid-stance, before the hip began to extend at an increasing rate during the second half of stance as the body weight was gradually unloaded. The hip extension angular velocity therefore reached a second peak, before beginning to decrease as the resultant hip joint moment became flexor dominant. This transition from extensor to flexor moment dominance at the hip joint during stance was consistent with many previous sprint kinetics analyses (e.g. Mann and Sprague, 1980; Mann, 1981; Johnson and Buckley, 2001; Hunter *et al*., 2004; Bezodis *et al*., 2008), and was required to absorb energy and thus decrease the extension angular velocity of the hip towards zero by toe-off. For sprinter N, and in some trials of sprinter Q, hip flexion actually commenced prior to toe-off, and positive flexor power was generated.

The time at which the resultant hip joint moment changes from extensor to flexor dominance during stance has varied widely in previous studies. This variation is well indicated by the results of Johnson and Buckley (2001), who observed flexor dominance to occur at approximately 45% of stance when analysing the mean group data, but found individual mean values to range from approximately 30 to 90%. The timings observed in the current study (Figure 5.15g) were similar to those observed during the second stance phase by Jacobs and van Ingen Schenau (1992). During the maximum velocity phase, Bezodis *et al*. (2008) observed this moment dominance change at around 80% of stance, whilst Mann and Sprague (1980) and Mann (1981) observed it to occur nearer one third of the way through a maximum velocity stance phase. It thus does not appear that the timing of flexor dominance necessarily relates directly to the phases of the sprint. These differences could possibly be due to ability and technique differences between the groups studied. For example, the sprinters studied by Mann and Sprague (1980) and Mann (1981) may have exhibited a more

powerful initial contribution from the hip extensor muscles, and thus required earlier hip flexor dominance in order to stop ground contact time increasing. This could partly be influenced by the training methods of sprinters in different studies, as they or their coach may have focussed on specific strength exercises favouring certain muscles, thus affecting when and how these muscles were recruited during a sprint. These temporal differences may also have been due to such factors as the dual role of the hip in stabilising the upper body (Winter, 1983), or to contrasting identification of the hip joint centre between studies, where differences of up to 30 mm have been found to affect the determined hip joint moments by up to 22% (Stagni *et al*., 2000).

Contributions of the rotational joint kinetics and kinematics to performance

As determined in Chapters 2 and 3, sprint performance is essentially a horizontal concept. Therefore, in order to fully understand the practical implication of the joint velocities, moments and powers, it was important to consider how these rotational joint motions affected overall performance in terms of horizontal motion. The contribution of a segment's rotational motion to horizontal translational velocity is dependent not only on the angular velocity of that segment, but also on the orientation of the segment, something which has been termed the *geometrical constraint* (van Ingen Schenau *et al*., 1987). For example, the proximal endpoint of a segment rotating about a fixed distal endpoint with constant angular velocity will possess a greater horizontal velocity when the segment is closest to a vertical orientation, due to a more favourable direction of the tangential velocity vector at that proximal endpoint (Figure 5.21). The geometrical constraint is therefore an important issue when considering how rotational joint motions affect performance of an essentially translational task.

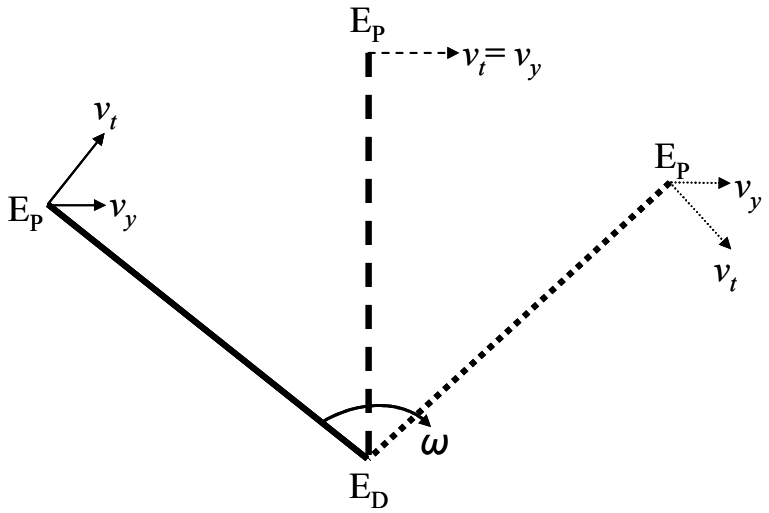

Figure 5.21. Illustration of the geometrical constraint. The proximal endpoint (E_P) of a segment rotating about a fixed distal endpoint (E_D) with constant angular velocity (ω) will possess a constant tangential velocity (v_t). However, this tangential velocity will relate most to horizontal velocity (v_y) when the segment is in a vertical orientation.

Another constraint which exists when considering the associations between rotational and translational motion is the *anatomical constraint* (van Ingen Schenau *et al*., 1987). This refers to the fact that as a joint approaches full extension, the angular velocity at that joint must be decelerated to zero in order to prevent injury to any of the biological structures crossing the joint. By considering these two constraints associated with rotational and translational motion, it is possible to further understand the reasons behind the techniques used during the first stance phase of a sprint, and how the previously described joint kinetics patterns helped to cause the desired increase in horizontal velocity.

An extensor moment at the hip, which was active during the late rear leg swing phase and the early part of the stance phase, would tend to increase the angle at the hip joint. This moment acted on both the thigh and trunk segments, and succeeded in increasing the hip joint angle during early stance (Figure 5.15e). This increase in hip joint angle from touchdown onwards was largely due to a clockwise rotation of the thigh segment rather than an anti-clockwise trunk rotation (Figure 5.18). An anti-clockwise trunk rotation would not be beneficial for performance, as it would translate the CM of the relatively massive trunk backwards relative to the hip joint,

which would not assist an increase in horizontal velocity. In human movement, the angular acceleration of a segment is seldom influenced by just a single resultant joint moment (Putnam, 1991; Hunter *et al*., 2004), and due to the linked-segment nature of the human body, all of the resultant joint moments and interactive moments in the system could affect the motion of any segment (Putnam and Dunn, 1987; Hunter *et al*., 2004). Despite the large hip extensor moment acting at the distal end of the trunk segment, a large rotation of the trunk was prevented by the significant gravitational moment of the segment itself (Figure 5.17) due to the segment CM being sufficiently far in front of the hip joint. The resultant moment generated about the hip joint may therefore have been a compromise between being as large as possible in order to generate a rapid clockwise rotation of the thigh segment without being so great that it created a potentially detrimental large anti-clockwise rotation of the trunk.

During the first half of stance, there was minimal rotation of the shank or either of the foot segments (Figures 5.18 - 5.20). It therefore appeared that the knee extensor moment, and the ankle and MTP plantarflexor moments were working together to maintain a stable lower end of the linked-segment system in relation to the thigh segment. This appeared to be a similar strategy to the limited ankle dorsiflexion used by sprinter P in the previous chapter (page 103), which was suggested to potentially assist extension of the proximal leg joints and thus performance. Similar joint kinetics to those observed in the current chapter have previously been observed at the 16 m mark of a sprint, where the ankle plantarflexor and knee extensor moments were also attributed to helping prevent the collapse of the lower leg (Hunter *et al*., 2004). This therefore provided a fixed knee joint centre, about which the thigh could rotate due to the large positive extensor power generated at the hip and knee. Owing to the fairly consistent orientation of the trunk and shank during this first half of stance, the increasing knee and hip angles were therefore largely indicative of the rapid thigh rotation (Figures 5.18 - 5.20). This helped to translate the stance thigh, trunk and swing leg segments forward, thus increasing the horizontal velocity of the whole body CM. These findings coincide with previous suggestions that success in sprinting is partly related to an ability to generate a high angular velocity of the stance thigh (Kunz and Kauffman, 1981; Mann and Sprague, 1983; Mann and Herman, 1985). Coupled with a stable trunk angle and near rigid joints in the lower leg and foot, this rapid clockwise thigh angular velocity assisted the forward

translation of the proximal, more massive segments of the body. The greater performance of sprinter Q may therefore be partly due to his ability to rotate the thigh segment over a greater range during stance, from a slightly more anti-clockwise initial orientation than sprinters N and R (Figure 5.19a). Sprinter Q was able to achieve this without an unfavourable increase in stance duration, which was likely assisted by the greater energy he generated at the knee joint compared to sprinters N and R (Figure 5.16).

Towards the end of stance, the knee and hip joints became increasingly extended (Figure 5.20), and thus the anatomical constraint (van Ingen Schenau *et al*., 1987) became a more pertinent issue. Also, because the thigh segment had rotated far beyond a vertical orientation, its contribution to horizontal velocity became increasingly less effective due to the geometrical constraint (van Ingen Schenau *et al*., 1987). However, the two foot segments remained in a favourable position to maintain the horizontal acceleration of the CM. During the latter part of stance, the more proximal segments (trunk, stance thigh and shank) therefore maintained a more stationary position with minimal rotation. Not only did this satisfy the anatomical constraint, and reduce the effects of the geometrical constraint, it also created a stable large mass which could be propelled forward by rotation of the foot segments due to the positive plantarflexion power generated at the ankle and MTP joints. Whilst both foot segments showed large changes in angle during the latter part of stance, these changes did not occur concurrently - the rearfoot started to rotate earlier, followed later by a more rapid rotation of the forefoot (Figure 5.18). This again reinforced the notion that the MTP joint cannot be ignored in sprinting, as there was considerable motion at this joint during the stance phase. Sprinter Q rotated the rearfoot segment over a greater range during stance (Figure 5.19b), and particularly evident was a greater rate of rotation during the final 25% of stance. Combined with the aforementioned thigh rotations, the joint kinetics of sprinter Q therefore appeared to augment his higher levels of performance by creating more rapid rotations of the thigh and foot segments (in particular the rearfoot), over a greater range of motion without any associated increase in stance time (compared to sprinter N). This may have been possible due to the greater power production and thus energy generated at the hip, knee and ankle joints during each of the respective positive power phases (Figure 5.16). The individual joint rotations appeared to be produced in such a way

that these joint powers were able to contribute to horizontal motion in the most effective fashion.

These results reinforce data from the second stance phase of a sprint, whereby sprinters were found to adopt a technique of initially rotating the body about the stance foot before extending the stance leg once the body's orientation was more favourable for this extension to benefit horizontal motion (Jacobs and van Ingen Schenau, 1992). However, these previous findings were based simply on the change in angle and distance between the stance foot and the CM, and the differences in horizontal velocity between the CM, the ankle, and the ground. The current results thus advance this theory by identifying the individual segment rotations responsible for the previously identified movement of the CM relative to the foot.

The timing of the segment rotations during stance (Figure 5.18) appeared to be consistent with the temporal pattern of peak positive joint powers (Figures 5.14 and 5.15). The large peak hip power reached early in stance would have assisted the clockwise rotation of the thigh, which would have been assisted by the peak knee joint power occurring shortly after mid-stance. The ankle and MTP positive joint power peaks occurred during the last 20% of stance, which assisted the rotation of the two foot segments. This proximal-to-distal pattern in the timing of the peak positive joint powers may potentially be related to a transfer of power owing to the action of biarticular muscles (Grégoire *et al*., 1984; van Ingen Schenau *et al*., 1987; Bobbert and van Ingen Schenau, 1988; van Ingen Schenau, 1989; Jacobs *et al*., 1996).

In order to satisfy the aforementioned anatomical constraint associated with joint extension, the joints must be decelerated as they approach full extension (van Ingen Schenau *et al*., 1987). If this were achieved through the action of mono-articular flexor muscles, the rotational energy generated during the latter range of extension would be dissipated as heat. However, the use of bi-articular muscles to decelerate the extending joints allowed the rotational energy to be transferred to an adjacent joint (Grégoire *et al*., 1984; Bobbert and van Ingen Schenau, 1988). The optimal joint extension pattern for power producing movements is therefore typified by a proximal-to-distal sequencing of peak joint powers, as power is transferred distally

from the hip to the knee via the bi-articular rectus femoris, and from the knee to the ankle via the bi-articular gastrocnemius (Grégoire *et al*., 1984, van Ingen Schenau *et al*., 1987; Bobbert and van Ingen Schenau, 1988; van Ingen Schenau, 1989; Jacobs *et al*., 1996). Without bi-articular muscles, a simultaneous extension of the leg joints would be optimal for power production in order to avoid the energy losses associated with deceleration of the joint angular velocities to satisfy the anatomical constraint (van Ingen Schenau, 1989). The proximal-to-distal sequencing in peak extension angular velocities, extensor moments and positive powers in the current study (Figures 5.14 and 5.15) therefore suggest that the bi-articular muscles played an important role in maximising the power output during the first stance phase, reinforcing similar findings from the second stance phase (Jacobs and van Ingen Schenau, 1992). Proximal-to-distal sequencing in peak joint powers has also been observed at the 16 m mark (Johnson and Buckley, 2001) and the maximum velocity phase (e.g. Bezodis *et al*., 2008) suggesting that this aspect of technique is important not only during the initial steps, but throughout the entire sprint. The techniques adopted therefore existed to overcome the geometrical and anatomical constraints associated with powerful leg extension (van Ingen Schenau *et al*., 1987; Bobbert and van Ingen Schenau, 1988) and to transfer the power to the specific joints where it could be most effectively used, with a minimal waste of energy, to maximise performance.

The proximal-to-distal joint sequencing may relate back to the issues surrounding the force and time contributions to impulse, as identified in Chapter 2. The techniques used by the sprinters in the current study indicate that peak joint powers were reached in a sequential fashion, and that joint angular velocities were reduced to zero prior to the joints reaching their full absolute extension limits. Whilst a concurrent extension of the stance leg joints would have decreased stance duration, the net force generated would have been far from optimal. Either not all joints would have been able to extend over their full range, or considerable energy would have been lost in reducing the rotational velocity at some joints (van Ingen Schenau, 1989). Impulse would therefore have been low, and despite the shorter stance duration, the external power production would also have been low due to the submaximal forces generated. In contrast, if the joints had extended considerably further towards their maximal extension, this would likely have increased the total impulse. However, the forces

generated about the joints during this extra range of extension would have been far from maximal due to both the geometrical constraints, and the need to satisfy the anatomical constraints (van Ingen Schenau *et al*., 1987). Therefore the impulse would have likely only been larger due to an increase in stance duration, as average force production would not have increased, and actually would most likely have decreased. These geometrical and anatomical constraints may also explain the results obtained in Chapter 4, where sprinter N was observed to exhibit an unfavourable additional increase in extension at the ankle joint towards the end of the block phase.

These findings once again highlight the importance of performance quantification, for simply determining the overall change in velocity during stance may not provide a full understanding of performance if stance phase durations are markedly different. The importance of the hip flexor moment is also potentially re-affirmed, because it would have helped to 'pull' the foot from the track at the end of stance, and without this hip flexor moment ground contact may not have been terminated as early, culminating in extra time spent generating low forces. In the current results, there was minimal energy absorption at the ankle or knee during late stance (Figures 5.14h and 5.15d). This suggested that the sprinters did not lose the ability to generate energy at these joints prior to toe-off, and that the energy absorption required to satisfy the anatomical constraints was either used favourably at distal joints, or occurred during the start of the subsequent swing phase. The sprinters could therefore recover and reposition the leg during this swing phase in preparation for the next stance phase where velocity could be further increased once more from an initially flexed-leg position.

5.4.4. Conclusion

The kinetic analysis performed in this chapter revealed that the stance leg resultant joint moments worked to provide a steady foot and shank about which the thigh segment could rapidly rotate. The horizontal velocity increase due to this motion was assisted by a virtually fixed trunk orientation, and thus much of the sprinter's mass was translated forward due to the hip and knee power which rotated the thigh. As the hip extended further, power was transferred to the knee joint to continue the rapid rotation of the thigh segment. Once the contribution of thigh rotation to horizontal velocity began to progressively decrease as it rotated further from the vertical, power

was transferred from the knee to the ankle joint. Here it was used favourably to rotate the two foot segments in a clockwise direction, as the ankle and MTP plantarflexor moments moved from assisting the knee extensor moment in fixing the shank and foot, to actively propelling the sprinter forward during late stance. By this point in stance, the rest of the body was considerably further ahead of the stance foot, and these rotations thus propelled the body forward as well as upward. The sprinter with the highest levels of performance (sprinter Q), in terms of horizontal external power production, was able to reduce the horizontal velocity of the foot to zero at touchdown. This meant that positive power could be generated at the knee throughout stance, as an initial flexor moment was not required to try and counter a large braking force. This sprinter generated greater positive peak powers and energy at each of the stance limb joints, and as was the case for all three sprinters, the peaks occurred in such a temporal fashion that the power could be transferred to the joints where it could be most favourably used to contribute to forward translation.

5.5. Chapter summary

A joint kinetics analysis was undertaken in order to further the understanding of how techniques are achieved during the start of a sprint. The techniques and performance were drawn together by associating the joint kinetics and kinematics with the individual segment rotations and thus linear translational motion. The impact moments previously observed at the knee and hip joints during sprinting were suggested to be due to data processing techniques, and a different methodological approach was taken in the current study. The results were analysed in an attempt to address research question iv - *how are the more advantageous sprint start kinematics achieved, and why do they lead to improved performance?*

The joint moment and power patterns were generally consistent with those previously reported during the early acceleration phase of a sprint. A novel finding was that in addition to considerable motion at the MTP joint, a plantarflexor moment in excess of 100 Nm also existed, highlighting the need for inclusion of this joint in subsequent sprint analyses investigating lower leg kinetics. The knee and hip joints provided much of the energy during early and mid-stance, as they rotated the thigh in a clockwise direction. This was largely possible due to the absorption of energy by the MTP and ankle joints, which helped to maintain a stable shank segment about

which the thigh could rotate in a clockwise direction. This caused a large forward translation of the CM, with greater power production at the knee appearing particularly important for overall average horizontal external power production and thus performance. A proximal-to-distal transfer of this power during late stance allowed acceleration to continue until toe-off, as the foot segments rotated in a clockwise direction, thus propelling the sprinter both forward and upward into the subsequent flight phase.

These empirical data increased the understanding of how techniques are achieved by international-level sprinters during the sprint start. Whilst certain aspects of technique, such as thigh rotation, horizontal foot velocity at touchdown, and the temporal pattern of joint angular velocities and powers, were identified as being potentially important aspects of technique, answers to research question vi - *can selected hypothetical technique adjustments identify further performance improvements?* - can only currently be speculated. Therefore, a theoretical model will be developed in an attempt to address research question v - *can a realistic representation of sprint start technique and performance be achieved with a forward dynamics computer simulation model?* This would allow subsequent alterations to be made to the technique of a sprinter to address research question vi and quantitatively determine how these changes would affect performance.

CHAPTER 6: DEVELOPMENT AND EVALUATION OF A SIMULATION MODEL OF A SPRINTER DURING THE FIRST POST-BLOCK STANCE PHASE

6.1. Introduction

In order to expand on the findings from the previous three empirical chapters (Chapter 3-5), a theoretical modelling research approach was also adopted. This offered a useful alternative mode of research, since comprehensive empirical data from repeated collections are difficult to obtain from international sprinters due to the strict focus of their training regimes (Kearney, 1999), which also restricts the undertaking of any experimental interventions. It was discussed in Chapter 2 that the clear scope for computer simulation models to enhance the current understanding of an activity such as the sprint start can only be realised if such models are utilised in conjunction with empirical data (Yeadon and Challis, 1994). Key findings from Chapter 5 were used in the determination and evolution of the structure of a forward dynamics model of a sprinter during the first stance phase. Selected empirical data from Chapter 5 were then used as inputs to the model, with the remaining input parameters determined through matching optimisations. The model output data were evaluated against further empirical data to ensure the model possessed an appropriate degree of accuracy and to address research question v - *can a realistic representation of sprint start technique and performance be achieved with a forward dynamics computer simulation model?*

6.1.1. General modelling assumptions

A linked-segment modelling approach was used to develop an appropriate theoretical representation of a sprinter during the first post-block stance phase. This assumed that a human can be represented by a series of rigid segments connected at frictionless joints. The movement was assumed to be planar in nature, and thus a 2D simulation model was developed which allowed sagittal plane movement about these joints. Air resistance was assumed to be negligible throughout and was ignored. Ground contact forces were modelled using spring-damper systems, an approach highlighted in Chapter 2 (section 2.4.1). A simple representation was initially developed, with model complexity subsequently increased as required.

6.2. One-segment spring-damper model

The simplest representation of a sprinter during stance is a single rigid rod with a fixed CM - located at a constant distance (*l*) from the distal end of the rod (O) - and a fixed moment of inertia. A linear spring-damper system is modelled at the distal end to represent the interaction between the rod and the ground during contact. These springs can extend from an initial resting length of zero at touchdown (t0), and the forces generated between the rod and the ground at any instant in time (t) can be calculated based on the instantaneous spring lengths and velocities.

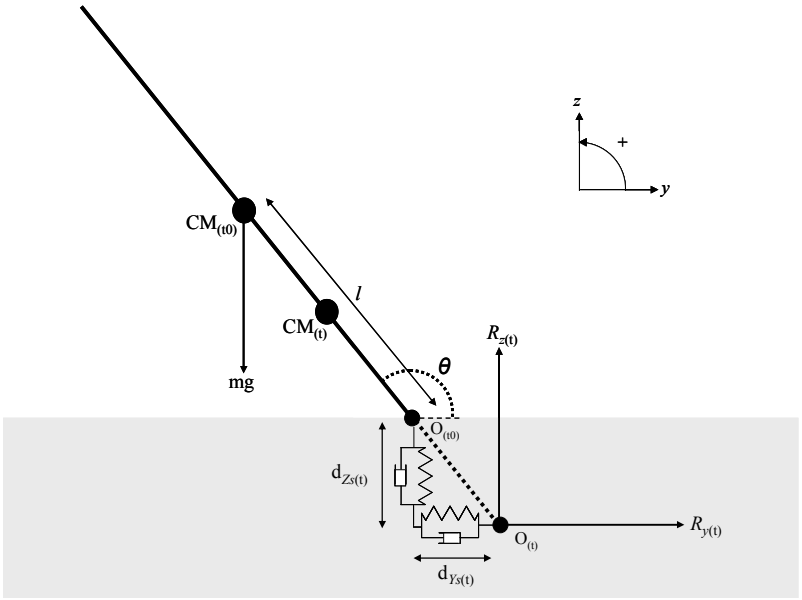

Figure 6.1. Illustration of the one-segment spring-damper model. See section 6.2.1 for definition of nomenclature.

6.2.1. Manual determination of equations of motion

As with any model system, the motion of this one-segment model can be simulated by determining the forces acting on it and formulating the associated equations of motion. This allows the motion of the system to be advanced throughout the contact phase. Questions relating to how the model inputs and parameters (e.g. initial velocities, plant angle, spring stiffness and damping) affect motion throughout the stance phase (and thus during the subsequent flight phase) can then be addressed.

At touchdown (t0), the distal end of the rod makes contact with the ground at point $O_{(t0)}$, with a plant angle of θ. During the subsequent ground contact phase, the

springs are extended from their original length (zero at t0). At any point in time (t) during ground contact, the distal end of the rod is at point $O_{(t)}$, and the springs possess a specific length in both the horizontal (d_{y_S}) and vertical (d_{z_S}) directions. Calculations can therefore be made relative to the point of contact ($O_{(t0)}$) to determine the motion of the system at any instant.

The position of the segment CM relative to the point of contact ($O_{(t0)}$) in both the horizontal ($d_{y_{CM}}$) and vertical ($d_{z_{CM}}$) directions can be calculated using trigonometry:

$$d_{y_{CM}} = d_{y_S} + l\cos\theta \quad [6.1]$$

$$d_{z_{CM}} = d_{z_S} + l\sin\theta \quad [6.2]$$

Equations 6.1 and 6.2 can be differentiated to obtain horizontal and vertical velocities of the CM:

$$v_{y_{CM}} = v_{y_S} - l\sin\theta\omega \quad [6.3]$$

$$v_{z_{CM}} = v_{z_S} + l\cos\theta\omega \quad [6.4]$$

Equations 6.3 and 6.4 can also therefore be differentiated to obtain horizontal and vertical accelerations of the CM:

$$a_{y_{CM}} = a_{y_S} - l\sin\theta\alpha - l\cos\theta\omega^2 \quad [6.5]$$

$$a_{z_{CM}} = a_{z_S} + l\cos\theta\alpha - l\sin\theta\omega^2 \quad [6.6]$$

The forces within each spring-damper system (F) can be characterised by a linear force-deformation relationship, where k and b are representative of the respective stiffness and damping co-efficients of the rod-ground interface:

$$F_y = -k_y d_{y_S} - b_y v_{y_S} \quad [6.7]$$

$$F_z = -k_z d_{z_S} - b_z v_{z_S} \quad [6.8]$$

The horizontal and vertical reaction forces at $O_{(t)}$ (R_y and R_z, respectively) can also be calculated using Newton's Second Law of Motion:

$$R_y = ma_{y_{CM}} \quad [6.9]$$

$$R_z - mg = ma_{z_{CM}} \quad [6.10]$$

where m is the mass of the segment, and g is the acceleration due to gravity (9.81 $m \cdot s^{-2}$). The angular momentum of the entire system about $O_{(t0)}$ (H_o) can be calculated as:

$$H_o = I\omega - mv_{y_{CM}} d_{z_{CM}} + mv_{z_{CM}} d_{y_{CM}} \quad [6.11]$$

where I is the moment of inertia of the segment. The rate of change of angular momentum (first derivative) about $O_{(t0)}$ is equal to the moment produced about $O_{(t0)}$ (M_o), thus:

$$M_o = \frac{\Delta H_o}{\Delta t} \quad [6.12]$$

By substituting equation 6.11 into equation 6.12, and resolving into horizontal and vertical components, a simplified expression for torque about $O_{(t0)}$ can be obtained:

$$M_o = \frac{\Delta(I\omega - mv_{y_{CM}} d_{z_{CM}} + mv_{z_{CM}} d_{y_{CM}})}{\Delta t}$$

$$M_o = I\alpha - ma_{y_{CM}} d_{z_{CM}} - mv_{y_{CM}} v_{z_{CM}} + mv_{z_{CM}} v_{y_{CM}} + ma_{z_{CM}} d_{y_{CM}}$$

$$M_o = I\alpha - ma_{y_{CM}} d_{z_{CM}} + ma_{z_{CM}} d_{y_{CM}} \quad [6.13]$$

The torque of the entire system about $O_{(t0)}$ can also be described by taking moments about $O_{(t0)}$, and can thus be calculated as:

$$M_o = -mgd_{y_{CM}} + R_z d_{y_S} - R_y d_{z_S} \quad [6.14]$$

Substituting equations 6.1, 6.9 and 6.10 into equation 6.14 yields:

$$M_o = -mg(l\cos\theta + d_{y_S}) + mgd_{y_S} + ma_{z_{CM}}d_{y_S} - ma_{y_{CM}}d_{z_S}$$

$$M_o = -mg(l\cos\theta) + ma_{z_{CM}}d_{y_S} - ma_{y_{CM}}d_{z_S} \qquad [6.15]$$

The two equations for torque (6.13 and 6.15) can therefore be equated to yield:

$$-mg(l\cos\theta) + ma_{z_{CM}}d_{y_S} - ma_{y_{CM}}d_{z_S} = I\alpha - ma_{y_{CM}}d_{z_{CM}} + ma_{z_{CM}}d_{y_{CM}}$$

$$I\alpha = -mg(l\cos\theta) + ma_{z_{CM}}d_{y_S} - ma_{y_{CM}}d_{z_S} + ma_{y_{CM}}d_{z_{CM}} - ma_{z_{CM}}d_{y_{CM}} \qquad [6.16]$$

By substituting equation 6.1 into equation 6.16 and simplifying, an expression for angular acceleration can be obtained:

$$I\alpha = -mg(d_{ycm} - d_{y_S}) + ma_{y_{CM}}(d_{z_{CM}} - d_{z_S}) - ma_{z_{CM}}(d_{y_{CM}} - d_{y_S})$$

$$\alpha = \frac{-mg(d_{ycm} - d_{y_S}) + ma_{y_{CM}}(d_{z_{CM}} - d_{z_S}) - ma_{z_{CM}}(d_{y_{CM}} - d_{y_S})}{I} \qquad [6.17]$$

Equations 6.9, 6.10 and 6.17 therefore yield three acceleration terms ($a_{y_{CM}}, a_{z_{CM}}, \alpha$) which can be subsequently integrated to calculate the velocity and displacement of the CM. The motion of this one-segment spring-damper system can therefore be fully determined from these equations of motion, using the following procedure:

- Equations 6.7 and 6.8 are used to obtain values for F_y and F_z.
- Because the horizontal and vertical reaction forces at $O_{(t)}$ are equal to the forces exerted by the corresponding spring-damper systems (i.e. $R_y = F_y$ and $R_z = F_z$), equations 6.9 and 6.10 are subsequently used to obtain values for $a_{y_{CM}}$ and $a_{z_{CM}}$, respectively.
- These linear accelerations are thus used with equation 6.17 to obtain the angular acceleration (α).
- From these three acceleration values ($a_{y_{CM}}, a_{z_{CM}}, \alpha$), the positions and velocities of the entire system (and the spring velocities and displacements) can be estimated at a specific small time step later.

- This iterative process continues, implementing the new positions and velocities back into equations 6.7 and 6.8, and repeating the process until a desired endpoint is reached.

These equations were manually implemented in a Matlab™ (v. 7.4.0, The MathWorks™, USA) script file, which was verified by running the simulation using the same input conditions as used by Wilson (2003) in a model of identical structure. These input conditions (Table 6.1) were developed by Wilson (2003) for use in a model of jumping for height. Although the current model is being developed for sprinting, the values presented in Table 6.1 provided appropriate data for the current purposes - to verify the correctness of model implementation.

Table 6.1. One-segment model inputs and the values of Wilson (2003) used to verify the manual implementation of the equations of motion.

Input	Equation nomenclature	Value
Segment length	l	1.00 m
Segment mass	m	70.00 kg
Segment moment of inertia	I	10 kg·m^2
Plant angle	θ	40°
Horizontal foot-ground interface stiffness	k_y	25,000 N·m^{-1}
Vertical foot-ground interface stiffness	k_z	50,300 N·m^{-1}
Horizontal foot-ground interface damping	b_y	0 N·s·m^{-1}
Vertical foot-ground interface damping	b_z	0 N·s·m^{-1}
Initial horizontal velocity	v_y (initial value)	6.7 m·s^{-1}
Initial vertical velocity	v_z (initial value)	0.0 m·s^{-1}

The equations of motion were integrated using a custom-written *for* loop throughout contact until the vertical spring returned to its original length, which was deemed to be representative of toe-off. Pilot tests revealed a fixed time step of 0.00001 s to be appropriate for obtaining sufficient accuracy when simulating the motion of this system. The instantaneous kinematics of the CM at 'toe-off' were extracted, and combined with equations of projectile motion in order to calculate the peak height of the CM during the subsequent flight phase. A peak height of 2.70 m was achieved

during this flight phase, matching that determined by Wilson (2003), and thus validating the manual implementation of the equations of motion within a Matlab™ script file.

6.2.2. Assisted determination of equations of motion

A one-segment model was not sufficient to accurately represent a sprinter during the first post-block stance phase, because the results presented in Chapter 5 revealed the unique roles associated with individual joints and segments, particularly those in the stance leg. An increase in model complexity was therefore required. However, as human body models become more sophisticated, the task of developing the equations that describe their motion also increases in complexity. As highlighted in section 2.4.2, software packages exist which allow the user to explicitly define the specific properties of a model system, and these packages can subsequently determine the associated equations of motion. It was therefore decided to utilise Simulink® (v.7.1, The MathWorks™, USA) to develop the model, with the SimMechanics® toolbox used to create the basic structure of the model. This reduced the potential for computational errors and improved the efficiency of the model development process.

The SimMechanics® toolbox contains *body* blocks which can be used to represent each segment within a model, as their properties (e.g. mass, moment of inertia, length and CM location) can be explicitly defined. *Joint* blocks from this toolbox can then be used to connect the body blocks, with the degrees of freedom at each joint also defined by the user. The system must also be connected to a *ground* block, which is in turn linked to a *machine environment* block where specific properties of the environment (e.g. gravitational constants, dimensionality) are defined. The associated motion is therefore determined from the user-defined properties of each individual block within the system, and the connections between them.

The simple one-segment model was recreated in Simulink® to verify the correct model system construction prior to extending the model to include additional joints and segments. Therefore, the system was defined using a series of blocks with custom-defined properties (Figures 6.2 and 6.3), rather than developing the equations of motion manually as in section 6.2.1. The model implementation could therefore

again be evaluated by determining the maximum height reached in the subsequent flight phase (Figure 6.4) and comparing it to the previously obtained value of 2.70 m.

The block system for the one-segment model is presented in Figures 6.2 to 6.4. Figure 6.2 illustrates the basic structure of the model system at its top-level, with a *body* block ('Segment') connected via a *joint* block ('Planar Joint') to the *Ground* and *Machine Environment* blocks. The initial joint conditions such as plant angle and linear velocities were specified by attaching an additional *Initial Joint Conditions* block to the *joint* block. The forces between the distal end of the segment and the ground were modelled in a separate subsystem (GRFs; Figure 6.3). The positions and velocities of this distal endpoint were sensed by *Joint Sensor* blocks, before being implemented into the spring-damper equations to calculate the forces. These forces were then applied to the segment via *Joint Actuator* blocks. A subsystem ('Terminate Simulation') was developed to stop the simulation when the vertical spring returned to its resting length, which represented toe-off (this was identical to the subsystem used to terminate simulation in the final model, as depicted in Appendix D, Figure D.4) Based on the CM kinematics at toe-off, variables relating to flight time, 'CM step height' (i.e. the height of the CM during the subsequent flight phase) and 'CM step distance' (i.e. the horizontal displacement of the CM during the subsequent flight phase) were calculated using equations of projectile motion in a separate subsystem (Projectile Motion Analysis; Figure 6.4).

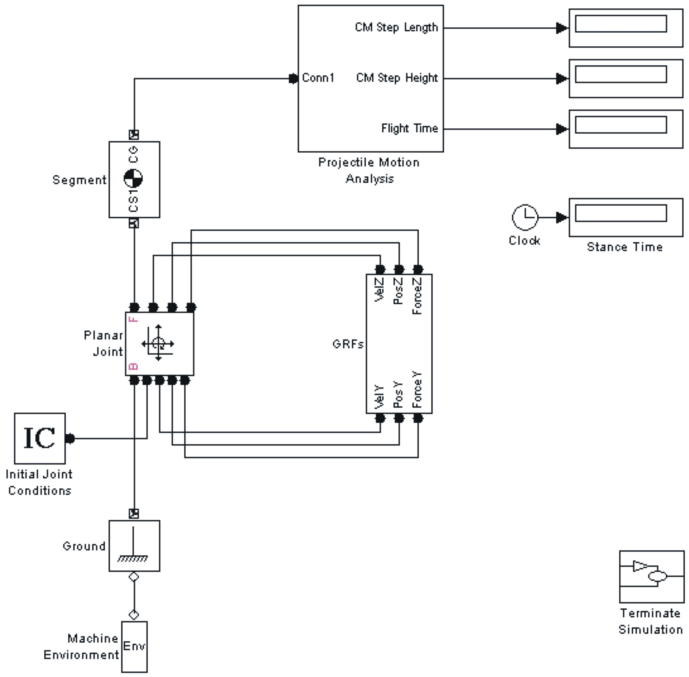

Figure 6.2. The overall top-level structure of the system used to recreate the one-segment model in Simulink®.

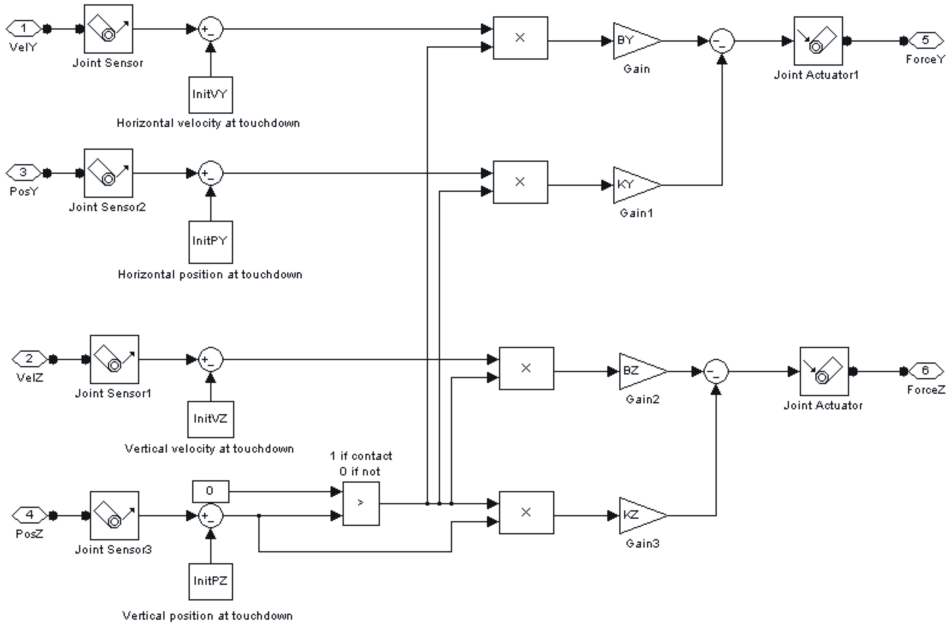

Figure 6.3. The subsystem ('GRFs' in Figure 6.2) used to model the ground reaction forces for the one-segment model in Simulink®. This is equivalent to equations 6.7 and 6.8 in the manual model development.

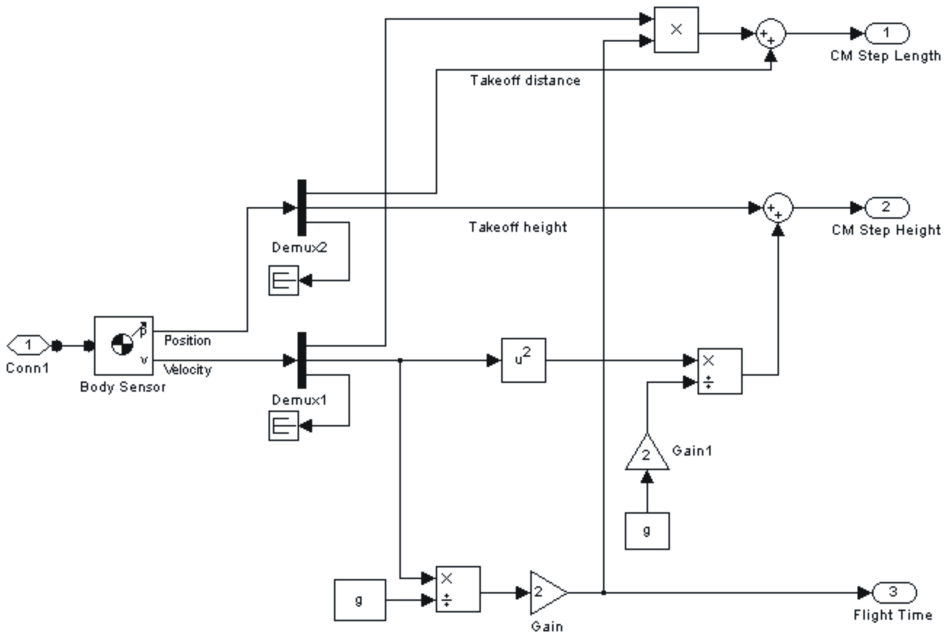

Figure 6.4. The subsystem ('Projectile Motion Analysis' in Figure 6.2) used to determine the flight phase kinematics for the one-segment model in Simulink®.

When this one-segment Simulink® model was run, a value of 2.70 m was obtained for CM jump height, identical to that obtained with the manual implementation. This proved that a multibody dynamic software package (i.e. Simulink®) could be used to recreate the simple one-segment model, reducing the time spent by the user developing the model. All subsequent model development could therefore take place within the Simulink® environment with full confidence in the automated equations of motion, provided the structure of the model was implemented correctly (verification of the final model structure is subsequently included in Section 6.3.2). The Simulink® model was therefore extended to include additional segments and a more complicated representation of ground contact, in order to achieve a more appropriate representation of reality.

6.3. Multi-segment model of a sprinter

The structure of the multi-segment model was based on the key findings presented in Chapter 5. Quantitative data from Chapter 5 were used alongside a qualitative analysis of the video clips to determine the properties which necessitated inclusion in the model representation.

6.3.1. Model structure, simplifications and assumptions

The data presented in Chapter 5 revealed the importance of the MTP joint in sprinting, and thus a two segment representation of the stance foot was included. The stance shank and thigh were also included as separate segments due to their clear importance in the first stance phase of a sprint. It was decided to include the swing thigh and shank as individual segments within the model, due to the relatively large changes in angle which were observed to occur at the swing hip and knee joints during stance. The swing foot was incorporated into the swing shank, as ankle and MTP motion of this swinging leg were deemed not to be critically important aspects of technique during the first post-block stance phase. The head, arms and trunk were grouped into a single segment (HAT) in order to prevent unnecessary overcomplication within the model, although they could be separated out into individual segments at a later time if required. The model therefore contained seven rigid segments (Figure 6.5). These were connected at revolute joints allowing rotation about a medio-lateral axis, thus permitting 2D motion to occur in the sagittal plane. The basic Simulink® structure of this model is presented in Figure 6.6.

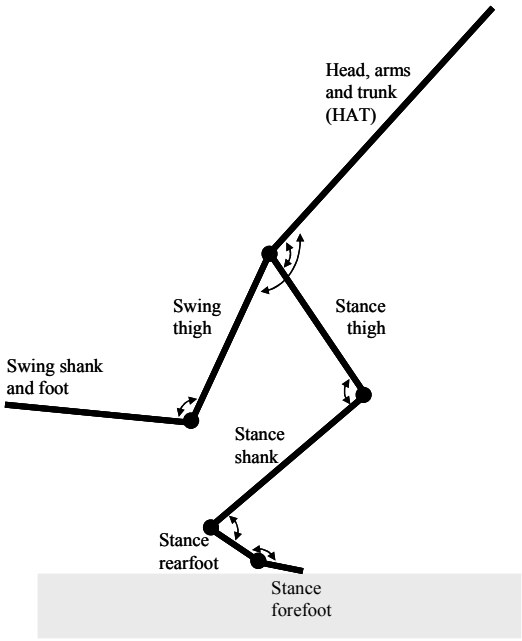

Figure 6.5. Determined structure of the multi-segment model of a sprinter during the first post-block stance phase.

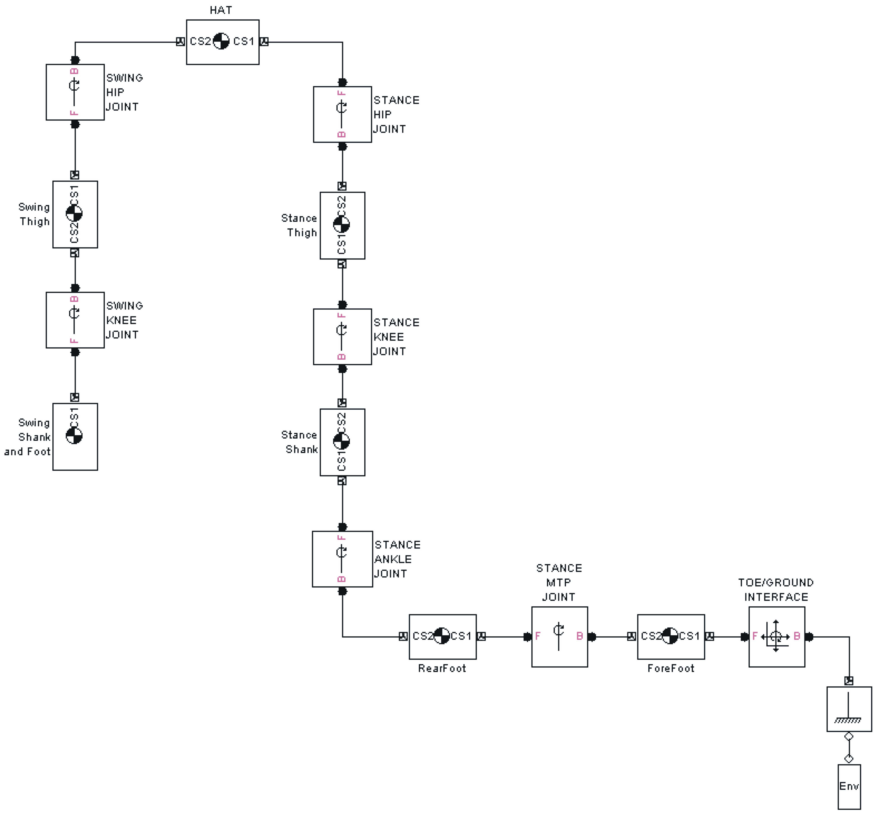

Figure 6.6. Basic structure used to create the multi-segment model representation using Simulink® software.

6.3.2. Verification of model structure

The model was checked at various stages during its creation to ensure correct development, and that no computational or theoretical errors had been made. With ground contact restricted to occur solely between the toe and the ground, the seven-segment model was firstly verified by constraining it to a fixed posture and sensing the forces between the toe and the ground to ensure that these were equal to body weight. The model was also simulated during free-fall, with the associated CM kinematics viewed to ensure they conformed to the laws of projectile motion (i.e. acceleration of the model CM was equal to acceleration due to gravity). Once the final ground contact model had been determined (see section 6.4) the ground reaction forces were compared with the linear motion of the whole body CM to ensure that the CM accelerations calculated from both corresponded exactly.

6.4. Modelling ground contact

A vital part of the simulation model was the interaction between the sprinter and the environment. As air resistance was assumed to be zero, aside from gravity the only external forces acting on the sprinter were those between the foot and the ground. These model forces were represented through spring-damper systems at the foot-ground interface, as has commonly been implemented in previous model representations of ground contact (e.g. Gilchrist and Winter, 1996; Marhefka and Orin, 1996, 1999; Bruneau and Ouezdou, 1999; Gittoes, 2004; King and Yeadon, 2004; Wilson *et al*., 2006).

It was important to obtain an accurate representation of this foot-ground interface in the model in order to ensure that the forces acting on the model system were close to those observed in Chapter 5. Qualitative analysis of the video clips obtained in Chapter 5 revealed that the toe always made the initial contact with the ground, and was soon followed by contact at the MTP joint. There was no rearfoot or heel contact with the ground, and the MTP joint always left the ground prior to toe-off. It was therefore decided to allow forces to be developed between the foot and the ground at both the toe and the MTP joint. Horizontal and vertical spring-damper systems were included at these points (Figure 6.7). During contact between the foot and the ground in sprinting, the soft tissue on the inferior surface of the foot, the spiked shoe, and the track surface will all deform to some extent. The spring-damper systems included in

the model were thus representative of the combined visco-elasticity of the soft tissue, spiked shoe and track surface.

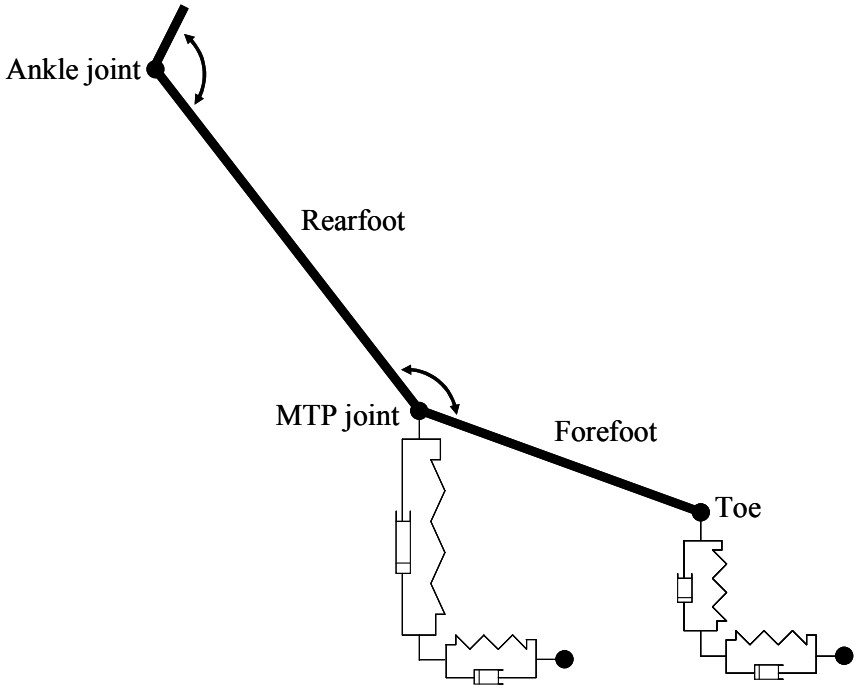

Figure 6.7. Illustration of the foot model used to represent ground contact.

The spring-damper systems used to model ground contact in the one-segment model earlier in this chapter (Section 6.2) were linear in nature, with stiffness totally dependent on spring length and damping on spring velocity, as indicated by equations 6.7 and 6.8 (and Figure 6.3). However, it was highlighted in Chapter 2 that the use of such equations can lead to discontinuity in the forces upon impact due to the initial velocity in the spring (Marhefka and Orin, 1996). The ground contact representation used in the seven-segment model therefore incorporated an additional function whereby the damping term was dependent on the spring length. This created a representation in which damping increased as the spring compressed, similar to the realistic situation where an increased area of the spiked shoe and track would come into contact (Wilson *et al*., 2006). The spring-damper force equations were therefore extended from those presented in equations 6.7 and 6.8, with the damping being additionally dependent on the change in spring length for the horizontal and vertical springs, respectively:

$$F_y = -k_y d_{y_S} - b_y \left| d_{y_S} \right| v_{y_S} \quad [6.18]$$

$$F_z = -k_z d_{z_S} - b_z \left| d_{z_S} \right| v_{z_S} \quad [6.19]$$

Another aspect of ground contact that has been included in previous spring-damper model representations is that when vertical spring compression is greater, larger horizontal forces are required in order to achieve a given horizontal displacement due to a greater frictional force. Horizontal forces have thus previously been considered to be dependent on the associated vertical motion (e.g. Wilson *et al*., 2006). Therefore, whilst the vertical forces could be represented using equation 6.19, the horizontal forces were modelled using equation 6.20, which included vertical spring displacement:

$$F_y = (-k_y d_{y_S} - b_y \left| d_{y_S} \right| v_{y_S}) d_{z_S} \quad [6.20]$$

Spring-damper systems defined by equations 6.19 and 6.20 were therefore incorporated to represent the respective vertical and horizontal motion at both the toe and MTP joint. Similar to the subsystems developed previously for the one-segment model (Figure 6.3), the toe system sensed the position and velocity within the joint between the toe and the ground, and actuated this joint with the forces calculated. The MTP system required a slightly different approach since it was not possible to include linear joints between the MTP and the ground due to over-determination of the model. The position of the proximal endpoint of the forefoot segment (i.e. the MTP joint) was therefore sensed, and this part of the forefoot *body* block was actuated via a *body actuator* block.

The sum of the forces from both the toe and MTP spring-damper systems thus yielded the total ground reaction force magnitudes acting on the model:

$$F_y = F_{y_{toe}} + F_{y_{MTP}} \quad [6.21]$$

$$F_z = F_{z_{toe}} + F_{z_{MTP}} \quad [6.22]$$

As stated previously, ground contact commenced with the toe, and terminated when the toe left the ground. The co-ordinates of the toe at touchdown were subtracted from all subsequent toe-co-ordinates to create initial resting spring lengths of zero (i.e. zero force at touchdown). Ground contact in the model was terminated when the vertical toe co-ordinate returned to a value greater than this initial vertical co-ordinate at touchdown, using a *Relational Operator* block in Simulink®. For each modelled trial, the toe co-ordinates at touchdown were determined from the 1000 Hz video clips collected in the investigation undertaken in Chapter 5, extracting the values from the instant of touchdown as identified using the force platform data.

The force platform could only be used to identify toe touchdown, and not MTP touchdown. A displacement threshold for the latter was thus required, below which MTP contact was assumed to be present. Therefore, when MTP vertical displacement fell below the set threshold level, the modelled MTP spring-damper systems activated, and forces were generated in the spring. For each modelled trial, the MTP threshold was estimated manually from the video data collected with camera 3 (1000 Hz) in Chapter 5, based on identification of the time at which the MTP joint appeared to make contact with the track. The corresponding vertical MTP co-ordinate at this instant in time was identified from the exported digitised data. This threshold value was allowed to vary by ± 0.01 m in the subsequent optimisations (section 6.6) to allow for any errors associated with digitising or the visual identification of MTP contact from the 1000 Hz video clip. The MTP force subsystem was therefore included within an *if action* subsystem, which was only activated if the vertical MTP co-ordinate was equal to, or less than, the specific threshold value. As the MTP rose back off the ground during the latter part of the stance phase, the vertical MTP spring-damper system began to return towards its resting level (i.e. length of zero), with MTP contact terminating when the spring had returned to its resting length (i.e. vertical MTP displacement reached the threshold co-ordinate and the *if action* subsystem was no longer activated).

6.5. Model implementation

Having developed the structure of the seven-segment model using Simulink® software, the model required implementation. This section describes the methods used to advance the simulation model and solve the differential equations associated

with the block structure at each time-step. The model inputs, including parameters, initial conditions and joint drivers, are detailed in terms of their structure and formulation. The model outputs required for the subsequent evaluation (section 6.6) and application (Chapter 7) are also described.

6.5.1. Integration methods

The manually-developed equations for the one-segment model were previously solved using a custom built integrator inside a *for* loop with a fixed-time step of 0.00001 s. However, purpose-built solvers exist within the Simulink® environment which can be chosen to suit the desired purpose. It was decided to use a variable-step solver for the multi-segment model, as this would reduce the step size when the model's states changed rapidly, and increase it when the states changed more slowly. This would therefore maintain a high level of accuracy when required, yet reduce potential time losses associated with fixed-step solvers during slowly-changing states. A Runge-Kutte integration algorithm was employed, through the *ode45* Dormand-Prince solver available within the Simulink® environment. Solutions were initially obtained between time boundaries defined by the author during developmental stages, with subsequent simulations terminated when the vertical toe spring returned to its resting length.

6.5.2. Model inputs

Model inputs were used to expand the original model structure by specifying the trial-specific properties associated with each block, and to determine how the model advanced through each time step when integrated. These inputs were calculated and defined in a Matlab™ script file (Appendix E), which was run prior to implementation of the model. Sprinter-specific inputs allowed customisation of the model, and thus the subsequent evaluation of model-generated data against empirical data collected from an individual athlete. This therefore also permitted the model to be used to identify aspects of technique which could facilitate performance on a single-sprinter level. Model inputs can be divided into *model parameters*, such as segmental inertia properties and the foot-ground interface stiffness and damping co-efficients, *initial conditions*, such as linear and angular displacements and velocities at touchdown, and *joint angular acceleration time-histories*, which were used to drive the motion about each joint.

Model parameters

The sprinter-specific segmental inertia parameters used in Chapter 5 (Appendix B) were also used with the model. These were obtained using 95 anthropometric measurements (Yeadon, 1990) taken directly from the sprinters, and provided length, CM location, mass and moment of inertia of each segment. Where segments were grouped in the model (i.e. HAT segment, swing shank and foot segment), combined inertia properties for the new segments were calculated through the summation of moments and the parallel axes theorem (Winter, 1990) assuming constant neutral angles between adjacent segments. Stiffness and damping parameters for the foot-ground interface were also required. The stiffness and damping characteristics of the foot vary depending on the frequency and loading rate of impact (Aerts and de Clercq, 1993; Ker, 1996). Combined with the fact that the novel representation of the foot in the current model contained two segments and spring-damper systems at the toe and MTP, the use of spring constants from previous literature was therefore not warranted. To achieve realistic model ground reaction forces, the stiffness and damping co-efficients at the foot-ground interface were thus obtained through a matching optimisation approach for each modelled trial (section 6.6). This allowed the foot-ground interface co-efficients to be systematically varied in combination, using an optimisation algorithm in an attempt to determine the stiffness and damping values which facilitated the closest match between the modelled trial and reality. Such an approach has been commonly adopted in previous theoretical research incorporating spring-damper systems to represent ground contact (e.g. Yeadon and King, 2002; Gittoes, 2004; Wilson *et al*., 2006).

Initial conditions

The initial conditions of the stance phase were required in order to describe the initial state of the model for each modelled trial. Initial horizontal and linear velocities of the stance toe were determined from the 1000 Hz video camera data collected in Chapter 5. Due to the structure of the model within Simulink®, these provided the only linear motion inputs. Linear segmental CM motions could then be determined using the angular motion at each of the joints. Whole body CM motion was obtained through the summation of segmental moments (Appendix D, Figure D.2). The initial joint angular positions and velocities were obtained from the kinematic data

presented in Chapter 5. Forefoot angle and angular velocity relative to the ground were also obtained as initial conditions for the rotational motion of the forefoot segment, which would subsequently be influenced by the forces generated in the toe and MTP spring-damper systems. The spring lengths were defined relative to the position of the toe at touchdown and of the MTP at MTP contact, respectively. This therefore meant that initial resting spring lengths were zero, and the springs subsequently extended and compressed as stance progressed.

Joint angular acceleration time-histories

Joint angular accelerations were used to drive the joints rather than joint torques because the aim of the model was to investigate how changes in technique could influence performance. This angle-driven approach therefore allowed the direct systematic manipulation of technique, which can be difficult to achieve with a torque-driven model (e.g. Yeadon and King, 2002). Joint angular acceleration time-histories were calculated from the filtered empirical data presented in Chapter 5. These were then integrated and combined with the initial joint conditions (velocity and position at each joint) to yield the associated angular velocity and displacement time-histories.

Despite the smoothing procedures adopted in Chapter 5, the joint angular acceleration time-histories may still have contained noise which could have resulted in erroneous inputs to the model. It was therefore decided to include an additional function which allowed these time-histories to vary slightly from their original values. Five terms of a Fourier series (ε_j) were added to the empirically-recorded angular acceleration time-histories (α_{Ej}) at each separate joint (*j*). This yielded new angular acceleration time-histories which acted as inputs for the model (α_{Mj}), similar to the procedures previously used by Wilson *et al*. (2006):

$$\alpha_{Mj}(t) = \alpha_{Ej}(t) + \varepsilon_j(t) \qquad [6.23]$$

It was decided to use a combination of sine and cosine terms so that the angular accelerations at touchdown, toe-off and the exact mid-point of stance were able to vary. The five sine terms used by Wilson *et al*. (2006) were unable to deviate from

zero at these points, and thus could not influence the associated joint angular accelerations. Sine waves with a frequency of 1, 3 and 5 Hz, and cosine waves with a frequency of 2 and 4 Hz were added to each joint angular acceleration time-history, using equation 6.24:

$$\varepsilon_j(t) = j_1 \sin(t) + j_2 \cos(2t) + j_3 \sin(3t) + j_4 \cos(4t) + j_5 \sin(5t) \qquad [6.24]$$

where j_n is the co-efficient for the term of frequency n Hz at joint j. The co-efficients of each term were initially set to zero, and thus the initial joint angular accelerations matched the empirically recorded time-histories. These co-efficients were then allowed to vary between specific limits in the matching optimisations (section 6.6) in an attempt to reduce the effects of any noise in the empirical time-histories.

6.5.3. Model Outputs

Because a forward dynamics approach was used to solve the equations of motion, the model produced solutions for the kinematic and kinetic aspects of the simulated motion. There were potentially numerous outputs that could be determined from the model through the attachment of *joint sensor* or *body sensor* blocks to specific joints or bodies of interest within the Simulink® environment. These model outputs were firstly used in the evaluation, and ultimately for the application of the model in an attempt to address specific research questions (Chapter 7). Joint angle time-histories throughout the stance phase were output directly from the model. The individual segment CM locations were obtained, and combined with their respective masses to calculate a trajectory of the whole body CM throughout stance. The horizontal and vertical ground reaction forces between the toe and the ground, and the MTP and the ground (and thus the composite ground reaction forces), were produced by motion within the spring-damper systems. Cumulative impulses from the entire stance phase were calculated from these ground reaction force time-histories through integration (Trapezium Rule), and thus also provided a value for the overall change in the CM velocity of the model from touchdown to toe-off (when divided by the mass of the sprinter). This enabled average horizontal external power (i.e. the performance measure) to be calculated using equation 3.4 (page 60).

6.6. Model evaluation

Model evaluation provides a level of confidence that can be associated with theoretical predictions (Yeadon and Challis, 1994). An appropriate evaluation compares the model outputs with empirical data, quantifying the accuracy of the model in replicating the system of interest. This section therefore assesses the appropriateness of the model for gaining insight into the first stance phase of a sprint.

6.6.1. Method of evaluation

Having developed the model structure, the model inputs (section 6.5.2) allowed the model to be customised to an individual. Input data from the highest-performing sprinter during the first stance phase analysed in Chapter 5 (i.e. sprinter Q) were therefore used to define the appropriate inputs to the model. Model input data from three randomly-selected trials of sprinter Q (subsequently referred to as trials E1, E2 and E3) were generated using a Matlab™ script file (Appendix E). These trial-specific input data were used in matching optimisations to determine the remaining input parameters (i.e. foot-ground interface stiffness and damping co-efficients, Fourier co-efficients for angular acceleration time-histories) which provided the closest match between the model and reality for each of the three trials. Based on pilot investigations, all horizontal foot-ground interface spring-damper co-efficients were allowed to vary between 0 and 1.0×10^{06}, and all vertical co-efficients between 0 and 1.0×10^{05}. The start values for the optimisation of these horizontal and vertical co-efficients were 1.0×10^{05} and 1.0×10^{04}, respectively. The Fourier co-efficients applied to the angular acceleration input parameters were allowed to vary between ± 2000. Variation was also permitted in the linear toe velocities at touchdown (± 0.25 $m \cdot s^{-1}$), the foot angle at touchdown (± 1º), the foot angular velocity at touchdown (± 25º$\cdot s^{-1}$) and the position at which the MTP was deemed to have made contact with the track (± 0.01 m) to account for errors in the digitised input data.

The matching optimisations were performed using a Latin Hypercube optimisation algorithm to minimise the difference between the model and actual ground reaction force time-histories by varying the specified input parameters within their pre-defined boundaries. This algorithm performed a pattern search, using both uphill and downhill searches to locate the global optimum, thus reducing the chance of convergence at a local optimum. A variable-step solver (*ode45*) was used for model

integration, with absolute and relative tolerances of 1.0×0.6^{-04} and 1.0×0.6^{-06}, respectively. Optimisations were programmed to restart after every 500 iterations to prevent the Hessian (the square matrix of second-order partial derivatives of the function being optimised) from becoming ill-conditioned, thus increasing the chance of the optimisation converging.

6.6.2. Determination of variables used in the evaluation

The variables used to evaluate a model should directly reflect the desired application of the model (Yeadon and King, 2002). It was therefore decided to identify specific variables relevant to the first step of a sprint as those variables deemed critical for determining the appropriateness of the model. Three of the evaluation categories were based on previous model evaluations - *configuration* (e.g. Yeadon and King, 2002; Hiley and Yeadon, 2007), *orientation* (e.g. Yeadon and King, 2002; Yeadon *et al*., 2006) and *ground reaction force accuracy* (e.g. Gittoes, 2004; Wilson *et al*., 2006). These were included in the current evaluation alongside *impulse* and *performance* categories, which to the author's knowledge have not previously been used to evaluate angle-driven models of human movement.

Configuration

The configuration score corresponded to how well the model joint angle time-histories matched the empirical data throughout the duration of the stance phase. This quantified the magnitude of the effect that each angular acceleration Fourier term had on the angular displacement time-histories. An RMS difference between the model and actual joint angle time-histories, based on data from each 1% of stance, was calculated. The mean value from the six joints (stance MTP, stance ankle, stance knee, stance hip, swing knee, swing hip) provided an evaluation score for configuration.

Orientation

Whilst the configuration score quantified the differences between actual and model kinematics at each joint, it provided no indication regarding whether the sum of these differences had a pronounced systematic effect on the overall motion of the sprinter. The angle of the trunk relative to the horizontal was influenced by the angles at the stance MTP, ankle, knee and hip joints. An RMS difference between the model and

actual trunk angle thus yielded a value which quantified the combined effect of these joint angles on the overall orientation of the sprinter, and provided an evaluation score for orientation.

Impulse

Having evaluated the model kinematics, it was important to quantify the level of accuracy with which certain kinetic variables could be represented within the model. The vertical impulse and net propulsive impulse which were generated between the sprinter and the ground were calculated, as these determined the overall change in velocity of the sprinter. These impulses were expressed as a percentage difference from the corresponding empirical values, and the vertical and net propulsive impulse percentage differences were averaged to obtain a single impulse score for the evaluation.

Ground reaction force accuracy

It was possible that a close match between model and empirical impulse data could be achieved without the force time-histories necessarily matching well. For example, if the model force time-history continually fluctuated equally above and below the empirical values, even if these fluctuations were large, a good impulse match would be achieved. In order to quantify how well the overall pattern of the force time-histories matched, an RMS difference value was calculated between the model and actual force data, based on data from each 1% of stance. This RMS value was then expressed as a percentage of the total force excursion (i.e. min - max range), and the horizontal and vertical percentage differences were averaged to yield an evaluation score for ground reaction force accuracy.

Performance

Whilst the four previously discussed values quantified the accuracy of kinematic and kinetic technique-related variables, a final aspect of the model which clearly required evaluation was the overall level of performance achieved by the model-based representation of the sprinter. The average horizontal external power generated during stance was calculated based on equation 3.4 (page 60), and was expressed as a percentage difference from the associated empirical value, yielding an evaluation score for performance.

Overall model accuracy

Five scores related to the overall accuracy of the model were therefore obtained during the evaluation. It has previously been proposed that errors in degrees can be equated to those in percent (Yeadon and King, 2002), and thus the mean value of these five scores yielded an overall score providing a reflection of the level of accuracy with which the model was representative of reality.

6.6.3 Evaluation results

The input parameters obtained using matching optimisations were used in a single simulation of the model. The subsequently generated model output data were written to text files allowing them to be evaluated against the empirical data. The previously-described kinematic and kinetic evaluation variables (section 6.6.2) were compared with the empirical data collected in Chapter 5 for all three evaluated trials (E1, E2 and E3). This section presents evaluation scores for all three trials and figures for one trial to provide a graphical representation of model accuracy (figures correspond to trial E3 as this was subsequently used in the investigations undertaken in Chapter 7).

Spring-damper co-efficients

Table 6.2 presents the optimised horizontal and vertical stiffness and damping co-efficients obtained for the toe and MTP foot-ground interface springs through matching optimisation, and used as inputs for the evaluation of each of the three trials. Whilst it is difficult to evaluate these co-efficients against empirical data, closer inspection of them reveals that they provided a sensible representation of ground contact. The large $k_{y_{Toe}}$ and $b_{y_{Toe}}$ co-efficients indicate that considerable horizontal forces were generated in the toe springs (Table 6.2). The MTP always made contact with the ground soon after touchdown, and remained in contact for the majority of stance. Large vertical forces were thus generated due to the magnitude of the vertical stiffness co-efficient ($k_{z_{MTP}}$) in the spring between the MTP joint and the ground (Table 6.2). The appropriateness of these co-efficients for representing ground contact was also confirmed by the evaluation scores related to the ground reaction forces (impulse, ground reaction force accuracy and performance) as will be discussed subsequently (pages 194-196).

Table 6.2. Optimised stiffness ($N \cdot m^{-1}$) and damping ($N \cdot s \cdot m^{-1}$) co-efficients for the representation of the foot-ground interface in the three evaluated trials.

Parameter	Trial E1	Trial E2	Trial E3
$k_{y_{Toe}}$	914,274	196,843	235,850
$k_{y_{MTP}}$	1,327	7,031	239,990
$b_{y_{Toe}}$	544,526	55,458	110,310
$b_{y_{MTP}}$	4,008	0	0
$k_{z_{Toe}}$	3,565	11,594	60
$k_{z_{MTP}}$	35,024	28,902	48,661
$b_{z_{Toe}}$	46	51	42
$b_{z_{MTP}}$	894	245	15,590

k represents a stiffness co-efficient, *b* represents a damping co-efficient, *y* refers to the horizontal springs, z refers to the vertical springs, *Toe* refers to the springs between the toe and the ground, *MTP* refers to the springs between the metatarsophalangeal joint and the ground.

The variation in spring-damper co-efficients between the three trials (Table 6.2) was not surprising since many forward dynamics models have previously identified large differences in the foot-ground interface parameters obtained from independent trials (e.g. Wilson, 2003; Gittoes, 2004). In the model developed by Gittoes (2004), optimised stiffness co-efficients ranging from 3.9×10^{05} to 1.9×10^{09} $N \cdot m^{-1}$ were determined for the toe springs, and from 9.5×10^{04} to 2.0×10^{09} $N \cdot m^{-1}$ for the heel springs. The damping co-efficients of Gittoes (2004) ranged from 1.6×10^{05} to 1.9×10^{08} $N \cdot s \cdot m^{-1}$ for the toe springs, and from 1.0×10^{04} to 2.0×10^{07} $N \cdot m^{-1}$ for the heel springs. Although these values cannot be directly compared to those obtained in the current model due the use of non-linear springs and horizontal forces independent of vertical spring compression by Gittoes (2004), they provide additional evidence to reinforce the notion that spring parameters are typically trial-specific, even when trials have been collected from a single subject. Although this variation in optimised spring-damper co-efficients did exist between trials in the current study, it is possible that these inter-trial differences may not have had a large effect on the overall optimised solution. For example, the horizontal stiffness for the MTP spring ($k_{y_{MTP}}$) was considerably larger in trial E3 (239,990 $N \cdot m^{-1}$) than in trials E1 and E2

(1,327 and 7,031 $N \cdot m^{-1}$, respectively). However, it is likely that the horizontal displacement range in this spring was small compared to that at the toe, and thus this co-efficient would not have had a major influence on the total horizontal forces generated between the foot and the ground. It is therefore important to determine the sensitivity of these foot-ground interface spring co-efficients, and a sensitivity analysis was subsequently undertaken (section 6.6.4).

The degree to which these spring-damper co-efficients provided sensible input data for the model can be further assessed by quantifying the level of accuracy associated with specific model output variables when using these inputs in the foot-ground interface. A close match between model and empirical output data would confirm that these values provided an appropriate representation of the visco-elastic properties of the track, spiked shoe and soft tissue on the sole of the foot. The following evaluation scores were therefore calculated for trials E1, E2 and E3 when running a simulation using the trial-specific inputs obtained from the matching optimisations.

Configuration

The RMS differences between the model and actual joint angle time-histories at each of the six joints for all three optimised matches are presented in Table 6.3. The mean values (i.e. configuration scores) are also presented. The joint angle time-histories throughout the stance phase for trial E3 are illustrated in Figures 6.8a-f.

Table 6.3. RMS differences between model and empirical joint angle time-histories throughout stance for the three evaluated trials.

	Trial E1	Trial E2	Trial E3
Stance MTP	8.5º	9.8º	5.6º
Stance ankle	10.4º	10.7º	6.5º
Stance knee	6.3º	10.1º	6.5º
Stance hip	8.0º	9.9º	2.4º
Swing knee	7.3º	10.5º	6.8º
Swing hip	8.4º	9.8º	6.8º
Mean (i.e. configuration score)	8.1º	10.1º	5.7º

The RMS differences between each of the six model joint angle time-histories and their corresponding empirical values (Table 6.3) were indicative of a good match between the model and reality. These values confirmed that the boundaries specified for the Fourier co-efficients applied to the empirical angular acceleration time-histories were sufficiently tight in order to prevent an excessive change in the individual joint kinematics of the model (e.g. Figure 6.8). The gradual drift between the model and empirical data in Figures 6.8a-f can be attributed to both the propagation of errors as the integration progressed through time, as well as to applying Fourier terms to acceleration, rather than displacement, time-histories. This gradual increase in the difference between model and empirical displacements has been previously observed by Yeadon and Hiley (2000), who also used angular acceleration time-histories to drive their model.

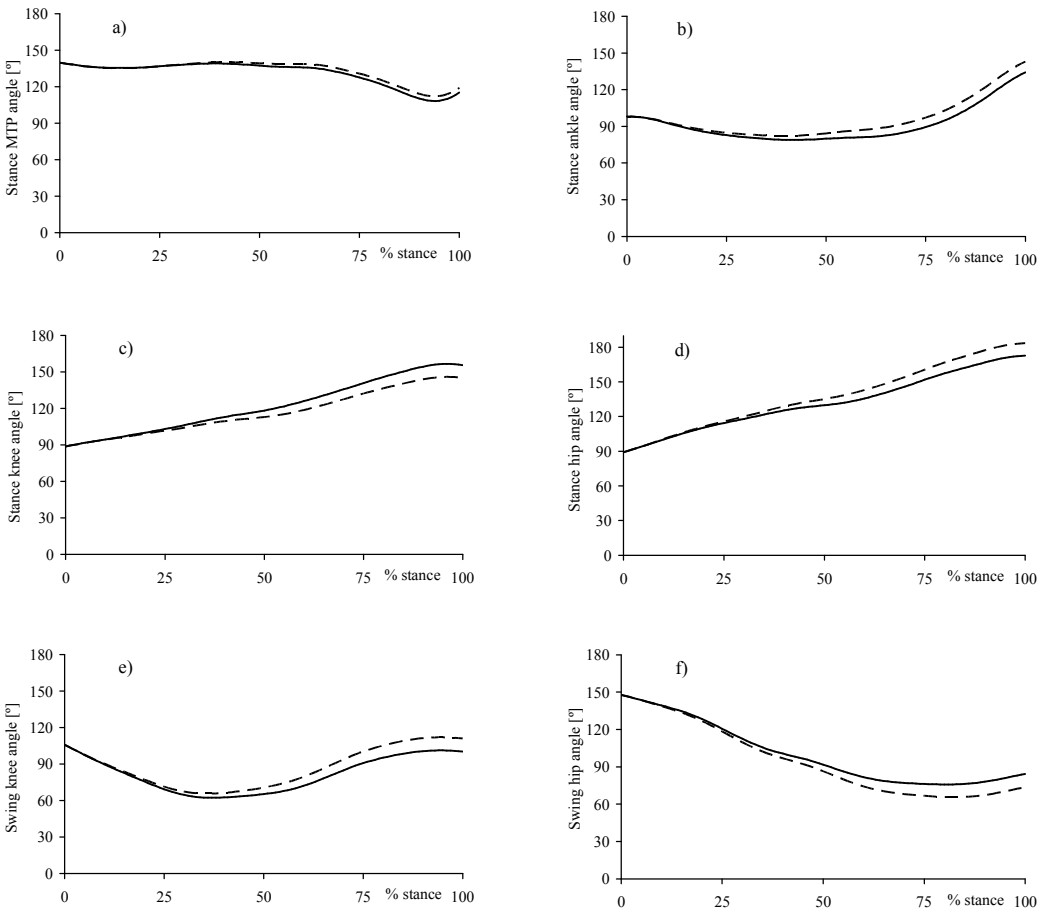

Figures 6.8a-f. Joint angle time-histories for the six angle-driven joints in trial E3 (empirical data = solid line; model data = dashed line).

Orientation

The RMS differences between the model and empirically-recorded trunk angle time-histories were 9.3º for trial E1, 11.6º for trial E2 and 8.6º for trial E3. Model and actual trunk angle time-histories from trial E3 are presented in Figure 6.9. As these orientation scores were not considerably larger than the mean configuration scores (Table 6.3), this confirmed that the differences in each individual joint angle time-history did not have a pronounced effect on the overall orientation (i.e. trunk angle relative to the horizontal) of the sprinter. These orientation scores also compared well with previous values of up to 6.1º presented in the evaluation of an angle-driven model of the stance phase preceding a jump (Wilson, 2003). The slightly lower values achieved by Wilson (2003) may be due to the matching optimisations favouring kinematic variables, since ground reaction force accuracy was not matched as closely by Wilson (2003) compared to the current model (as will be subsequently discussed). It was important to achieve a close match in the kinetic variables in this angle-driven model of sprinting, as the impulses generated determined the change in velocity of the sprinter, and thus the levels of performance.

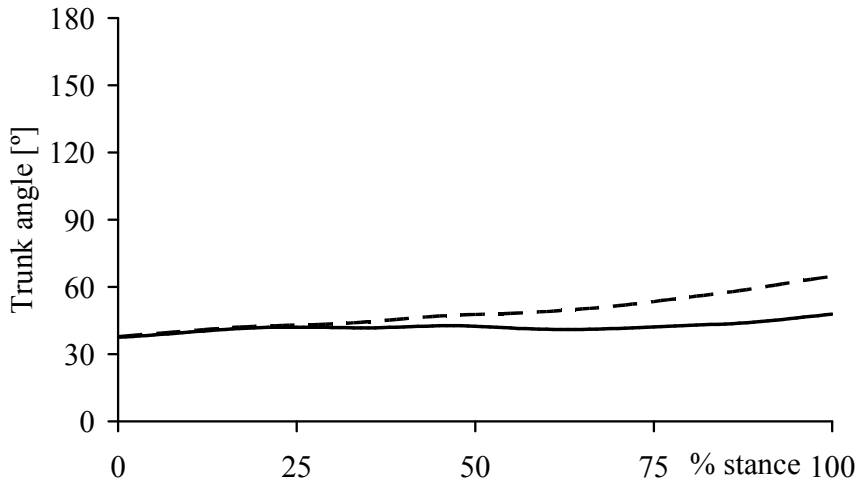

Figure 6.9. Trunk angle (relative to the horizontal) time-histories from the evaluation of trial E3 (empirical data = solid line; model data = dashed line).

Impulse

The percentage differences in net propulsive impulse and in vertical impulse between the model and actual data for each of the three evaluated trials are presented in Table 6.4. The mean value is also presented, providing an impulse score for the evaluation.

Table 6.4. Net propulsive impulse and vertical impulse differences between model and empirical data for each of the three evaluated trials.

	Trial E1	Trial E2	Trial E3
Net propulsive impulse	11.9 %	8.8 %	1.0 %
Vertical impulse	5.7 %	0.5 %	1.7 %
Mean (i.e. impulse score)	8.8 %	4.7 %	1.4 %

To the author's knowledge, impulse has not previously been used as a variable with which to evaluate the accuracy of a forward dynamics model. Impulse determines the change in velocity of a sprinter during each ground contact phase, and is therefore a critical variable in sprinting, and consequently in the simulation model. The small differences in both horizontal and vertical impulse between the model and empirical data indicated that the model could successfully replicate realistic ground reaction impulses during the first stance phase of a sprint.

Ground reaction force accuracy

The RMS differences between model and actual force time-histories (expressed as a percentage of force excursion) were 17.1% and 14.7% for the horizontal and vertical forces respectively for trial E1, 15.1% and 9.1% for trial E2, and 7.8% and 8.7% for trial E3. These low percentage differences indicated that the close match in the impulse data was achieved alongside a realistic ground reaction force pattern, and that accurate impulses were not achieved through unrealistic force time-histories. The mean values of the horizontal and vertical forces accuracies were 15.9%, 12.1% and 8.3% for trials E1, E2 and E3, respectively. Model and the corresponding empirical ground reaction force time-histories for trial E3 are presented in Figure 6.10a-b.

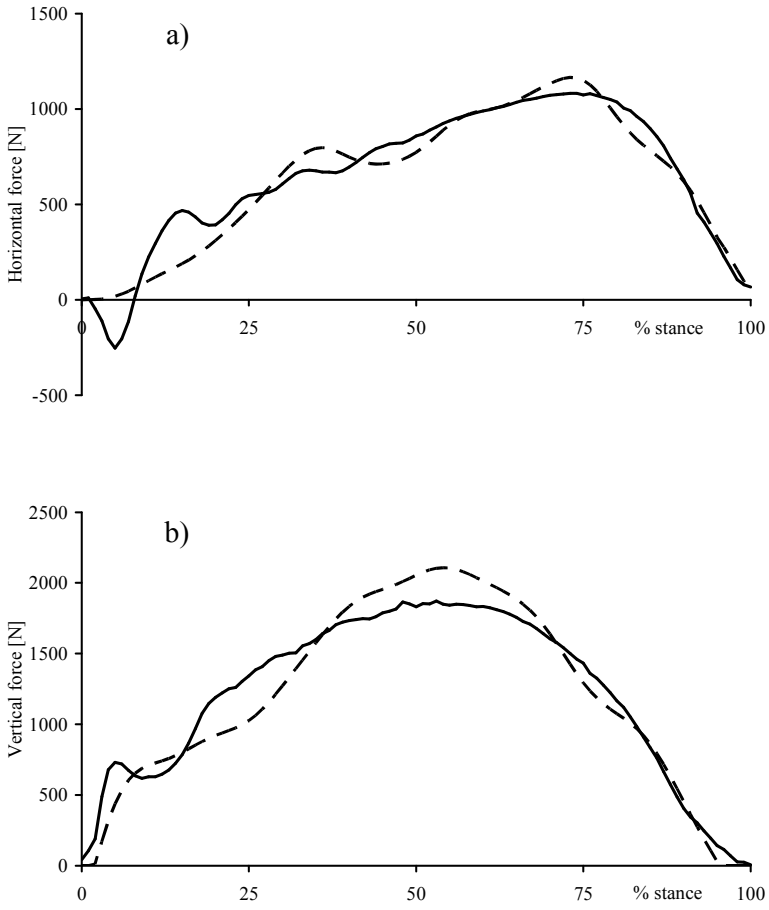

Figures 6.10a-b. Horizontal (a) and vertical (b) ground reaction force time-histories from the evaluation of trial E3 (empirical data = solid line, model data = dashed line).

The accuracy with which the ground reaction forces were represented in the model compared favourably with previous angle-driven models. In the two trials evaluated by Wilson *et al*. (2006), mean (i.e. average of horizontal and vertical results) RMS differences in force time-histories expressed as a percentage of force excursion were 13.2 and 21.7%. From an evaluation of six separate trials, Gittoes (2004) reported corresponding values ranging from 14.3 to 20.5% for the horizontal forces and 11.6 to 18.9% for the vertical forces. Figure 6.10a indicated the optimal matching solution for trial E3 did not replicate the small braking forces present during early stance. The model was developed based on data from sprinter Q, who exhibited only minor braking forces during this time (Figure 5.12a). The algorithms used in the matching optimisations may therefore have converged towards foot-ground interface stiffness and damping co-efficients which provided a very close match with the propulsive

forces, as the minimal braking force magnitudes had little influence on the function being optimised. However, due to the low magnitude of these braking forces, and based on the associated scores obtained in previous evaluations of angle-driven models, the ground reaction force accuracy scores obtained in the current model were clearly representative of a good match between model and empirical data.

Performance

The differences in average horizontal external power between the model representation and reality were 13.6%, 10.0% and 2.0% for trials E1, E2 and E3, respectively. This confirmed that a close match with overall performance could be achieved in addition to the good match obtained with the previously presented kinematic and kinetic technique-related data, particularly for trial E3. External power production has not previously been used to evaluate the accuracy of an angle-driven model, possibly due to the increased difficulty encountered when trying to match kinetic model variables with empirical data (e.g. Wilson *et al*., 2006). However, it was deemed vital to obtain an accurate representation of this variable with the current model, due to the previous identification of average horizontal external power as the most appropriate measure of sprint start performance (Chapter 3). This provided confirmation that not only could the model match technique during the first stance phase of a sprint with sufficient accuracy, an appropriate match could also be achieved in the resulting levels of performance obtained by the model.

Overall model accuracy

Table 6.5 summarises the evaluation scores for each of the 5 components for all three evaluated trials, and presents the mean values for each trial. The scores in degrees and percentages were given equal weighting (Yeadon and King, 2002), thus yielding overall evaluation scores of 11.1%, 9.7% and 5.2% for trials E1, E2 and E3 respectively. These evaluation results indicated a good match between the model and the actual empirical data, and the mean scores compared well with previously published overall evaluation scores from angle-driven models based on both kinematic and kinetic data (e.g. 5.6 and 9.4%, Wilson *et al*., 2006).

Table 6.5. Overall scores for all three evaluated trials.

	Trial E1	Trial E2	Trial E3
Configuration	8.1º	10.1º	5.7º
Orientation	9.3º	11.6º	8.6º
Impulse	8.8%	4.7%	1.4%
Ground reaction force accuracy	15.9%	12.1%	8.3%
Performance	13.6%	10.0%	2.0%
Mean	11.1%	9.7%	5.2%

Resultant joint moments

The resultant joint moments at each of the stance leg joints were also included in the model output data. It was highlighted in the review of literature (section 2.4.5) that one limitation of angle-driven models is that the predicted joint moments may be beyond the scope of the human system being modelled. Therefore, although these moments were not explicitly used to quantify the model accuracy (since the aim of the model was not to manipulate joint kinetics) they provided a further verification of the appropriateness of the model. The peak extensor/plantarflexor moments at each of the joints (and flexor moment at the hip), and the times at which these occurred (expressed as a percentage of stance), are presented in Table 6.6 for trial E3 (alongside empirical data in parentheses).

Table 6.6. Model representations of peak joint moments for trial E3, and the times at which they occurred, expressed as a percentage of stance.

	Peak moment [Nm]	Time of peak moment [% stance]
MTP plantarflexor	20 (142)	74 (60)
Ankle plantarflexor	295 (283)	56 (55)
Knee extensor	353 (250)	49 (48)
Hip extensor	357 (264)	3 (4)
Hip flexor	-368 (-326)	93 (91)

Values in parentheses are the corresponding empirical values for this trial.

Although the model MTP moment was lower than the actual value, this may have been affected by the assumptions regarding the model structure used to represent ground contact. The peak moments at the remaining three stance leg joints were

close to their corresponding empirical values, both in terms of their magnitude and in particular their temporal occurrence. Most importantly, none were excessively larger than trained sprinters could be expected to achieve (e.g. Bezodis *et al*., 2008), confirming that the inputs used in trial E3 did not cause unrealistic resultant joint moments. Time-histories of these four model-based resultant joint moments are presented in Appendix F.

6.6.4. Sensitivity analysis

The close overall matches between model and empirical data for the three evaluated trials (Table 6.5) confirmed that the previously discussed spring-damper co-efficients obtained through matching optimisations (Table 6.2) provided suitable input data for the foot-ground interface within the model. Whilst some variation in the spring-damper co-efficients existed between trials, it was not clear to what extent variation in these and other input parameters could affect the output data. A sensitivity analysis was therefore undertaken to quantify the sensitivity of the model to changes in its inputs, including the initial foot kinematics and Fourier series co-efficients in addition to the foot-ground interface spring-damper co-efficients.

Systematic sensitivity analysis of model robustness

The spring-damper co-efficients, Fourier series co-efficients, MTP contact threshold value and linear toe-velocities at touchdown were all separately varied by ± 10% from their optimised values obtained during the trial E3 matching optimisation. The forefoot angle and angular velocity at touchdown were varied by ± 1% and ± 5% respectively, since a 10% change in these values was considered to be markedly larger than would be expected from digitising errors (e.g. a 10% error in forefoot angle at touchdown would equate to a 16º difference). The effect of these changes on both net propulsive impulse and vertical impulse was quantified, and expressed as a percentage change from the impulse magnitudes obtained during the successful matching optimisation of trial E3 (Table 6.7).

Table 6.7. Sensitivity of net propulsive and vertical impulses (% change) to a ± 10% change in the model input parameters for trial E3.

Input parameter	Net propulsive impulse		Vertical impulse	
	(+10%)	(-10%)	(+10%)	(-10%)
$k_{y_{Toe}}$	-0.62	0.37	-1.01	0.82
$k_{y_{MTP}}$	0.51	-0.63	-0.53	0.40
$b_{y_{Toe}}$	0.08	-0.10	-0.04	0.04
$b_{y_{MTP}}$	0.00	0.00	0.00	0.00
$k_{z_{Toe}}$	0.00	0.00	0.00	0.00
$k_{z_{MTP}}$	2.39	-2.62	1.68	-2.14
$b_{z_{Toe}}$	0.00	0.00	0.00	0.00
$b_{z_{MTP}}$	-0.06	0.04	0.26	-0.26
All j_n	-5.25	4.56	-2.82	2.46
Forefoot θ_i*	4.31	-5.47	-4.09	3.65
Forefoot ω_i*	-1.84	1.58	-4.48	4.40
MTP contact threshold	3.56	-2.87	1.56	-1.65
Initial horizontal toe velocity	0.93	-0.96	1.06	-1.07
Initial vertical toe velocity	0.05	0.38	4.30	-3.95

* Forefoot θ_i adjusted by ± 1%, and forefoot ω_i adjusted by ± 5% because a 10% error in the estimation of forefoot angle and angular velocity at touchdown was deemed to be unrealistically large. j_n = Fourier co-efficient at joint n.

The results of this sensitivity analysis (Table 6.7) revealed a generally high level of robustness associated with the model. Individually changing the foot-ground interface stiffness and damping parameters by 10% only resulted in a maximum change in net propulsive impulse of 2.62%, and in vertical impulse of 2.14%, and for some co-efficients the effect was negligible. Adjusting all Fourier series co-efficients by 10% produced changes of around 5% in the net propulsive impulse and 2.5% in the vertical impulse. These values were representative of a 'worst-case scenario', since all 30 Fourier co-efficients (i.e. five terms at each of the six joints) were adjusted by 10%, and thus a low level of model sensitivity would clearly be expected with errors in any one of the individual Fourier co-efficients. Changes to the forefoot angular data and the MTP thresholds produced errors between 1.56 and 5.47%. It was expected that these parameters would have had the largest influence on the

sensitivity of the model, since they were directly associated with each other and with the foot-ground interface co-efficients. Therefore any changes in these parameters, unaccompanied by changes in the other associated parameters could potentially cause larger errors. However, the fact that the average of the absolute values of the 12 errors associated with changes to these three parameters (MTP contact threshold, forefoot θ_i and ω_i) was 3.29% indicated a good level of robustness in the model with respect to changes in the foot kinematics at touchdown, which play a major role in defining the initial state of the model. The low level of sensitivity associated with the initial toe velocities at touchdown were further proof of the high robustness within the model, and even when vertical toe velocities were altered by 10%, errors in vertical impulse did not exceed 4.30% despite the clear interaction between these inputs and the foot-ground interface damping co-efficients.

Independent sensitivity analysis of model robustness

The sensitivity of the eight spring-damper co-efficients obtained for the foot-ground interface for trial E3 through matching optimisation procedures was also independently assessed. In order to achieve this, the spring-damper co-efficients from both trials E1 and E2 (Table 6.2) were separately used in the foot-ground interface for trial E3 alongside the remaining input data from trial E3. With these spring-damper co-efficients fixed, the match between model and reality was optimised by allowing the kinematic inputs (Fourier co-efficients, foot angular and linear data, MTP threshold) to vary within their pre-determined limits (as specified in section 6.6.1) to account for error in the digitised input data. The accuracy of the optimal match was then evaluated as before, using the variables outlined in section 6.6.2. Results of these independent sensitivity analyses are presented in Table 6.8.

The overall evaluation scores for these two independent evaluations were 7.4% and 7.0% (Table 6.8). These were only slightly larger than the original overall evaluation score for trial E3 (5.2%; Table 6.5). This therefore indicated that the use of an independent set of foot-ground interface co-efficients obtained using a matching optimisation from another trial still yielded accurate model output data, and the model was thus not overly sensitive to changes in these input parameters. This provided further confidence in the model, as the use of trial-specific spring-damper co-efficients would not limit the applicability of the output data.

Table 6.8. Evaluation scores from the independent analysis of the sensitivity of trial E3 to the use of spring-damper co-efficients from trials E1 and E2.

	Trial E1 co-efficients	Trial E2 co-efficients
Configuration	8.1°	7.1°
Orientation	11.5°	10.6°
Impulse	2.3%	4.6%
Ground reaction force accuracy	14.3%	9.4%
Performance	1.0%	3.3%
Mean	7.4%	7.0%

The model was shown to be relatively insensitive to both independent and systematic changes to numerous model inputs, highlighting that changes in the input parameters had only minimal effect on the output data. The first analysis revealed that the impulse outputs, which were associated with both technique and performance, were relatively insensitive to systematic changes in several input parameters. Secondly, the independent analysis revealed that the sensitivity of the model to the use of two independently-obtained sets of foot-ground interface co-efficients was also low. This was highlighted by only small increases in the five kinematic and kinetic evaluation scores (Table 6.8) compared to those values obtained from the matching optimisation of trial E3 (Table 6.5). These sensitivity analyses therefore further informed the model evaluation, increasing the confidence with which the seven segment angle-driven model could be applied to gain insight into technique and performance during the first stance phase of a sprint.

6.6.5. Model evaluation summary

The model evaluation has quantified the appropriateness of the model for gaining insight into the intended system. The differences between model output and empirical data presented in Table 6.5 revealed a sufficiently close match between the model and reality, with a particularly good match for trial E3. Both kinematic and kinetic aspects of technique, and the resulting performance were evaluated, and none of these model outputs were considerably more poorly matched with reality than any

of the others. The model therefore provided a suitable overall match, and did not favour one or more aspects of reality at the expense of others.

The use of five terms of a Fourier series in combination with each angular acceleration time-history provided an appropriate means through which to allow the model kinematics to vary slightly, whilst still achieving an appropriate representation of the individual joint kinematics (and the resulting trunk angle) of a sprinter during the first stance phase of a sprint. Closer matches between impulse and the ground reaction force time-histories were achieved than in previous angle driven models (e.g. Gittoes, 2004; Wilson *et al*., 2006). This may have partly been due to the inclusion of a two-segment foot with ground contact permitted beneath both the toe and MTP joint (Figure 6.7), allowing a more realistic representation of the ground reaction forces to be achieved (Figure 6.10a-b). Additionally, the use of spring-damper functions incorporating greater damping as spring compression increased, and a greater requirement for horizontal force as vertical spring compression increased (based on the equations developed by Wilson *et al*., 2006) allowed the forces to increase from zero at touchdown, also assisting the match with empirically-recorded data.

6.7. Chapter summary

The development of a seven-segment angle-driven forward dynamics model, representative of a sprinter during the first post-block stance phase was described. The Simulink® structure used to define this final model is presented in Appendix D, including the full top-level model structure and some of the contributing subsystems. The inputs required for customisation and driving of the model were outlined and described, and the Matlab™ script file calculating and defining these inputs is provided in Appendix E.

An evaluation of the accuracy with which the model could replicate reality was undertaken, addressing research question v - *can a realistic representation of sprint start technique and performance be achieved in a computer simulation model?* It was shown that the chosen model structure was suitable for representing the kinematic and kinetic aspects of technique, and that performance could also be accurately quantified. By driving the model with joint angular acceleration time-histories,

aspects of technique can thus be readily manipulated in an attempt to investigate the direct effects of changes in technique upon performance during the first post-block stance phase. The model can therefore be applied in Chapter 7 to address research question vi - *can selected hypothetical technique adjustments identify further performance improvements?*

CHAPTER 7: INVESTIGATING THE EFFECTS OF TECHNIQUE ADJUSTMENTS ON PERFORMANCE THROUGH SIMULATION

7.1. Introduction

The evaluation of the forward dynamics model developed in Chapter 6 indicated a high level of accuracy associated with this model-based representation of the first stance phase of a sprint. The simulation model can therefore be confidently applied to further the insight developed from the previous inter-subject comparisons based on empirical data collected and analysed in Chapters 3 to 5. With the modelling approach, specific technique changes can be implemented and the direct performance consequences observed - something that is difficult to achieve with sprinters in an experimental setting, particularly when analysing international-level sprinters. A series of model-based simulations can thus be undertaken to address research question vi - *can selected hypothetical technique adjustments identify further performance improvements?* The aim of this chapter was therefore to use the simulation model to conduct a series of investigations designed to systematically examine the effects of altering specific aspects of first stance phase technique upon the consequent levels of performance attained.

7.2. Methods

The simulation model developed and evaluated in Chapter 6 was used to investigate the effects of altering technique on first stance phase performance. Data from trial E3 were used as model inputs, as the evaluation results presented in section 6.6.3 indicated that this trial provided the closest match with reality (Table 6.5). These inputs included specific empirical data obtained from the investigation undertaken in Chapter 5 alongside further co-efficients and values obtained through the matching optimisations undertaken in Chapter 6. The sensitivity analyses described in section 6.6.4 indicated that these input parameters were insensitive to both systematic changes (Table 6.7) and to the use of independent stiffness and damping co-efficients within the ground contact part of the model (Table 6.8). The inputs from trial E3 therefore provided appropriate values with which to simulate the motion of the modelled system and also to use as a basis from which to investigate technique adjustments.

Three investigations were undertaken in this chapter, with the implemented technique adjustments based on the concluded importance of the empirical results obtained in Chapters 3-5. These investigations involved altering either the kinematics at touchdown or the kinematics during the stance phase:

1. Alterations to hip (1A), knee (1B) and ankle (1C) angle at touchdown.
2. Alterations to ankle angle during stance.
3. Alterations to horizontal toe velocity at touchdown.

For investigations 1 and 3, specific model inputs were adjusted by altering the appropriate values within the inputs script file (Appendix E). For investigation 2, a custom-developed function was directly combined with the ankle joint angular acceleration time-history within the Simulink model itself. This function was included in the joint angle-driver subsystem in addition to the previously optimised Fourier series co-efficients specific to trial E3. The function served to modify the angular accelerations (and thus displacements) whilst maintaining a consistent overall range of motion. All adjustments to the input kinematics were based on the within and between-subject variation observed in the empirical data collected in Chapter 5, and the resultant joint moments were output from the model to ensure that they remained within realistic limits in each of the simulations undertaken.

Investigation 1 was formulated based on results obtained throughout the thesis, including the large range in kinematics at touchdown observed within the group of 13 sprinters in Chapter 3 (Table 3.6), the differences in touchdown distance between sprinters N and Q observed in Chapter 4 (page 98) and the range in stance leg joint angles observed at touchdown between sprinters N, Q and R in Chapter 5 (Figures 5.14 and 5.15). For investigations 1A and 1C, the touchdown angles at the ankle and hip were adjusted from the trial E3 values by ± 5º at 1º intervals (i.e. there were 10 simulations in these investigations; touchdown angles of -5º, -4º, -3º, -2º, -1º, +1º, +2º, +3º, +4º, +5º relative to trial E3 as 0º). Due to the larger inter-subject differences observed in the data previously presented in section 5.3.3 (Figure 5.15a) knee joint angles at touchdown were varied by ± 10º at 1º intervals in investigation 1B.

Investigation 2 involved a series of simulations designed to alter the ankle joint angle time-history during the stance phase. Specifically, this investigation aimed to reduce

the amount of dorsiflexion occurring at the ankle joint during the early part of the stance phase. These changes were formulated based on data presented in Chapter 4, where it was suggested that the reduced dorsiflexion of sprinter P may have assisted his achievement of higher performance levels by permitting enhanced knee and hip extension (Table 4.6). However, due to the descriptive nature of the analysis undertaken in Chapter 4 and the relatively small differences observed between sprinters (8º of dorsiflexion for sprinter P and 11º for sprinters N and Q), this could not be confidently concluded. It was therefore decided to systematically manipulate the amount of dorsiflexion which occurred during the early part of the stance phase in the model to better understand its relation to performance.

An adjustment was required which reduced the amount of dorsiflexion during early stance without altering the overall net change in ankle angle throughout stance. This ensured that the angular displacement changes did not simply affect performance by increasing the overall net range in motion at the ankle joint. In order to achieve this, a function was added to the joint angular acceleration time-history which increased the positive (i.e. plantarflexion direction) acceleration during early stance, before subsequently decreasing it later in stance. However, this could not be a simple increase followed by a decrease of equal and opposite magnitude, since due to the nature of altering an acceleration time-history, the earlier increase would have had a larger effect on the overall displacement time-history. A Fourier series (ε) containing a sine and a cosine wave was therefore used to achieve the desired changes in joint angle (this function is illustrated in Figure 7.1):

$$\varepsilon(t) = a \cdot \cos\left(\frac{t}{2}\right) - b \cdot \sin\left(\frac{t}{4}\right) \qquad [7.1]$$

Co-efficients *a* and *b* were adjusted so that the total amount of dorsiflexion decreased, but the total net plantarflexion during stance was unaltered (i.e. ankle angle at toe-off remained the same as in trial E3). For each simulation, co-efficient *a* was adjusted from 0 to 5000 at intervals of 1000, and the value for *b* which provided the desired amount of net plantarflexion was manually determined.

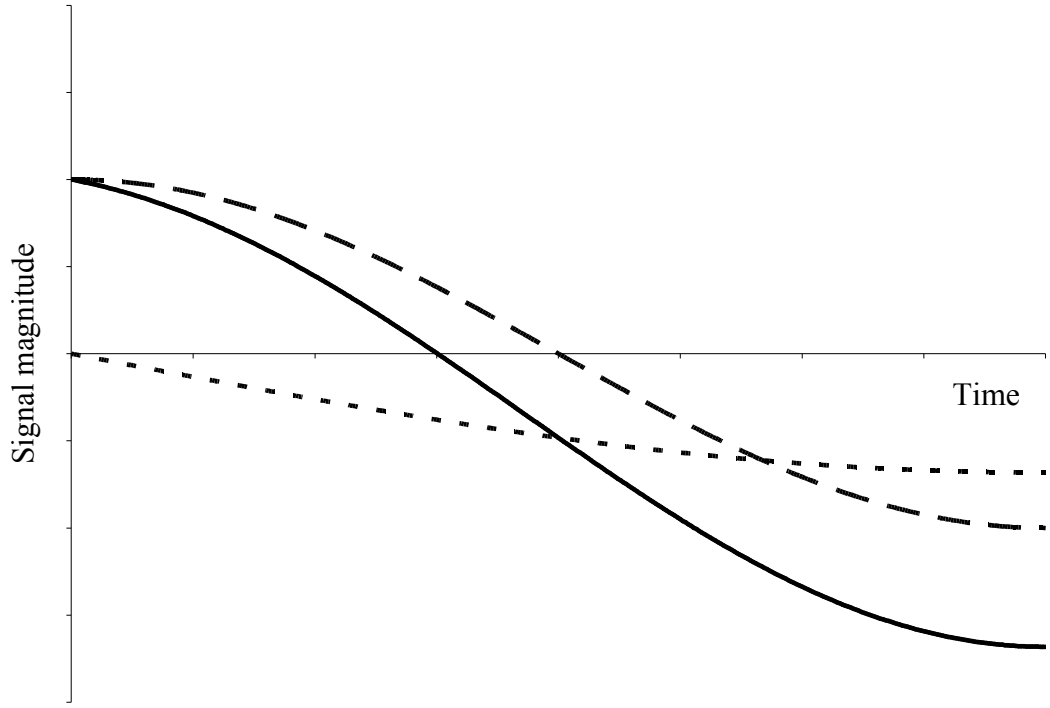

Figure 7.1. The shape of the cosine wave (dashed line), sine wave (dotted line) and the combined function (i.e. Fourier series; solid line) applied to the ankle joint angular acceleration time-history in investigation 2. The effect of functions of this form on the ankle angular displacement time-history during stance can be seen subsequently in Figure 7.6.

Investigation 3 involved systematic alterations to the horizontal velocity of the stance toe relative to the ground at touchdown. This investigation was formulated based on data presented in Chapter 5, which revealed a strong trend between toe velocity at touchdown and peak braking force magnitude (Figure 5.13a). Data from sprinter Q, who exhibited only small braking forces during early stance (Figure 5.12a), were used to develop and evaluate the model in Chapter 6. The model did not replicate these braking forces, possibly because the spring-damper co-efficients were determined in matching optimisations. As suggested in Chapter 6, the optimisation algorithm may have converged towards spring-damper co-efficients which provided a close match with the propulsive forces, due to the large magnitude of the propulsive forces (relative to the small braking forces) having a greater influence on the function being optimised. Despite this limitation, the model still provided an appropriate means with which to determine the effects of horizontal toe velocity at touchdown on horizontal force development, as toe velocity could also influence the

rate of propulsive force development between the foot and the ground. When averaged across the five trials analysed in Chapter 5, sprinter Q exhibited a mean (± *s*) touchdown velocity of 0.00 ± 0.15 $m \cdot s^{-1}$ (Table 5.5). In trial E3, touchdown velocity was -0.18 $m \cdot s^{-1}$, and thus in investigation 3 toe velocity at touchdown was varied at 0.05 $m \cdot s^{-1}$ intervals from -0.38 to 0.17 $m \cdot s^{-1}$ in each of the simulations. This provided a range of values encompassing those of sprinter Q in Chapter 5, and also reduced the toe velocity to slightly lower values than that observed in trial E3.

For each investigation, a series of individual simulations were run using the range of adjusted input data. Each simulation was advanced until the toe left the ground and the stance phase thus terminated. Output data from each simulation were recovered, and these were compared against the reference output data from the simulation of trial E3 with no modified inputs. The key output used for comparison was average horizontal external power production during the stance phase, which provided the measure of performance (subsequent references to performance in this chapter therefore relate to average horizontal external power production). The overall change in horizontal velocity achieved during stance and the total duration of the stance phase were also recovered. This allowed the determination of how the difference in average horizontal external power production was associated with these two important variables. The power, velocity and time data were expressed as percentages relative to the original reference values from trial E3.

In order to assist the understanding associated with the observed results in some of the investigations, further output data were obtained. These included horizontal and vertical impulses generated during stance, the ground reaction force time-histories, and the distance between the stance foot and the CM at touchdown (i.e. touchdown distance). For each investigation, the percentage changes in average horizontal external power, velocity generation during stance and stance phase duration from all simulations were plotted against the corresponding input data to illustrate the effects of the systematic technique alterations on these performance-related variables.

7.3. Results and discussion

The results of each investigation into the effects of altering the technique associated with trial E3 will initially be discussed. This will be followed in section 7.3.6 by a

general discussion of the combined theoretical results alongside previous empirical results from Chapters 3-5.

7.3.1. Investigation 1A - alterations to hip angle at touchdown

The results of this investigation revealed a negative linear trend between hip angle at touchdown and average horizontal external power (Figure 7.2). Therefore as the model-based representation of the sprinter commenced stance with an increasingly flexed hip angle relative to that in trial E3, consequent levels of performance progressively improved. Negative relationships also existed between touchdown hip angle and both change in velocity during stance and stance phase duration (Figure 7.2). Although a decrease in stance phase duration would potentially be a beneficial consequence of altering technique, the current results indicated that the concurrent decreases in the change in horizontal velocity achieved during stance as a result of increasing hip angle at touchdown clearly outweighed this. Decreasing hip angle at touchdown was therefore a favourable strategy for increasing performance in trial E3, despite the associated slight lengthening of stance phase duration.

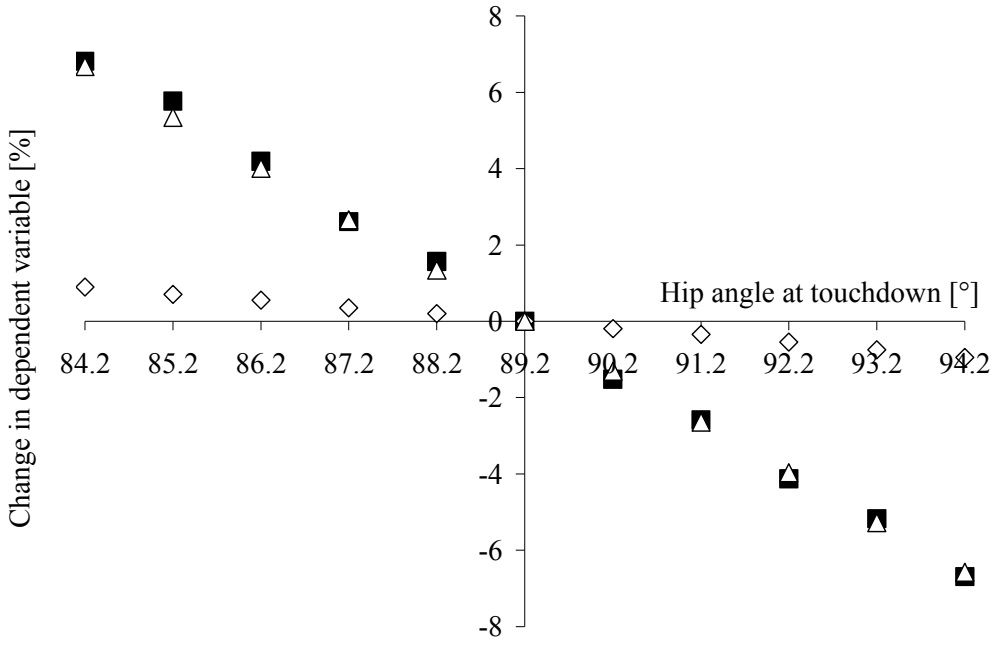

Figure 7.2. The effect of changing hip angle at touchdown (from 89.2º in trial E3) on average horizontal external power (squares), velocity (triangles) and stance duration (diamonds).

7.3.2. Investigation 1B - alterations to knee angle at touchdown

When knee angle at touchdown was altered, a curvilinear relationship with average horizontal external power was observed (Figure 7.3). At all knee joint angles below the 88.8º associated with trial E3, levels of performance decreased, with slightly greater decrements apparent as the joint became increasingly flexed. As the knee joint angle at touchdown increased above 88.8º, performance continued to increase up to the simulation using 91.8º as an initial knee joint angle. However, the level of performance began to decrease beyond this value, dropping below the level associated with trial E3 once knee angle at touchdown reached 93.8º. By the time the initial knee joint angle was 10º greater than in trial E3, performance had decreased by 6.7%.

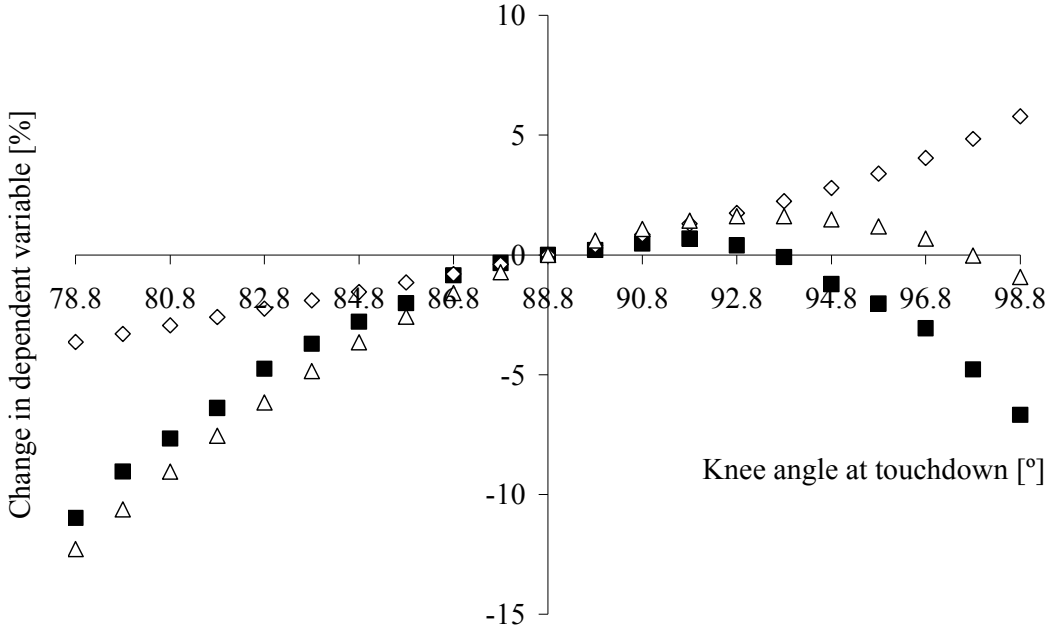

Figure 7.3. The effect of changing knee angle at touchdown (from 88.8º in trial E3) on average horizontal external power (squares), velocity (triangles) and stance duration (diamonds).

These results suggested that the level of performance in trial E3 could be improved slightly by increasing the knee angle at touchdown. An optimum level of performance (a 0.7% increase from the average horizontal external power generated in trial E3) was associated with a 3º increase in knee angle at touchdown. However, continuing to extend the knee beyond this was not beneficial for performance, as the average horizontal external power generated decreased and soon dropped below the

levels observed in trial E3. The maximum potential increase in average horizontal external power associated with altering knee angle at touchdown was clearly less than that associated with altering the hip angle at touchdown (or ankle angle - as will be subsequently shown in section 7.3.3). However, as highlighted in Chapter 1, even the slightest improvements in performance can be the difference between winning a medal or not in competitive international-level sprinting, and thus this kinematic change could yield sufficiently beneficial improvements in performance. Therefore, although the knee angle of sprinter Q at touchdown in trial E3 was not far from optimal, slightly higher values did yield performance improvements. This finding indicates well one of the benefits associated with a modelling approach, since the coach and athlete can concentrate on fine tuning technique rather than spending unnecessary time using a trial and error process.

The change in velocity achieved during the stance phase followed a similar curvilinear trend to the average horizontal external power data, peaking between the 92.8 and 93.8º simulations (both of these simulations were associated with a 1.62% increase in velocity), and decreasing below the trial E3 values in the 97.8º and 98.8º simulations (Figure 7.3). However, a decrease in the change in velocity during stance as touchdown knee angle became increasingly extended was not the sole factor associated with reductions in performance relative to trial E3. Stance duration followed a relatively linear positive trend from touchdown knee angles of 78.8º to around 93-94º, but beyond this the rate of increase in stance phase duration became greater. By the simulation in which knee angle had been extended by 10º at touchdown, stance phase duration had increased by 5.8%. The decreased average horizontal external power observed when commencing stance from more extended knee angles was therefore associated with an unfavourable increase in stance time in addition to the detrimental decrease in the change in horizontal velocity.

In order to try and further understand the observed trends in stance duration and change in velocity during stance, further output data were analysed. Decreasing knee angle at touchdown meant that the CM and the stance foot became horizontally closer (Figure 7.4a). This linear trend continued as knee angle was increased above the value associated with trial E3 (88.8º) and the CM moved progressively further forward at touchdown relative to the stance toe. A decrease in knee angle at

touchdown was also associated with an increase in vertical impulse, and a decrease in horizontal impulse (Figure 7.4b). As knee angle at touchdown increased beyond 88.8º, the negative relationship with vertical impulse continued, and values began to decrease relative to trial E3. However, whilst horizontal impulse increased slightly at knee angles above 88.8º, it soon began to decrease again, and by 97.8º it had dropped below the horizontal impulse value associated with trial E3.

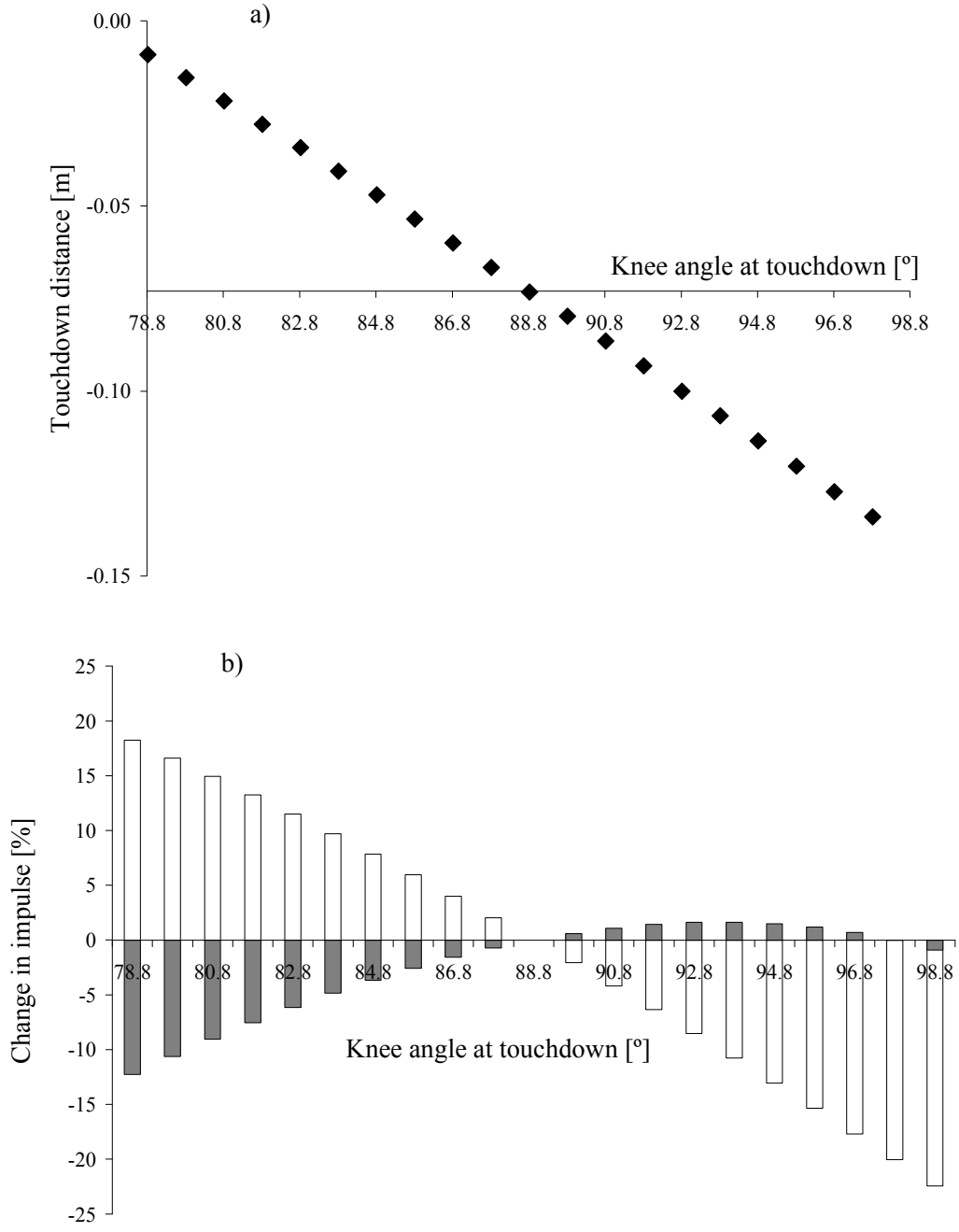

Figure 7.4. The effect of changing knee angle at touchdown (from 88.8º in trial E3) on (a) touchdown distance at the onset of stance and (b) the change in horizontal (grey bars) and vertical (white bars) impulse production during stance.

It is possible that the reduction in vertical impulse as knee angle at touchdown increased above 88.8º (Figure 7.4a) may have influenced the observed increases in stance duration (Figure 7.3). These greater knee angles at touchdown clearly reduced the potential for vertical force generation (i.e. there were reductions in vertical impulse despite longer stance durations). Whilst this did not affect performance as knee angles initially increased above the trial E3 value, in the simulations where the knee was extended at touchdown above an angle of around 93-94º, stance duration had to increase at a greater rate in order for sufficient vertical impulse to be generated to propel the sprinter off the ground and into the next step. Additionally, horizontal impulse production did not continue to increase as knee angle extended above 93-94º despite the associated increases in stance time. The results of this investigation therefore also suggested that too large a knee angle at touchdown (and the associated increase in distance between the stance toe and the CM) may place the leg in a less favourable position for producing horizontal force. Therefore, whilst positioning the CM further ahead of the stance toe at touchdown could improve performance from that observed in trial E3, too large an increase in this distance appeared to be detrimental for performance due to limiting the ability for both horizontal and vertical force production.

7.3.3. Investigation 1C - alterations to ankle angle at touchdown

The output data from investigation 1C revealed that decreasing ankle angle at touchdown (i.e. increased dorsiflexion at touchdown) induced an increase in the change in velocity achieved during stance (Figure 7.5). Although this was accompanied by a concurrent increase in stance phase duration, the changes to average horizontal external power production (i.e. performance) associated with these changes indicated that the increases in velocity far outweighed the extra time spent achieving them (Figure 7.5). A more plantarflexed ankle at touchdown was clearly not beneficial for performance - a 5° increase in ankle angle was associated with an 18% decrease in average horizontal external power.

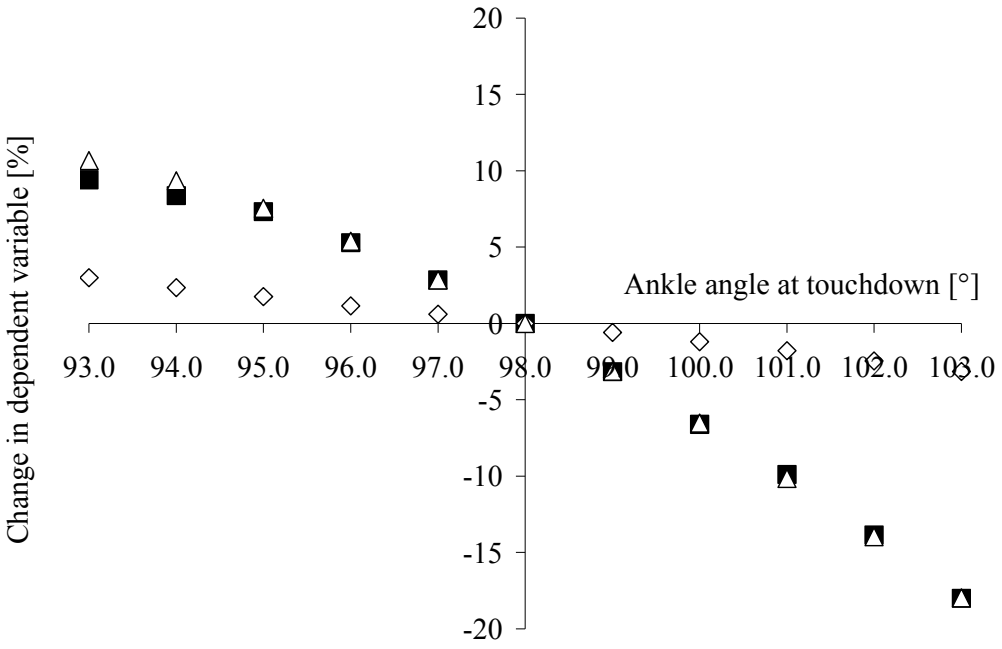

Figure 7.5. The effect of changing ankle angle at touchdown (from 98.0º in trial E3) on average horizontal external power (squares), velocity (triangles) and stance duration (diamonds).

In this investigation, the total overall range of dorsiflexion was fixed because the initial joint angular velocity and the angular acceleration time-history remained unchanged. However, the large reductions in performance associated with increased ankle angle at touchdown could have been partly influenced by the subsequent plantarflexion occurring throughout a less favourable range of ankle joint angles. In reality, an altered ankle joint angle at touchdown would likely also influence the amount of dorsiflexion present during the early part of the stance phase, and thus the ankle joint angle from which plantarflexion commenced. In all of the empirical data collected from the first stance phase throughout this thesis, there existed a considerable amount of dorsiflexion during early stance, the amounts of which varied both within and between sprinters (e.g. Table 4.6 and Figure 5.14). Investigation 2, which focussed on altering the kinematics at the ankle joint during stance in an attempt to progressively reduce the amount of dorsiflexion that occurred during the early part of stance, may therefore provide further insight regarding ankle joint kinematics during the first stance phase of a sprint.

7.3.4. Investigation 2 - alterations to ankle angle during stance

Fourier series of the form described in equation 7.1 and illustrated in Figure 7.1 were combined with the ankle joint angular acceleration time-history to successfully alter the ankle joint angle time-histories. In trial E3, there was a total of 15.8° of dorsiflexion at the ankle joint during early stance. For the five simulations carried out in this investigation, the degrees of dorsiflexion during early stance were 13.9, 12.1, 10.7, 9.6 and 8.6°, respectively (Figure 7.6).

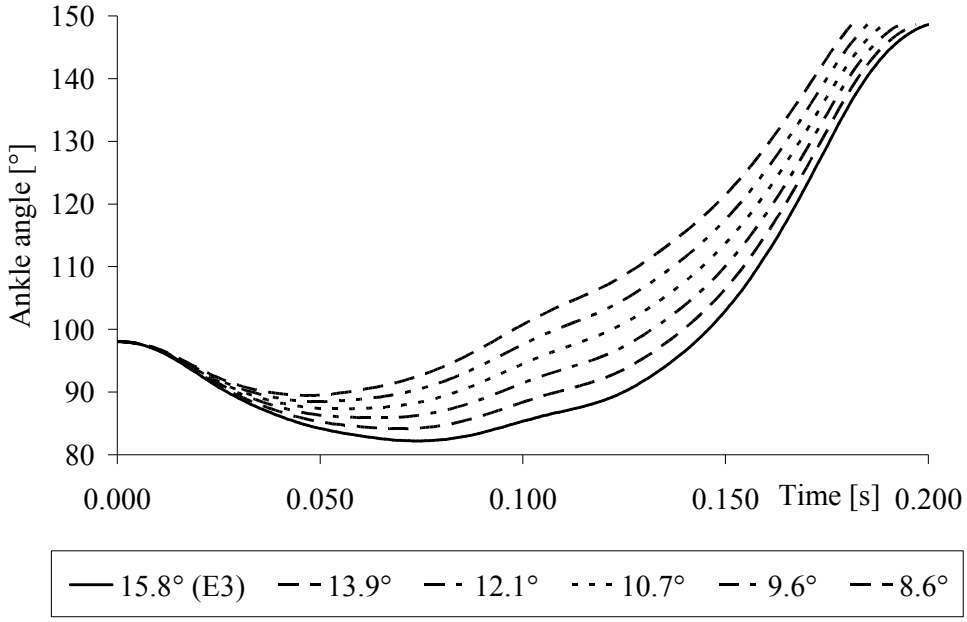

Figure 7.6. The original ankle joint angle time-history from trial E3 (solid line), and the five altered time-histories used in investigation 2. Values in the legend relate to the total amount of dorsiflexion at the ankle joint during early stance.

It was found that by reducing the amount of dorsiflexion present at the ankle joint during the early part of stance, average horizontal external power increased in a curvilinear fashion, with increasing performance improvements apparent as the amount of dorsiflexion reduced (Figure 7.7). A reduction in dorsiflexion was also accompanied by a concurrent reduction in the duration of the stance phase. In the 13.9º and 12.1º simulations, this outweighed the influence of smaller changes in horizontal velocity during stance relative to the original change in horizontal velocity in trial E3 (Figure 7.7). Limiting dorsiflexion therefore initially improved performance by reducing the amount of time spent in stance, the reductions in which

outweighed slight decreases in the associated change in velocity achieved. It was not until dorsiflexion was reduced by more than 6º that changes in velocity began to increase markedly from the trial E3 values, and these changes were accompanied by even greater percentage decreases in stance time.

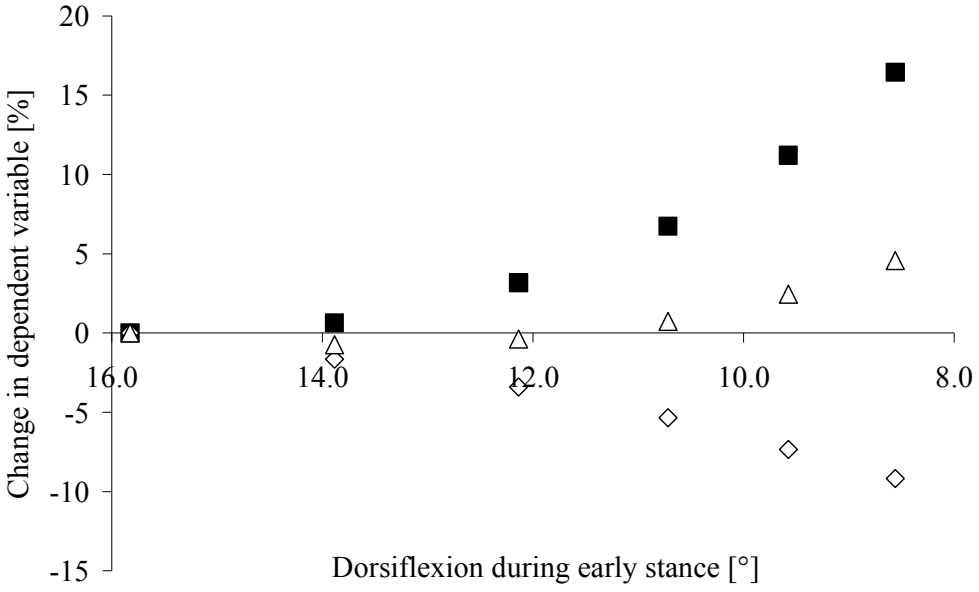

Figure 7.7. The effect of decreasing the amount of ankle joint dorsiflexion during early stance (from 15.8° in trial E3) on average horizontal external power (squares), velocity (triangles) and stance duration (diamonds).

An explanation for the performance results observed in investigation 2 was obtained by studying the horizontal ground reaction force time-histories associated with each of the simulations undertaken in this investigation (Figure 7.8). By limiting the amount of dorsiflexion during the early part of the stance phase, greater horizontal force was developed earlier in stance. The same change in velocity could therefore be achieved in a shorter time duration. As the amount of dorsiflexion was reduced further, it was possible to generate sufficient horizontal forces to achieve a greater change in velocity in an even shorter stance duration, and thus reducing dorsiflexion from the 15.8º observed in trial E3 was clearly beneficial for the resulting levels of performance.

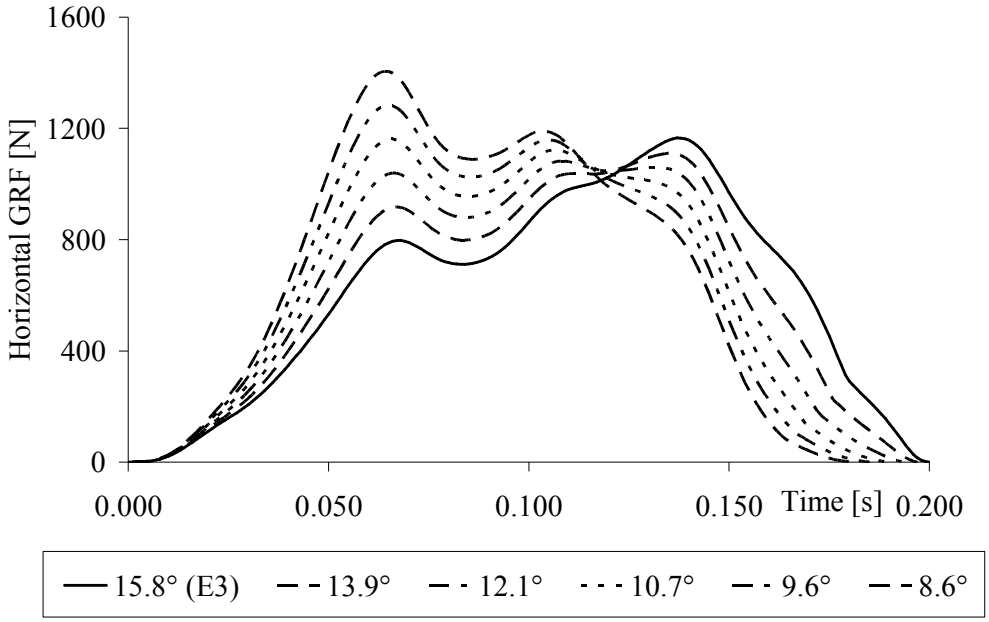

Figure 7.8. The effect of decreasing the amount of ankle joint dorsiflexion during early stance on horizontal ground reaction force production. Values in the legend relate to the total amount of dorsiflexion at the ankle joint during early stance.

7.3.5. Investigation 3 - alterations to toe velocity at touchdown

The final investigation undertaken in this chapter involved a series of simulations in which the horizontal velocity of the toe was altered at touchdown. It was found that as horizontal toe touchdown velocity increased at 0.05 $m \cdot s^{-1}$ intervals from the trial E3 value of -0.18 $m \cdot s^{-1}$ (with respect to the ground), the average horizontal external power produced throughout stance decreased (Figure 7.9). As horizontal toe velocity relative to the track reduced further below -0.18 $m \cdot s^{-1}$, and the toe was thus moving increasingly backwards relative to the track at touchdown, performance levels increased. Increases in horizontal toe velocity at touchdown were also associated with concurrent small increases in stance phase duration (Figure 7.9). However, the increased horizontal toe velocity caused a large reduction in the change in horizontal velocity achieved during stance (Figure 7.9). Therefore the reductions in performance which occurred as a result of the foot contacting the ground with a less backwards, and subsequently increasingly forward, horizontal velocity were largely associated with a decrease in overall CM horizontal velocity generation, and with only slight increases in stance duration.

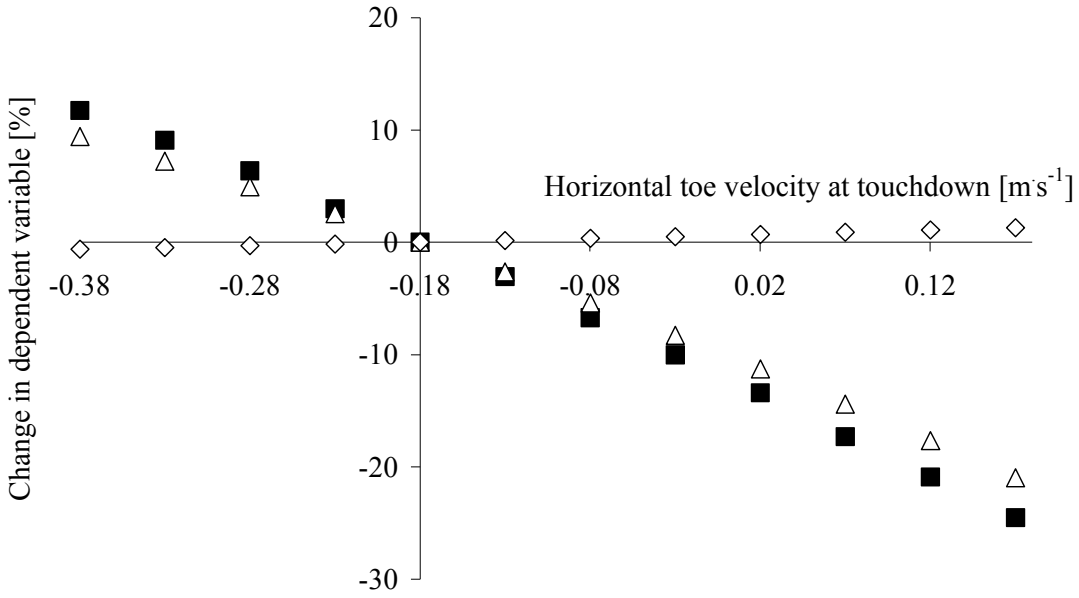

Figure 7.9. The effect of altering horizontal toe velocity at touchdown (from -0.18 $m \cdot s^{-1}$ in trial E3) on average horizontal external power (squares), velocity (triangles) and stance duration (diamonds).

It has been suggested that increases in the forward horizontal velocity of the foot at touchdown are associated with an increase in braking force (Putnam and Kozey, 1989; Jacobs and van Ingen Schenau, 1992; Hunter *et al*., 2005). Although the model did not replicate braking forces for trial E3, it was previously suggested that toe velocity at touchdown would also influence the subsequent development of propulsive forces. The horizontal force time-histories associated with the 12 simulations undertaken in investigation 3 were therefore output from the model. By initiating stance with the toe moving at an increasingly negative (i.e. backwards) velocity relative to the track, the rate of horizontal force development increased during early stance (towards the dashed line in Figure 7.10 associated with a toe velocity of -0.38 $m \cdot s^{-1}$ at touchdown). This also facilitated the generation of greater peak propulsive forces. As stance times were only marginally lower than in trial E3, the overall horizontal impulse generation was thus also increased. In contrast, as horizontal toe velocity at touchdown became increasingly positive, the rate of horizontal force development decreased (towards the dotted line in Figure 7.10 associated with a toe velocity of 0.17 $m \cdot s^{-1}$ at touchdown). These model-based force time-histories therefore offered an explanation for the observed increases in

performance - a reduction of the forward horizontal velocity of the foot at touchdown to increasingly negative (i.e. backwards) velocities increased the rate of propulsive force development.

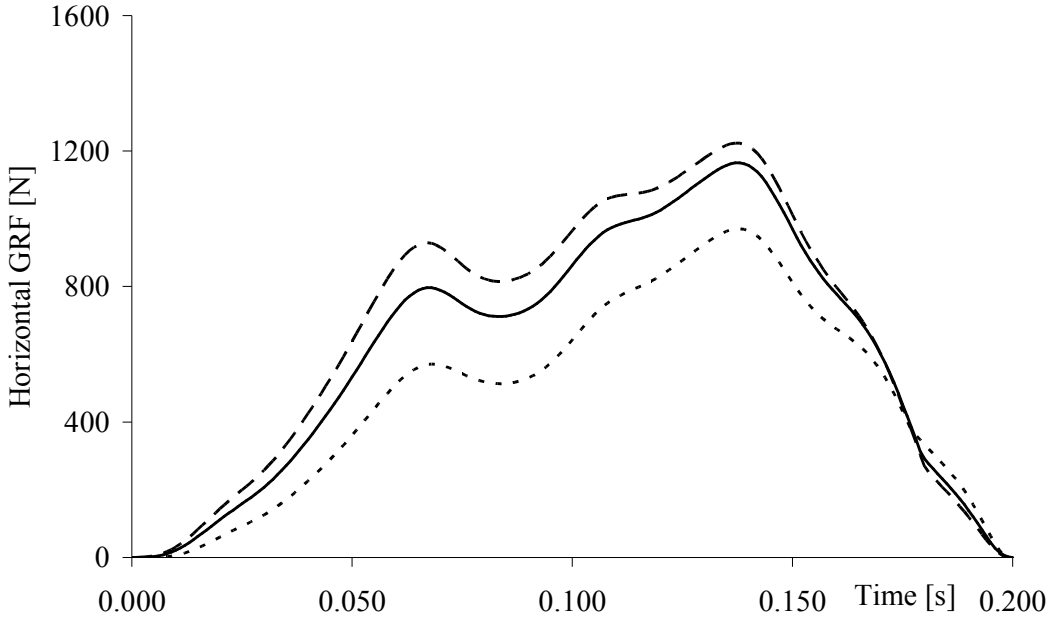

Figure 7.10. The effect of altering horizontal toe velocity at touchdown on horizontal ground reaction force production. Presented values are from trial E3 (-0.18 $m \cdot s^{-1}$, solid line) and the two extreme simulations (-0.38 $m \cdot s^{-1}$, dashed line; 0.17 $m \cdot s^{-1}$, dotted line).

7.3.6. General discussion and conclusions

The results of the investigations undertaken in this chapter addressed research question vi – *can selected hypothetical technique adjustments identify further technique improvements?* This was carried out based on simulations using input data from sprinter Q in trial E3. The results of these investigations can be extended in an attempt to increase the understanding developed from the empirical data presented in previous chapters in response to research questions iii – *which kinematic technique variables are associated with higher levels of performance?* and iv – *how are the more advantageous sprint start kinematics achieved, and why do they lead to improved performance*?

The findings of investigation 1A reinforced discussion developed from the empirical data in Chapter 5. By landing with a more flexed hip, the trunk would initially be

rotated in a more clockwise direction relative to the thigh (when viewed from the right hand side with the sprinter running from left to right). There would therefore be a larger gravitational moment associated with the trunk segment about the hip joint, which would help to prevent an unfavourable anticlockwise rotation of this segment due to the hip extensor moment present at touchdown (Figure 5.17). This would thus keep the trunk in a more favourable position relative to the stance thigh. Clockwise rotation of the thigh segment due to extension at the knee joint would consequently translate the relatively massive trunk segment in a slightly more beneficial horizontal direction. Contrastingly, a greater angle between the stance thigh and trunk segments would likely induce an increasingly vertical change in motion throughout stance. The model-based results therefore provided additional data to reinforce previous suggestions regarding the importance of the gravitational moment of the trunk segment, and how it could be increased by a more flexed hip angle at touchdown.

The results of investigation 1B identified that as the distance between the stance toe and the CM at touchdown systematically decreased, vertical impulse production increased and horizontal impulse production tended to decrease (Figure 7.4). These results concurred with empirical data presented in Chapter 4, where sprinter N exhibited higher levels of first stance phase performance than sprinter Q. Sprinter N landed with his CM on average 0.07 m further ahead of his stance foot than sprinter Q. During the subsequent stance phase, sprinter N achieved a much greater increase in horizontal velocity (Table 4.5), whereas sprinter Q exhibited a greater increase in vertical motion (Figure 4.2). These changes in horizontal and vertical motion would have been directly determined by the respective impulse production. The data from investigation 1B therefore reinforced the theory developed from the results in Chapter 4 and that of Jacobs and van Ingen Schenau (1992) - by increasing the distance which the CM is positioned in front of the foot at touchdown, a more favourable impulse profile is generated. This yields a greater horizontal rather than vertical increase in motion as the leg extends during the subsequent stance phase. However, the model-based data suggested this only to hold true up to a limit. As the CM was positioned increasingly far ahead of the stance foot, the subsequent leg extension was less favourable due to a reduction in the ability to generate both horizontal and vertical forces. Although the motion of the CM is determined once a sprinter leaves the blocks (in accordance with the laws of projectile motion),

repositioning of the individual segments relative to the CM during flight could therefore lead to subsequent improvements in first stance phase performance, provided the CM is not too far in front of the foot at touchdown.

Reducing the ankle angle at touchdown in investigation 1C revealed that commencing stance from a more dorsiflexed position than in trial E3 was beneficial for the performance of sprinter Q. However, whilst these changes suggested potential performance improvements, it was proposed that a more appropriate investigation of the ankle joint kinematics would be to alter the joint angle time-history throughout stance. Investigation 2 therefore systemically reduced the amount of dorsiflexion occurring at the stance ankle joint, and results showed that a reduction in the amount of dorsiflexion during the early part of stance could improve performance from the levels observed in trial E3. In Chapter 4, sprinter P was able to limit the initial dorsiflexion occurring at the stance ankle compared to sprinters N and Q (Table 4.6), and achieved higher levels of performance (Table 4.5). However, for sprinter P, these performance improvements were associated with a greater increase in horizontal velocity rather than a reduction in stance time (relative to the stance times of sprinters N and Q, Table 4.5). It is therefore also possible that a reduction in ankle dorsiflexion during early stance could be used to assist other aspects of technique, for example by providing a 'stiffer' base for the more proximal knee and hip joints to extend against. It was observed in Chapter 5 that an ability to keep a relatively stable foot and shank orientation during early stance allowed the thigh to rotate about a fixed knee joint and thus propel the relatively massive trunk and swing leg segments forward. Sprinter P may therefore have accompanied the reduction in ankle dorsiflexion with another aspect of technique (such as his greater knee extension during stance of 53º compared to 35 and 42º for sprinters N and Q, respectively) to elicit greater increases in velocity rather than reducing stance time. In the model-based representation of trial E3, knee and hip angle time-histories remained unaltered. If additional inputs were allowed to vary, it is possible that a reduction in dorsiflexion could assist an increased extension of the more proximal stance leg joints, rather than facilitating a reduction in stance time. However, it may also be possible that the techniques used by sprinters P and Q were sufficiently different, and that alterations to stance ankle dorsiflexion affected them in contrasting ways. Whether a reduced amount of dorsiflexion is used to reduce stance duration

(simulation 2 of trial E3) or potentially to increase horizontal force generation through assisting increased extension of the more proximal leg joints (sprinter P in Chapter 4), it appears that such a strategy is beneficial for performance.

The results of investigation 3 suggested that if the backwards horizontal velocity of the foot at touchdown was increased, the magnitude of the horizontal propulsive forces generated would also increase. As stance time was only marginally reduced, levels of performance were thus increased. Although the model did not replicate braking forces, these results could also offer a potential explanation for how braking force magnitudes could be reduced if present. It is possible that if the model were customised to either sprinter N or R, braking forces may be observed due to the much increased forward horizontal toe velocities they exhibited at touchdown (Table 5.5) and the link between these velocities and the forces generated within the model (equation 6.20; page 180). Whilst the results of investigation 1B did not identify whether alterations to horizontal toe velocity could affect the magnitude of the braking force, they did indicate that such alterations would affect the generation of horizontal propulsive forces, particularly during the early stance phase. This does not directly reinforce suggestions related to the relationship between foot velocity and braking force magnitude from previous descriptive empirical data, both in the current thesis and in published research studies (e.g. Putnam and Kozey, 1989; Jacobs and van Ingen Schenau, 1992; Hunter *et al*., 2005). However, the results do add further weight to this theory by suggesting that as the backwards velocity of the foot increased, horizontal propulsive force generation was improved. Future model simulations could be used with input data from different sprinters in an attempt to determine how these foot velocities at touchdown could influence both the braking and propulsive forces during the subsequent stance phase.

7.3.7. Conclusion

The systematic alterations to model inputs, and the observed changes in average horizontal external power production, provided a good indication of whether the performance of sprinter Q in trial E3 would be expected to increase or decrease with specific changes to technique. Furthermore, by reporting the changes to the overall horizontal velocity increase during stance, and the associated duration of the stance phase, it was determined whether performance improvements were represented by an

increase in velocity, a decrease in the time spent in stance, or a combination of these two factors. Single inputs were altered in each investigation. Although this 'law of the single variable' is useful when attempting to determine the specific outcomes associated with an isolated change to a model input, it must be considered that attempting to implement an individual technique change may in reality also be associated with concurrent changes to other aspects of technique. For example, the increased ankle angles at touchdown in investigation 1C would potentially be associated with concurrent alterations to the amount of dorsiflexion occurring during early stance and to the other stance leg joint angles at touchdown. Although these were investigated separately in investigations 1A, 1B and 2, to the author's knowledge combinations of technique changes have not previously been applied in angle-driven models in an attempt to replicate increasingly realistic system-wide alterations in technique, and future simulations could aim to focus on this. Additionally, the model could be customised to other sprinters in an attempt to determine how the techniques of different sprinters can be individually improved, and how specific the strategies identified in this chapter were to sprinter Q. However, whilst there is clearly scope for further investigation using this simulation model, the results presented in this chapter identified several important aspects of technique which could be adjusted in an attempt to improve performance.

7.4. Chapter summary

This chapter outlined a series of simulations undertaken to determine the effects of manipulating first stance phase technique upon performance. The model was applied to address specific theoretical questions relating to the effects of technique changes on performance, and thus addressed research question vi - *can selected hypothetical technique adjustments identify further performance improvements?* Systematic alterations to stance leg joint angles at touchdown, horizontal toe velocity at touchdown, and the amount of ankle joint dorsiflexion present during early stance all identified changes which could lead to improvements in performance. The performance results of these model-based investigations were explained through the description of numerous output variables. Several of these findings also reinforced theories developed from empirical data in previous chapters, thus furthering the understanding developed in response to research questions iii - *which kinematic technique variables are associated with greater performance?* and iv - *what are the*

underlying kinetics behind these techniques and why do they lead to improved performance? Future lines of investigation were proposed, including simulations focussing on combining alterations to input parameters in an attempt to mimic system-wide changes that would be expected in reality. A further potential application of this forward dynamics model could be to develop a specific function allowing numerous automated simulations in which many input parameters are permitted to vary slightly within realistic boundaries. The optimisation of this function based on maximisation of performance would therefore facilitate the identification of a technique during the first stance phase associated with optimum levels of performance.

CHAPTER 8: DISCUSSION

8.1. Introduction

The aim of this thesis was to understand the aspects of sprint start technique that contribute to higher levels of performance. The research questions in Chapter 1 focussed the investigations undertaken throughout the thesis towards achieving this aim. The six research questions are therefore revisited in this chapter to outline how they were addressed by the series of investigations described in Chapters 3 to 7, and to summarise the key findings of this thesis. Following this, the appropriateness of specific aspects of the methodology used throughout the thesis will be discussed and potential future investigations will be proposed.

8.2. Addressing the research questions

From the initial conception of this study, it was identified that if aspects of technique were to be associated with levels of performance, the identification of an appropriate single measure of performance was paramount. This led to the first research question:

i. **Does the choice of performance measure influence the identification of different levels of sprint start performance?**

In Chapter 3, twelve trained sprinters were ranked from 'best' to 'worst' for each of ten different measures of block phase performance (based on the measures used in the previous sprint start research reviewed in Chapter 2). Spearman's rank order correlation co-efficients revealed that no two measures were perfectly correlated, and thus research question i was answered with a 'yes'. This confirmed the notion developed from critiquing the previous results of Mendoza and Schöllhorn (1993; Figure 2.1), that the choice of variable with which to measure performance could affect the conclusions reached in a sprint start study. Due to this failure for any two performance measures to provide identical assessments of performance, there was thus a clear need to address the second research question:

ii. **What is the most appropriate measure of sprint start performance, and can it be accurately quantified in a field environment?**

Using a theoretical argument (section 3.3.2), it was shown that the commonly used velocity-based measures (e.g. block velocity) could favour techniques associated with increased contact times. This was due to the direct influence of horizontal impulse, which could conceivably lead to a large block velocity through an increase in the time spent pushing in the blocks. This clearly conflicted with the 'least possible time' nature of sprint performance (Mendoza and Schöllhorn, 1993). Block velocity may therefore not be the most appropriate variable with which to quantify performance due to its potential for bias towards those sprinters spending a longer time generating force in the blocks. It was therefore advocated that the chosen performance measure should also reflect the length of time over which a change in velocity was achieved. Performance was therefore quantified based on average horizontal external power production, as maximal power production from the very start of a sprint has been shown to be a favourable strategy in sprinting due to the associated reduction in the time spent running at submaximal velocities (de Koning *et al*., 1992; van Ingen Schenau *et al*., 1994). Average horizontal external power quantifies the overall net power generated by a sprinter against the track/blocks in an attempt to translate the CM in a horizontal direction. It thus provides an appropriate measure of sprint start performance, and when normalised to account for differences in morphology, yields objective comparisons between sprinters.

An equation was presented (equation 3.4, section 3.2.3) which enabled the calculation of average horizontal external power during a specific phase of interest from velocities at either end of this phase, the associated phase duration, and knowledge of the mass of the sprinter. Therefore, in order to assess the second part of research question ii, the externally valid high-speed video protocol used to collect these velocity and time data from sprint training sessions at the track was replicated in a laboratory (section 3.3.3). This allowed the determination of whether performance data could be accurately obtained in a field environment. The calculation of 95% limits of agreement (Bland and Altman, 1986) revealed that velocity could be measured to within ± 0.048 $m \cdot s^{-1}$ of criterion force platform values, and when combined with the video-based estimate of time duration, average horizontal external power data could be measured to within ± 24 W of the magnitudes expected from well-trained sprinters. These values were contextualised

against previously recorded data, and the errors associated with the high-speed video protocol equated to less than 1.6% of the average horizontal external power values expected from a trained sprinter during a typical block exit.

The accuracy of an LDM device, used to obtain performance data over 30 m for addressing research question i, was also quantified (section 3.3.4). It was shown that whilst the LDM device provided appropriate data from these distances, it should not be used during the first 5 m of a sprint due to the substantial changes in the posture of a sprinter. This changing posture yielded sufficient differences between the horizontal displacement profiles of the lumbar point (at which the LDM device was aimed) and the CM. The velocity data associated with the lumbar point (and measured with the LDM device) were therefore not able to sufficiently replicate the velocity profile of the CM during the early parts of a sprint. As the subsequent investigations concentrated on the block and first stance phases, the LDM device was not used to collect any further data.

Having determined that performance could be accurately quantified through the measurement of average horizontal external power via a high-speed video protocol, it was possible to relate specific aspects of technique with successful performance, thus allowing the third research question to be investigated:

iii. Which kinematic technique variables are associated with higher levels of sprint start performance?

The data collected in Chapter 3 from the group of trained sprinters, and in Chapter 4 from the three international-level sprinters allowed research question iii to be addressed for both the block phase (Chapters 3 and 4) and the first stance phase (Chapter 4). During the block phase, Pearson's product moment (r) correlations revealed only one statistically significant relationship between the mean values of specific technique variables and the resulting levels of performance within a group of 13 trained sprinters. This was an association between greater peak front hip extension angular velocity and higher levels of performance ($r = 0.56$, $p < 0.05$). There were also trends for the rear hip action to be linked with greater performance, through increased peak extension angular velocity ($r = 0.37$, $p = 0.22$), an increased range of

extension during the push against the rear block (r = 0.41, p = 0.17) and a greater joint angle at rear block exit (r = 0.51, p = 0.08). Combined with a trend for an increased push duration with the rear leg to be associated with higher performance levels (r = 0.50, p = 0.09), these data suggested that increased rear hip extension may also be an aspect of technique that could enhance block phase performance. Kinematic data obtained during the block phase had not previously been reported, and these results identified specific aspects of technique which provided a potential explanation behind previous suggestions for an increased push with the rear leg as a strategy to facilitate performance (Payne and Blader, 1971; Lemaire and Robertson, 1990).

The block phase data analysed in Chapter 4 confirmed the importance of hip joint extension for block performance, as the highest performing sprinter (P) exhibited greater hip joint extension and average extension angular velocities. The role of the rear hip was again apparent, and the observed kinematic data were used alongside previously published EMG data (Guissard and Duchateau, 1990; Mero and Komi, 1990) to explain its importance. Activation throughout rear block contact and the potential for power generation from the musculature surrounding the rear hip were identified as possible reasons behind its proposed beneficial influence. The kinematic data presented in section 4.3.1 also identified an interesting aspect of technique which led to an increase in block velocity, but which was detrimental for performance. Sprinter N exhibited an increased plantarflexion of the front ankle during the late part of the block phase, and achieved a higher block velocity than sprinters P and Q. However, this was a less powerful technique than that of sprinter P as it was largely due to spending additional time in the blocks. These empirical data thus furthered the previous theoretical justification regarding the choice of average horizontal external power in response to research question ii.

The large range in kinematic data collected at first stance touchdown from the group of 13 trained sprinters in Chapter 3 (section 3.3.5) led to the inclusion of the first stance phase in subsequent investigations. In Chapter 4, data revealed the stance knee joint to extend from touchdown onwards (section 4.3.2), unlike at the 16 m mark (Johnson and Buckley, 2001) or during the maximum velocity phase (Bezodis *et al*., 2008) where an initial period of knee flexion has been observed. Increased extension

of the stance leg joints was suggested as being important for the achievement of higher levels of performance (e.g. sprinter P), and it was proposed that this may be assisted by an ability to reduce ankle dorsiflexion during early stance. Further support was given to reducing dorsiflexion for improved performance in Chapter 7. The results of the simulations in investigation 2 revealed that a systematic reduction in the amount of dorsiflexion in trial E3 led to improved levels of performance. There thus appears to be clear benefit for a sprint coach to include eccentric or plyometric ankle strength exercises in training if trying to improve the start performance of a sprinter. This could allow the same amount of horizontal impulse to be generated in less time, or potentially could facilitate increased extension at the more proximal stance knee and hip joints by providing a more stable base.

Another interesting aspect of technique was observed in Chapter 4 when comparing sprinters N and Q, who exhibited less total leg joint extension than sprinter P but similar amounts to each other. Despite this, sprinter N achieved greater levels of performance than sprinter Q. There was a noticeable difference in their overall configuration at touchdown, as sprinter N typically landed with his stance foot MTP 0.07 m further behind his CM than sprinter Q. It was suggested that the leg extension of sprinter N was therefore directed in a more favourable horizontal direction, assisting his generation of average horizontal external power, and thus performance. In contrast, the leg extension of sprinter Q had an increased effect on vertical CM motion, and performance consequently suffered. These suggestions were reinforced by the results of investigation 1B in Chapter 7. Alterations in the distance between the CM and stance foot at touchdown, achieved through changing knee angle, were found to influence vertical and horizontal impulse production, and ultimately performance. These findings reinforced data previously presented by Jacobs and van Ingen Schenau (1992), and suggested that although the path of the CM is determined from the moment a sprinter leaves the blocks, there appears to be potential benefit in attempting to reposition the body segments around the CM during flight so that the foot is slightly further back at touchdown. However, the results of investigation 1B suggested that as the CM became increasingly further ahead, performance levels could decrease due to a reduced ability to generate force. This combination of empirical and theoretical data also provided one answer to the fourth research question, by identifying how and why alterations to touchdown distance could affect

performance. In order to identify additional causes behind this and other kinematic aspects of technique, an inverse dynamics analysis was undertaken in Chapter 5 to calculate the joint kinetics (resultant moments, powers and work), and these therefore were used to further address research question iv:

iv. How are the more advantageous sprint start kinematics achieved, and why do they lead to improved performance?

The joint moment time-histories revealed several interesting aspects of sprint start technique. Firstly, a considerable plantarflexor moment was observed at the MTP joint during stance. The MTP joint has rarely been included in kinetic sprint analyses, and these data suggested that it should not be omitted during the first stance phase. Whilst it was not clear from the current data whether inclusion of the MTP joint would affect analyses undertaken during subsequent stance phases of a sprint, recently documented motion at the MTP joint in a kinematic analysis of the maximum velocity phase of sprinting (Krell and Stefanyshyn, 2006) suggested that it may be an important feature of the foot action throughout a sprint. Failure to include the MTP joint could therefore lead to artificially high ankle joint moments due to neglecting a moment at the distal end of the rearfoot segment. This could also subsequently introduce error into the moments calculated at the knee and hip joints.

Kinetic results presented in section 5.3.3 revealed the ankle joint to be a large net energy generator during the first stance phase. Based on previously published data from subsequent phases of a sprint, it was suggested that this net energy generation at the ankle joint decreased as a sprint progressed. The generation of positive power at the knee joint appeared to be important for performance, and may have been associated with the knee being able to extend throughout stance during this early part of a sprint, as highlighted previously. Sprinter Q exhibited only minimal horizontal braking and vertical impact forces, and he was consequently able to generate an extensor moment at the knee from the onset of stance. He thus generated around double the energy of sprinters N and R at the knee joint, which may have assisted his greater average horizontal external power production during stance in Chapter 5. At the hip joint, resultant moments were found to exhibit a similar pattern to those

commonly observed in latter phases of a sprint – a large extensor moment at touchdown which became flexor dominant after mid-stance.

Due to the importance of horizontal translation in sprinting, the joint kinetics were subsequently related to performance through their effects on horizontal motion. The MTP and ankle plantarflexor and knee extensor moments appeared to work synergistically during the early part of stance. These moments created a stable lower leg about which the thigh could rotate due to the action of the knee and hip extensor moments. A large clockwise thigh rotation therefore occurred, which due to its orientation at touchdown, provided a means by which the large mass of the upper body and swing leg could be moved in a favourable horizontal direction. These findings were again partly reinforced by the model-based investigations undertaken in Chapter 7, where a larger gravitational moment of the trunk segment about the hip joint, and a more stable distal end of the stance leg (due to reduced dorsiflexion), were associated with improvements in the performance of sprinter Q in trial E3.

As the thigh rotated beyond a vertical orientation during stance, its rotation contributed less to horizontal motion due to the *geometrical constraint* (van Ingen Schenau *et al*., 1987; Figure 5.21). The two stance foot segments, however, remained in a favourable position to augment horizontal motion, and power appeared to be transferred in a proximal-to-distal fashion to assist this. It was suggested that this was achieved via the bi-articular muscles, allowing the rotational energy to be effectively transferred rather than dissipated as the hip and knee joints decelerated in order to satisfy the *anatomical constraint* (van Ingen Schenau *et al*., 1987). Clockwise rotation (when viewed from the right hand side with the sprinter running from left to right) of the rearfoot and forefoot segments during the late stance phase therefore continued the forward propulsion of the CM. These segmental rotations and joint moments explained the previously identified movement of the CM relative to the foot during an early sprint start stance phase (Jacobs and van Ingen Schenau, 1992). This also provided an understanding of how the kinematic aspects of the techniques observed in Chapter 4 were achieved, by identifying a specific kinetic strategy which would assist the direction of leg extension in a more favourable horizontal direction.

As has been highlighted in parts of the response to research questions iii and iv, a simulation model was developed in an attempt to extend the empirical-based understanding of the first stance phase. In order to confidently use the model, and to consequently theorise how performance could potentially be improved, the accuracy of the model had to be evaluated in response to the fifth research question:

v. Can a realistic representation of sprint start technique and performance be achieved with a forward dynamics computer simulation model?

A seven-segment angle-driven forward dynamics model was developed in Chapter 6. The model included a novel representation of the foot-ground interface. This incorporated a two segment foot, contact was permitted beneath the toe and MTP joints, and forces were modelled using spring-damper equations. The model evaluation (section 6.6) included assessment of impulse and average horizontal external power in addition to the commonly used measures of configuration, orientation and ground reaction force accuracy. Compared against empirical data from sprinter Q, the model was shown to be able to accurately reproduce kinematic and kinetic technique variables, as well as yielding an accurate overall measure of performance. For the trial subsequently used in the theoretical investigations in Chapter 7, configuration and orientation RMS differences between the model and empirical data were 5.7º and 8.6º, respectively. Stance phase impulses were modelled to within 1.4%, and were associated with ground reaction force accuracies within 8.3% of the empirical values - levels of error which compared favourably with previous angle-driven forward dynamics models (e.g. Gittoes, 2004; Wilson *et al*., 2006). When comparing average horizontal external power, model-based performance for the trial used in subsequent investigations was within 2.0% of the associated empirical values.

The sensitivity analysis of the model (section 6.6.4) revealed the model to be relatively insensitive to changes in the inputs, even when spring-damper co-efficients from the matching optimisations of two independent trials were used in conjunction with input data from trial E3. The overall evaluation accuracy score only increased from 5.2% to 7.4% and 7.0% when using spring-damper co-efficients from trials E1 and E2 with the remaining input data from trial E3, and no single component of the

evaluation was largely affected. The forward dynamics model therefore offered an appropriate representation of the system it was intended to represent - the technique and performance of a sprinter during the first stance phase. The model thus provided a suitable tool with which to address the final research question:

vi. Can selected hypothetical technique adjustments identify further performance improvements?

The series of investigations undertaken in Chapter 7 identified a number of technique adjustments which improved the performance of sprinter Q during the first stance phase. By changing the angles of the stance leg joints at touchdown by as little as 1º, performance could be increased by up to 2.9% (e.g. reduced ankle angle), without any need to alter the subsequent rate of extension at the joint during stance. It was also shown that a reduction in stance ankle dorsiflexion during early stance improved performance for sprinter Q by reducing the time spent in stance without detrimentally affecting the generation of horizontal velocity. A link was suggested with the higher levels of performance of sprinter P who was able to limit ankle dorsiflexion, which potentially provided a more rigid base from which knee and hip extension could be increased. This was also one example of how the model simulations potentially reinforced some of the insight gained from the empirical research towards research questions iii and iv.

Reducing the horizontal velocity of the foot from small positive values to increasingly negative (i.e. backwards) values in the model was also shown to lead to improved performance, and this was due to an increase in the rate and magnitude of propulsive force development. Although this did not directly reinforce previous theories relating to foot velocity and braking force magnitudes (Putnam and Kozey, 1989; Jacobs and van Ingen Schenau, 1992; Hunter *et al*., 2005) - as the model did not replicate the small braking forces of sprinter Q - it provided confirmation that the horizontal velocity of the foot at touchdown could have an important effect on the horizontal force development. If input data from other sprinters with large forward foot touchdown velocities were used in the model, it is possible that braking forces would be observed and could be influenced by further changes in these inputs.

8.3. Discussion of methodological approach

This section will discuss the key aspects of the methodologies used in the investigations undertaken throughout the thesis. This includes the measurement of performance, the use of manual video analyses to obtain empirical data, the choice of group-based or multiple single-subject analyses, and the use of both inverse and forward dynamics approaches.

8.3.1. Measurement of sprint start performance

A key issue which was addressed early in this thesis was the measurement of performance. This has clear importance not only for biomechanists, but also for coaches wishing to objectively assess the performance levels of their sprinters. It was shown using both a theory-based argument (section 3.3.2) and empirical data (section 4.4.1) that the commonly-adopted measurement of block velocity to quantify block phase performance could provide biased measures due to the additional effects of the time spent pushing in the blocks. Average horizontal external power was defined and subsequently proposed as the most appropriate measure of performance, and it is recommended that this should be used to objectively quantify sprint start performance in the future.

8.3.2. Manual video analysis

A manual video analysis approach was chosen as it provided an appropriate means with which to obtain externally valid data from sprinters at the track, which would not be possible using an automatic motion analysis system. As with all of the investigations undertaken in this thesis, two-dimensional analyses were undertaken due to the largely planar nature of both the movement and the overall aim in sprinting. A protocol was developed, using a four-point calibration, narrow fields of view, high resolution images and specific methods for the determination of velocity. Not only was such an approach unobtrusive, thus allowing externally valid performance data to be collected at the training sessions of international-level sprinters, it was also proven to maintain the internal validity of these data. It was shown that kinetic data, such as the chosen performance measure – average horizontal external power – could be accurately calculated from these high-speed video clips, and thus manual video analyses were suitable for addressing the aim of this thesis with an appropriate degree of accuracy.

8.3.3. Group-based and multiple single-subject analyses

Having identified an appropriate performance measure, the initial technique investigation (Chapter 3) utilised a group-based study design, by analysing the techniques of 13 trained sprinters. Mean values for specific technique variables were therefore correlated with the associated performance levels of each sprinter in an attempt to identify aspects of technique associated with higher performing sprint starters. Whilst this provided a good starting point for the thesis, the wide variation in techniques meant that no clear trends were observed between any single aspect of technique and the resulting levels of performance. It was therefore decided to continue the investigation using a multiple single-subject approach.

A multiple single-subject approach allowed specific individual techniques to be assessed without masking important effects by averaging a range of techniques and performances. This was also necessary because it was important to analyse the techniques of internationally-competitive sprinters if high levels of performance were to be attained, and by its very nature, the collection of high-level performance data from a large number of sprinters is contradictory. The analysis of international-level sprinters in Chapters 4 and 5 therefore provided sprint start data associated with high-level performance, particularly in Chapter 5 by which time the three sprinters analysed in this chapter had reached the final of European or World indoor competitions (where the start is of even greater importance due to the distance covered being only 60 m). The multiple single-subject analysis allowed differences in individual techniques to be identified (e.g. the greater front hip and knee extension of sprinter P compared to the greater ankle plantarflexion of sprinter N in Chapter 4), whilst still allowing general aspects of international-level sprint start technique to be identified (e.g. the segmental rotation contributions to performance in Chapter 5).

8.3.4. Inverse dynamics analysis

In order to address research question iv - *how are the more advantageous sprint start kinematics achieved, and why do they lead to improved performance?* – an inverse dynamics analysis was undertaken in Chapter 5. This allowed the underlying joint kinetics to be described, through the calculation of resultant joint moments, powers and work. Although this does not allow the measurement of these variables from

individual muscles due to the indeterminacy problem, the overall dominance of muscle groups crossing a particular joint provided considerable useful insight with which research question iv was answered.

Extensive attention was given to the processing of the data required as inputs to the inverse dynamics analysis. Based on an argument previously developed by van den Bogert and de Koning (1996) and Bisseling and Hof (2006), a pilot analysis was undertaken in section 5.2.4 to investigate the effects of various force and video data cut-off frequencies on the resultant knee joint moment time-history. It was determined that the use of different cut-off frequencies between the high-speed video and force platform data could lead to artificial peaks in the time-histories soon after impact, and this was suggested to be due to the loss of high frequency segmental accelerations in the kinematic data. Artificially large internal joint forces would therefore be calculated, leading to high frequency and magnitude artefact in the resultant joint moment time-histories shortly after touchdown. When video and force data cut-off frequencies were matched, these artefacts were not apparent as the frequency components of both the kinematic and kinetic acceleration data were thus also matched. Whilst numerous previously published sprint kinetics articles (e.g. Mann and Sprague, 1980; Mann, 1981; Johnson and Buckley, 2001; Hunter *et al*., 2004; Bezodis *et al*., 2008) have identified high frequency flexor and extensor peaks in the knee joint moment soon after touchdown, the resultant knee joint moment time-histories calculated in the current study and presented in section 5.3.3 contained no such peaks. Based on the data presented from the pilot analysis in section 5.2.4, it is suggested that the methods adopted in the current study yielded a more appropriate representation of the true resultant joint moment time-histories. However, these methods warrant further investigation during subsequent phases of a sprint to justify their use, as the aforementioned research reporting impact peaks in the resultant knee joint moment soon after touchdown has all been undertaken during later phases of a sprint.

8.3.5. Forward dynamics analysis

The development and application of a forward dynamics model of the sprint start offered a novel means through which to increase the understanding of technique and performance. Several simplifying assumptions regarding the mechanical properties

used to represent the sprinter were made in the development of the model (sections 6.3 and 6.4). These included the chosen structure of the seven-segment model (including a two-segment foot), and the use of angular acceleration time-histories to drive the motion at the joints and thus simulate whole body motion. Numerous input parameters were required to initiate the model, and many of these were obtained directly from the empirical data presented in Chapter 5. The other inputs, such as the Fourier co-efficients used to vary the joint angular acceleration time-histories and the spring-damper co-efficients used to represent the properties of the foot-ground interface, were obtained through matching optimisations. Although a matching optimisation approach has been widely used to obtain input parameters in previous forward dynamics models (e.g. King and Yeadon, 2002; Hiley and Yeadon, 2003a; Gittoes, 2004; Wilson *et al*., 2006), it is important that when using such an approach, the accuracy with which the model can replicate the system it intends to represent is evaluated (Yeadon and Challis, 1994). A detailed model evaluation therefore assessed the assumptions made when developing the model, quantifying the replication accuracy and providing confidence in the output data obtained from simulation of the model system.

Although some variation existed between the optimised stiffness and damping co-efficients in the three evaluated trials, this has been a common feature of spring-damper systems used to represent the foot-ground interface in previous forward dynamics models incorporating ground contact phases (e.g. Gittoes, 2004; Wilson *et al*., 2006). Sensitivity analyses of the eight spring-damper co-efficients revealed that the model was not overly-sensitive to these inputs, and that the inter-trial range in the magnitude of these co-efficients would thus not have a major effect on the model outputs. Whilst it is difficult to evaluate these co-efficients against empirical data, the values obtained through the matching optimisations provided appropriate inputs for the model, as indicated by the close overall match between the model and empirical data quantified in the evaluations. The optimised spring-damper co-efficients were therefore considered to provide a suitable representation of the properties of the track, spiked shoe and soft tissue on the sole of the foot for use in the model. The model evaluations also provided evidence to support the chosen model structure, such as the use of seven segments, including a two segment foot, and the use of angular acceleration time-histories to drive the model. The close kinematic matches

achieved (i.e. configuration and orientation scores) indicated that the use of five terms of a Fourier series provided a sufficient means with which to allow the kinetic variables (impulse, ground reaction force accuracy and performance scores) to match more closely, but not to the extent where the kinematic technique variables were markedly altered. The evaluation scores presented in section 6.6.3 therefore indicated that the model provided an appropriate representation of a sprinter during the first stance phase of a sprint.

Although a close degree of match was obtained between model and empirical data, it is acknowledged that a perfect match was not achieved. It is therefore possible that further model development could continue to improve this match. Although the use of a HAT segment was appropriate for addressing the questions posed in this thesis, subsequent separation of these segments could improve the match with empirical data. Furthermore, the model had difficulty in reproducing the braking forces experienced during the initial part of stance, and the subsequent expansion of the ground contact model to a more complicated form may improve this. The combination of Fourier series with the angular acceleration time-histories allowed slight adjustments to be made to the inputs driving the model. These functions were relatively simple and affected the entire stance phase, and more complex functions could potentially be applied to specific regions within stance to further improve the accuracy of the model. However, despite these limitations, the current degree of matching achieved between model and empirical data compared favourably with previously-published angle-driven models. The model was therefore appropriate for addressing the relevant research questions and achieving the stated aim. These further model advancements were thus beyond the scope of the current thesis and provide an interesting direction for future research.

The investigations undertaken using the simulation model in Chapter 7 provided theoretical data which clearly increased the understanding obtained from the empirical investigations. However, despite its many benefits, forward dynamics simulations possess some limitations, no matter how closely the model matches reality. Due to the ‘law of the single variable’ associated with this type of theoretical research, it was possible to implement specific alterations to individual aspects of technique. However, although this provided a greater understanding of how a single

input could affect performance, it is likely that such changes would be accompanied by concurrent changes in other variables. This may have led to some slight exaggeration in the performance gains associated with specific technique changes, although it is also possible that concurrently simulated technique changes could facilitate even greater improvements in performance. Despite this, due to the close match achieved with reality in the current model, the general performance trends observed when systematically manipulating an input parameter would likely have yielded a good indication of the direction of change in performance - whether that type of technique change would result in improvements or deteriorations in performance. Future simulation modelling could therefore endeavour to couple changes based on informed theory - for example it is possible that an increase in hip flexion during swing would be accompanied by an increase in knee extension, due to the nature of the biarticular muscles spanning these two joints. The effect of such actions on configuration at touchdown could therefore potentially be combined in future investigations. However, whatever changes are implemented, it must ultimately be remembered that such changes must be realistic, and achievable by the sprinter the model intends to represent.

8.4. Future investigations

The investigations undertaken throughout this thesis advanced the current understanding of sprint start technique and performance. However, this research has also identified and provided several potential future lines of enquiry. An interesting future investigation would be to conduct inverse dynamics analyses during other phases of a sprint in which both sets of input data are filtered with the same cut-off frequency. The results could be compared to previously published data to determine how they influence the current knowledge surrounding joint kinetics in sprinting.

To the author's knowledge, this was the first time a forward dynamics model has been used to simulate and systematically manipulate the technique of a sprinter. A model framework therefore now exists, and in the current study only the first stance phase was simulated. Collection of full kinematic and kinetic data from any of the subsequent steps of a sprint could be used to develop appropriate input data. This would allow application of the model to later phases in an attempt to determine how

they compare with the start, and ultimately to increase the understanding of technique and performance across an entire sprint.

The use of a simulation model to investigate specific research questions hinted at the powerful potential for theoretical research to continue developing the current understanding of sprinting. One possible application would be to develop increasingly complicated functions in order to manipulate more specific aspects of technique. There is also clear possibility to adapt the model into a torque-driven version to directly investigate questions related to the effects of a sprinter's strength and muscle co-ordination on performance. Furthermore, during either the start or any phase of a sprint, the combined, systematic adjustment of numerous input parameters would provide an interesting future area of research focussing on how to achieve optimum sprint performance.

8.5. Thesis conclusion

The aim of this thesis was to understand the aspects of sprint start technique that contribute to higher levels of performance. Six specific research questions were developed to achieve this objective, and these questions were addressed through a series of empirical and theoretical investigations. An objective and obtainable measure of performance was identified. Subsequent descriptive analyses of kinematic and kinetic data from trained and international-level sprinters identified several aspects of technique that were associated with improvements in this performance measure. To further the empirical understanding, a simulation model was developed which included specific features such as a two-segment foot to facilitate a close match between the model and reality. Application of the model identified theoretical technique adjustments that could be made to enhance performance, and also reinforced some of the insight gained from the empirical research. This thesis thus identified several important aspects of technique that can be applied in an attempt to improve sprint start performance.

REFERENCES

Ackland, T. R., Henson P. W. and Bailey, A. (1988). The uniform density assumption: its effect upon the estimation of body segment inertia parameters. *International Journal of Sports Biomechanics*, **4**, 146-155.

Aerts, P. and de Clercq, D. (1993). Deformation characteristics of the heel region of the shod foot during simulated heel strike: the effect of varying midsole hardness. *Journal of Sports Sciences*, **11**, 449-461.

Alexander, M. (1989). The relationship between muscle strength, sprinting kinematics and sprinting speed in elite sprinters. *Track and Field Journal*, **35** (2), 7-21.

Alexander, R. M. (1990). Optimum take-off techniques for high and long jumps. *Philosophical Transactions of the Royal Society of London Series B-Biological Sciences*, **329**, 3-10.

Altman, D. G. and Bland, J. M. (1983). Measurement in medicine: the analysis of method comparison studies. *The Statistician*, **32**, 307-317.

Angeloni, C., Riley, P. O. and Krebs, D. E. (1994). Frequency content of whole body gait kinematic data. *IEEE Transactions on Rehabilitation Engineering*, **2**, 40-46.

Arsac, L. M. and Locatelli, E. (2002). Modeling the energetics of 100-m running by using speed curves of world champions. *Journal of Applied Physiology*, **92**, 1781-1788.

Atkinson, G. and Nevill, A. (1997). Comment on the use of concordance correlation to assess the agreement between two variables. *Biometrics*, **53**, 775-777.

Atkinson, G. and Nevill, A. M. (1998). Statistical methods for assessing measurement error (reliability) in variables relevant to sports medicine. *Sports Medicine*, **26**, 217-238.

Atkinson, G. and Nevill, A. M. (2001). Selected issues in the design and analysis of sport performance research. *Journal of Sports Sciences*, **19**, 811-827.

Atkinson, G., Davison, R. C. R. and Nevill, A. M. (2005). Performance characteristics of gas analysis systems: what we know and what we need to know. *International Journal of Sports Medicine*, **26**, S2-S10.

Atwater, A. E. (1982). Kinematic analyses of sprinting. *Track and Field Quarterly Review*, **82**, 12-16.

Badoux, D. M. (1964). Friction between feet and ground. *Nature*, **202**, 266-267.

Bates, B. T. (1996). Single-subject methodology: an alternative approach. *Medicine and Science in Sports and Exercise*, **28**, 631-638.

Bates, B. T., James, C. R. and Dufek, J. S. (2004). Single-subject analysis. In *Innovative Analyses of Human Movement* (edited by N. Stergiou), pp. 3-28. Champaign, IL: Human Kinetics.

Baumann, W. (1976). Kinematic and dynamic characteristics of the sprint start. In *Biomechanics V-B* (edited by P. V. Komi), pp. 194-199. Baltimore, MD: University Park Press.

Belli, A., Kyröläinen, H. and Komi, P. L. V. (2002). Moment and power of lower limb joints in running. *International Journal of Sports Medicine*, **23**, 136-141.

Bezodis, I. N., Kerwin, D. G. and Salo, A. I. T. (2008). Lower-limb mechanics during the support phase of maximum-velocity sprint running. *Medicine and Science in Sports and Exercise*, **40**, 707-715.

Bhowmick, S. and Bhattacharyya, A. K. (1988). Kinematic analysis of arm movements in sprint start. *Journal of Sports Medicine and Physical Fitness*, **28**, 315-323.

Bisseling, R. W. and Hof, A. L. (2006). Handling of impact forces in inverse dynamics. *Journal of Biomechanics*, **39**, 2438-2444.

Bisseling, R. W., Hof, A. L., Bredeweg, S. W., Zwerver, J. and Mulder, T. (2007). Relationship between landing strategy and patellar tendinopathy in volleyball. *British Journal of Sports Medicine*, **41**, E8.

Bland, J. M. and Altman, D. G. (1986). Statistical methods for assessing agreement between two methods of clinical measurement. *Lancet*, **327**, 307-310.

Bland, J. M. and Altman, D. G. (1995). Comparing methods of measurement: why plotting difference against standard method is misleading. *Lancet*, **346**, 1085-1087.

Bland, J. M. and Altman, D. G. (1999). Measuring agreement in method comparison studies. *Statistical Methods in Medical Research*, **8**, 135-160.

Bland, J. M. and Altman, D. G. (2003). Applying the right statistics: analyses of measurement studies. *Ultrasound in Obstetrics & Gynecology*, **22**, 85-93.

Bobbert, M. F. and van Ingen Schenau, G. J. (1988). Coordination in vertical jumping. *Journal of Biomechanics*, **21**, 249-262.

Bobbert, M. F., Huijing, P. A. and van Ingen Schenau, G. J. (1987). Drop jumping 1: the influence of jumping technique on the biomechanics of jumping. *Medicine and Science in Sports and Exercise*, **19**, 332-338.

van den Bogert, A. J. and de Koning, J. J. (1996). On optimal filtering for inverse dynamics analysis. In *Proceedings of the IXth Biennial Conference of the Canadian Society for Biomechanics* (edited by J. A. Hoffer, A. Chapman, J. J. Eng, A. Hodgson, T. E. Milner and D. Sanderson), pp. 214-215. Vancouver, Canada: University Press.

van den Bogert, A. J. and Su, A. (2008). A weighted least squares method for inverse dynamic analysis. *Computer Methods in Biomechanics and Biomedical Engineering*, **11**, 3-9.

Borzov, V. (1978). The optimal starting position in sprinting. *Legkaya Atletika*, **4** (10), 173-174.

Brewin, M. A., Yeadon, M. R. and Kerwin, D. G. (2000). Minimising peak forces at the shoulders during backward longswings on rings. *Human Movement Science*, **19**, 717-736.

Bruneau, O. and Ouezdou, F. B. (1999). Distributed ground/walking robot interaction. *Robotica*, **17**, 313-323.

Burkholder, T. J. and Lieber, R. L. (1996). Stepwise regression is an alternative to splines for fitting noisy data. *Journal of Biomechanics*, **29**, 235-238.

Caldwell, G. E. and Forrester, L. W. (1992). Estimates of mechanical work and energy transfers: demonstration of a rigid body power model of the recovery leg in gait. *Medicine and Science in Sports and Exercise*, **24**, 1396-1412.

Cappozzo, A. and Gazzani, F. (1983). Comparative evaluation of techniques for the harmonic analysis of human motion data. *Journal of Biomechanics*, **16**, 767-776.

Cavagna, G. A., Saibene, F. P. and Margaria, R. (1963). External work in walking. *Journal of Applied Physiology*, **18**, 1-9.

Cavagna, G. A., Margaria, R. and Arcelli, E. (1965). A high-speed motion picture analysis of the work performed in sprint running. *Research Film*, **5**, 309-319.

Challis, J. H. (1999). A procedure for the automatic determination of filter cutoff frequency for the processing of biomechanical data. *Journal of Applied Biomechanics*, **15**, 303-317.

Challis, J. H. and Kerwin, D. G. (1996). Quantification of the uncertainties in resultant joint moments computed in a dynamic activity. *Journal of Sports Sciences*, **14**, 219-231.

Chandler, R. F., Clauser, C. E., McConville, J. T., Reynolds, H. M. and Young, J. W. (1975). *Investigation of inertia properties of the human body*. AMRL-TR-74-137. Aerospace Medical Research Laboratory, Wright-Patterson Air Force Base, Ohio.

Chelly, S. M. and Denis, C. (2001). Leg power and hopping stiffness: relationship with sprint running performance. *Medicine and Science in Sports and Exercise*, **33**, 326-333.

Chou, L. S., Song, S. M. and Draganich, L. F. (1995). Predicting the kinematics and kinetics of gait based on the optimum trajectory of the swing limb. *Journal of Biomechanics*, **28**, 377-385.

Clauser, C. E., McConville, J. T. and Young, J. W. (1969). *Weight, volume, and centre of mass of segments of the human body*. AMRL-TR-69-70. Aerospace Medical Research Laboratory, Wright-Patterson Air Force Base, Ohio.

Čoh, M. and Tomažin, K. (2006). Kinematic analysis of the sprint start and acceleration from the blocks. *New Studies in Athletics*, **21** (3), 23-33.

Čoh, M., Peharec, S. and Bačić, P. (2007). The sprint start: biomechanical analysis of kinematic, dynamic and electromyographic parameters. *New Studies in Athletics*, **22** (3), 29-38.

Čoh, M., Jošt, B., Škof, B., Tomažin, K. and Dolenec, A. (1998). Kinematic and kinetic parameters of the sprint start and start acceleration model of top sprinters. *Gymnica*, **28**, 33-42.

Cole, G. K., Nigg, B. M., van den Bogert, A. J. and Gerritsen, K. G. M. (1996). Lower extremity joint loading during impact in running. *Clinical Biomechanics*, **11**, 181-193.

Collet, C. (1999). Strategic aspects of reaction time in world-class sprinters. *Perceptual and Motor Skills*, **88**, 65-75.

van Coppenolle, H., Delecluse, C., Goris, M., Bohets, W. and Vanden Eynde, E. (1989). Technology and development of speed: evaluation of the start, sprint and body composition of Pavoni, Cooman and Desruelles. *Athletics Coach*, **23** (1), 82-90.

Cousins, S. and Dyson, R. (2004). Forces at the front and rear blocks during the sprint start. In *Proceedings of XXII International Symposium on Biomechanics in Sports* (edited by M. Lamontagne, D. G. E. Robertson and H. Sveistrup), pp. 198-201. Ottawa, Canada: University Press.

Davies, C. T. M. and Rennie, R. (1968). Human power output. *Nature*, **217**, 770-771.

Dempster, W. T. (1955). *Space requirements of the seated operator*. WADC-TR-55-159. Aerospace Medical Research Laboratory, Wright-Patterson Air Force Base, Ohio.

Dickinson, A. D. (1934). The effect of foot spacing on the starting time and speed in sprinting and the relation of physical measurements to foot spacing. *Research Quarterly*, **5**, 12-19.

Dixon, S. J. and Kerwin, D. G. (2002). Variations in achilles tendon loading with heel lift intervention in heel-toe runners. *Journal of Applied Biomechanics*, **18**, 321-331.

Dufek, J. S., Bates, B. T., Stergiou, N. and James, C. R. (1995). Interactive effects between group and single-subject response patterns. *Human Movement Science*, **14**, 301-323.

Durkin, J. L., Dowling, J. J. and Andrews, D. M. (2002). The measurement of body segment inertial parameters using dual energy X-ray absorptiometry. *Journal of Biomechanics*, **35**, 1575-1580.

Elftman, H. (1940). The work done by muscles in running. *American Journal of Physiology*, **129**, 672-684.

Faverial, J., Basset, F., Azizah, M. G. and Teasdale, N. (2000). Kinetic and kinematic analysis of the sprint start. *Archives of Physiology and Biochemistry*, **108**, 135.

Fortier, S., Basset, F. A., Mbourou, G. A., Faverial, J. and Teasdale, N. (2005). Starting block performance in sprinters: a statistical method for identifying discriminative parameters of the performance and an analysis of the effect of providing feedback over a 6-week period. *Journal of Sports Science and Medicine*, **4**, 134-143.

Gagnon, M. (1978). A kinetic analysis of the kneeling and the standing starts in female sprinters of different ability. In *Biomechanics VI-B* (edited by E. Asmussen and K. Jorgensen), pp. 46-50. Baltimore, MD: University Park Press.

Gerritsen, K. G. M., van den Bogert, A. J. and Nigg, B. M. (1995). Direct dynamics simulation of the impact phase in heel-toe running. *Journal of Biomechanics*, **28**, 661-668.

van Gheluwe, B. (1981). A biomechanical simulation model for airborne twist in backward somersault. *Journal of Human Movement Studies*, **7**, 1-22.

Giakas, G. and Baltzopoulos, V. (1997a). A comparison of automatic filtering techniques applied to biomechanical walking data. *Journal of Biomechanics*, **30**, 847-850.

Giakas, G. and Baltzopoulos, V. (1997b). Optimal digital filtering requires a different cut-off frequency strategy for the determination of higher derivatives. *Journal of Biomechanics*, **30**, 851-855.

Gilchrist, L. A. and Winter, D. A. (1996). A two-part, viscoelastic foot model for use in gait simulations. *Journal of Biomechanics*, **29**, 795-798.

Gilchrist, L. A. and Winter, D. A. (1997). A multisegment computer simulation of normal human gait. *IEEE Transactions on Rehabilitation Engineering*, **5**, 290-299.

Gittoes, M. J. R. (2004). *Contributions to Impact Loading in Females During Vertical Drop Landings*. Unpublished Doctoral dissertation, University of Bath.

Grégoire, L., Veeger, H. E., Huijing, P. A. and van Ingen Schenau, G. J. (1984). Role of mono- and biarticular muscles in explosive movements. *International Journal of Sports Medicine*, **5**, 301-305.

Guissard, N. and Duchateau, J. (1990). Electromyography of the sprint start. *Journal of Human Movement Studies*, **18**, 97-106.

Guissard, N., Duchateau, J. and Hainaut, K. (1992). EMG and mechanical changes during sprint starts at different front block obliquities. *Medicine and Science in Sports and Exercise*, **24**, 1257-1263.

Gutierrez-Davila, M., Dapena, J. and Campos, J. (2006). The effect of muscular pre-tensing on the sprint start. *Journal of Applied Biomechanics*, **22**, 194-201.

Hafez, A. M. A., Roberts, E. M. and Seireg, A. A. (1985). Force and velocity during front foot contact in the sprint start. In *Biomechanics IX-B* (edited by D. A. Winter, R. W. Norman, R. P. Wells, K. C. Hayes and A. E. Patla), pp. 350-355. Champaign, IL: Human Kinetics.

Hanavan, E. P. (1964). A mathematical model of the human body. AMRL-TR-64-102, AD-608-463. Aerospace Medical Research Laboratories, Wright-Patterson Air Force Base, Ohio.

Harland, M. J. and Steele, J. R. (1997). Biomechanics of the sprint start. *Sports Medicine*, **23**, 11-20.

Harrison, A. J., Jensen, R. L. and Donoghue, O. (2005). A comparison of laser and video techniques for determining displacement and velocity during running. *Measurement in Physical Education and Exercise Science*, **9**, 219-231.

Hatze, H. (1980). A mathematical-model for the computational determination of parameter values of anthropomorphic segments. *Journal of Biomechanics*, **13**, 833-843.

Hatze, H. (1981a). A comprehensive model for human motion simulation and its application to the take-off phase of the long jump. *Journal of Biomechanics*, **14**, 135-142.

Hatze, H. (1981b). The use of optimally regularized Fourier-series for estimating higher-order derivatives of noisy biomechanical data. *Journal of Biomechanics*, **14**, 13-18.

Henry, F. M. (1952). Force-time characteristics of the sprint start. *The Research Quarterly*, **23**, 301-318.

Hiley, M. J. and Yeadon, M. R. (2003a). Optimum technique for generating angular momentum in accelerated backward giant circles prior to a dismount. *Journal of Applied Biomechanics*, **19**, 119-130.

Hiley, M. J. and Yeadon, M. R. (2003b). The margin for error when releasing the high bar for dismounts. *Journal of Biomechanics*, **36**, 313-319.

Hiley, M. J. and Yeadon, M. R. (2007). Optimization of backward giant circle technique on the asymmetric bars. *Journal of Applied Biomechanics*, **23**, 300-308.

Hill, A. V. (1938). The heat of shortening and the dynamic constants of muscle. *Proceedings of the Royal Society*, **B126**, 136-195.

Hof, A. L. (1996). Scaling gait data to body size. *Gait & Posture*, **4**, 222-223.

Hopkins, W. G. (2000). Measures of reliability in sports medicine and science. *Sports Medicine*, **30**, 1-15.

Hoster, M. and May, E. (1978). Notes on the biomechanics of the sprint start. *Athletics Coach*, **13** (2), 2-7.

Hunter, J. P., Marshall, R. N. and McNair, P. J. (2004). Segment-interaction analysis of the stance limb in sprint running. *Journal of Biomechanics*, **37**, 1439-1446.

Hunter, J. P., Marshall, R. N. and McNair, P. J. (2005). Relationships between ground reaction force impulse and kinematics of sprint-running acceleration. *Journal of Applied Biomechanics*, **21**, 31-43.

IAAF. (2008). http://www.iaaf.org/oly08/index.html. Accessed 26th November 2008.

van Ingen Schenau, G. J. (1989). From rotation to translation: constraints on multi-joint movements and the unique action of bi-articular muscles. *Human Movement Science*, **8**, 301-338.

van Ingen Schenau, G. J., Bobbert, M. F. and Rozendal, R. H. (1987). The unique action of bi-articular muscles in complex movements. *Journal of Anatomy*, **155**, 1-5.

van Ingen Schenau, G. J., de Koning, J. J. and de Groot, G. (1994). Optimisation of sprinting performance in running, cycling and speed skating. *Sports Medicine*, **17**, 259-275.

van Ingen Schenau, G. J., Jacobs, R. and de Koning, J. J. (1991). Can cycle power predict sprint running performance? *European Journal of Applied Physiology*, **63**, 255-260.

Ito, A., Saito, M., Fuchimoto, T. and Kaneko, M. (1992). Progressive changes of joint power in sprint start. *Journal of Biomechanics*, **25**, 708.

Jacobs, R. and van Ingen Schenau, G. J. (1992). Intermuscular coordination in a sprint push-off. *Journal of Biomechanics*, **25**, 953-965.

Jacobs, R., Bobbert, M. F. and van Ingen Schenau, G. J. (1996). Mechanical output from individual muscles during explosive leg extensions: the role of biarticular muscles. *Journal of Biomechanics*, **29**, 513-523.

Jensen, R. K. (1978). Estimation of the biomechanical properties of three body types using a photogrammetric method. *Journal of Biomechanics*, **11**, 349-358.

Jessop, D.M. and Pain, M.T.G. (2007). Effect of the number of foot segments and viscoelastic properties of the foot in an angle driven model of the sprint start. In *23rd Proceedings of the BASES Biomechanics Interest Group* (edited by J. Vanrenterghem), p. 17. Liverpool, UK: University Press.

Johnson, M. D. and Buckley, J. G. (2001). Muscle power patterns in the mid-acceleration phase of sprinting. *Journal of Sports Sciences*, **19**, 263-272.

Jonkers, I., Spaepen, A., Papaioannou, G. and Stewart, C. (2002). An EMG-based, muscle driven forward simulation of single support phase of gait. *Journal of Biomechanics*, **35**, 609-619.

Kane, T. R., Likins, P. W. and Levinson, D. A. (1983). *Spacecraft Dynamics*. New York, NY: McGraw-Hill.

Kearney, J. T. (1999). Sport performance enhancement: design and analysis of research. *Medicine and Science in Sports and Exercise*, **31**, 755-756.

Ker, R. F. (1996). The time-dependent mechanical properties of the human heel pad in the context of locomotion. *Journal of Experimental Biology*, **199**, 1501-1508.

King, M. A. and Yeadon, M. R. (2002). Determining subject-specific torque parameters for use in a torque-driven simulation model of dynamic jumping. *Journal of Applied Biomechanics*, **18**, 207-217.

King, M. A. and Yeadon, M. R. (2004). Maximising somersault rotation in tumbling. *Journal of Biomechanics*, **37**, 471-477.

King, M. A., Wilson, C. and Yeadon, M. R. (2006). Evaluation of a torque-driven model of jumping for height. *Journal of Applied Biomechanics*, **22**, 264-274.

Kistler, J. W. (1934). A study of the distribution of the force exerted upon the blocks in starting the sprint from various starting positions. *Research Quarterly*, **5**, 27-32.

de Koning, J. J., de Groot, G. and van Ingen Schenau, G. J. (1992). A power equation for the sprint in speed skating. *Journal of Biomechanics*, **25**, 573-80.

Korchemny, R. (1992). A new concept for sprint start and acceleration training. *New Studies in Athletics*, **7** (4), 65-72.

Krell, J. B. and Stefanyshyn, D. J. (2006). The relationship between extension of the metatarsophalangeal joint and sprint time for 100 m Olympic athletes. *Journal of Sports Sciences*, **24**, 175-180.

Kunz, H. and Kauffman, D. A. (1981). Biomechanical analysis of sprinting: decathletes versus champions. *British Journal of Sports Medicine*, **15**, 177-181.

Lemaire, E. D. and Robertson, D. G. E. (1990). Force-time data acquisition-system for sprint starting. *Canadian Journal of Sport Sciences*, **15**, 149-152.

de Leva, P. (1996). Adjustments to Zatsiorsky-Seluyanov's segment inertia parameters. *Journal of Biomechanics*, **29**, 1223-1230.

Liu, W. and Nigg, B. M. (2000). A mechanical model to determine the influence of masses and mass distribution on the impact force during running. *Journal of Biomechanics*, **33**, 219-224.

Mann, R. (1981). A kinetic analysis of sprinting. *Medicine and Science in Sports and Exercise*, **13**, 325-328.

Mann, R. (1985). Biomechanical analysis of the elite sprinter and hurdler. In *The Elite Athlete* (edited by N. K. Butts, T. T. Gushiken and B. Zarins), pp. 43-80. New York, NY: Spectrum Publications Inc.

Mann, R. and Herman, J. (1985). Kinematic analysis of Olympic sprint performance: men's 200 meters. *International Journal of Sport Biomechanics*, **1**, 151-162.

Mann, R. and Sprague, P. (1980). A kinetic analysis of the ground leg during sprint running. *Research Quarterly for Exercise and Sport*, **51**, 334-348.

Mann, R. and Sprague, P. (1983). Kinetics of sprinting. In *Proceedings of I International Symposium on Biomechanics in Sports* (edited by J. Terauds), pp. 305-316. San Diego, CA: University Press.

Mann, R., Kotmel, J., Herman, J., Johnson, B. and Schultz, C. Kinematic trends in elite sprinters. In *Proceedings of II International Symposium on Biomechanics in Sports* (edited by J. Terauds, K. Barthels, E. Kreighbaum, R. Mann and J. Crakes), pp. 17-33. Colorado Springs, CO: University Press.

Marhefka, D. W. and Orin, D. E. (1996). Simulation of contact using a nonlinear damping model. *Robotics and Automation*, **2**, 1662-1668.

Marhefka, D. W. and Orin, D. E. (1999). A compliant contact model with nonlinear damping for simulation of robotic systems. *IEEE Transactions on Systems, Man and Cybernetics - Part A: Systems and Humans*, **29**, 566-572.

McLaughlin, T. M., Dillman, C. J. and Lardner, T. J. (1977). Biomechanical analysis with cubic splines. *Research Quarterly*, **48**, 569-582.

Mendoza, L. and Schöllhorn, W. (1993). Training of the sprint start technique with biomechanical feedback. *Journal of Sports Sciences*, **11**, 25-29.

Menely, R. C. and Rosemier, R. A. (1968). Effectiveness of four track starting positions on acceleration. *The Research Quarterly*, **39**, 161-165.

Mero, A. (1988). Force-time characteristics and running velocity of male sprinters during the acceleration phase of sprinting. *Research Quarterly for Exercise and Sport*, **59**, 94-98.

Mero, A. and Komi, P. V. (1986). Force-velocity, EMG-velocity, and elasticity-velocity relationships at submaximal, maximal and supramaximal running speeds in sprinters. *European Journal of Applied Physiology and Occupational Physiology*, **55**, 553-561.

Mero, A. and Komi, P. V. (1990). Reaction-time and electromyographic activity during a sprint start. *European Journal of Applied Physiology and Occupational Physiology*, **61**, 73-80.

Mero, A. and Komi, P. V. (1994). EMG, force, and power analysis of sprint-specific strength exercises. *Journal of Applied Biomechanics*, **10**, 1-13.

Mero, A., Luhtanen, P. and Komi, P. V. (1983). A biomechanical study of the sprint start. *Scandinavian Journal of Sports Science*, **5**, 20-28.

Mero, A., Kuitunen, S., Harland, M., Kyröläinen, H. and Komi, P. V. (2006). Effects of muscle-tendon length on joint moment and power during sprint starts. *Journal of Sports Sciences*, **24**, 165-173.

Miller, D. and Nelson, R. (1973). *Biomechanics of Sport: A Research Approach*. Philadelphia, PA: Lea and Febiger.

Morin, J. B., Jeannin, T., Chevallier, B. and Belli, A. (2006). Spring-mass model characteristics during sprint running: correlation with performance and fatigue-induced changes. *International Journal of Sports Medicine*, **27**, 158-165.

Mungiole, M. and Martin, P. E. (1990). Estimating segment inertia properties: comparison of magnetic resonance imaging with existing methods. *Journal of Biomechanics*, **23**, 1039-1046.

Onyshko, S. and Winter, D. A. (1980). A mathematical model for the dynamics of human motion. *Journal of Biomechanics*, **13**, 361-368.

Pain, M. T. G. and Hibbs, A. (2007). Sprint starts and the minimum auditory reaction time. *Journal of Sports Sciences*, **25**, 79-86.

Pandy, M. G., Zajac, F. E., Sim, E. and Levine, W. S. (1990). An optimal-control model for maximum-height human jumping. *Journal of Biomechanics*, **23**, 1185-1198.

Parry, T. E., Henson, P. and Cooper, J. (2003). Lateral foot placement analysis of the sprint start. *New Studies in Athletics*, **18** (1), 13-22.

Payne, A. H. and Blader, F. B. (1971). The mechanics of the sprint start. In *Biomechanics II* (edited by J. Vredenbregt and J. Wartenweiler), pp. 225-231. Baltimore, MD: University Park Press.

Payne, A. H., Slater, W. J. and Telford, T. (1968). The use of a force platform in the study of athletic activities: a preliminary investigation. *Ergonomics*, **11**, 123-143.

Pezzack, J. C., Norman, R. W. and Winter, D. A. (1977). Assessment of derivative determining techniques used for motion analysis. *Journal of Biomechanics*, **10**, 377-382.

di Prampero, P. E., Fusi, S., Sepulcri, L., Morin, J. B., Belli, A. and Antonutto, G. (2005). Sprint running: a new energetic approach. *Journal of Experimental Biology*, **208**, 2809-2816.

Putnam, C. A. (1991). A segment interaction analysis of proximal-to-distal sequential segment motion patterns. *Medicine and Science in Sports and Exercise*, **23**, 130-144.

Putnam, C. A. and Dunn, E. G. (1987). Performance variations in rapid swinging motions: effects on segment interaction and resultant joint moments. In *Biomechanics X-B* (edited by B. Jonsson), pp. 661-665. Champaign, IL: Human Kinetics.

Putnam, C. A. and Kozey, J. W. (1989). Substantive issues in running. In *Biomechanics of Sport* (edited by C. L. Vaughan), pp. 1-33. Boca Raton, FL: CRC Press.

Reis, V. M. and Fazenda, L. M. (2004). Associations between the placement on the starting blocks and indoor sprint performance. *International Journal of Performance Analysis in Sport*, **4**, 54-60.

Riemer, R., Hsiao-Wecksler, E. T. and Zhang, X. (2008). Uncertainties in inverse dynamics solutions: a comprehensive analysis and an application to gait. *Gait & Posture*, **27**, 578-88.

Riley, P. O. and Kerrigan, D. C. (1998). Torque action of two-joint muscles in the swing period of stiff-legged gait: a forward dynamic model analysis. *Journal of Biomechanics*, **31**, 835-840.

Robertson, D. G. E., Caldwell, G. E., Hamill, J., Kamen, G. and Whittlesey, S. N. (2004). *Research Methods in Biomechanics*. Champaign, IL: Human Kinetics.

Rodano, R., Rabufetti, M. and Squadrone, R. (1994). Mathematical model for the estimate of the centre of mass kinematics in sprint start. In *Proceedings of XII International Symposium on Biomechanics in Sports* (edited by A. Barabas), pp. 43-46. Budapest, Hungary: University Press.

Roos, P. E. (2007). *Contributions to Successful Trip Recovery in Younger and Older Adults*. Unpublished Doctoral dissertation, University of Bath.

Salo, A. and Bezodis, I. (2004). Which starting style is faster in sprint running - standing or crouch start? *Sports Biomechanics*, **3**, 43-54.

Salo, A. I. T. and Scarborough, S. (2006). Changes in technique within a sprint hurdle run. *Sports Biomechanics*, **5**, 155-166.

Salo, A. I. T., Keränen, T. and Viitasalo, J. T. (2005). Force production in the first four steps of sprint running. In *Proceedings of XXIII International Symposium on Biomechanics in Sports* (edited by Q. Wang), pp. 313-317. Beijing, China: The China Institute of Sport Science.

Schot, P. K. and Knutzen, K. M. (1992). A biomechanical analysis of 4 sprint start positions. *Research Quarterly for Exercise and Sport*, **63**, 137-147.

Seyfarth, A., Blickhan, R. and van Leeuwen, J. L. (2000). Optimum take-off techniques and muscle design for long jump. *Journal of Experimental Biology*, **203**, 741-750.

Sigerseth, P. O. and Grinaker, Y. F. (1962). Effect of foot spacing on velocity in sprints. *Research Quarterly*, **33**, 599-606.

Slawinski, L., Billat, V., Koralstein, J. P. and Tavernier, M. (2004). The use of the lumbar point for the estimation of potential and kinetic mechanical power in running. *Journal of Applied Biomechanics*, **20**, 324-331.

Smith, G. (1989). Padding point extrapolation techniques for the Butterworth digital filter. *Journal of Biomechanics*, **22**, 967-971.

van Soest, A. J., Schwab, A. L., Bobbert, M. F. and van Ingen Schenau, G. J. (1993). The Influence of the biarticularity of the gastrocnemius-muscle on vertical-jumping achievement. *Journal of Biomechanics*, **26**, 1-8.

Son, J., Hwang, S. and Kim, Y. (2008). An algorithm to estimate muscle force from joint angle using Simulink. In *Proceedings of XXVI International Symposium on Biomechanics in Sports* (edited by Y-H. Kwon, J. Shim, J. K. Shim and I-S. Shin) pp. 170-172. Seoul, Korea: Seoul National University Press.

Soudan, K. and Dierckx, P. (1979). Calculation of derivatives and fourier coefficients of human motion data, while using spline functions. *Journal of Biomechanics*, **12**, 21-26.

Stagni, R., Leardini, A., Cappozzo, A., Benedetti, M. and Capello, A. (2000). Effects of hip joint centre mislocation on gait analysis results. *Journal of Biomechanics*, **33**, 1479-1487.

Stefani, R. T. (2006). The relative power output and relative lean body mass of World and Olympic male and female champions with implications for gender equity. *Journal of Sports Sciences*, **24**, 1329-1339.

Stefanyshyn, D. J. and Nigg, B. M. (1997). Mechanical energy contribution of the metatarsophalangeal joint to running and sprinting. *Journal of Biomechanics*, **30**, 1081-1085.

Stergiou, N. and Scott, M. M. (2005). Baseline measures are altered in biomechanical studies. *Journal of Biomechanics*, **38**, 175-178.

Stock, M. (1962). Influence of various track starting positions on speed. *Research Quarterly*, **33**, 607-614.

Thelen, D. G., Anderson, F. C. and Delp, S. L. (2003). Generating dynamic simulations of movement using computed muscle control. *Journal of Biomechanics*, **36**, 321-328.

Thomas, J. R. and Nelson, J. K. (1999). *Research Methods in Physical Activity*. Champaign, IL: Human Kinetics.

Vagenas, G. and Hoshizaki, T. B. (1986). Optimization of an asymmetrical motor skill: sprint start. *International Journal of Sport Biomechanics*, **2**, 29-40.

Vaughan, C. L. (1982). Smoothing and differentiation of displacement-time data - an application of splines and digital filtering. *International Journal of Bio-Medical Computing*, **13**, 375-386.

Vint, P. F. and Hinrichs, R. N. (1996). Endpoint error in smoothing and differentiating raw kinematic data: an evaluation of four popular methods. *Journal of Biomechanics*, **29**, 1637-1642.

Whitsett, C. E. (1963). *Some dynamic response characteristics of weightless man*. AMRL-TDR-63-18, AD-412-541. Aerospace Medical Research Laboratory, Wright-Patterson Air Force Base, Ohio.

Willems, P. A., Cavagna, G. A. and Heglund, N. C. (1995). External, internal and total work in human locomotion. *Journal of Experimental Biology*, **198**, 379-393.

Wilson, C. (2003). *Optimisation of Performance in Running Jumps*. Unpublished Doctoral dissertation, Loughborough University.

Wilson, C., King, M. A. and Yeadon, M. R. (2006). Determination of subject-specific model parameters for visco-elastic elements. *Journal of Biomechanics*, **39**, 1883-1890.

Winter, D. A. (1978). Calculation and interpretation of mechanical energy of movement. *Exercise and Sport Sciences Reviews*, **6**, 183-201.

Winter, D. A. (1983). Moments of force and mechanical power in jogging. *Journal of Biomechanics*, **16**, 91-97.

Winter, D. A. (1990). *Biomechanics and Motor Control of Human Movement*. New York: Wiley.

Wojtyra, M. (2003). Multibody simulation model of human walking. *Mechanics Based Design of Structures and Machines*, **31**, 357-379.

Woltring, H. J. (1985). On optimal smoothing and derivative estimation from noisy displacement data in biomechanics. *Human Movement Science*, **4**, 229-245.

Wood, G. A. (1982). Data smoothing and differentiation procedures in biomechanics. *Exercise and Sport Sciences Reviews*, **10**, 308-362.

Wood, G. A. and Jennings, L. S. (1979). On the use of spline functions for data smoothing. *Journal of Biomechanics*, **12**, 477-479.

Yeadon, M. R. (1990). The simulation of aerial movement 2: a mathematical inertia model of the human-body. *Journal of Biomechanics*, **23**, 67-74.

Yeadon, M. R. and Brewin, M. A. (2003). Optimised performance of the backward longswing on rings. *Journal of Biomechanics*, **36**, 545-552.

Yeadon, M. R. and Challis, J. H. (1994). The future of performance-related sports biomechanics research. *Journal of Sports Sciences*, **12**, 3-32.

Yeadon, M. R. and Hiley, M. J. (2000). The mechanics of the backward giant circle on the high bar. *Human Movement Science*, **19**, 153-173.

Yeadon, M. R. and King, M. A. (2002). Evaluation of a torque-driven simulation model of tumbling. *Journal of Applied Biomechanics*, **18**, 195-206.

Yeadon, M. R., Kato, T. and Kerwin, D. G. (1999). Measuring running speed using photocells. *Journal of Sports Sciences*, **17**, 249-257.

Yeadon, M. R., Kong, P. W. and King, M. A. (2006). Parameter determination for a computer simulation model of a diver and a springboard. *Journal of Applied Biomechanics*, **22**, 167-176.

Yu, B. and Hay, J. G. (1996). Optimum phase ratio in the triple jump. *Journal of Biomechanics*, **29**, 1283-1289.

Yu, B., Gabriel, D., Noble, L. and An, K. N. (1999). Estimate of the optimum cutoff frequency for the Butterworth low-pass digital filter. *Journal of Applied Biomechanics*, **15**, 318-329.

Zajac, F. E., Wicke, R. W. and Levine, W. S. (1984). Dependence of jumping performance on muscle properties when humans use only calf muscles for propulsion. *Journal of Biomechanics*, **17**, 513-523.

Zatsiorsky, V. and Seluyanov, V. (1983). The mass and inertia characteristics of the main segments of the human body. In *Biomechanics VIII-B* (edited by H. Matsui and K. Kobayashi), pp. 1152-1159. Champaign, IL: Human Kinetics.

Zernicke, R. F., Caldwell, G. E. and Roberts, E. M. (1976). Fitting biomechanical data with cubic spline functions. *Research Quarterly*, **47**, 9-19.

APPENDIX A: EQUATIONS USED TO NORMALISE DATA

The following equations were presented by Hof (1996). In the current thesis, these were used to normalise certain kinematic and kinetic variables, based on a sprinter's mass (m), leg length (l) and the acceleration due to gravity (g = 9.81 m·s^{-2}). The addition of a subscript N to the symbol representing a variable defines the normalised value of that variable.

Distance (d):

$$d_N = \frac{d}{l}$$

Energy/Work (E):

$$W_N = \frac{W}{m \cdot g \cdot l}$$

Force (F):

$$F_N = \frac{F}{m \cdot g}$$

Moment (M):

$$M_N = \frac{M}{m \cdot g \cdot l}$$

Power (P):

$$P_N = \frac{P}{m \cdot g^{1/2} \cdot l^{3/2}}$$

APPENDIX B: SUBJECT-SPECIFIC INERTIA DATA

The following are the inertia data determined for the sprinters studied in Chapter 5, using the methods of Yeadon (1990).

Table B.1. Individual segmental masses expressed as a percentage of whole body mass.

Segment	Sprinter N	Sprinter Q	Sprinter R
Head	5.67	5.10	6.43
Trunk	44.09	43.78	45.67
Left upper arm	2.73	2.44	2.53
Right upper arm	2.63	2.66	2.63
Left forearm	1.56	1.56	1.30
Right forearm	1.51	1.74	1.36
Left hand	0.44	0.36	0.42
Right hand	0.42	0.43	0.46
Left thigh	14.69	15.35	12.89
Right thigh	13.82	14.57	13.48
Left shank	5.01	4.90	5.29
Right shank	5.07	5.13	5.31
Left rearfoot	0.99	0.88	0.93
Right rearfoot	1.01	0.86	0.95
Left forefoot	0.18	0.12	0.16
Right forefoot	0.18	0.12	0.19

Table B.2. Individual segmental CM locations expressed as a percentage of the distance from the proximal to the distal endpoint.

Segment	Sprinter N	Sprinter Q	Sprinter R
Head	49.76	49.01	52.48
Trunk	51.63	51.39	50.52
Left upper arm	45.69	47.17	46.26
Right upper arm	46.09	45.61	45.94
Left forearm	40.55	41.34	42.49
Right forearm	40.77	40.84	41.98
Left hand	38.38	36.96	38.71
Right hand	38.90	38.53	39.81
Left thigh	41.75	41.48	41.27
Right thigh	41.47	41.80	40.58
Left shank	42.26	41.62	41.58
Right shank	42.35	42.00	42.24
Left rearfoot	44.94	43.01	44.53
Right rearfoot	44.12	43.16	44.12
Left forefoot	36.48	36.36	38.16
Right forefoot	36.85	37.06	38.35

Table B.3. Individual segmental moments of inertia ($kg \cdot m^2$) about the transverse axis.

Segment	Sprinter N	Sprinter Q	Sprinter R
Head	0.02673	0.02230	0.01860
Trunk	1.47178	1.36386	0.95197
Left upper arm	0.01474	0.01371	0.01016
Right upper arm	0.01397	0.01485	0.01057
Left forearm	0.00737	0.00849	0.00370
Right forearm	0.00695	0.00945	0.00366
Left hand	0.00089	0.00068	0.00050
Right hand	0.00082	0.00089	0.00054
Left thigh	0.20272	0.24889	0.10490
Right thigh	0.19039	0.20993	0.10654
Left shank	0.06100	0.06428	0.03753
Right shank	0.06333	0.06877	0.03588
Left rearfoot	0.00208	0.00184	0.00100
Right rearfoot	0.00211	0.00171	0.00095
Left forefoot	0.00008	0.00004	0.00004
Right forefoot	0.00008	0.00005	0.00005

APPENDIX C: RESULTANT JOINT MOMENTS AND JOINT POWER AT THE MTP AND ANKLE DURING STANCE

These figures show the MTP and ankle joint resultant moments and powers with different *y*-axis scaling to those presented in Figure 5.9.

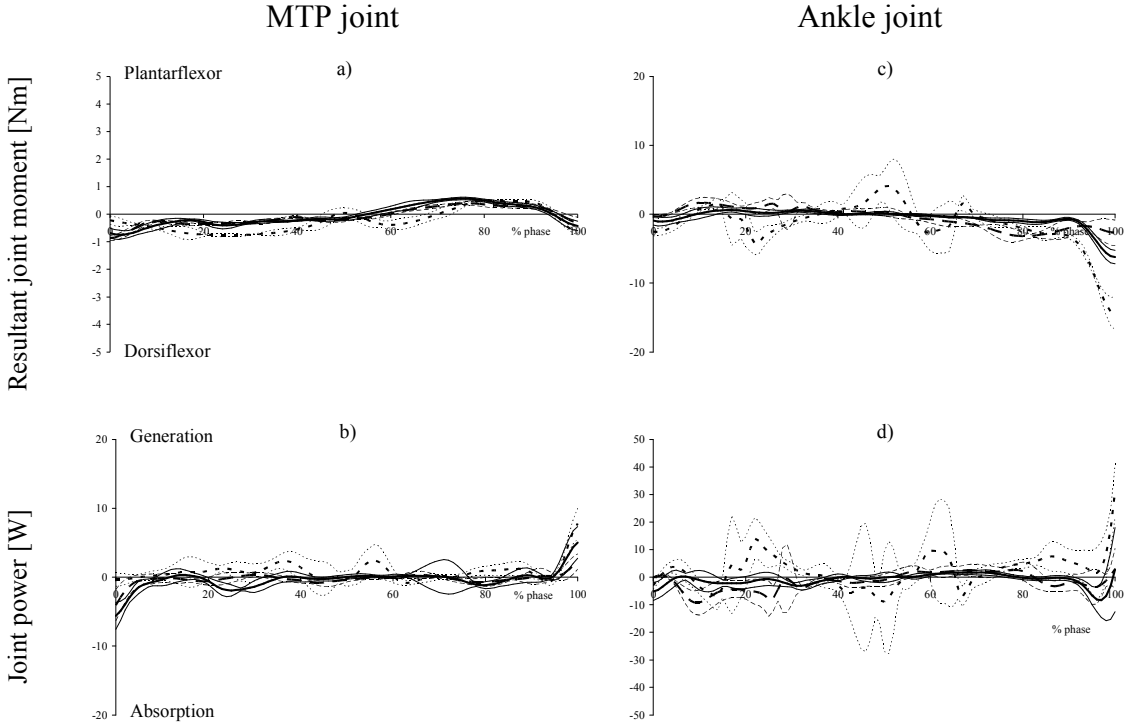

Figure C.1a-d. MTP and ankle angular kinematic and kinetic time-histories during the rear leg swing phase (i.e. from rear foot off the block until first stance touchdown) expressed relative to phase duration (mean ± *s*; sprinter N = dotted line; sprinter Q = dashed line; sprinter R = solid line). These are the same data as presented in Figures 5.9 c, d, g and h, but on a larger scale.

APPENDIX D: SIMULINK® MODEL STRUCTURE

The following four figures illustrate components of the overall structure used to develop the seven-segment model in Simulink®, as described in Chapter 6.

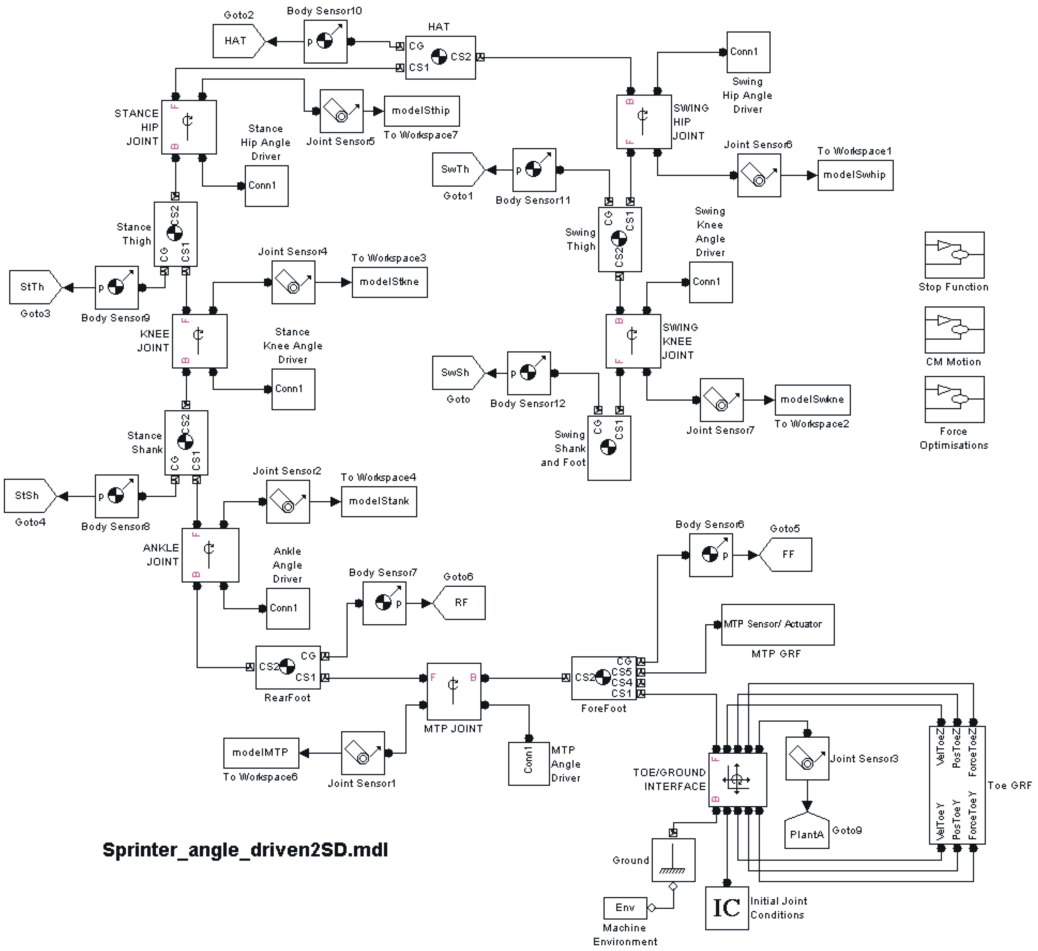

Figure D.1. Top-level structure used in the seven-segment Simulink® model.

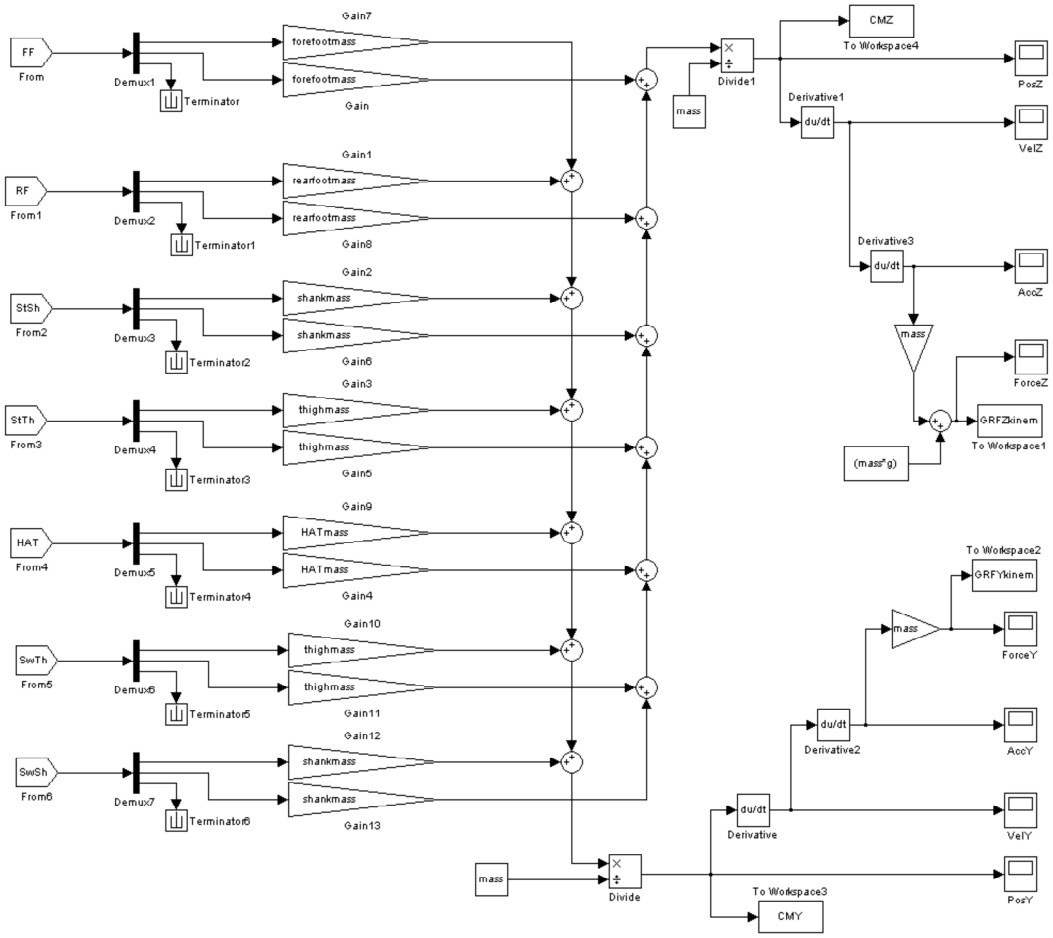

Figure D.2. Simulink® subsystem ('CM Motion' in Figure D.1) used to reconstruct the motion of the whole body centre of mass.

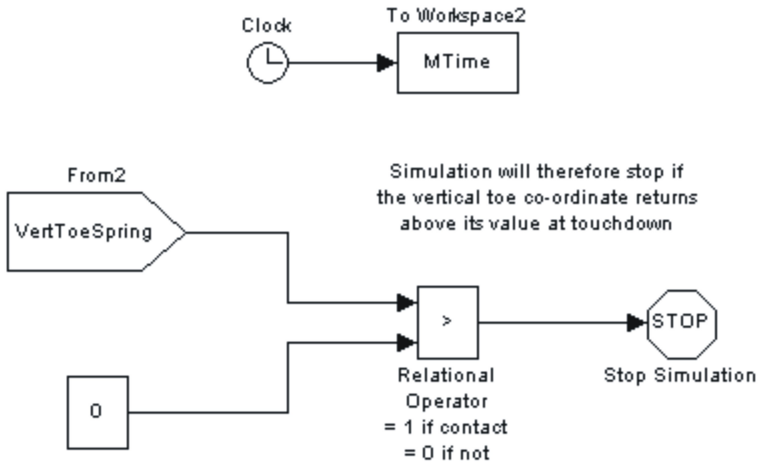

Figure D.3. Simulink® subsystem ('Stop Function' in Figure D.1) used to terminate a simulation when the vertical toe spring returned to its resting length.

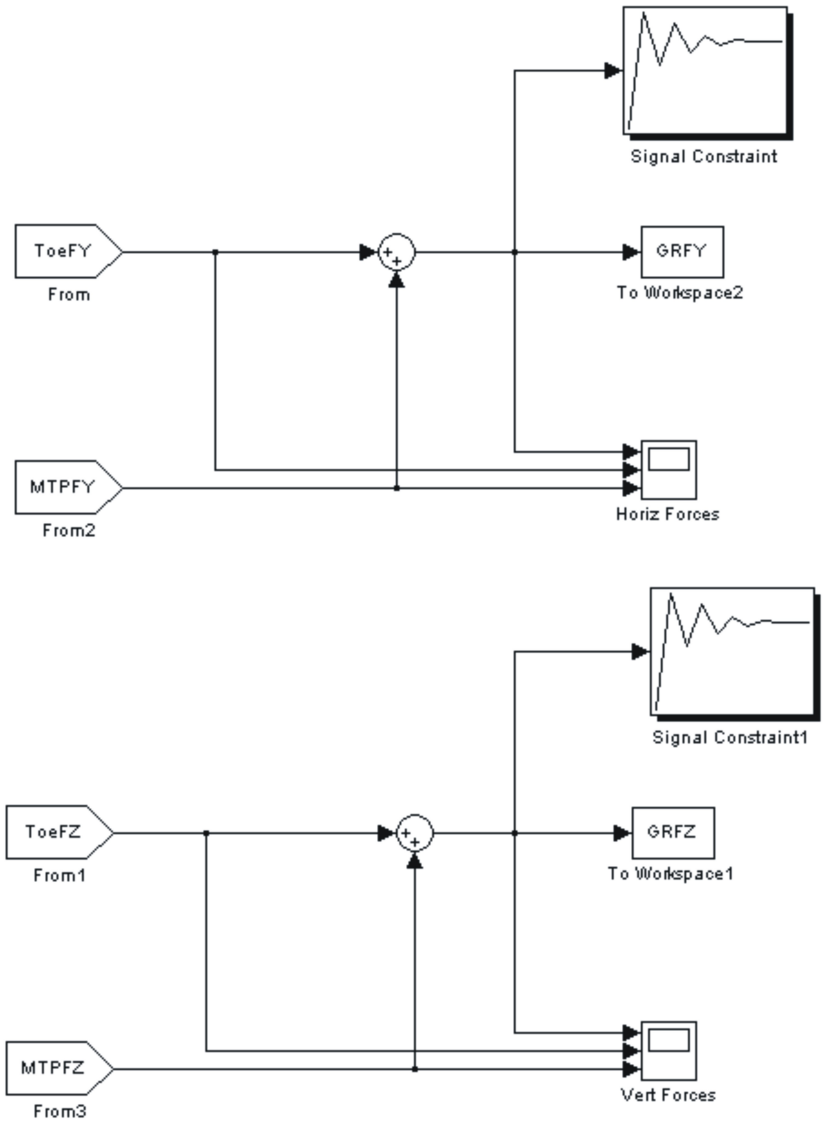

Figure D.4. Simulink® subsystem ('Force Optimisations' in figure D.1) used in the matching optimisations to obtain model input parameters.

APPENDIX E: CODE WRITTEN TO PROVIDE MODEL INPUT DATA

```
%=====================================================================
% Model_Inputs_2SD.m
%
% Written by Neil Bezodis.
%
% Purpose is to generate/specify the input data required for use in
% the forward dynamics model "Sprinter_angle_driven2SD.mdl"
%=====================================================================


% Clear workspace and command window, and close any open figures:
clear all
close all
clc


%=========================================
% DEFINE VARIABLES FOR TRIAL BEING MODELLED
%=========================================

% Define directory for file loading/saving:
directory = 'H:\Matlab';

% Specify which sprinter is being modelled in order to obtain
correct anthropometrics, etc (R = 1, N = 2, Q = 3):
sprinter  = 3;

% Specify trial being modelled in order to obtain correct timing of
events, phase durations, etc:
trial     = 12;

% Define input file containing filtered joint centre data:
inputfile  = '071218_T12V.txt';
% Define input file containing force data (for matching optims):
inputfile2 = '071218_T12F.txt';

% Define time of t/d and t/o, and block velocities for each trial:
touchdowns = [0.556 0.567 0.552 0.545 0.565 0.552 0.606 0.561 0.553
0.595 0.579 0.533 0.597 0.559];
takeoffs   = [0.732 0.771 0.745 0.730 0.747 0.743 0.782 0.758 0.748
0.764 0.771 0.721 0.785 0.748];
blockvels  = [3.14 3.23 3.47 3.15 3.30 3.75 3.07 3.15 3.61 3.07 3.19
3.40 3.06 3.50];

% Identify t/d, t/o and block velocity for trial of interest:
tdtime   = touchdowns(:,trial);
totime   = takeoffs(:,trial);
blockvel = blockvels(:,trial);

% Calculate stance phase duration (required for joint angular
acceleration Fourier series calculations):
sttime = totime - tdtime;
```

```
%====================================
% OPEN AND LABEL STANCE (S) VIDEO DATA
%====================================

% Open video data file using custom-designed function:
dataS = nb_fopen(directory, inputfile, 41, inf, 0);

% Label necessary columns:
timeS  = dataS(:,1);
vertxS = dataS(:,2);
vertyS = dataS(:,3);
neckxS = dataS(:,4);
neckyS = dataS(:,5);
lshoxS = dataS(:,6);
lshoyS = dataS(:,7);
rshoxS = dataS(:,8);
rshoyS = dataS(:,9);
lelbxS = dataS(:,10);
lelbyS = dataS(:,11);
lwrixS = dataS(:,12);
lwriyS = dataS(:,13);
lhanxS = dataS(:,14);
lhanyS = dataS(:,15);
relbxS = dataS(:,16);
relbyS = dataS(:,17);
rwrixS = dataS(:,18);
rwriyS = dataS(:,19);
rhanxS = dataS(:,20);
rhanyS = dataS(:,21);
lhipxS = dataS(:,22);
lhipyS = dataS(:,23);
rhipxS = dataS(:,24);
rhipyS = dataS(:,25);
lknexS = dataS(:,26);
lkneyS = dataS(:,27);
lankxS = dataS(:,28);
lankyS = dataS(:,29);
lmtpxS = dataS(:,30);
lmtpyS = dataS(:,31);
ltoexS = dataS(:,32);
ltoeyS = dataS(:,33);
rknexS = dataS(:,34);
rkneyS = dataS(:,35);
rankxS = dataS(:,36);
rankyS = dataS(:,37);
rmtpxS = dataS(:,38);
rmtpyS = dataS(:,39);
rtoexS = dataS(:,40);
rtoeyS = dataS(:,41);
mshoxS = (lshoxS + rshoxS)/2;
mshoyS = (lshoyS + rshoyS)/2;
mhipxS = (lhipxS + rhipxS)/2;
mhipyS = (lhipyS + rhipyS)/2;

% Define which leg is swing/stance leg (sprinters Q and R, swing =
left leg; sprinter N, swing = right leg):
if sprinter == 2
     st_hipx = lhipxS;
     st_knex = lknexS;
     st_ankx = lankxS;
     st_mtpx = lmtpxS;
```

```
     st_toex = ltoexS;
     sw_hipx = rhipxS;
     sw_knex = rknexS;
     sw_ankx = rankxS;
     sw_mtpx = rmtpxS;
     sw_toex = rtoexS;
     st_hipy = lhipyS;
     st_kney = lkneyS;
     st_anky = lankyS;
     st_mtpy = lmtpyS;
     st_toey = ltoeyS;
     sw_hipy = rhipyS;
     sw_kney = rkneyS;
     sw_anky = rankyS;
     sw_mtpy = rmtpyS;
     sw_toey = rtoeyS;
else
     st_hipx = rhipxS;
     st_knex = rknexS;
     st_ankx = rankxS;
     st_mtpx = rmtpxS;
     st_toex = rtoexS;
     sw_hipx = lhipxS;
     sw_knex = lknexS;
     sw_ankx = lankxS;
     sw_mtpx = lmtpxS;
     sw_toex = ltoexS;
     st_hipy = rhipyS;
     st_kney = rkneyS;
     st_anky = rankyS;
     st_mtpy = rmtpyS;
     st_toey = rtoeyS;
     sw_hipy = lhipyS;
     sw_kney = lkneyS;
     sw_anky = lankyS;
     sw_mtpy = lmtpyS;
     sw_toey = ltoeyS;
end


%==========================================
% FIRST STANCE ANGULAR KINEMATIC CALCULATIONS
%==========================================

% Calculate joint angles using custom-designed function:

% Trunk angle (relative to the horizontal):
trunk_ang = nb_ang(mhipxS, mhipyS, mshoxS, mshoyS);

% Stance hip angle:
st_hip_ang = nb_r_ang(st_hipx, st_hipy, mshoxS, mshoyS, st_knex,
st_kney, 1);

% Swing hip angle:
sw_hip_ang = nb_r_ang(sw_hipx, sw_hipy, mshoxS, mshoyS, sw_knex,
sw_kney, 1);

% Stance knee angle:
st_kne_ang = nb_r_ang(st_knex, st_kney, st_hipx, st_hipy, st_ankx,
st_anky, 0);
```

```
% Swing knee angle:
sw_kne_ang = nb_r_ang(sw_knex, sw_kney, sw_hipx, sw_hipy, sw_ankx,
sw_anky, 0);

% Stance ankle angle:
st_ank_ang = nb_r_ang(st_ankx, st_anky, st_knex, st_kney, st_mtpx,
st_mtpy, 1);

% Stance mtp angle:
st_mtp_ang = nb_r_ang(st_mtpx, st_mtpy, st_ankx, st_anky, st_toex,
st_toey, 1);

% Plant angle:
plant_ang = nb_ang(st_toex, st_toey, st_mtpx, st_mtpy);

% Convert angles to required SimMechanics convention:
st_mtp_ang = st_mtp_ang - 180;
st_ank_ang = st_ank_ang - 180;
st_kne_ang = 180 - st_kne_ang;
st_hip_ang = st_hip_ang - 180;
sw_hip_ang = sw_hip_ang * (-1);
sw_kne_ang = sw_kne_ang - 180;

% Interpolate angular data to 1000 Hz using custom-designed
% function:
[timeK, trunk_angK]  = nb_interp(timeS, trunk_ang, 1000);
[timeK, st_hip_angK] = nb_interp(timeS, st_hip_ang, 1000);
[timeK, sw_hip_angK] = nb_interp(timeS, sw_hip_ang, 1000);
[timeK, st_kne_angK] = nb_interp(timeS, st_kne_ang, 1000);
[timeK, sw_kne_angK] = nb_interp(timeS, sw_kne_ang, 1000);
[timeK, st_ank_angK] = nb_interp(timeS, st_ank_ang, 1000);
[timeK, st_mtp_angK] = nb_interp(timeS, st_mtp_ang, 1000);
[timeK, plant_angK]  = nb_interp(timeS, plant_ang, 1000);

% Interpolate linear toe data to 1000 Hz using custom-designed
% function:
[timeK, st_toexK]  = nb_interp(timeS, st_toex, 1000);
[timeK, st_toeyK]  = nb_interp(timeS, st_toey, 1000);

% Calculate velocities (linear and angular) using custom-designed
% function:
trunk_w   = nb_2cd(trunk_angK, 1000);
st_hip_w  = nb_2cd(st_hip_angK, 1000);
sw_hip_w  = nb_2cd(sw_hip_angK, 1000);
st_kne_w  = nb_2cd(st_kne_angK, 1000);
sw_kne_w  = nb_2cd(sw_kne_angK, 1000);
st_ank_w  = nb_2cd(st_ank_angK, 1000);
st_mtp_w  = nb_2cd(st_mtp_angK, 1000);
plant_w   = nb_2cd(plant_angK, 1000);
st_toex_v = nb_2cd(st_toexK, 1000);
st_toey_v = nb_2cd(st_toeyK, 1000);
st_mtpx_v = nb_2cd(st_mtpxK, 1000);
st_mtpy_v = nb_2cd(st_mtpyK, 1000);

% Calculate angular accelerations using custom-designed function:
trunk_a   = nb_2cd(trunk_w, 1000);
st_hip_a  = nb_2cd(st_hip_w, 1000);
sw_hip_a  = nb_2cd(sw_hip_w, 1000);
st_kne_a  = nb_2cd(st_kne_w, 1000);
```

```
sw_kne_a  = nb_2cd(sw_kne_w, 1000);
st_ank_a  = nb_2cd(st_ank_w, 1000);
st_mtp_a  = nb_2cd(st_mtp_w, 1000);
plant_a   = nb_2cd(plant_w, 1000);
st_toex_a = nb_2cd(st_toex_v, 1000);
st_toey_a = nb_2cd(st_toey_v, 1000);
st_mtpx_a = nb_2cd(st_mtpx_v, 1000);
st_mtpy_a = nb_2cd(st_mtpy_v, 1000);

% Identify 1000 Hz touchdown and takeoff frames for this trial:
td = find(timeK == tdtime);
to = find(timeK == totime);

% Identify joint angles at touchdown:
plant_td_ang = plant_angK(td);
stmtp_td_ang = st_mtp_angK(td);
stank_td_ang = st_ank_angK(td);
stkne_td_ang = st_kne_angK(td);
sthip_td_ang = st_hip_angK(td);
trunk_td_ang = trunk_angK(td);
swkne_td_ang = sw_kne_angK(td);
swhip_td_ang = sw_hip_angK(td);

% Find toe/MTP positions at touchdown:
toex_td = st_toexK(td);
toey_td = st_toeyK(td);
mtpx_td = st_mtpxK(td);
mtpy_td = st_mtpyK(td);

% Identify angular velocities at touchdown:
plant_td_w = plant_w(td);
stmtp_td_w = st_mtp_w(td);
stank_td_w = st_ank_w(td);
stkne_td_w = st_kne_w(td);
sthip_td_w = st_hip_w(td);
trunk_td_w = trunk_w(td);
swkne_td_w = sw_kne_w(td);
swhip_td_w = sw_hip_w(td);

% Identify linear velocities at touchdown:
toex_td_v = st_toex_v(td);
toey_td_v = st_toey_v(td);
mtpx_td_v = st_mtpx_v(td);
mtpy_td_v = st_mtpy_v(td);

% Chop time and joint angular acceleration data to just stance:
timeK2   = timeK(td:to);
st_hip_a = st_hip_a(td:to);
sw_hip_a = sw_hip_a(td:to);
st_kne_a = st_kne_a(td:to);
sw_kne_a = sw_kne_a(td:to);
st_ank_a = st_ank_a(td:to);
st_mtp_a = st_mtp_a(td:to);
plant_a  = plant_a(td:to);

% Reset time so that first frame (i.e. touchdown) = 0.000 s...
timeK2 = timeK2 - timeK2(1);
```

```
%=========================================================================
% CREATE APPROPRIATE MATRICES FOR SIMULINK ANGULAR ACCELERATION
DRIVERS
%=========================================================================

plant(:,1) = timeK2;
plant(:,2) = plant_a;

stmtp(:,1) = timeK2;
stmtp(:,2) = st_mtp_a;

stank(:,1) = timeK2;
stank(:,2) = st_ank_a;

stkne(:,1) = timeK2;
stkne(:,2) = st_kne_a;

sthip(:,1) = timeK2;
sthip(:,2) = st_hip_a;

swhip(:,1) = timeK2;
swhip(:,2) = sw_hip_a;

swkne(:,1) = timeK2;
swkne(:,2) = sw_kne_a;


%=========================================
% SPRINTER-SPECIFIC SEGMENTAL INERTIA DATA
%=========================================

% Sprinter R:
if sprinter == 1
    mass      = 60.5;  % without spikes (kg)
    height    = 1.700; % in metres

    % Forefoot:
    forefootmass   = 0.001725*mass; % segment mass % of total mass
    forefootMoI    = 0.000043;      % sagittal plane MoI
    forefootlength = 0.0715;        % segment length (m)
    forefootCMpc   = 1 - 0.38252;   % segment CM from prox. to dist.

    % Rearfoot:
    rearfootmass   = 0.009425*mass;
    rearfootMoI    = 0.000977;
    rearfootlength = 0.1350;
    rearfootCMpc   = 1 - 0.443245;

    % Divide spike mass between the foot segments:
    footlength        = forefootlength + rearfootlength;
    forefootspikemass = (forefootlength/footlength)*0.2;
    rearfootspikemass = (rearfootlength/footlength)*0.2;
    forefootmass      = forefootmass + forefootspikemass;
    rearfootmass      = rearfootmass + rearfootspikemass;

    % Shank:
    shankmass   = 0.053035*mass;
    shankMoI    = 0.036709;
    shanklength = 0.3975;
```

```
    shankCMpc   = 1 - 0.419065;

    % Thigh:
    thighmass   = 0.131865*mass;
    thighMoI    = 0.10572;
    thighlength = 0.3975;
    thighCMpc   = 1 - 0.40924;

    % HAT (Combined head, arms and trunk segment):
    HATmass   = 0.60788*mass;
    HATMoI    = 0.951969;
    HATlength = 0.837;
    HATCMpc   = 1 - 0.58820;

    % Include spike mass in total mass value...
    mass      = mass + 0.4;

% Sprinter N:
elseif sprinter == 2
    mass      = 82.6;  % Without spikes
    height    = 1.810;

    % Forefoot:
    forefootmass   = 0.00176*mass;
    forefootMoI    = 0.0000825;
    forefootlength = 0.0830;
    forefootCMpc   = 1 - 0.366665;

    % Rearfoot:
    rearfootmass   = 0.01001*mass;
    rearfootMoI    = 0.002093;
    rearfootlength = 0.1565;
    rearfootCMpc   = 1 - 0.44532;

    % Divide spike mass between the foot segments:
    footlength        = forefootlength + rearfootlength;
    forefootspikemass = (forefootlength/footlength)*0.2;
    rearfootspikemass = (rearfootlength/footlength)*0.2;
    forefootmass      = forefootmass + forefootspikemass;
    rearfootmass      = rearfootmass + rearfootspikemass;

    % Shank:
    shankmass   = 0.050405*mass;
    shankMoI    = 0.062165;
    shanklength = 0.437;
    shankCMpc   = 1 - 0.423045;

    % Thigh:
    thighmass   = 0.142575*mass;
    thighMoI    = 0.1965575;
    thighlength = 0.4355;
    thighCMpc   = 1 - 0.416065;

    % HAT (Combined head, arms and trunk segment):
    HATmass   = 0.59049*mass;
    HATMoI    = 1.471782;
    HATlength = 0.887;
    HATCMpc   = 1 - 0.59583;
```

```
    % Include spike mass in total mass value:
    mass      = mass + 0.4;

% Sprinter Q:
else
    mass      = 86.9;
    height    = 1.790;

    % Forefoot:
    forefootmass   = 0.00124*mass;
    forefootMoI    = 0.000045;
    forefootlength = 0.0710;
    forefootCMpc   = 1 - 0.367125;

    % Rearfoot:
    rearfootmass   = 0.00872*mass;
    rearfootMoI    = 0.0017725;
    rearfootlength = 0.1540;
    rearfootCMpc   = 1 - 0.43084;

    % Divide spike mass between the foot segments:
    footlength        = forefootlength + rearfootlength;
    forefootspikemass = (forefootlength/footlength)*0.2;
    rearfootspikemass = (rearfootlength/footlength)*0.2;
    forefootmass      = forefootmass + forefootspikemass;
    rearfootmass      = rearfootmass + rearfootspikemass;

    % Shank:
    shankmass   = 0.05016*mass;
    shankMoI    = 0.066525;
    shanklength = 0.447;
    shankCMpc   = 1 - 0.41812;

    % Thigh:
    thighmass   = 0.149600*mass;
    thighMoI    = 0.229411;
    thighlength = 0.4555;
    thighCMpc   = 1 - 0.41639;

    % HAT (Combined head, arms and trunk segment):
    HATmass   = 0.58056*mass;
    HATMoI    = 1.363860;
    HATlength = 0.834;
    HATCMpc   = 1 - 0.59556;

    % Include spike mass in total mass value:
    mass      = mass + 0.4;
end


%================================================
% FORCE PLATFORM DATA (FOR MATCHING OPTIMISATIONS)
%================================================

% Open video data file using custom-designed function:
dataF = nb_fopen(directory, inputfile2, 3, inf, 1);
```

```
% Label necessary columns:
timeF = dataF(:,1);
FX    = dataF(:,2);
FY    = dataF(:,3);

% Adjust time vector so first value = 0.000 s
timeF = timeF - timeF(1);


%=================================================
% GROUND CONTACT SPRING PARAMETER INITIAL ESTIMATES
%=================================================

% Threshold for MTP contact:
RestingMTPPos = 0.0450;

% Horizontal toe stiffness:
ToeKH = 150000;

% Vertical toe stiffness:
ToeKV = 100000;

% Horizontal toe damping:
ToeBH = 150000;

% Vertical toe damping:
ToeBV = 10000;

% Horizontal MTP stiffness:
MTPKH = 150000;

% Vertical MTP stiffness:
MTPKV = 100000;

% Horizontal MTP damping:
MTPBH = 150000;

% Vertical MTP damping:
MTPBV = 10000;


%====================================
% INITIAL FOURIER SERIES CO-EFFICIENTS
%====================================

% These start from zero so that the initial angular acceleration
% time-histories at each joint are equal to the empirical values:

% Stance MTP:
stmtp1 = 0;
stmtp2 = 0;
stmtp3 = 0;
stmtp4 = 0;
stmtp5 = 0;

% Stance ankle:
stank1 = 0;
stank2 = 0;
```

```
stank3 = 0;
stank4 = 0;
stank5 = 0;

% Stance knee:
stkne1 = 0;
stkne2 = 0;
stkne3 = 0;
stkne4 = 0;
stkne5 = 0;

% Stance hip:
sthip1 = 0;
sthip2 = 0;
sthip3 = 0;
sthip4 = 0;
sthip5 = 0;

% Swing knee:
swkne1 = 0;
swkne2 = 0;
swkne3 = 0;
swkne4 = 0;
swkne5 = 0;

% Swing hip:
swhip1 = 0;
swhip2 = 0;
swhip3 = 0;
swhip4 = 0;
swhip5 = 0;


%=============
% End of code.
%=============
```

APPENDIX F: RESULTANT JOINT MOMENT TIME-HISTORIES FROM THE MODEL EVALUATION OF TRIAL E3

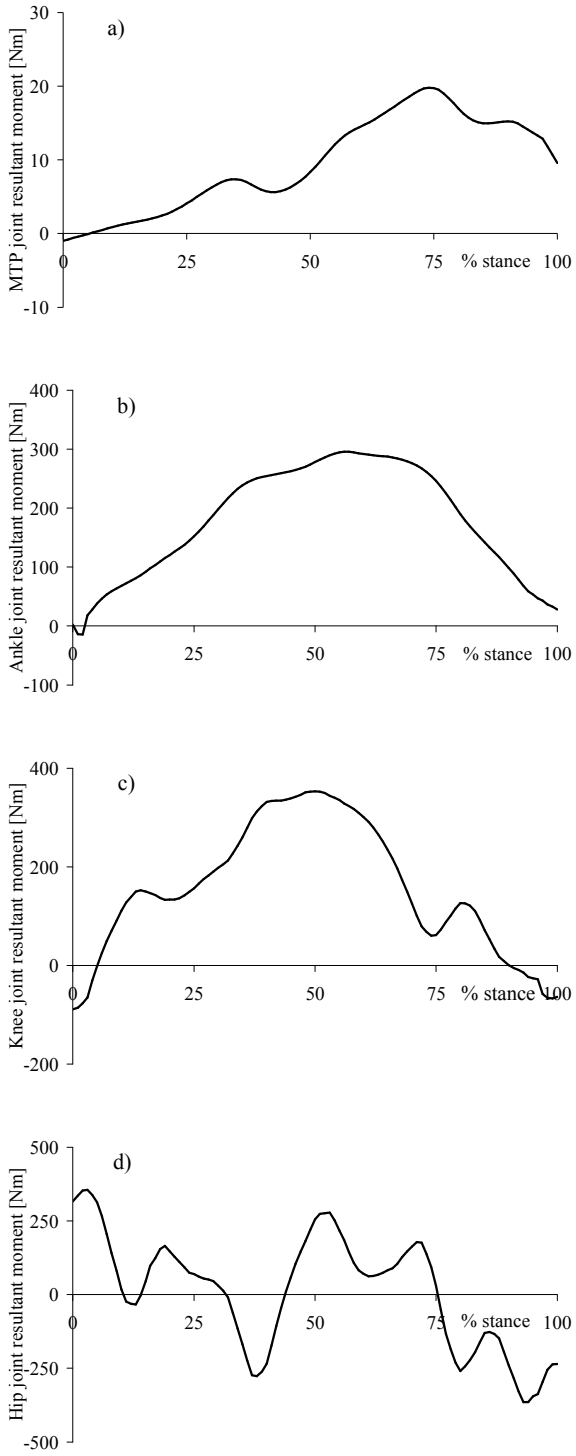

Figures F.1a-d. MTP (a), ankle (b), knee (c) and hip (d) resultant joint moments from the model evaluation of trial E3.